Selective Transport and Separation of Biomolecules using Charged Membranes

Thesis

Submitted to the

Bhavnagar University, Bhavnagar

for the degree of

DOCTOR OF PHILOSOPHY

in

CHEMISTRY

By

ARUNIMA SAXENA

Under the guidance of

Dr. VINOD KUMAR SHAHI

Scientist

Electro-Membrane Processes Division

Central Salt and Marine Chemicals Research Institute

Bhavnagar-364002, Gujarat, India

May 2009

CANDIDATE'S STATEMENT

I hereby declare that the work incorporated in the present thesis is original and has not been submitted to any University/Institute for the award of a Diploma or Degree. I further declare that the results presented in the thesis consideration made therein, contribute in general to the advancement of knowledge in Chemistry and in particular to **"Selective transport and separation of biomolecules using charged membranes".**

ARUNIMA SAXENA

केन्द्रीय नमक व समुद्री रसायन अनुसंधान संस्थान
गिजुभाई बधेका मार्ग, भावनगर- ३६४ ००२

CENTRAL SALT & MARINE CHEMICALS RESEARCH INSTITUTE
Gijubhai Badheka Marg, Bhavnagar, 364-002, Gujarat, INDIA

Dr. Vinod K. Shahi,
Scientist
Electro-Membrane Processes Division

Date: 04/05/2009
No. EMP/VKS/AS-Ph.D.-09

CERTIFICATE BY THE Ph. D. GUIDE

This is to certify that the contents of this thesis entitled "**Selective transport and separation of biomolecules using charged membranes**" is the original resaerch work of **Mrs. Arunima Saxena**, carried out under my guidence in the Electro-Membrane Processes Division at Central Salt & Marine Chemicals Reserach Institute, Bhavnagar-364002.

Further, I hereby certify that the work has not submitted either partly or fully to any other University or Institution for the award of any other Diploma or Degree.

(**Vinod K. Shahi**)

☏: (O) Phone: 091-278-2569445 (Mobile) 091-9925125760; Fax: 091-278-2567562/2566970.
E-mail: vkshahi@csmcri.org; vinodshahi1@yahoo.com

Dedicated

to

My father-in-law

(Late) Sri. Narendraprasad Srivastava

for his honourable support

&

My respected parents

Dr. Ashok Saxena and

Dr. (Mrs.) Vinapani Saxena,

whose motivation and encouragements

have given me the fortune

that I have

today.

Acknowledgements

First and foremost, with utmost regards and sincerity, I take this opportunity to thank to my research guide Dr. Vinod K. Shahi, Scientist, Electro-Membrane Processes Division, Central Salt and Marine Chemicals Research Institute, Bhavnagar, under whose scholarly and infallible guidance this research work was accomplished. His dynamic inspiration, invaluable suggestion and keen interest in this work have always been source of energy and knowledge to me in my endeavor. I have exceedingly benefited from his vast knowledge, lasting enthusiasm, and exceptional personality. Not even professional ground, even in individually, he always edify ethical values in my persona like a well-wisher. He will always present as a blaze of inspiration in my entire life.

It is my profound privilege to verbalize my feelings of gratitude and thanks to Dr. P. K. Ghosh, Director, Central Salt and Marine Chemicals Research Institute and Discipline Coordinator, Electro-membrane processes discipline Dr. G. Ramchandariah, who have always been encouraging like a beacon with their kind words and deeds.

Words prove inadequate when one sets out to thank someone so dedicated to work with vivid incarnation of knowledge, inspiration and sensible discussion during the course of work- Dr. Arvind Kumar, Dr. R. S. Shukla and. Dr. S. K. Thampy.

I would like to express some special words of thanks to Mr. B. S. Makwana, Mrs. B. G. Shah, Mr. M. N. Parmar and Mr. Kalpesh Vyas for their be of assistance.

I feel proud to express my heartiest thanks to my research colleagues like Dr. G. S. Gohil, Dr. Subba Reddy, Dr. Sunil Dave, Mr. Bijay P. Tripathi, Mr. Mahendra Kumar and Mr. Umesh Shelke. I thank to my friends for the great time I had with them Mrs. Ulka Sathapathy, Miss Amrita Ghosh, Ms. Kavita Pathak, Mr. Renjith S. Pillai Mr. Tejvant Singh, Mr. Santosh Agrawal, Mr. Govind Sethia,

Mr. Shailandra Jaiswal and Miss Payal Sanadhya for their timely help and cooperation.

I am duty bound to thank Discipline Coordinator, Analytical Science Discipline, for their kind support for instrumental facilities.

Finance assistance received from Department of Biotechnology, Department of Atomic Energy, Government of India, New Delhi and Council of scientific and Industrial Research (CSIR), Government of India, New Delhi has been gratefully and coordinately acknowledged.

I would like to express my heartfelt thanks to my loving brother (Mr. Arunabha Saxena), sister with her husband (Mrs. Apurava Shrivastava, Mr. Prashant Shrivastava) and respected mother-in-law Mrs. Premlata Srivastava whose continuous back-up and encouragement have been a source of inspiration and the only flame of my success.

With core of my heart, I am thankful to Mrs. Madhulika Shahi, Ms. Bhavya Shahi, Ms. Himanshi Shahi and Mr. Anmol Shahi for sharing plenty of sweet and cheery movements.

I whole heartedly express my thanks to someone for whom words would fall short at present but feelings remain and who, I think do not require words but understand my feelings -my beloved husband Dr. Anjanee Kumar Srivastava. During this period he always induced me to deliver my duties toward my work. His unconditional moral support and continuous motivation in every circumstances, results the successful completion of this work.

Last but not least; I am gratified to the Almighty, who has provided sound health and strength to me for walk on the path of light and success.

ARUNIMA SAXENA

CONTENTS

PREFACE

It is often a requirement in the chemical and biochemical sciences to separate a component from mixture based on its molecular size or charge of individual component. The increasing complexity of chemical and in particular, biochemical, or biological systems has required more sophisticated, selective and efficient technique to resolve/separate individual components. Ultrafiltration is an efficient and scalable bio-separation technique, has been extensively studied in recent years and shown great potential for downstream processing of biotech processes (*e.g.,* protein concentration/fractionation). Although protein separation using ultrafiltration has become a routine and successful operation in biotechnology, fractionation of proteins is still a technological challenge and its effectiveness and efficiency are strongly dependent on operating conditions, such as pH, salt concentration, permeate flux, and system hydrodynamics. Additionally, ultrafiltration is size based membrane separation processes and it is difficult to achieve high selectivity for protein fractionation with similar molecular weights or molecular size of both components.

Electro-driven separation in the porous gels is also commonly used to separate proteins based on their charged nature. Many electrophoretic processes have been developed under various electrical field conditions from constant applied voltages or currents to single- or multiple-dimensional pulsed electrical fields for the separation of biomolecules. In all these afore-mentioned processes only one property of given molecule; either its molecular size or charge and iso-electric point was used to achieve its separation under only one driving force either pressure gradient or electrical gradient. All processes involve only one selectivity parameter (either molecular size or charge) and one driving force, which result less selectivity and membrane throughput. Only few reports are available, in which, nature of charge on the protein, its molecular size, nature and extent of charge on the membrane

matrix was used to increase the selectivity of separation with high membrane throughput under coupled driving forces (pressure and potential gradient).

During the course of my research efforts, we developed different types of hydrophilic modified charged ultrafiltration membrane for studying the transmission of proteins in different environments under simultaneous action of driving forces for achieving high selectivity and maximum membrane throughput because of three selectivity parameters (i.e., charge on the membrane matrix, nature of charge and molecular size of the protein) and dual driving forces.

This thesis is divided into six chapters.

Chapter I: Membrane processes are increasingly reported for various applications in both upstream and downstream technology, such as microfiltration, ultrafiltration, emerging processes as membrane chromatography, high performance tangential flow filtration and electrophoretic membrane contactor. Membrane-based processes are playing critical role in the field of separation/purification of biotechnological products. Membranes became an integral part of biotechnology and improvements in membrane technology are now focused on high resolution of bioproduct. In bioseparation, applications of membrane technologies include protein production/purification, protein–virus separation. This chapter provides an overview of recent developments and published literature in membrane technology, focusing on special characteristics of the membranes and membrane-based processes that are now used for the production and purification of proteins.

Chapter II: This chapter deals with experimental procedures for the electrochemical and physicochemical characterization of charged ultrafilter membrane. Detailed about the methodologies used for the estimation of membrane water uptake, membrane conductivity, ion-exchange capacity, counter-ion transport numbers, permselectivity, electro-osmotic permeability etc as well different techniques, such as FT-IR, NMR, TGA, DMA, SEM, HPLC etc, used for the characterizations of different charged ultrafilter membranes,

were included. Measured properties of these membranes help us to find out suitability of membranes for desired electro-membrane applications. Also, experimental procedure of electro-ultrafiltration and electrochemical membrane reactor for separation/purification of biomolecule/protein under coupled driving forces or electrical forces are described in chapter II.

Chapter III: First part of this chapter deals with functionalization of chitosan either by introducing a phosphonic acid group or by quaternization of existing primary ammonium groups in order to make it a water-soluble material. Functionalized chitosans and poly(vinyl alcohol) (PVA)-based nanoporous charged membranes were prepared in aqueous media and gelated in methanol at 10 ◦C to tailor their pore structure. Elaborate electrochemical and permeation experiments were conducted in order to predict suitability of these membranes for the separation of mono- and bivalent electrolytes based on their hydrated ionic radius. Observations were correlated with equivalent pore radius of the different membranes as estimated by membrane permeability measurements.

Second part of chapter III, concerns with preparation of *N*-methylene phosphonic chitosan-silica (PC-Si) and quaternized chitosan-silica (QC-Si) composite charged ultrafilter membranes by acid catalyzed sol–gel method in the aqueous media and gelated in methanol for tailoring their pore structure. These membranes were employed for developing a simple membrane process for pH sensitive protein fractionation under coupled driving forces (pressure and electric gradient). Protein transmission (selectivity) and membrane throughput across both membranes were studied using binary mixture of protein under different gradients. Relatively high separation value of individual protein from binary mixture and filtrate velocity suggests the practical usefulness of this novel process and biopolymer membranes.

Chapter IV: First part of chapter IV concerns with a simple membrane process for the protein fractionation using sulfonated poly(ether sulfone) ultrafilter membrane under coupled driving forces (pressure and potential difference). Different extent of sulfonation of poly(ether sulfone) was carried

out under controlled conditions and negatively charged membranes with different charge density were prepared under optimum conditions. Transmission of proteins across these membranes were studied under simultaneous action of pressure and electrical gradient at different pH (pH > p*I* or pH < p*I*). Polarity of electrical potential was set in such a way that both type of migrations (pressure or electrical driven) occurred in the same direction. It was observed that transmission of protein can be governed by varying nature of the charge on it (pH), nature and extent of the charge on the membrane matrix, polarity of the applied potential gradient with an ultrafilter membrane of given pore dimensions. In this novel processes, charge on the protein, nature and extent of the charge on the membrane interfaces, polarity of the potential gradient all are governing the transport of given protein across the membrane, which resulted high selectivity and membrane throughput under coupled driving forces.

In the second part of chapter IV, organic-inorganic hybrid charged membranes by sol-gel process were developed in aqueous media and gelated in non-aqueous media with desired pore dimensions and charge density at the membrane interfaces. These membranes were used for developing a simple membrane process for protein separation/fractionation by iso-electric focusing of one component under coupled driving forces (pressure and electric gradient). Protein transmission (selectivity) and membrane throughput (filtration speed) across both membranes were studied using their binary mixture using varying gradients and pH of solution. Also, no appreciable membrane fouling was observed due to cleverly application of electric gradient and back flushing of foulants protein from the membrane interface and indirectly cleaning. Due to coupling of driving forces high filtration speed (flux) in combination with high selectivity was achieved, which is urgent for efficient down stream processing and indicated the usefulness of developed process.

Chapter V: A simple membrane process for the protein fractionation has been developed using acidic functionalized (sulphonated, carboxyleted

and phosphorylated) ultrafilter membranes, based on the interpolymer of poly(vinyl chloride) (PVC) and styrene–divinyl benzene (DVB) copolymer, under coupled driving forces (pressure and potential difference). Ionic functional groups incorporated into polymer have decided effect on physical properties of the ultrafilter membrane. Protein transmission (selectivity) and membrane throughput across both membranes were studied using binary mixture of protein under different gradients at different pH. It was observed that transmission of protein can be governed by varying nature of the charge on it (pH), nature and extent of the charge on the membrane matrix, polarity of the applied potential gradient with an ultrafilter membrane of given pore dimensions. In this novel processes, charge on the protein, nature and extent of the charge on the membrane interfaces, polarity of the potential gradient all are governing the transport of given protein across the membrane, which resulted high selectivity and membrane throughput under coupled driving forces.

Chapter VI: In this chapter an electrochemical membrane reactor based on an in-house-prepared anion-exchange membrane was reported to achieve single-step separation and acidification (ion substitution) of lactates to lactic acid. The physicochemical and electrochemical properties of the anion-exchange membrane under standard and operating conditions reveal its suitability for the proposed reactor. Experiments using synthetic solutions of sodium and ammonium lactates of different concentrations were carried out to study the feasibility of the process. This process was completely optimized in terms of operating conditions such as the initial concentration of lactate in the catholyte, the applied potential gradient, the lactate flux, the recovery, the energy consumption, and the current efficiency. It was observed that ammonium lactate can be more efficiently and more rapidly separated and acidified than sodium lactate. A representative experiment with fermentation broth was also conducted for the separation and acidification of sodium lactate in the presence of polysaccharides, carbohydrates, salts, and coloring materials. It was concluded that the electrochemical membrane

reactor is an efficient and simple device for the recovery and acidification of lactates from uncharged molecules such as polysaccharides, carbohydrates, and other coloring agents as these molecules are not able to cross the anion-exchange membrane in a single-step separation for producing lactic acid.

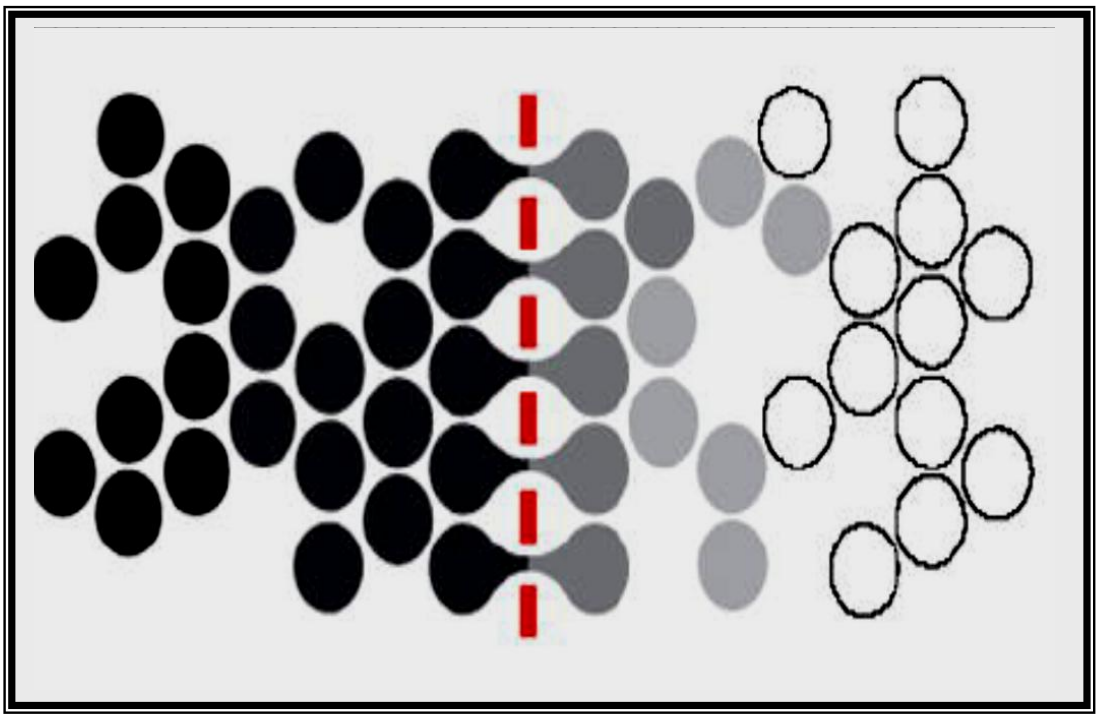

CHAPTER I

INTRODUCTION

In simpler terms, a membrane can be described as an interphase, usually heterogeneous, acting as a barrier to the flow of molecular and ionic species present in the liquids and/or vapours contacting the two surfaces. During the last three decades, membranes attracted the attention of chemists, chemical and biotechnical engineers due to their unique separation principle, i.e. the selective transport and efficient separation in compare with other unit operations. Separations with membranes do not require additives, and they can be performed isothermally at low temperatures with less energy consumption compared to other thermal separation processes. Due to the unique properties of membranes, up scaling and downscaling of membrane separation processes as well as their integration into other separation or reaction processes are easy. The success attending any membranes based unit operation, such as demineralization, desalination/purification of water, bio-separation of fermentation products, milk fractionation, decaidification of fruit juices, etc., depends on the availability of the suitable membranes. Recently, membrane based processes gained importance in biotechnology due to their ability for size and/or charge based protein separation with high purity and throughput [1-6]. Most protein based products needs to be purified before they can be used. They need for purification is due to the following: (i) requirement of high purity; (ii) concentration enrichment; (iii) removal of specific impurities (e.g. toxins from therapeutic products); (iv) prevention of catalysis other than the type desired (as with enzymes); (v) Prevention of catalysis poisoning (as with enzymes); (vi) recommended product specifications; (vii) enhancement protein stability; (viii) reduction of protein denaturation. Over the last two decades, new membranes modules and systems have been developed specially to meet the requirements of the biotechnology industries.

Membranes have traditionally been used for size-based separations with high-throughput but relatively low-resolution requirements. These uses include micro-filtration (MF), clarification, sterile filtration and ultrafiltration (UF) for protein concentration and buffer exchange. Current research and

development efforts are directed toward drastic improvements in selectivity while maintaining the inherent high-throughput characteristics of membranes. Although, essentially all membrane processes are used for bio-separation, but greatest interests have been shown in the pressure driven technologies such as MF or UF (Fig. 1.1.1). Recently, electric or ultrasonic fields were imposed simultaneously to increase throughput and membrane selectivity as well as reducing membrane fouling which is a common phenomenon in pressure driven membrane separation technologies. During last two decades, membrane technologies were frequently used for the size or charge based protein separation/fractionation. MF membranes were tailored to retain cells and cells debris while allowing proteins and smaller molecules to pass into filtrate. UF membranes were designed to provide high retention

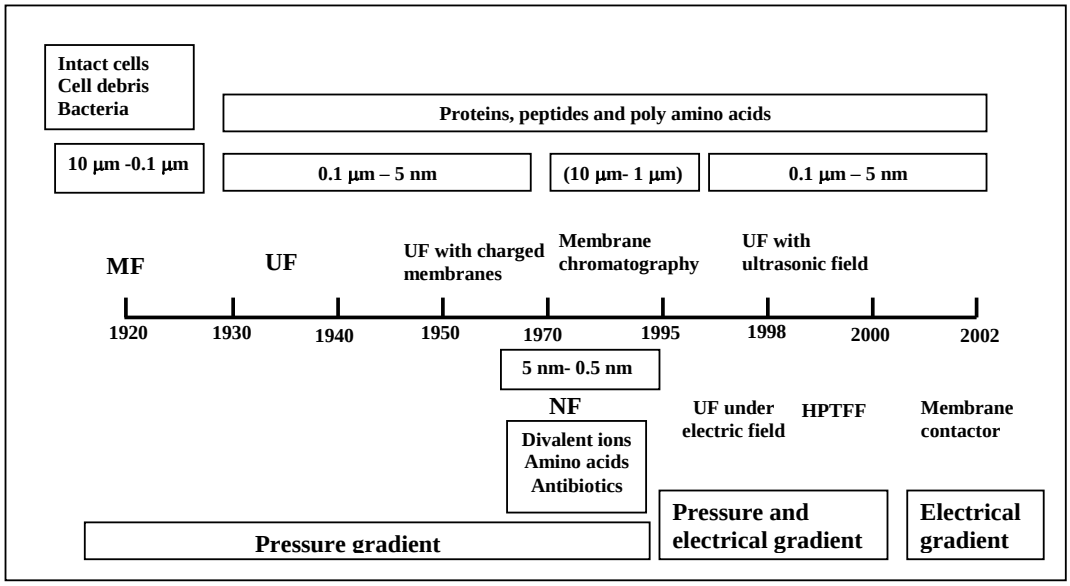

Figure 1.1.1. Milestones in the development of membrane technologies for protein separation/ purification.

of proteins and other macromolecules. These membrane processes involve the filtration of biological solutions containing proteins, peptides, amino acids, salts and other compounds like organic acids, sugars, vitamins, etc. Some examples include concentration of whey proteins during the production of a variety of dairy products, filtration of wine or the purification of downstream solutions in biotechnology [7]. Nanofiltration (NF) was defined as

a process that separates solvent, monovalent salts, small organics from divalent ions and larger species. Conventional UF is limited to separation of solutes that differ in 10 fold in size. High-performance tangential flow filtration (HPTFF) is a new technology for protein and peptide purification. HPTFF is a two dimensional purification method that exploits differences in both size and charge characteristics of protein/biomolecules. Thus this methodology can be used to separate protein with same molecular weight. During recent years, electrophoretic membrane contactor process was also developed for size and charge based protein separations. Membrane chromatography is used as an alternative to conventional resin-based chromatography columns for a large range of chromatographic purification schemes, including ion-exchange, hydrophobic, reversed-phase, and affinity chromatography. Purification/separation procedures using membrane chromatography have been reported for a wide variety of biological compounds such as proteins, DNA and viruses.

The objective of this chapter is to provide an overview of recent development in membrane science and technologies, focusing on the special characteristics of membranes and processes that are now used in the production and purification of recombinant protein products.

1.1. Pressure-driven membrane technologies for separation/purification of proteins

Although essentially all membrane processes are used for protein separation/purification, the greatest interest has been in the application of the pressure-driven processes of MF, UF and NF. MF is now established unit operation in environmental engineering, biotechnology, life sciences and medicine as well as several other areas [2,8-12]. MF membranes are especially well suited for the separation of fine particles in the size range of 0.1–10.0 μm. While UF membranes with 1-100 nm pore size were designed to provide high retention of proteins and other macromolecules [4]. The UF process has become particularly important for concentrating proteinaceous

solutions. Examples of commercial membrane processes involved the filtration of protein solutions in the presence of electrolytes, concentration of whey proteins in the dairy industry, protein recovery from blood plasma, protein concentration in downstream processing, etc [13]. NF is another promising technology that separates solutes based on solute charge and size. Several research papers published on the application of NF for peptide fractionation in model systems of amino acids and peptides, which was based on a molecular sieve effect and/or on a charge effect depending on the membrane type and the feed phase composition [14-16].

1.1.1. Proteins separation/purification by MF

MF is widely used for the separation, purification and clarifying of protein-containing solutions, e.g. for the recovery of extra cellular proteins produced via fermentation and for the removal of bacteria and viruses in the final formulation of therapeutic proteins. In all these processes the macromolecules and proteins involved are much smaller in size than the pores of the MF membrane and should not normally be retained by the membranes [17,18]. The basic operational concept of MF leads to a solute concentration that is higher and close to the membrane surface than it is in the bulk feed stream [19]. This is so-called concentration polarization, which causes due to diffusive flow of solute back to the bulk feed. That is the reason for the process permeates flux falling below the flux of clean fluid through the membrane. After a given period steady state conditions will be achieved. The effect of concentration polarization can be very served in MF applications because the fluxes are high and the mass transfer coefficients are low as a result of the low diffusion coefficients of macromolecular solutes and of small particulates, colloids and emulsions. Module configuration of MF include hollow fibber, tubular, flat plate, spiral wound and rotating devices. The two standard modes of operation are dead-end and cross-flow configurations are shown in Fig. 1.1.2. In the cross-flow mode, the fluid to be filtered flows parallel to the membrane surface and permeates through the membrane due

to pressure difference. The cross-flow reduces the formation of the filter cake to keep it at a low level.

Much effort is still being devoted to developing new membrane modules with improved mass-transfer characteristics for UF and MF processes. This includes rotating disk filters [20, 21] cylindrical Taylor vortex devices [22], conically shaped rotors [23], and helical coiled Dean vortex systems [24,25]. Dean vortex devices have very high mass-transfer rates, owing to the presence of centrifugal flow instabilities. These devices show significant increases in protein transmission and capacity, although fouling remains a problem in many applications. An alternative approach was used for high frequency back pulsing to clean the membrane surface. High frequency back pulsing was shown to improve flux, reduce fouling and increase protein transmission in the purification of conjugated vaccine products [27].

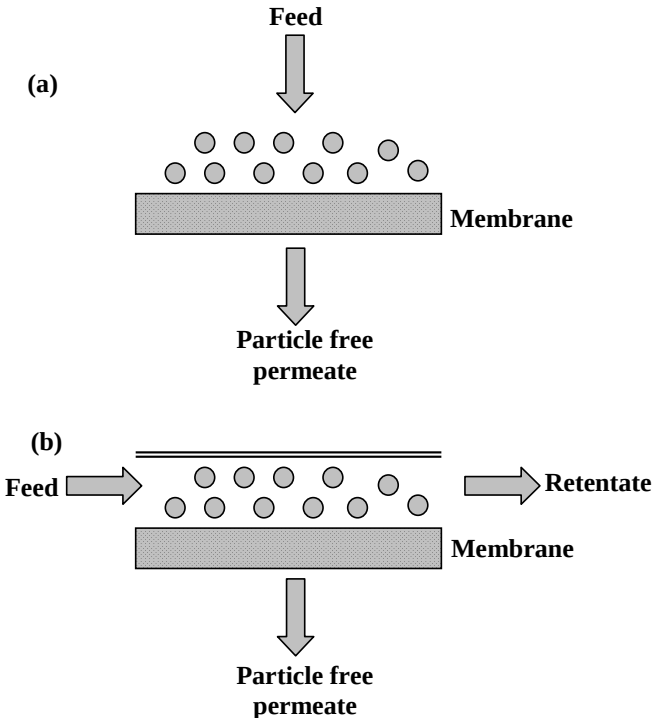

Figure 1.1.2. Comparison between: (a) dead-end, (b) cross-flow configuration.

MF is commonly used to recover macromolecules and retain suspended colloidal particles, and are being integrated into both up-stream and down-stream processes [8,9]. A large range of MF applications is reported to pre-treatment steps, removal of small molecules from bigger protein molecules, clarify suspensions for cell harvesting, and sterilize liquids to remove viruses and bacteria [4,28]. Other membrane processes include

membrane bioreactors, where enzymes, micro-organisms or antibodies were suspended in solutions and compartmentalized by a membrane in a reaction vessel or immobilized within the membrane matrix itself. The sterile filtration (bacterial removal) was achieved in dead-end configuration using 0.2 μm pore size membranes have been validated for the absolute removal of *Brevundimonas diminuta* [29]. However, such sterilizing filters can pass very small micro-organisms under some process conditions. Therefore, some users employ 0.1 μm pore size membranes to provide enhanced sterility assurance in pharmaceutical process [30]. Membrane manufacturers are developing membrane filters with increasing resolution for virus and protein separation [10]. This was of significant importance to the biotechnology industry because incidents of parvovirus are particularly difficult to remove, as they are both small (about 20 nm diameters) and highly resistant to many thermal and chemical methods of inactivation. Continues improvements in understanding the effects of solution environment on molecules, particles retention, and fouling [31] have also led to further enhancements in UF and MF performances. For example, numbers of recent studies have demonstrated that it is possible to control the rate of protein transport through membranes by adjusting the solution pH or the ionic strength [32-34]. The process has to be operated at the iso-electric point (p*I*) of the transmitted protein and far away from the p*I* of the retained protein. To enhance the separation, the ionic strength was kept low so that the thickness of the diffuse double layer of the charged solute was pronounced, leading to high retention, whereas the uncharged solute readily permeated the membrane.

Poly(ethersulfone) (PES) becomes a kind of “standard” material for many membrane manufacturers, because it is reliably available in well-defined qualities and (almost) unlimited quantities [35,36]. PES based MF membranes were employed for biological applications like selective permeation, protein recognition/purification, controlled release, isolation of soya proteins etc. [37,38]. They have a wide range of applications in the food

industry, including processed meat, nutritional beverages, infant formulas, and dairy product replacements. Critical functional properties necessary in protein ingredients include solubility, water and fat absorption, emulsion stabilization, whip ability, gelation, foaming and good organoleptic properties [39,40]. Many physical, chemical and enzymatic modifications have been used to expand the range of functional properties in soy proteins [41-43]. These modifications can be costly in terms of the process itself as well as losing some other properties at the expense of improving the targeted ones. Chemical modification also posed the problem of removing any unreacted reagents from the final product. Soy protein fractionation using chemical methods have been reported [44].

1.1.1.1. Advanced MF under electric field

Electrically enhanced membrane filtration (EMF) is an advanced technique, which consists in superimposing an electrical field to a conventional membrane filtration unit. In EMF, the electrical field acts as an additional driving force to the trans-membrane pressure. Accordingly, differences in protein electrophoretic mobility are coupled to the membrane sieving effect to enhance the selectivity of membrane fractionation in EMF. It has been mainly used as a strategy to improve protein solutions permeation flux by preventing concentration polarization and membrane fouling [45-48]. Furthermore, selectivity enhancement for biomolecules separation (amino acids and peptides) was recently obtained using EMF [49-52]. However, only few studies reported the effect of EMF on complex protein solutions separation selectivity [53].

The purification and separation of protein has been widely used in electro-dialysis (ED), UF and MF when comparing studies on the use of conventional membranes for different protein separation [54,55]. The newly developed techniques superimposed additional forces such as pressured hydraulic force. Recently dynamic filtration has represented a further possibility for reducing the surface layer on the membrane of rotating disc filtration [55,56]. However, the principle disadvantage of this technique is

that it cannot be used in high concentrations of protein. Another superimposed force, that is, an electric field, was induced as a force on charged protein in order to reduce the surface layer of a membrane. Park et al. studied the purification of protein through membrane process under the influence of an electric field and explained how filtration time was reduced by the use of an electric field. In this case, concentration of protein in the membrane process in the presence of an electric field was reduced by over 300% in comparison with the membrane process without an electric field. For this investigation, polyvinylidene fluoride (PVDF) membrane and hemoglobin as a protein was used. It was observed that an electric field is a superimposed force which, induced as a force on charged protein to reduce the surface layer formation at the membrane interface and that led the development of EMF [56-59].

Pouliot et al. studied the effect of applying an external electrical field during lactoferrin (LF) and whey protein solutions by MF under influence of electrical field strength (0–3333 V m^{-1}) and polarity on the permeation flux and protein transmission through micro-filter membrane with flat-sheet module [60]. In this case, electrical field had an important impact on protein transmission. Selectivity enhancements were obtained, particularly when the cathode was on the retentate side. In that configuration (3333 V m^{-1}), the separation factors obtained between LF and the two main whey proteins β-LG and α-LA were, respectively, 3.0 and 9.1. PVDF membrane with 0.5 μm of pore size diameters was used for this study.

1.1.2. Proteins separation by UF

Protein fractionation is rapidly becoming more selective through improvements in membrane and module design. Compared to chromatographic methods, membrane separation techniques offer advantages of lower cost and ease to scale-up for commercial production. However, the lack of membrane selectivity and its fouling due to protein absorption during filtration has severely restricted UF applications [61]. Now, UF has been widely used as preferred method for protein concentration and

buffer exchange, and replaced size-exclusion chromatography in these applications [62].

UF membranes, based on variety of synthetic polymers, have high thermal stability, chemical resistivity, and restricted the use of fairly harsh cleaning chemicals [4,63]. The choice of membrane was usually guided by its molecular weight cut-off (MWCO), which is defined as the equivalent molecular weight of the smallest protein that would exhibit above 90% rejection. Although this choice is arbitrary, but it has been adopted by most of the UF membrane user community. However, the experimental conditions and systems used to evaluate 90% MWCO have not been standardized [63]. Hollow fiber, flat-sheet cassettes, spiral wound cartridges, tubular modules, and enhanced mass transfer devices have been developed for UF. These modules provide physical separation of the retentate and filtrate streams, mechanical support for the membrane (if needed), high membrane packing densities (membrane area per device volume), easy access for cleaning and replacement, and good mass transfer characteristics. Spiral wound modules are sensitive for plugging/fouling, and are more difficult to clean. However, they have more limited range of scalability than hollow fiber modules or flat-sheet cassettes. Rotating and Dean Vortex systems have been also developed for UF. These devices showed high mass transfer coefficients but lower packing densities [64]. Additionally, their scale-up (or down) is difficult due to changes in hydrodynamic conditions [65].

PES is widely used UF membrane material, because of its high rigidity, creep resistance, good thermal and dimensional stabilities [66]. Ghosh et al. studied purification of lysozyme (LYS) from chicken egg white using hollow-fiber PES UF membrane (30 kDa MWCO) [67]. UF of fermented cheese whey broth was also studied using a lab scale cross-flow membrane system with PES membranes (5, 20 kDa MWCO) [68]. Separation of β-LG from whey protein was achieved by its fractionation using two-stage UF with PES membrane (30 and 10 kDa MWCO) in stirred rotating disk module followed by ion-exchange membrane chromatography [69]. Other types of polymeric

UF membranes such as polyacrylonitrile membrane [70,71], regenerated cellulose membrane [72], cellulose acetate membrane [73,74] and ceramic membranes [75] etc., were extensively studied for the separation of proteins. A schematic diagram of UF membrane set-up used for protein separation/purifications is shown in Fig. 1.1.3. Fractionation of dairy wastewater into lactose-enriched and protein-enriched streams using UF membrane technique was also studied. Three regenerated cellulose membranes of 3, 5 and 10 kDa MWCO were used to determine the efficiency of the process. The performance was determined under various processing conditions that include the operating temperature and trans-membrane pressure across and the concentration of lactose in the feed solution [76].

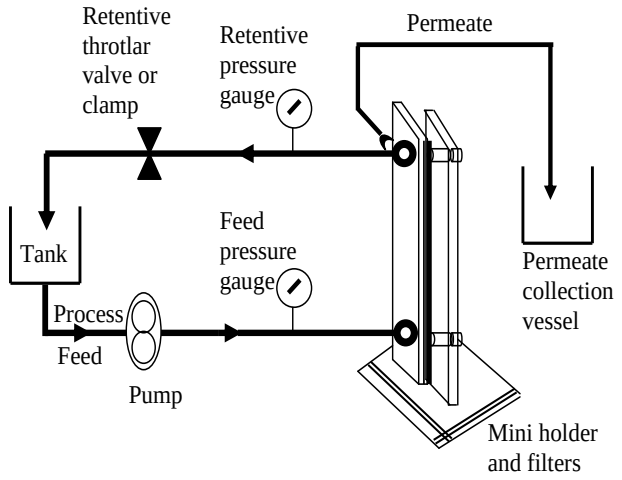

Figure 1.1.3. A schematic diagram for the ultrafiltration membrane set-up

1.1.3. Advanced UF techniques for proteins separations

Recently UF technique was modified for developing advanced technique with low membrane fouling, high selectivity and permeate flux in order the meet the industrial requirements for protein separations.

1.1.3.1. Protein separation using charged UF membranes

Charged UF membrane separation process involved both size and charge based exclusion rather than simply size based separation of protein molecules, as in the case of UF. A positively or negatively charged UF membrane with definite pore structure and MWCO was generally used for selective protein separation because of high interactions between

transporting species and membrane surface with extremely low fouling due to electro-static repulsion between membrane surface and foulants. pH and ionic strength of the feed solution were adjusted to control the charge on the proteins and attenuate charge shielding from reduction of the double layer. Although protein concentration by UF has become a routine and successful operation in biotechnology, fractionation of proteins using UF is still a technological challenge and its effectiveness and efficiency are strongly dependent on operating parameters such as pH, salt concentration, permeate flux, and system hydrodynamics. Additionally, UF is size based separation processes and it is difficult to achieve high selectivity with high throughput. Zydney and co-workers have studied electrostatic interactions between charged proteins and charged membranes [77-81] and demonstrated that pH values and ionic strengths have profound effects on protein separation. This is promising technology for separation of proteins differing in molecular mass by at least factor of 10, with high resolution by UF with charged membranes [82]. In this case, charged membranes were used for the fractionation of proteins at their iso-electric point (IEP) in binary or ternary solution. Nystrom et al. studied UF with charged membranes and separated enzymes from fermentation broth and myoglobin from bovine serum albumin (BSA) [83,84]. High selectivity was achieved for the smaller protein at its IEP. Zydney and co-workers also studied electrostatic interactions between charged proteins and charged membranes and demonstrated that pH values and ionic strengths have profound effects on protein separation [80,81,85].

Fractionation of a protein mixture (myoglobin and cytochrome C) was also attempted with positively (sulphonated) and negatively charged (aminated with quaternary group) PES based UF membranes near to isoelectric pH of one of the proteins. High transmission of the neutral protein and strong electrostatic repulsion of the charged protein with the membrane matrix was observed. This opened up exciting new opportunities for exploiting electrostatic interactions in the optimization of membrane systems for protein purification [86]. Cellulosic UF membranes with positive charges

were also used to separate different monoclonal antibody (mAb) therapeutics from Chinese hamster ovary cell protein impurities [87]. Excellent work on developing a theoretical understanding of charged UF membrane separations was carried out by Zydney and collaborators [8,88]. More than 900-fold purification and 94% yield of BSA from an antigen binding fragment (FAB) of recombinant DNA antibody using a negatively charged membrane to obtain very strong retention of the negatively charged BSA [89].

Suen et al. studied separation of BSA, LYS and γ-globulin using plate-and-frame modules with charged UF membranes made of with either cellulose phosphate or diethylaminoethyl cellulose [90]. In this single plate-and-frame module, operating conditions were greatly influenced the separation performance. At the elution stage, a better performance was achieved by using the cross-flow mode. Other operating conditions such as the number of membranes in a stack, the pH value at adsorption, and the mixed mode in the membrane stack also affected the separation performance. Cation-exchange membranes (cellulose phosphate, thickness 0.23 mm) and anion exchange membranes (diethylaminoethyl cellulose, thickness 0.2 mm) were also found to be suitable for the separation of targeted protein with better recovery [90]. Fractionation of LYS and chicken egg white by UF were also studied using commercially available negatively charged membranes made of by regenerated cellulose or PES with 30 kDa MWCO. In optimized conditions, 99% LYS transmission with 2400 folds selectivity was obtained [91]. Effect of solution pH on the transmission of ovalbumin, myoglobin, and lysozyme in a rotating (Taylor vortex) module was also studied [92]. Very large reduction in protein transmission at pH < p*I* was attributed to the significant adsorption of the positively charged proteins on the negatively charged polyacrylonitrile (PAN) membrane under optimized conditions [70,71,92].

UF was traditionally performed using polymeric membranes such as polyethersulfone, polysulfone, cellulose acetate, and regenerated cellulose. However, these polymeric membranes are susceptible to chemical degradation by strong alkali or acid cleaning solutions leading to a significant

reduction in membrane life. In addition, some polymeric membranes have limited mechanical stability, leading to a reduction in permeability at high pressures and possible membrane failure, particularly in systems employing rapid high-pressure back pulsing. These membranes are also incompatible with steam sterilization, potentially increasing the overall bio-burden in subsequent processing steps [93,94]. These limitations have motivated the development of a variety of inorganic UF membranes with greatly enhanced chemical, thermal, and mechanical stability. Zydney et al. [93] synthesized nanoporous carbon UF membrane from a polymeric precursor mixture of poly (ethylene glycol) (PEG) and poly (furfural alcohol) (PFA). Performance characteristics for the nanoporous carbon were only slightly below those of commercial polymeric UF membranes. Additionally these membranes were stable even after prolonged exposure to 3N NaOH solutions. Using this membrane about 0.62 sieving coefficient for BSA was achieved. UF separation of lysozyme and BSA was also studied using both zirconia membrane and zirconia modified with a positively charged polymer (polyvinyl imidazole) at different ionic strengths. Best selectivity (transmission of lysozyme/transmission of BSA) was obtained at low ionic strength with both membranes [95,96]. Chaufera et al. studied inorganic membranes chemically modified by a polyethyleneimine coating bearing positive charges for fractionation of negatively charged proteins at pH 7, α-LA (target protein) and β-LG (contaminant protein) from whey protein in order to reach a high selectivity of α-LA in the permeate [97]. Variation of retention of a single protein, either positively charged lysozyme or negatively charged BSA in a buffer solution at pH 7 was investigated by varying the ionic strength with unmodified or chemically modified zirconia UF membranes. Chemical modification was obtained by coating polyvinylimidazole, amine group reacted further with bis-epoxiranes in order to have, both, a partly quaternized amine group and a pH-stable network on the membrane surface [96].

1.1.3.2. UF in the presence of electric field (Electro-ultrafiltration)

The use of electric field in UF goes back to the first study carried out by Bechhold by imposing electric field in UF and utilized a combination of electro-osmosis and electrophoresis to purify colloids in an apparatus he called an 'electro-ultrafiltration' (EUF) [98]. EUF is an effective method to decrease gel layer formation on the membrane surface and to increase the filtration flux, owing to electro-kinetic phenomena such as electrophoresis and electro-osmosis [99,100-105]. Basic principle of EUF is presented in Fig. 1.1.4. This process aroused from a combination of a number of mechanisms, including ion association, ion adsorption or ion dissolution. The electrochemical properties of the membrane surface and the dispersed materials or solutes can have a significant influence on the nature and magnitude of the interactions between the membrane and the substances being used and their separation characteristics. The utilization of such properties by the application of external electric fields improved substantially the membrane performance. The conventional electro-filtration can also be the effective means of reducing both the concentration polarization and membrane deposition but it has some drawbacks which make this method uneconomical and difficult to handle for certain processes [106]. The electric field imposed an electrophoretic effect on the charged molecules dragging them away from the membrane surface. The concentration polarization layer

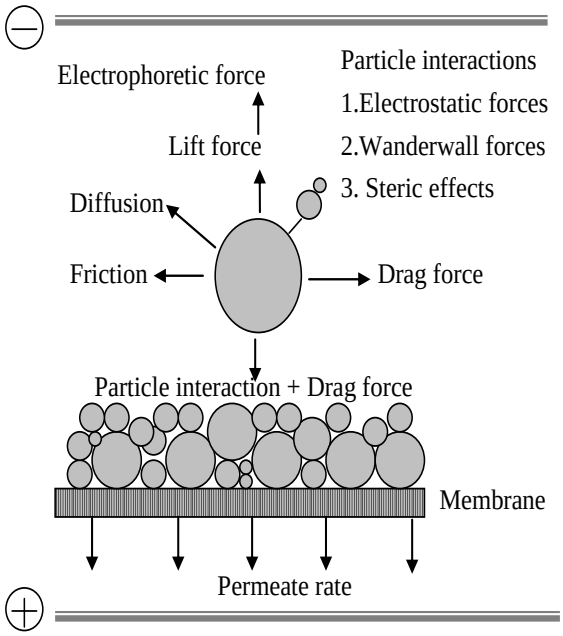

Figure 1.1.4. Principle of electro-ultrafiltration

is thereby reduced and the flux increases. The solvent flow through the membrane might also be enhanced by the electro-osmotic effect; but this effect is considered secondary [107,108].

Generally, two electrodes were positioned, on either side parallel to the UF membrane, used to apply the electric gradient. The field vector perpendicular to the membrane provokes a displacement of colloid species towards the electrode with the opposite sign. This phenomenon is called electrophoresis. Several reports are available concerning to use EUF for separation or concentration of protenecious solutions [48,53,109-116]. In most cases, the electric field was applied by two parallel electrode plates. The simplest configuration is to insert the electrodes into the suspension and permeate channels. This construction has two major disadvantages: i. alteration of the product pH by electrolysis products; and ii. deposition of the particles at the electrodes [107].

When an electric field is applied to the separator, permeate is either concentrated or diluted by differences in the charge of solute and the direction of the electric potential gradient. The accumulation of the solutes on the membrane surface is limited by the imposed electrophoretic force. In addition, the filtration rate through the filter cake is dramatically enhanced due to electro-osmosis as a secondary electro-kinetic phenomenon. This method is best suited for the separation of protein since its surface charge changes according to the solution pH [117-122]. As biological products like proteins and peptides are sensitive to shear stress and temperature, the coupled effects of electric field and pressure served as an additional driving force for the separation, which is an interesting way to improve the membrane permeates flux with out increasing the shear stress [99,123,124]. Since proteins carry a net electrical charge, an electrical field may be used to reduce the influence of polarized layer. By applying a suitable external dc electric field, the protein molecules were transmitted through the membrane due to the electrostatic attraction and concentration polarization was reduced [45]. EUF was also studied as a membrane cleaning procedure, in which

electrical fields attracted the particles with opposite charge from the membrane surface, and initial permeate flux was restored by eliminating fouling up to large extent [125,126]. It was observed that as the voltage increased, the cake layers deposited on the membrane surface became thinner. Eventually when the critical voltage, at which the foulants were stationary, reached no particle deposition on the membrane surface was observed. Applying at the critical voltage has greatly mitigated membrane fouling problems and prolonged the frequency of its cleaning [109].

Bier et al. reported the membrane technique using an electric field to dewater colloidal suspensions [127]. In this case the electric field served as an additional driving force for the separation. Numerous research paper published, in which electrical fields have also been used to control membrane fouling and filter cake formation, enhance the filtration rate and increases the separation efficiency of the UF of proteins by altering the structure of the protein gel layer formed on the UF membrane surface [128-131]. The use of electric fields in the protein UF process has demonstrated that the initial permeate flux can be restored almost instantaneously by means of an exponential curve [136]. The permeability of protein was proportional to hydraulic pressure with an electric field, indicating that the protein quickly is oriented in the field direction through the membrane pores [137].

Effects of direct current electric field on the transient and dynamically balanced filtration rate in dead-end inclined and downward UF were explored under constant pressure using protein (BSA) solution. It was found that, in downward EUF, the dynamically balanced filtration rate was directly proportional to the electric field strength. Also, in inclined EUF, filtration rate increased (30-50%) with field strength above the critical electric field strength [45,47,138]. A three-fold flux increase was also reported by Oussedik et al. for BSA filtration by EUF [47]. EUF was used to improve the filtration rate and increase the selectivity while separating, e.g. amino acids and peptides [49]. During EUF the impact of operating parameters on fouling including flux, velocity, trans-membrane pressure and electric field were also studied

with BSA in the concentration range of 1-5 g/1 and demonstrated a 25-50% increase of the flux permeate compared to the case of without any electric field [139]. Kappler et al. used different UF membranes in a two-sided electro-filter apparatus with flushed electrodes brought significant enhancement of the protein fractionation process. Due to electrophoretic effects, the filtration velocity could be kept on a very high level for a long time, furthermore, the selectivity of a binary separation process carried out exemplarily for BSA and lysozyme could be greatly increased in the current case up to a value of more than 800. Thus, the new two-sided electro-UF technique achieves both high product purity and short separation times [140]. Saxena and Shahi prepared negatively charged UF membranes by different degree of sulfonation of PES [141]. These membranes showed different extent of charge density on the membrane matrix. Adsorption study at various pH of the protein solution was performed and it was observed that protein binding capacity of the membranes was strongly dependent on the pH of the protein solution as well extent of charge on the membrane matrix. Using these membrane transmission characteristics of BSA and LYS were investigated under single or coupled driving forces *i.e.* pressure difference and applied potential gradient. It was found that membrane flux and observed protein transmission through the membrane increased under the simultaneous action of driving forces and pH of the protein solution (*i.e.* their iso-electric points), and extent of the charge on the membrane matrix have strong influence on the observed transmission of the protein. Schematic diagram for the mode of UF experiments were conducted without any applied potential gradient is presented in Fig. 1.1.5(A). While Fig. 1.1.5(B) represents ultrafiltartion experiment with applied potential gradient and electrical polarity. Polarity of the applied potential was fixed so that electrode in the feed side became anode and towards permeate side became cathode so that only positively charged BSA (BSA^{+}) are facilitated to cross through the negatively charged membrane under the influence of coupled driving forces (pressure and potential difference). In other cases negatively charged BSA

(BSA$^-$) or zwitterions BSA (BSA^0) are suppose to be exhibit very low transmission under given polarity and charged nature of the membrane. It was concluded that

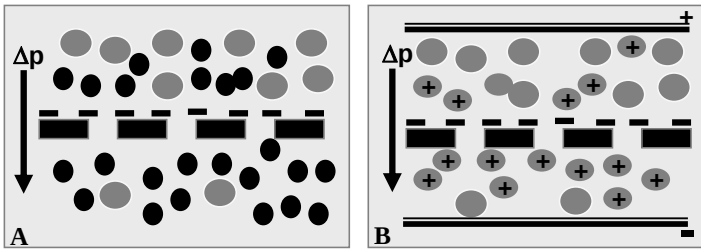

Figure 1.1.5. Schematic presentation of: (A) ultrafiltration; and (B) ultrafiltration under applied potential gradient.

transmission of protein can be governed by varying nature of the charge on it (pH), nature and extent of the charge on the membrane matrix, polarity of the applied potential gradient with an ultrafilter membrane of given pore dimension. Coupling of the driving forces always results more membrane throughput with relatively high selectivity. Based upon these results, it is possible to achieve selective and efficient transport/separation of BSA-LYS at pH 4.8. Furthermore, this study established the basis for the development of new process and hydrophilic modified ultrafilter membrane for the fractionation of proteins depending on their iso-electric points. In this processes, charge on the protein, nature and extent of the charge on the membrane interfaces, polarity of the potential gradient all are governing the transport of given protein across the membrane, which will result high selectivity and membrane throughput. As spin off charged nature of the membrane matrix and bipolar electrical environment avoids the fouling of the membrane, which was the common phenomenon for the protein fractionation by UF membrane.

The conventional EUF can be effective means of reducing both the concentration polarization and membrane deposition but it has some drawbacks which make this method uneconomical and difficult to handle for certain processes. The disadvantages of this process are: (a) limitation of the process stream for relatively low conductivity of feed stream, (b) a high-energy requirement, (c) substantial heat production, and (d) changes in the process feed due to reaction at the electrode. For this reason, attention has been

directed to the use of pulsed electric fields [133,134]. This process has the same mechanism at work in preventing fouling as conventional electro-filtration. The only difference is that in pulsed electric fields, the electric field can be applied at certain intervals, which can be adjusted to suit the process. In some cases, this process can enhance the flux better than the conventional electro-filtration [135]. Applying the electric pulse on dead-end filtration has also been reported to reduce the rate of fouling [142-145]. A pulsed electric field consumes less energy than a constant field, and for some systems a pulsed electric field results in an even higher flux compared to a constant field [47,146]. In order to minimize energy consumption, several researchers have proposed pulsed electric field rather than steady fashion [147,148]. Electrophoretic membrane cleaning was carried using electric pulses with process variables are the strength of the applied voltage, pulse interval and pulse duration. They observed it that the application of the electric pulse in the cleaning membrane surface was an effective means in reducing fouling and restoring high permeation rate. Application of electric pulses across the membrane resulted in an increase in permeation rate due to the removal of deposited materials on the membrane surface. It was identified from the data, the most suitable and effective conditions to give the highest average filtration flux can be attained by applying higher voltage, shorter pulse interval and longer pulse duration [149-151]. Side view of the dead-end EUF module is a shown in Fig. 1.1.6. Bowen et al. used electric pulsed to clean the cross flow filtration; they found out that applying longer pulse duration might have changed the properties of

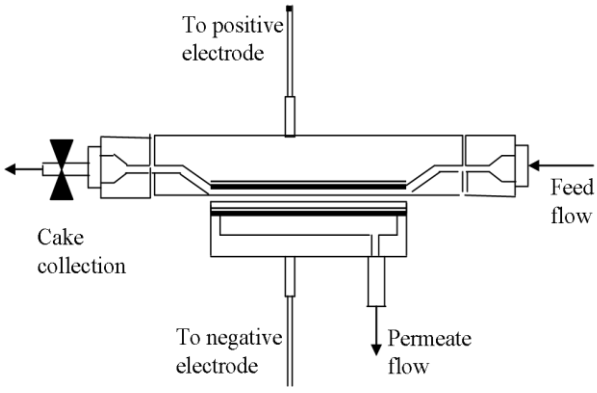

Figure 1.1.6. Side view of the dead-end EUF module

filter cake [144]. Thus longer pulse duration seemed to produce an increase in resistance to fluid flow that caused the average flux to decrease [145].

1.1.3.3. UF in the presence of ultrasonic field

One of the critical issues in the performance of protein UF processes is the declination of permeates flux with respect to time that occurs as a result of both concentration polarization and membrane fouling. Concentration polarization occurs when a concentration gradient of the retained components is formed on or near the membrane surface. This phenomenon is predominantly a function of membrane hydrodynamics. Conversely, fouling is the result of accumulation of proteins drawn toward filtering surface by convective flow of filtrate through the membrane [152,153]. Various methods have been used to reduce the negative effects of concentration polarization and fouling for enhance the permeate flux and membrane separation efficiency. Ultrasonic physical effects and sonochemical effects are also used in membrane technology in order to clean surfaces to prevent formation of filter cake and to enhance filtration and separation rates [154,155]. Cleaning procedures are significantly enhanced by cavitation and acoustic streaming induced by ultrasonic waves. In the field of UF number of researchers have also demonstrated the effective use of ultrasound (US) to enhance the permeate flux [156-165]. Ultrasonic techniques provide an alternative and attractive method for membrane fouling control. Ultrasound generates acoustic streaming and cavitation bubbles in a liquid medium (e.g., water). Cavitation bubbles causes microstreaming, microstreamers, microjets, and shock waves [159]. Ultrasound is the sonic wave at frequencies ranging from 16 kHz to 1019 Hz. When the ultrasonic energy at high power is applied to a liquid, capitation takes place, which means the formation, growth, and sudden collapse of bubbles in liquids. The acoustic streaming and shear forces imposed by cavitations bubbles reduce the fouling on membrane surface. This leads to an increase of permeate flux [166].

Several mechanisms were proposed to particle release from a particle-fouled surface as a result of ultrasound illustrated in Fig. 1.1.7 [167-169]. Acoustic streaming does not require the collapse of cavitation bubbles and it was defined as the absorption of acoustic energy resulting in fluid flow [168]. This removal mechanism is expected to be important near surfaces with loosely attached particles or with readily dissolvable surfaces [170]. Higher frequency ultrasound tends to have higher energy absorption and thus greater acoustic streaming flow rates than lower frequencies for the same power intensity [167]. In addition, higher power intensities lead to greater acoustic streaming flow rates due to higher energy gradients in solution between acoustically and non-acoustically stimulated areas. This mechanism causes bulk water movement toward and away from the membrane cake layer, with velocity gradients near the cake layer that may scour particles from the surface.

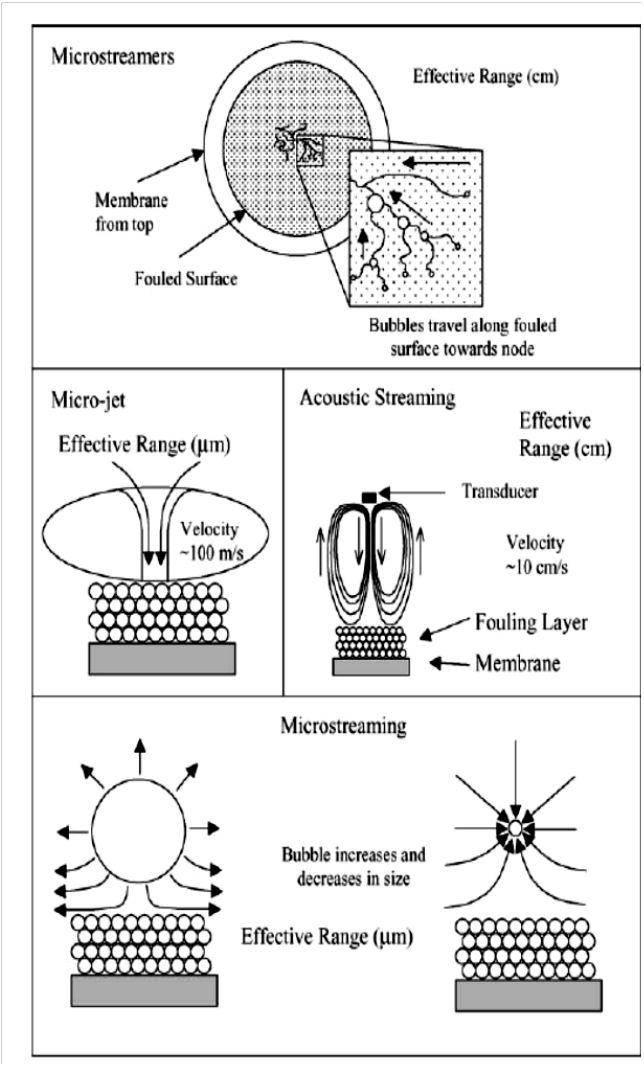

Figure 1.1.7. Possible mechanisms for particle removal/detachment observed with ultrasonic cleaning

Only few works has been done on the effect of ultrasonic wave on separation performance of protein mixture by UF. Tenga et al. studied the

effect of ultrasound on the flux and solute rejection in cross-flow UF of BSA-lysozyme binary protein mixture using PES membrane (30 kDa MWCO). They observed that ultrasonic wave not only enhanced the UF flux but also increased the lysozyme rejection. In particular example, ultrasound wave (25 kHz and 240 W) resulted in an increase of UF flux by 135% and 120% with PES membrane at pH: 11 in the upward and downward modes, respectively, in contrast to the case of without any ultrasound [171]. Effect of ultrasound on the flux and solute rejection in cross-flow UF in the (A) downward and (B) upward modes is shown in Fig. 1.1.8. Enhanced flux in continuous UF processes were suggested an interrupted ultrasound and more hydrophilic ultrafilter membranes in the upward operating mode for high performance [153]. It was noticed that the effectiveness of ultrasound in membrane filtration depends on many factors, such as orientation and position of ultrasonic field, ultrasonic frequency and power, ultrasonic radiation angle, position of ultrasonic vibration plate in the membrane module, membrane material, membrane housing, operating pressure and the fouling material [171]. It was widely believed that ultrasonic cavitation, acoustic streaming, ultrasonic-induced vibration of membrane and ultrasonic heating [172,173] was the main causes for the enhanced separation performance and permeate flux.

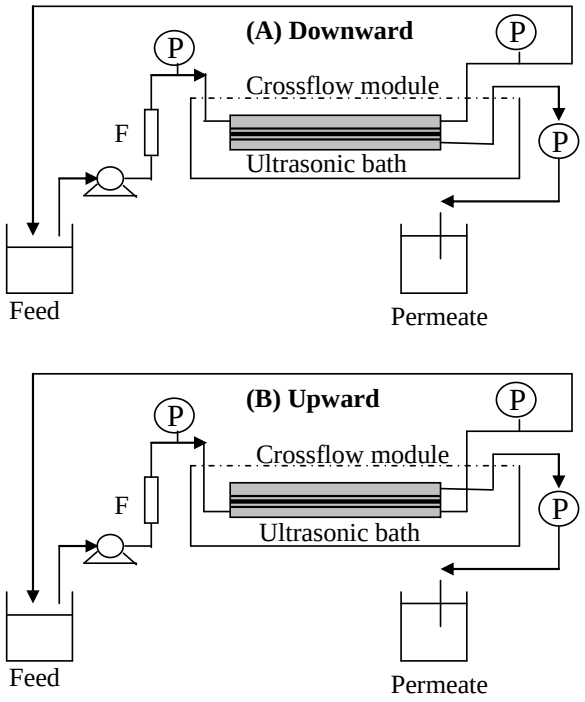

Figure 1.1.8. Experimental set up of cross-flow UF in the downward and upward modes

Muralidhara and Tarleton reported that both, electric and ultrasonic fields can reduce membrane fouling and in turn of enhanced flux. They

observed a synergistic effect when both the fields were applied simultaneously [174-176]. In addition Wakeman and Williams also observed that filtrate flux could be markedly increased by the simultaneous addition of electric and ultrasound fields. Both electrical and ultrasonic fields reduced the fouling when applied individually, but the extent of improvement by the ultrasonic field could be minimal. The improvement by the electric field is invariably considerably greater than that due to the ultrasonic field, particularly when the particles are well dispersed (high zeta potential) [19].

1.1.3.4. High-performance tangential flow filtration

High-performance tangential flow filtration (HPTFF) is also an emerging technology that enables the separation of proteins with similar size. HPTFF technology has become possible by exploiting several new discoveries. It has been demonstrated that optimum selectivity and throughput were obtained in the pressure-dependent flux regime. Selectivity and throughput could also be enhanced through module design and process configurations that reduce the trans-membrane pressure gradient. Optimizations of buffer pH and ionic strength have a significant impact on the sieving behaviour of proteins in membrane systems [65,88,89,177]. HPTFF is a two-dimensional unit operation that exploits both size and charge mechanisms. In addition, protein concentration, purification and buffer exchange can be accomplished in a single unit operation.

Conventional tangential flow filtration is limited to the separation of solutes that differ by ten-fold in size (e.g., cell-protein, virus-protein and protein-buffer). However, HPTFF is a two-dimensional purification method that exploited differences in both size and charge characteristics of biomolecules. Molecules that differ less than three-fold in size can be separated using highly selective charged membranes with careful optimization of buffer and fluid dynamics. Current protein separation processes often used ion-exchange chromatography, UF and size exclusion chromatography (SEC) for concentration, purification and buffer exchange. HPTFF made it possible to perform all of these steps in a single unit

operation by reducing production costs. It provided a high-resolution purification while maintaining the inherent high throughput and high yield characteristics of conventional UF.

The success of the HPTFF is based on several important factors such as operating pressure, flux and selectivity. Operating in pressure-dependent flux regime results in both the highest selectivity and mass throughput [177-179]. The best combination of selectivity and throughput was derived from a set of optimization equations using experimental flux and sieving data [180]. Optimizing buffer pH and ionic strength to increase flux difference between product and impurity further enhanced the resolution of the method [85]. Choice of automated process development systems depends on membrane selection, buffer choice and fluid dynamic optimization. Industrial-scale systems were based on the linear scale-up principles previously developed for UF [181,182]. Emerging trends for membrane development are being focused on enhanced pore size distribution and novel membrane chemistry. Despite significant enhancement in resolution, HPTFF has equivalent throughput to UF, measured in mass of product processed per unit membrane area and time. A limitation of the technology is the susceptibility to fouling by feed streams containing precipitates. In addition, high ionic strength feed streams have reduced selectivity and throughput.

The resolution of protein separation by HPTFF was further enhanced by the use of charged membranes. The sieving of positively charged proteins was dramatically lower with positively charged membranes due to like charge repulsion. These electro-static repulsions prevented the proteins to enter in the membrane pores, which enhanced protein transmission and reduced membrane fouling. Selection of buffer pH, where the product protein was positively charged and the impurity proteins were neutral charged resulted in extremely low product flux with high flux of impurities [89]. This is in sharp contrast to conventional UF processes, in which at least 10-fold difference in size for effective separation is required. HPTFF has been used to separate monomers from oligomers based on their difference in size [88], protein

variants differing at only a single amino acid residue [183], and an antigen-binding fragment from a similar size impurity [88]. In addition, HPTFF was potentially used for the purification process to remove specific impurities (e.g., proteins, DNA, or endotoxins) and/or eliminate protein oligomers or degradation products. In addition, it effected simultaneous purification, concentration, and buffer exchange, providing an opportunity to combine several different separation steps into a single scalable unit operation.

Commendable efforts were rendered to separate proteins by HPTFE. Van et al. [88,89] used Immunoglobulin-ovalbumin protein mixture as a model to understand the effect of membrane cut-off and variability on HPTFF protein separations. It has recently been shown that excellent HPTFF separations could be obtained even for molecules differing in size by less than two-fold. Although the ultimate range of HPTFF applications in bio-processing (and related fields) remains to be determined, this membrane technology has potential to play a vital role in the development of new and improved separation processes for many macromolecular species. 99-fold purification of an antigen-binding fragment of a monoclonal antibody (FAB) from BSA by operating the membrane process near the iso-electric point of the BSA and using a positively-charged membrane was obtained with high rejection of the positively-charged FAB [89].

HPTFF exploited a number of different strategies to achieve high resolution separations, including: (1) proper choice of pH and ionic strength to maximize differences in the hydrodynamic volume of the product and impurity, (2) use of electrically charged membranes to enhance the retention of like charged proteins, (3) operation in the pressure-dependent regime to maximize the selectivity, and (4) use of a dia-filtration mode to wash impurities through the membrane [184]. Since the selectivity in HPTFF is a function of the local filtrate flux, and thus the local trans-membrane pressure, the selectivity can be further improved by maintaining a nearly uniform trans-membrane pressure throughout the module. Conventional membrane modules typically have a large variation in trans-membrane

pressure drop due to the parasitic pressure losses associated with flow along the retentate channel. A simple approach for minimizing this trans-membrane pressure variation is necessary to establish a co-current flow on the filtrate side of the membrane by using a recirculation pump to generate a pressure gradient in the filtrate channel that balances the gradient in the retentate. Comparison of flow and pressure profiles for conventional TFF module and co-flow arrangement to maintain a uniform trans-membrane pressure throughout the module has shown in Fig. 1.1.9. Van et al. have proposed closed-loop cascade system for protein fractionation, based on HPTFF [88]. This system overcomes some of the problems associated with conventional MF/UF configurations and equipment and is reported to give high degree of protein fractionation [184].

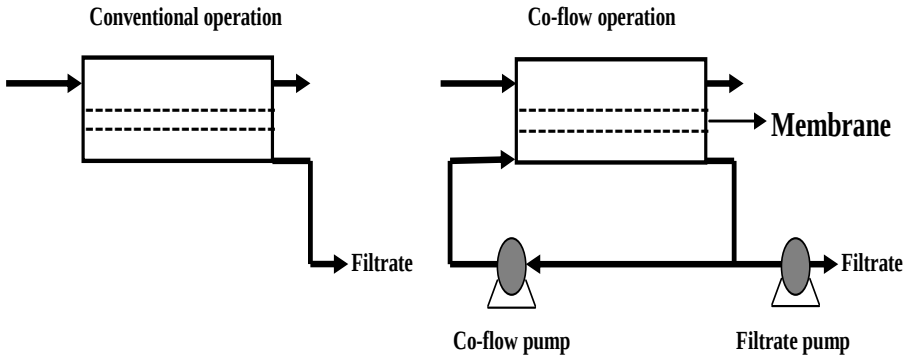

Figure.1.1.9. Comparison of flow and pressure profiles for conventional TFF module and a module using cross-flow arrangement to maintain a uniform trans-membrane pressure throughout the module

1.1.4. Protein separation/purification by nanofiltration

Nanofiltration (NF) is particularly useful for separation of peptides due to the suitable cut-off of the NF membranes and because of the electrochemical effects, which play an important role in the case of charged molecules. Negatively charged membranes have been applied to enrich cationic peptides with antibacterial properties from cheese whey [185,186]. A preliminary study on the desalting of peptide fractions from whey protein hydrolysate using NF membranes has revealed the possible occurrence of

specific rejection phenomena involving negatively charged peptides by NF membranes [187]. Pouliot et al. [188] has investigated the separation of peptides from tryptic hydrolysates of whey proteins with charged UF/NF membranes. Variation in pH and the ionic strength of the hydrolysate phase has proved charge effects on peptides separation performance [188].

1.1.5. Membrane fouling during protein separation by UF and MF

Fouling of MF/UF membrane during practical application for protein separation resulted from its adsorption on membrane surface significantly increases hydraulic resistance to flow, which reduced filtration flux rate and induced unfavourable effect on efficiency and economics of protein recovery processes [189,190]. Proteins are difficult foulants to deal because they readily adsorb onto membrane surfaces and pore walls. This leads to the formation of a secondary barrier that decreased permeate flux and changed solute selectivity. Therefore, to reduce fouling by rendering the membrane surface hydrophilic is one of the big challenges for achieving better membrane performance [191]. Membrane fouling referred to the irreversible alteration in membrane properties, caused by specific interactions feed stream components and membrane.

Fouling can occur by several forms in particular deposition of denatured or agglomerated proteins at the surface of the membrane, or adsorption of proteins inside the pore structure of the membranes. Many authors have studied the fundamental mechanisms involved in membrane fouling by protein suspensions, which may be grouped as follows.

(i) The formation of a gel layer due to concentration polarization [192].

(ii) Adsorption of species on the membrane surface and inside the pore structure [193].

(iii) Deposition and pore blocking after the formation of protein aggregates due to denaturation [194].

Modelling of the flux decline during filtration provided better understanding on membrane fouling and predictive tools for successful scale-up or scale-down of MF systems. Previous studies [195-197] have described the flux decline during protein filtration using the classical fouling models: complete pore blockage, intermediate pore blockage, pore constriction and cake filtration. Ho and Zydney [198] developed a combined membrane fouling model accounting for both, pore blockage and cake filtration to describe flux decline. Schematic diagram for all three mechanisms include pore narrowing, blockage, gel layer formation and pore plugging as shown in Fig. 1.1.10. The model shows a smooth transition from pore blockage to cake filtration, and is in good agreement with flux decline data obtained during bovine serum albumin filtration using polycarbonate track etched membranes. Although the combined pore blockage and cake filtration model described the flux decline during bovine serum albumin (BSA) filtration through the membrane pores, internal fouling was completely neglected. Internal fouling caused by protein adsorption in complicated membrane structure may be important for cases in which the feed stream has a relatively low concentration of foulant. For example, Taniguchi et al. reported some irreversible internal fouling by low molecular weight species.

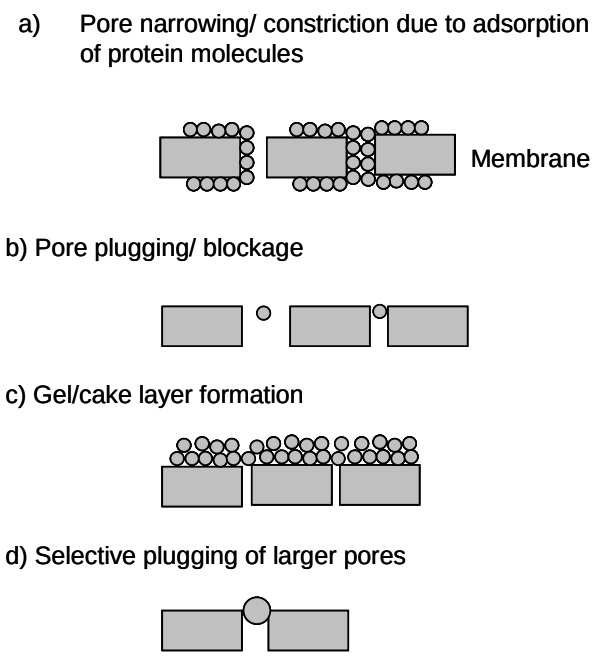

Figure 1.1.10. Schematic diagram for all four mechanisms including pore narrowing, blockage, gel layer formation and pore plugging.

Internal fouling is also important in cases where fouling is not expected to occur by a size-based mechanism, such as clarification applications [199].

Two techniques are currently used to characterize membrane fouling. Measurements of the flux decline at constant pressure, and the measurement of the pressure increase in constant flow rate permeation. Most studies of fouling have been concerned with UF membranes but from a technological point of view, the fouling of MF membranes by protein adsorption can be more important [200,201]. Only few investigations have been devoted to protein interactions with MF membranes. Hlavacek and Bouchet studied dead-end filtration of BSA solution by MF membranes and quantified fouling by means of the constant filtration rate equation [202]. However, the different roles of adsorption, gel formation and the deposition of aggregates were not clear. Fouling of MF membranes were also investigated by measuring the pressure drops across two membranes fed in series by a constant rate pump, which enables a distinction to be made between surface fouling and internal fouling of the membrane. In the case of the MF of BSA solutions, the technique showed how the type of pump and the operating temperature influenced membrane fouling and how protein denaturation and adsorption increased different types of fouling [17]. Fouling of MF membranes with BSA and γ-globulin were studied to investigate how surface properties of membranes and proteins affect adsorption and deposition. Electrical properties of the solute and the membrane should be previously known in order to interpret fouling in terms of their mutual interaction [203,204].

In order to improve the properties of conventional MF membranes, micro-sieves were introduced about a decade ago [205,206]. Micro-sieves differ from conventional MF membranes by their well structured morphology and controlled porosity, which results in good separation behaviour and high flow rates [207,208]. The main advantage of micro-sieves compared to conventional membranes is the larger permeate flux, which allows low-pressure operation and savings in the operational costs [209]. Another advantage of micro-sieves over MF membranes is their structural design, a

very thin selective layer and perfectly shaped straight pores. These features would be a great advantage against fouling because of the smooth surfaces and the fact that proteins cannot be trapped inside the pore network such as normally occurs in polymeric membranes. However, for economical and sustainable industrial processes, cleaning should be performed at the lowest frequency possible. In pressure-driven processes, protein fouling of MF membranes is nowadays still an issue. Several studies [210-212] proved that, even with pore sizes much larger than the protein size, fouling under dynamic condition occurs due to aggregate formation [211,213], by hydrophobic and/or electrostatic interactions or van der Waals forces [212]. In the case of BSA, Kelly and Zydney [214] proposed fouling mechanism based on deposition and subsequent pore blockage due to protein aggregates on the surface. At longer filtration times, the flux decline is usually governed by a cake filtration mechanism. The initial fouling due to pore blockage caused by aggregates has been corroborated by several authors, and extensively studied and modelled for BSA [215-217] and other protein systems [218].

Surface modification has been widely used for the improvement of protein adsorption resistance and permeation property of hydrophobic membranes. It is well known that by increase in membrane surface hydrophilicity can effectively minimize protein adsorption and prevent membrane fouling. Various methods, such as coating [219], surface graft polymerization [220,221], and chemical modification [222-225], have been reported in the literature to reduce the UF membrane fouling during protein separation. Nakao et al. studied that protein fouling during UF was entirely due to the formation of a secondary (gel) layer on the upper surface of the membrane. This layer provided an additional resistance to both, solute and solvent transport across the membrane [226]. Jiang et al. synthesized pegylated PES via a reaction of sulfonated PES with oligomeric poly (ethylene glycol) (PEG). The modified membranes showed superior resistance to BSA adsorption in compare with unmodified counterparts. Furthermore, UF

experiments revealed that both pegylated PES and sulfonated PES could enhance the permeation properties of PES membranes, but the pegylated PES reduced BSA fouling in a wider pH range and endowed membranes with better permeation properties. The improved antifouling property rendered longer operation lifespan of modified membranes [66]. A model to predict the effect of pH and ionic strength on fouling in the cross-flow UF of protein solutions was also presented. The model was experimentally tested with 1 g/l BSA using Amicon H1P30-20 modules, for a range of pressures, ionic strengths and pH [227]. Reports on performance of the surface-modified PVDF membranes during UF of BSA and the enzyme solution suggested that the modified membranes exhibited non-fouling properties, whereas the PES membranes showed severe fouling problems [228]. The modified membranes showed increased hydrophilicity, which has translated into decrease in protein fouling relative to the unmodified PES membrane. Relatively higher filtration performances compared with commercial low protein adsorbing membranes was observed [229].

Efforts were also dedicated for the photo-modification of UF membranes for achieving low fouling during the filtration of biological solutions. Nystrom and Jarvinen, photochemically modified PES membranes (6 kDa MWCO) using monomers containing dextran and poly (ethylene oxide) groups to decrease membrane fouling during the filtration of BSA, lysozyme, and whey [230]. Yamagishi et al. described the grafting of wide varieties of hydrophilic vinyl monomers onto the surface of PES UF membranes to reduce protein fouling during the BSA filtration [231]. Effect of the deposited protein (BSA) layer on water (solvent) flux has been studied in detail by many researchers [232,233]. They determined that maximum BSA adsorption occurred at the isoelectric point (pH: 4.8), at which approximately 80 monolayers were surmise after 8 h use of PES membrane (30 kDa MWCO). The long-term flux reached a minimum at pH: 5, at which protein has no net charge. Therefore, spacing between the packed protein molecules was less compared to the situation when protein molecules have a net charge and

repel each other [233,234]. Thus, the deposited layer was porous at low BSA concentration (less than gel forming concentration). Zydney et al. also observed that BSA filtration and adsorption caused significant reductions in the diffusive, convective, and hydraulic transport characteristics of the fully retentive PES membranes [191].

1.2. Electrophoretic membrane contactor for the separation of proteins

'Electrophoresis' is an electrically driven operation that constitutes a purification step used at the later stage of the downstream process because of their high resolution at the analytical scale. Different studies were devoted to find out the operating modes for scale up of electrophoretic separations. One of them is continuous flow electrophoresis (CFE), which was carried in a flowing buffer film. Different experimental and theoretical studies were carried out to understand the transport phenomena involved in this process [235-237]. From these works, the limitations of CFE were pointed out and their origin was identified [238]. Proper resolution/separation was achieved under well optimized conditions [237]. The limitations were in terms of production capacity or productivity, demonstrated and it had a strong relationship between resolution and productivity [236]. Finally, it was found that the productivity could not be increased over a certain limit, typically about few milligrams per hour.

To overcome these limitations, electro-membrane operations offered the possibility to increase the productivity without compromising from separation efficiency. The most common electro-membrane operation is 'electrodialysis' (ED) in which cation-exchange membrane (CEM) and anion-exchange membrane (AEM) are used. The use of porous membranes in the place of ion-exchange membranes were investigated to extend the field of electrodialysis applications for biological molecules like polyamino acids, peptides and proteins. In that case, the porous membrane acts as a contactor and the separation is achieved with respect to the difference between the

mass flow rates of the species. According to the membrane and solute properties, this difference can have various origins, like different electrophoretic mobility, sieving effects or a coupling of both [239-243]. The scalable preparative electrophoresis technique was used as a 'Gradiflow' apparatus [239]. It has been used for several applications like the separation of proteins from plasma, algal extracts [239] and egg-white [240,241]. The influence of the voltage, pH solute concentration and membrane has been studied over this process. However, no comprehensive work and no theoretical approach were devoted to understanding various transport phenomena involved in the process. Electrophoretic membrane contactor was developed for the separation of binary mixture of proteins by using ion-exchange and ultrafilter membranes.

The electrophoretic membrane contactor is schematically presented in Fig. 1.2.1(A & B). The separation chamber itself is composed of two compartments delimited by a porous membrane, acting as a contactor between the two streams in which the mass transfer takes place. The purified buffered solution is continuously fed into the chamber. The only driving force is a voltage, applied in a perpendicular direction to the feed flow. Two electrodes are located in compartments, which are separated from the separation chamber itself by ion-exchange membranes. As soon as a voltage is applied, the charged components contained in the feed would migrate from one compartment toward the other through the porous membrane. The mass flow of solute depends on its electrophoretic mobility, which is fixed by the pH of the buffered solution. Then, solutes having distinct electrophoretic mobilities were carried through the membrane at different rates. Two outlet streams with different compositions are thus obtained. The compartments in which the outlet concentration of the target solute are respectively lower and higher than the inlet, called "dilute" and "concentrate" respectively .

An electro-dialysis process could be operated in two different operating modes. The first one depicted in Fig. 1.2.1 (A), where the same solution, containing the species to be separated, was fed on both sides of the

membrane. This configuration would be further called “separation mode”. The second mode of operation, illustrated for the purification of a negatively charged component was depicted in Fig. 1.2.1 (B). In that case, the solution to be purified was fed in one compartment. The other compartment, which is the elution compartment, was fed with the buffer. The solute A, which migrates through the membrane, is then collected in that compartment. That configuration would be later called the “elution mode”. These two modes of operation could be used to achieve different objectives to favor quantitative or qualitative aspects. Indeed, as far as the production is concerned, the separating mode would be preferable. On the contrary, for achieving higher purification, the eluting mode would be used.

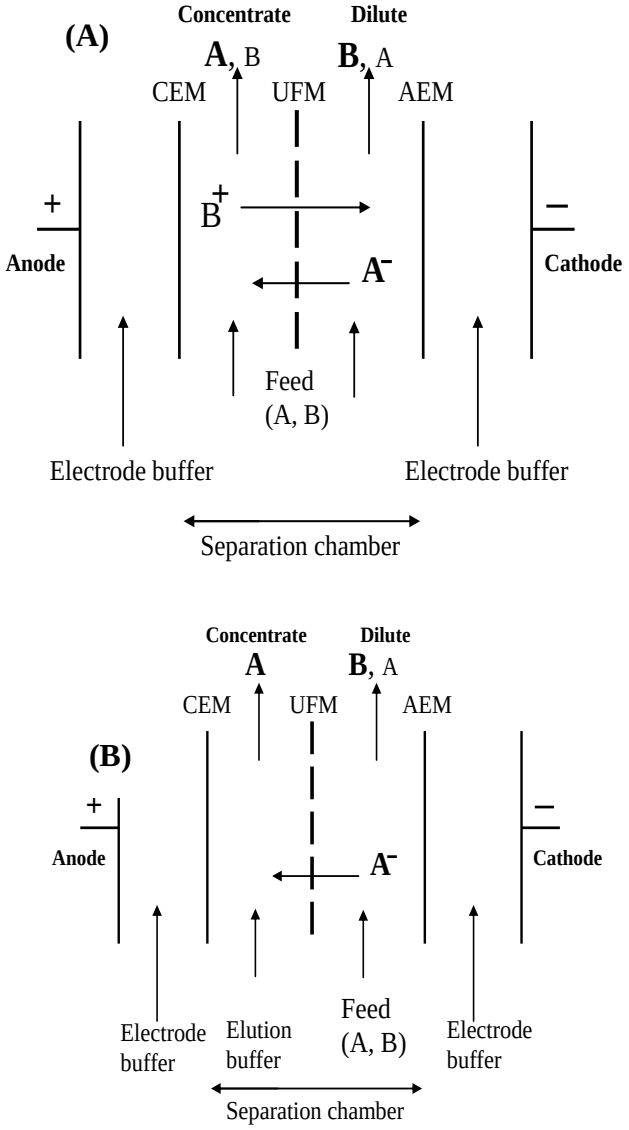

Figure 1.2.1. (A) Schematic drawing of the electrophoretic membrane contactor: separation mode; UFM: ultrafiltration membrane; AEM: anion exchange membrane; CEM: cation exchange membrane. (B) Schematic drawing of the electrophoretic membrane contactor: elution mode

Galier studied the purification of α-LA from a mixed solution containing α-LA and bovine hemoglobin using electrophoretic membrane contactor [242]. Three parameters were chosen to characterize the process performances, i.e. the productivity, purity and the product yield. It was confirmed that the productivity could be enhanced, by a factor of 5 by increasing the inlet concentration. It was further demonstrated that the increase of productivity was achieved without reducing the purity and the product yield. β-LG, one of the major whey components, can release by enzymatic hydrolysis of different bioactive peptidic sequences according to the enzyme used. However, the protein hydrolysates have to be fractionated to obtain peptides in a more purified form. Poulin [243] studied the feasibility of separating peptides from a β-LG hydrolysate using electrophoretic membrane contactor and studied the effect of pH on the migration of basic/cationic and acid/anionic peptides. It was concluded that electrophoretic membrane contactor appeared to be a selective method of separation since amongst a total of 40 peptides in the raw hydrolysate, only 13 were recovered. Amongst these 13 migrating peptides, three acid/anionic peptides migrated in one compartment, while three basic/cationic peptides migrated to another. Thus electrophoretic membrane contactor is an interesting way to separate bioactive peptides and other charged molecules of interest from complex feed-stocks in the food, pharmaceutical, fine chemical and fermentation industries.

1.3. Integrated membrane technologies for protein separation

Over the past decade, many traditional chemical industries have been undergoing a change in their orientation from conventional chemicals to life-science products. Despite discussion about what a life sciences company should consist of, the required technology for the future will not change [244]. Recent developments in biotechnology, together with recognition of the need for renewable resources have accelerated biotech research and

development in academia, industries and government-funded laboratories. The success of biotechnology for bulk product manufacturing will heavily depend on engineering solutions in the downstream process in which separation and purification have a crucial role with respect to commercial development. Development of efficient bio-separation methods is important for a broad range of business areas including pharmaceuticals, nutrition and health products, bio-based materials and crop production chemicals. Depending on the value of the end product and the scale of production, the processing required varies significantly. Key factors that have an impact on the choice of separation strategy include process throughput, particle size of the product, impurities and desired concentration of product.

Membrane systems are extensively used throughout the various biological and chemical industries to control variety of products. These membrane processes are successful because they are effective and economically implemented at the large stage, which is required for industrial applications. A combination of different membrane processes gives interesting benefits, which cannot be achieve by single membrane operation. The possibility of redesigning overall industrial production by the integration of various already developed membrane operations is becoming of particular interest. Because of the synergic effects are reach batter [245]. Integration membrane technology also shows simplicity of the units and possibility of advanced levels of autoimmunization. Membrane hybrid technology works best when developed as one concept. This clearly lies in the influence that process have on each other The rationalization of industrial production by use of these technologies permits low environmental impacts, low energy consumption, and higher quality of final products [246].

Various membrane operations (MF, UF, NF, etc.) have introduced in industrial production lines as an alternative of existing units for fractionation of protenecious products. The categories are as follows of different field of integrated membrane separation processes for purification and fractionation of protein products [247].

A lot of work has performed to recover valuable protenecious components from dairy waste streams [248-250]. Dairy proteins are valuable products and, used as high-value food additives, nutraceuticals and therapeutics. Recently a number of papers have published to recover the protein using MF, UF and NF processes [251,252]. The largest membrane area was installed in the dairy industry. It has been estimated 2,000,00 m^2 membrane area were installed for the fractionation of milk and whey. About 2/3 of the membrane area installed in the dairy industry is used for the treatment of whey and about 1/3 for milk [253].

1.3.1. Biotechnology industry

Uses of membrane technologies in biotechnology or bio-separation sector recently became an essential tool. In biotechnological downstream processing product is obtained at low concentration in a complex liquid. The product has to be separated from a mixture of a cell mass, substrate components, additive and by-products. Since the products are often labile, the separation has to be done rapidly and under gentle condition. The process has to be carried out in a closed system when working with pathogenic organism. Downstream treatment is an essential step in the fermentation process. Different module configurations and pre-treatments are common in this production step. The choice of the process depends on the sensitivity of the product and the viscosity. The optimization of a process also includes the adjusting of the membrane to the fermentation conditions [384,385]. Numerous applications of membrane technologies for the recovery of valuable bio-product from fermentation broth have been reported in the literature. Lactic acid is one such value-added product that was produced from processing cheese whey or sugar cane molasses by fermentation. The processes of lactic acid production include two key stages, which are (a) fermentation and (b) product recovery. The biggest challenge in lactic acid production lies in the recovery and not in the fermentation step. Usually, most of the separation of micro-organisms from fermentation broth was performed by centrifugation. Recently, cross-flow MF has been used to

separate cells in continuous fermentation processes [254]. A successful lactic acid recovery approach has been that of continuous fermentation in a cell-recycled reactor where the cells are separated by a filtration unit and returned to the fermentor while the product is removed in the permeate [255,256]. The long-term performance of membrane units at high cell densities was affected by the fouling of filtration membranes, which require extensive cleaning protocols [257].

Other typical examples of membrane technologies in the biotech or pharmaceutical sector were recently reported. This include recovery of heterogeneous immunoglobulin (IgG) from transgenic goat milk by MF [258], concentration and purification of recombinant Brain-Derived Neurotrophic Factor (rBDNF) inclusion bodies from E. coli cell suspensions by cross-flow MF and diafiltration [259], recovery of naturally glycosylated therapeutic proteins produced from animal cell cultures by MF [260], recovery and purification of yeast alcohol dehydrogenease (ADH) from bakers' yeast as typical of downstream processing for the extraction of an intracellular enzyme product [259]. The work of on the optimization of monoclonal antibody recovery from transgenic goat milk by MF is an interesting example. The optimization involved varying pH, trans-membrane pressure, milk feed concentration, membrane module type, and axial velocity. Operation in the pressure-dependent regime at low uniform trans membrane pressures using permeate circulation in co-flow, at the p*I* of the protein is shown to increase IgG recovery from less than 1% to over 95%. Such methodology is generally applicable to the recovery of target proteins found in other complex suspensions of biological origin. [260]. Much effort is still being devoted to developing new membrane modules with improved mass-transfer characteristics for UF and MF processes. This includes rotating disk filters [261,262], cylindrical Taylor vortex devices [263], conically shaped rotors [264], and helical coiled ‘Dean vortex systems’. Dean vortex devices have very high mass-transfer rates, owing to the presence of centrifugal flow instabilities. These devices show significant increases in protein transmission

and capacity, although fouling remains a problem in many applications. An alternative approach is to use high frequency back pulsing to continually clean the membrane surface. High frequency back pulsing was shown to improve flux, reduce fouling and increase protein transmission in the purification of conjugated vaccine products [265].

Membranes have been traditionally used to separate species of different size such as proteins from cells, fermentation broths, cell debris and separation of low molecular weight components from proteins. Since long it has been an integral part of biotechnology processes, the well known examples are MF and UF, which have become routine methods for protein separation/fractionation. The development of membrane chromatography, HPTFF and electrophoretic membrane contactor enable for the complete purification/separation of proteins using membrane systems. Although not implemented in any commercial processes, small-scale studies using this process show comparable yield, purification, and product quality with a conventional process. Continued efforts to develop improved membrane materials, modules, and process designs should enable membrane systems to play an important role in the next generation of biotechnology processes.

New applications of membrane processes continue to emerge, such as membrane biosensors and molecularly imprinted polymeric membranes for separation of molecules. Their industrial success will depend on their advantages over the existing technologies. Thus, deep understanding of physical and chemical phenomena across the membrane interfaces under the operating conditions will help to improve their performance in the biotechnology-based industries. Future trends of membranes in biotechnology will be driven by higher selectivity, lower cost of production, and enhanced membrane throughput. There is also trend towards increased use of disposable systems (bioreactors, ultrafilter-membranes, and buffer bags), which are attractive for production scale manufacturing, eliminating the need for the development and validation of cleaning cycles. Future developments will determine whether such a membrane-based process can

provide the required product quality, purity, yield and throughput with low cost for biotechnology industry.

References

[1] Ulbricht M. Polymer 2006;47:2217.

[2] Baker RW. Membrane technology and applications. Chichester: Wiley; 2004.

[3] Blanch HW, Clark DS. Biochemical Engineering. New York: Marcel Dekker; 1996.

[4] Van Reis R, Zydney AL. J Membr Sci 2007;297:16.

[5] Nagarale RK, Gohil GS, Shahi VK. Adv Colloid Interface Sci 2006;119:97.

[6] Saxena A, Gohil GS, Shahi VK. Ind Eng Chem Res 2007;46:1270.

[7] Darnon E, Morin E, Belleville MP, Rios GM. Chem Eng Process 2003;42:299.

[8] Zeman LJ, Zydney AL. Microfiltration and Ultrafiltration: Principles and applications. New York: Marcel Dekker; 1996.

[9] McGregor WC. Membrane separation in biotechnology. New York: Marcel Dekker; 1986.

[10] Van Reis R, Zydney AL. Curr Opin Biotechnol 2001;12:208.

[11] Ho WSW, Sirkar KK. Membrane Handbook. Kluwer: Academic Publishers Dordrecht; 1992.

[12] Bowen WR, Hall NJ. Biotechnol Bioeng 1995;46:28.

[13] Richard BW, Williams PM. Adv Colloid Interface Sci 2007;134:3.

[14] Garem AJ, Leaonil G, Daufin JL, Maubois. Lait 1996;76:267.

[15] Kimura S, Tamano A. Membranes and Membrane Processes. New York: Plenum Press; 1986.

[16] Tsuru T, Shutou T, Nakao SI, Kimura S. Sep Sci Technol 1994;29:971.

[17] Xu-Jiang Y, Dodds J, Leclerc D. Filtr Sep 1995;32:795.

[18] Kelly ST, Zydney AL. J Membr Sci 1995;107:115.

[19] Wakeman RJ, Williams CJ. Sep Purif Technol 2002;26:3.

[20] Jaffrin MY, Ding LH, Akoum O, Brou A. J Membr Sci 2004;242:155.

[21] Lee SS, Burt A, Russoti G, Buckland B. Biotechnol Bioeng 1995;48:386.

[22] Parnham CS, Davis RH. Biotechnol Bioeng 1995;41:55.

[23] Vogel JH, Kroner KH. Biotechnol Bioeng 999;63:663.

[24] Luque S, Mallubhotla H, Gehlert G, Kuriyel R, Dzengeleski S, Perl S. Biotechnol Bioeng 1999;63:247.

[25] Schutyser M, Rupp R, Wideman J, Belfort G. Biotechnol Prog 2002;18:322.

[26] Levesley JA, Hoare M. J Membr Sci 1999;158:29.

[27] Meacle F, Aunis A, Thornton R, Lee A. J Membr Sci 1999;161:171.

[28] Charcosset C. Biotechnol Adv 2006;24:482.

[29] Kuriyel R, Zydney AL. Methods in biotechnology downstream processing. Humana Press; 2000.

[30] Sundaram S, Auriemma M, Howard G, Brandwein H, Leo F. J Pharm Sci Technol 1999;53:186.

[31] Aimar P, Meireles M, Bacchin P, Sanchez V. Membrane processes in separation and purification. Applied Science Dordrecht: Kluwer Academic Publishers; 1993.

[32] Baruah GL, Venkiteshwaran A, Belfort G. Biotechnol Prog 2005;21:1013.

[33] Nystrom M, Aimar P, Luque S, Kulovarra M, Metsamuuronen S. Colloids Surf 1998;138:185.

[34] Van Reis R, Frautschy LN, Goodrich EM, Saksena S, Kuriyel R, Simpson CM. Biotechnol Bioeng 1997;56:71.

[35] Ulbricht M, Schuster O, Ansorge W, Ruetering M, Steiger P. Sep Purif Technol 2007;57:63.

[36] Fang JK, Chiu HC, Wu JY, Suen SY. React Funct Polym 2004;59:171.

[37] Varshosaz J, Falamarzian M. Eur J Pharm Biopharm 2001;51:235.

[38] Tarvainen, T, Nevalainen T, Sundell A, Svarfvar B, Hyrsyla J, Paronen P, Jarvinen K. J Controlled Release 2000;66:19.

[39] Kinsella JE. Crit Rev Food Sci 1976;7:219.

[40] Chovea BE, Grandison AS, Lewis MJ. Food Hydrocolloids 2007;21:1379.

[41] Campbell NF, Shih FF, Hamada JS, Marshall WF. J Agric Food Chem 1996;44:759.

[42] Henn L, Netto M. J Agric Food Chem 1998;46:3009.

[43] Lhocine L, Boye J, Arcand Y. J Food Sci 2006;71:137.

[44] Achouri A, Boye J, Yaylayan V, Yeboah F. J Food Sci 2005;70:270.

[45] Iritani E, Mukai Y, Kiyotomo Y. J Membr Sci 2000;164:51.

[46] Von Zumbusch P, Kulcke W, Brunner G. J Membr Sci 1998;142:75.

[47] Oussedik S, Belhocine D, Grib H, Lounici H, Piron DL, Mameri N. Desalination 2000;127:59.

[48] Robinson CW, Siegel MH, Condemine A, Fee C, Fahidy TZ, Glick BR. J Membr Sci 1993;80:209.

[49] Bargeman G, Dohmen-Speelmans M, Recio I, Timmer M, Van der Horst C. Lait 2000;80:175.

[50] Lapointe JF, Gauthier SF, Pouliot Y, Bouchard C. Biotechnol Bioeng 2006;94:223.

[51] Bargeman G, Houwing J, Recio I, Koops GH, Van der Horst HC. Biotechnol Bioeng 2002;80:599.

[52] Bargeman G, Koops GH, Houwing J, Breebaart I, Van der Horst HC, Wessling M. Desalination 2002;149:369.

[53] Lentsch S, Aimar P, Orozco JL. J Membr Sci 1993;80:221.

[54] Serra C, Wiesner M, Laine J. Chem Eng Sci 1999;72:1.

[55] Holeschovsky U, Cooney C. AIChE J 1991;37:1219.

[56] Lararova Z, Serro W. Sep Sci Technol 2002;37:515.

[57] Galier S, Balmann H. J Membr Sci 2001;194:117.

[58] Park YG. Desalination 2006;191:404.

[59] Byers C, Amarnath A. Chem Eng Progr 1995;63:1.

[60] Brisson G, Britten M, Pouliot Y. J Membr Sci 2007;297:206.

[61] Larive CK, Lunte SM, Zhong M, Perkins MD, George S, Wilson, Giridharan Gokulrangan, Williams Todd, Afroz Farhana, Scho1neich Christian, Derrick Tiffany S, Russell MC, Knipp SB. Anal Chem 1999;71:389R.

[62] Kurnik RT, Yu AW, Blank GS, Burton AR, Smith D, Athalye AM, Van Reis R. Biotechnol Bioeng 1995;45:149.

[63] Zydney AL, Kuriyel R. Methods in Biotechnology: Downstream Protein Processing. Totowa: Humana Press; 2000.

[64] Gehlert G, Luque S, Belfort G. Biotechnol Prog 1998;14:931.

[65] Van Reis R, Zydney AL. Encyclopedia of Bioprocess Technology: Fermentation, Biocatalysis, and Bioseparation. New York: John Wiley & Sons; 1999.

[66] Shi Q, Su Y, Zhu S, Li C, Zhaoa Y, Jiang Z. J Membr Sci 2007;303:204.

[67] Ghosh R, Silva1 SS, Cui Z. Biochem Eng J 2000;6:19.

[68] Li Y, Shahbazi A, Kadzere CT. J Food Eng 2006;75:574.

[69] Bhattacharjee S, Bhattacharjee C, Datta S. J Membr Sci 2006;275:141.

[70] Balakrishnan M, Agarwal GP. J Membr Sci 1996;112:75.

[71] Yang MC, Tong JH. J Membr Sci 1997;132:63.

[72] Tuccelli R, McGrath PV. US Patent 1996;5:522 991.

[73] Sivakumar M, Malaisamya R, Sajitha CJ, Mohana D, Mohana V, Rangarajan R. Eur Polym J 1999;35:164.

[74] Muller CH, Agarwal GP, Melin TH, Wintgens TH. J Membr Sci 2003;227:51.

[75] Almecija MC, Ibanez R, Guadix A, Guadix EM. J Membr Sci 2007;288:28.

[76] Chollangi A, Hossain MM. Chem Eng and Process 2007;46:398.

[77] Pujar NS, Zydney AL. J Chromatogr A 1998;796:229.

[78] Saksena S, Zydney AL. J Membr Sci 1997;125:93.

[79] Burns DB, Zydney AL. AIChE J 2001;47:1101.

[80] Cheang B, Zydney AL. Biotechnol Bioeng 2003;83:201.

[81] Burns DB, Zydney AL. J Membr Sci 2000;172:39.

[82] Tholmmes J, Etzel M. Biotechnol Prog 2007;23:42.

[83] Nystrom M, Ehsani N, Ojamo H. Bioseparation 1991;21:87.

[84] Ehsani N, Nystrom M. Bioseparation 1995;5:1.

[85] Burns DB, Zydney AL. Biotechnol Bioeng 1999;64:27.

[86] Nakao S, Osada H, Kurata H, Tsuru T, Kimura S. Desalination 1988;70:191.

[87] Van Reis R. U.S. Patent 2006;7:153 426.

[88] Van Reis R, Gadam S, Frautschy L, Orlando S, Goodrich E, Saksena S, Kuriyel R, Simpson C, Pearl S, Zydney AL. Biotechnol Bioeng 1997;56:71.

[89] Van Reis R, Brake JM, Charkoudian J, Burns DB, Zydney AL. J Membr Sci 1999;159:133.

[90] Lin SY, Suen SY. J Membr Sci 2002;204:37.

[91] Lu J, Wan Y, Cui Z. Ind Eng Chem Res 2005;44:7610.

[92] Balakrishnan M, Agarwal GP. J Membr Sci 1996;112:47.

[93] Shah TN, Henry C, Foley, Zydney AL. J Membr Sci 2007;295:40.

[94] Bhave RR. Inorganic Membranes: Synthesis, Characteristics and Applications. New York: Van Nostrand Reinhold; 1991.

[95] Millesime L, Dulieu J, Chaufer B. Bioseparation 1996;6:135.

[96] Millesime L, Dulieu J, Chaufer B. J Membr Sci 1995;108:143.

[97] Lucasa D, Baudrya MR, Millesimea L, Chaufera B, Daufin G. J Membr Sci 1998;148:1.

[98] Bechhold H. Ultrafiltration and Electro-ultrafiltration. New York: Chemical Catloge Company; 1926.

[99] Yukawa H, Shimura K, Suda A. J Chem Eng Japan 1983;16:305.

[100] Weber K, Stahl W. Chem Eng Technol 2003;26:44.

[101] Yoshida H, Kitajyo K, Nakayama M. Drying Technol 1999;17:539.

[102] Yukawa H, Shimura K, Suda A, Maniwa A. J Chem Eng Japan 1983;16:246.

[103] Yu JW, Neretnieks I. Chem Eng Sci 1996;51:4355.

[104] Henry JD, Lawler LF, Alex Kuo Jr CH. AIChE 1977;23:851.

[105] Radovich JM, Chao IM. J Coat Technol 1982;54:33.

[106] Zumbusch PV, Kulcke W, Brunner G. J Membr Sci 1998;142:75.

[107] Weigert T, Altmann J, Ripperger S. J Membr Sci 1999;159:253.

[108] Enevoldsen AD, Hansen EB, Jonsson G. J Membr Sci 2007;299:28.

[109] Sung M, Huang CP, Weng YH, Lin YT, Li KC. Sep Purif Technol 2007;54:170.

[110] Fair BD, Jamiesson AM. J Colloid Interface Sci 1980;73:130.

[111] Wakeman RJ, Tarleton ES. Filtr Sep 1986;23:174.

[112] Guizard C, Legault F, Idrissi N, Larbot A, Gavach C. J Membr Sci 1988;38:147

[113] Rios GM, Rakatoarisoa H, fuente BT. J Membr Sci 1988;38:147.

[114] Iritani E, Ohashi K, Murase T. J Chem Eng Jpn 1998;14:79.

[115] Zhou D, Zhao H, Price WE, Wallace GG. J Membr Sci 1995;98:173.

[116] Nakakura H, Yamashita A, Sambuichi M, Osasa K. J Chem Eng Jpn 1997;30:1020.

[117] Wakeman RJ. Trans IChemE Part C Food Bioprod Proc 1998;76:53.

[118] Kimura S, Nomura T. Membrane 1982;7:245.

[119] Karthik V, DasGupta S, De S. J Membr Sci 2002;199:29.

[120] Turkson AK, Mikhlin JA, Weber ME. Sep Sci Technol 1990;24:1261.

[121] Verdegan BM. Sep Sci Technol 1986;21:603.

[122] Visvanathan C, Aim RB. Sep Sci Technol 1989;24:383.

[123] Moulik SP, Cooper FC, Bier M. J Colloid Interface Sci 1967;24:427.

[124] Radovitch JM, Mason NS, Spark RE. Sep Sci Technol 1980;15:1491.

[125] Tarazaga CC, Campderros ME, Padilla AP. J Membr Sci 2006;278:219.

[126] Weng YH, Chaung-Hsieh LH, Lee HH, Li KC, Huang CP. J Hazard Mater 2005;122:171.

[127] Bier M. Electrophoresis. Vol. 1, New York: Academic Press; 1959.

[128] Nakao SI, Nomura T, Kumura S. AIChE J 1979;25:615.

[129] Hong J, Lee CK. Membrane Separation Coupled with Electrophoresis. Acad Sci: 1983.

[130] Radovich JM, Behnam B, Mullon C. Sep Sci Technol 1985;20:315.

[131] Henry JD, Lawler CH, Kuo CHA. AlChE J 1997;23:851.

[132] Carlos CT, Mercedes EC, Antonio PP. J Membr Sci 2006;278:219.

[133] Wakeman RJ, Tarleton ES. Chem Eng Sci 1987;42:829.

[134] Visvanathan C, Aim RB. Sep Sci Technol 1989;24:829.

[135] Iritani E, Ohashi K, Murase T. Chem Eng Jpn 1992;25:383.

[136] Carlos CT, Mercedes EC, Antonio PP. J Membr Sci 2006;283:339.

[137] Ku JR, Stroeve Pieter. Langmuir 2004;20:2030.

[138] Zumbusch PV, Thesis, TU Hamburg-Harburg 1996.

[139] Mameri N, Oussedik SM, Khelifa A, Belhocine D, Ghrib H, Lounici H. Desalination 2001;138:291.

[140] Kappler T, Posten C. J Biotechnol 2007;128:895.

[141] Saxena A, Shahi VK. J Membr Sci 2007;299:211.

[142] Bowen WR, Sabuni HAM. Ind Eng Chem Res 1992;31:515.

[143] Wakeman RJ. Filt Sep 1986;19:316.

[144] Bowen WR, Ahmad AL. AlChE J 1997;43:959.

[145] Ahmad AL, Electrophoretic membrane cleaning in dead-end ultrafiltration processes. Regional Symposium on Chemical Engineering, Johore Bharu-Malaysia, 1997.

[146] Weigert T, Altmann J, Ripperger S. J Membr Sci 1999;159:253.

[147] Wakeman RJ, Sabri MN. Chem Eng Res Des 1995;73:455.

[148] Bowen WR, Sabuni HAM. Ind Eng Chem Res 1994;33:1245.

[149] Ahmad AL, Ariffin N, Joseph A. Force balance model in electrophoretic dead-end membrane separation process. World Engineering Congress 99, Kuala Lumpur-Malaysia, 1999.

[150] Ahmad AL, Lau KK, Abu Bakar MZ. J Membr Sci 2005;262:138.

[151] Ahmad AL, Ibrahim N, Bowen WR. Sep Purif Technol 2002;29:105.

[152] Muthukumaran S, Kentish SE, Ashokkumar M, Stevens GW. J Membr Sci 2005;258:106.

[153] Teng MY, Lin SH, Wu CY, Juang RS. J Membr Sci 2006;281:103.

[154] Crawford AE. Ultrasonics 1963;1:65.

[155] Semmelink A. Ultrasonically enhanced liquid filtering, in Proceedings of Ultrasonics International Conference. England: Science and Technology Press; 1973.

[156] Mason TJ, Paniwnyk L, Lorimer JP. Ultrason Sonochem 1996;3:S253.

[157] Kobayashi T, Chai X, Fujii N. Sep Purif Technol 1999;17:31.

[158] Masselin I, Chasseray X, Durand-Bourlier L, Laine JM, Syzaret PY, Lemordant D. J Membr Sci 2001;181:213.

[159] Li J, Sanderson RD, Jacobs EP. J Membr Sci 2002;205:247.

[160] Chai X, Kobayashi T, Fujii N. Sep Purif Technol 1999;15:139.

[161] Chai X, Kobayashi T, Fujii N. J Membr Sci 1998;148:129.

[162] Simon A, Gondrexon N, Taha S, Cabon J, Dorange G. Sep Sci Technol 2000;35:2619.

[163] Ahner N, Gottschlich D, Narang S, Roberts D, Sharma S, Ventura S. Sep Sci Technol 1993;28;895.

[164] Kobayashi T, Hosaka Y, Fujii N. Ultrasonics 2003;41:185.

[165] Lamminen MO, Walker HW, Weavers LK. J Membr Sci 2004;237:213.

[166] Suslick K. Sonochem Sci 1990;247:1439.

[167] Suslick KS. Ultrasound Its Chemical, Physical, and Biological Effects. New York: 1988.

[168] Leighton TG. The Acoustic Bubble. San Diego: Academic Press; 1994.

[169] Starritt HC, Duck FA, Humphrey VF. Phys Med Biol 1991;36:146.

[170] Crum LA. Ultrason Sonochem 1995;2:S147.

[171] Tenga MY, Lina SH, Juangb RS. Desalination 2006;200:280.

[172] McNamara WB, Didenko YT, Suslick KS. Nature 1999;401:772.

[173] Chai X, Kobayashi T, Fujii N. J Membr Sci 1998;148:129.

[174] Wakeman RJ, Tarleton ES. Filtr Sep 1990;27:412.

[175] Tarleton ES. Filtr Sep 1988;25:402.

[176] Muralidhara HS, Senapati N, Ensminger D, Chauhan SP. Filtr Sep 1986;23:351.

[177] Zydney AL, Van Reis R. High performance tangential flow filtration in Membrane Separations in Biotechnology. New York: Marcel Dekker; 2001.

[178] Van Reis R. US Patent 1996;5:490 937.

[179] Van Reis R. US Patent 2000;6:054 051.

[180] Van Reis R, Saksena S. J Membr Sci 1997;129:19.

[181] Charles Christy, George Adams, Ralf Kuriyel, Glen Bolton, Seilly Alina. Desalination 2002;144:133.

[182] Ebersold MF, Zydney AL. Biotechnol Prog 2004;20:543.

[183] Van Eijndhoven RHCM, Saksena S, Zydney AL. Biotechnol Bioeng 1995;48:40.

[184] Zydney AL, Reis RV. Membrane Separations in Biotechnology New York: Marcel Dekker; 2001.

[185] Recio I, Slangen CJ, Visser S. Lait 2000;80:187.

[186] Pouliot Y, Gauthier SF, Lheureux J. Lait 2000;80:113.

[187] Wijers MC, Pouliot Y, Gauthier SF, Pouliot M, Nadeau L. Lait 1998;78:621.

[188] Pouliot Y, Wijers MC, Gauthier SF, Nadeau L. J Membr Sci 1999;158:105.

[189] Marshall AD, Munro PA, Tragardh G. J Membr Sci 1997;130:23.

[190] Weia J, Helma GS, Corner-Walkera N, Houb X. Desalination 2006;192:252.

[191] Boyd RF, Zydney AL. Biotechnol Bioeng 1998;59:451.

[192] Trettin DR, Doshi MR. Chem Eng Commun 1979;1:507.

[193] Aimar P, Baklouti S, Sanchez V. J Membr Sci 1986;29:207.

[194] Meireles M, Aimar P, Sanchez V. Biotechnol Bioeng 1991;38:528.

[195] Jiraratananon R, Uttapap D, Sampranpiboon P. J Membr Sci 1998;140:57.

[196] Tracey EM, Davis RH. J Colloid Interface Sci 1994;167:104.

[197] Duclos-Orsello C, Li W, Ho CC. J Membr Sci 2006;280:856.

[198] Ho CC, Zydney AL. J Colloid Interface Sci 2000;232:389.

[199] Taniguchi M, Kilduff JE, Belfort G. Environ Sci Tech 2003 ;37:1676.

[200] Clark WM, Banal A, Sontakke M, Ma YH. J Membr Sci 1991;55:21.

[201] Bowen WR, Gan Q. J Colloid Interface Sci 1991:144:254.

[202] Hlavacek M, Bouchet F. J Membr Sci 1993;82:285.

[203] Martinez F, Martin A, Pradanos P, Calvo JI, Palacio L, Hernandez A. J Colloid Interface Sci 2000;221:254.

[204] Herrero C, Pradanos P, Calvo JI, Tejerina F, Hernandez A. J Colloid Interface Sci 1997;187:344.

[205] Van Rijn CJM, Nano and Micro Engineered Membrane Technology. Elsevier: Amsterdam; 2004.

[206] Kuiper S, Van Rijn CJM, Nijdam W, Elwenspoek MC. J Membr Sci 1998;150:1.

[207] Girones M, Lammertink RGH, Borneman Z, Wessling M. J Membr Sci 2005;259:55.

[208] Girones M, Akbarsyah IJ, Nijdam W, Van Rijn CJM, Jansen HV, Lammertink RGH, Wessling M. J Memb Sci 2006;283:411.

[209] Girones M, Lammertink RGH, Wessling M. J Membr Sci 2006;273:68.

[210] Belfort G, Davis RH, Zydney AL. J Membr Sci 1994;96:1.

[211] Kelly ST, Zydney AL. J Membr Sci 1995;107:115.

[212] Marshall AD, Munro PA, Tragardh G. Desalination 1993;91:65.

[213] Guell C, Czekaj P, Davis RH. J Membr Sci 1999;155:113.

[214] Kelly ST, Zydney AL. Biotechnol Bioeng 1997;55; 91.

[215] Tracey EM, Davis RH. J Colloid Interf Sci 1994;167:104.

[216] Bowen WR, Calvo JI, Hernandez A. J Membr Sci 1995;101:153.

[217] Ho CC, Zydney AL. J Colloid Interf Sci 2000;232:389.

[218] Palacio L, Ho CC, Zydney AL. Biotechnol Bioeng 2002;79:260.

[219] Pieracci J, Wood DW, Crivello JV, Belfort G. Chem Mater 2000;12:2123.

[220] Chen H, Belfort G, J Appl Polym Sci 1999;72:1699.

[221] Kim IC, Choi JG, Tak TM. J Appl Polym Sci 1999;74:2046.

[222] Blanco JF, Sublet J, NguyenQT, Schaetzel P. J Membr Sci 2006;283:27.

[223] Hancock LF, Fagan SM, Ziolo MS. Biomaterials 2000;2:725.

[224] Park JY, Acar MH, Akthakul A, Kuhlman W, Mayes AM. Biomaterials 2006;27:856.

[225] Ying L, Wang P, Kang ET, Neoh KG. Macromolecules 2002;35:673.

[226] Nakao S, Yumoto S, Kimura S. J Chem Eng Japan 1982;15:463.

[227] Mignard D, Glass DH. J Membr Sci 2001;186:133.

[228] Weia J, Helma GS, Corner-Walkera N, Houb X. Desalination 2006;192:252.

[229] Pieraccia J, Crivellob JV, Belfort G. J Membr Sci 1999;156:223.

[230] Nystrom M, Jarvinen P. J Membr Sci 199;60:275.

[231] Yamagishi H, Crivello J, Belfort G. J Membr Sci 199;105:249.

[232] Chan R, Chen V. J Membr Sci 2004;242:169.

[233] Fane AG, Fell CJD, Suki A. J Membr Sci 1983;16:195.

[234] Munoz-Aguados MJ, Wiley D, Fane AG. J Membr Sci 1996;117:175.

[235] Nath S, Schutte H, Hustedt H, Deckwer WD. Biotechnol Bioeng 1993;42:829.

[236] Dalens F, Balmann HR, Sanchez V. Bioseparation 1995;5:127.

[237] Balmann HR, Cerro RM, Sanchez V. Electrophoresis 1998;19:1117.

[238] Jouve N, Clifton MJ. J Int Heat Mass Transfer 1991;34:2461.

[239] Horvath ZS, Corthals GL, Wrigley CW, Margolis J. Electrophoresis 1994;15:968.

[240] Margolis J, Corthals GL, Horvath ZS. Electrophoresis 1995;16:98.

[241] Rylatt DB, Napoli M, Ogle D, Gilbert A, Lim S, Nair CH. J Chromatogr A 1999;865:145.

[242] Liu Z, Huang Z, Chong J, Yang H, Ding F, Yuan N. Sep Sci Technol 1996;31: 1427.

[243] Liu Z, Zhao Y, Shen Z, Ding F, Yuan N. Sep Sci Technol 1997;32:1303.

[244] Galier S, Balmann HR. J Membr Sci 2004;241:79.

[245] Poulin JF, Amiot J, Bazinet L. J Biotechnol 2006;123:314.

[246] Keller K, Friedmann T, Boxman A. Trends Biotechnol 2001;19:438.

[247] Dutre B, Triigiirdh G. J Food Eng 1995;25:233.

[248] Simon A, Vandanjon L, Levesque G, Bourseau P. Desalination 2002;144:313.

[249] Skelton R. Membrane Technology: Technical and Applications Brief. Paper presented at a meeting of the Society of Chemical Industry: London; 1986.

[250] Chakravorty B, Singh, DP. Desalination 1990;78:279.

[251] Fane AG, Friend JP. Chemeca 1977;77:203.

[252] Porter M. Ind Eng Chem 1972;11:234.

[253] Akred AR, Fane AG, Friend JP. Ultrafiltration Membranes and Applications Plenum Press: NY; 1979.

[254] Grossman S, Bergman M. US patent 1992;5:093 474.

[255] Leuenherger BH. Food Hydrocolloids 1991;5:353.

[256] Jeantet R, Maubois JL, Boyaval P. Enzyme Microb Technol 1996;19:614.

[257] Senthuran A, Senthuran V, Mattiasson B, Kaul R. Biotechnol Bioeng 1997;55:841.

[258] Hjorleifsdottir S, Holst O, Mattiasson B. Bioprocess Engi 1991;6:29.

[259] Vogel JH, Kroner KH. Biotechnol Bioeng 1999;63:663.

[260] Levesley JA, Hoare M. J Membr Sci 1999;158:29.

[261] Jaffrin MY, Ding LH, Akoum O, Brou A. J Membr Sci 2004;242:155.

[262] Lee SS, Burt A, Russotti G, Buckland B. Biotechnol Bioeng 1995; 48:386.

[263] Parnham CS, Davis RH. Biotechnol Bioeng 1995;47:155.

[264] Luque S, Mallubhotla H, Gehlert G, Kuriyel R, Dzengeleski S, Pearl S. Biotechnol Bioeng 1999;63:247.

[265] Yebo Li, Abolghasem S, Charles TK. J Food Eng 2006;75:574.

CHAPTER II

EXPERIMENTAL METHEDOLOGIES

2.1. Spectroscopic characterization of charged membranes

Spectroscopy is essentially a technical procedure by which the energy difference between the allowed states of a system is measured by determining the frequencies of the corresponding light absorbed. Organic molecules absorb radiation, in discrete 'packets' of $\Delta E = h\nu$, which are also called quanta of energy. The absorbed quanta of energy bring about different kinds of excitation in the molecule and each requires its own distinctive energy ΔE. That is each type of excitation corresponds to the absorption of light in a different region of the electromagnetic spectrum [1]. Ultraviolet and visible light brings about movement of valence shell electrons, typically from a filled bonding molecular orbital to an unfilled anti-bonding orbital. The energy needed for this transfer lies in the range 40-300 k cal $mole^{-1}$. Infrared radiation causes vibrational excitation of the molecular frame work of a compound (ΔE is 1-10 k cal $mole^{-1}$); quanta of microwave radiation effect rotation around bonds (ΔE ~10^{-4}k cal $mole^{-1}$) and radio waves reorient nuclear spins (ΔE ~10^{-6}k cal $mole^{-1}$), a phenomenon which forms the basis of nuclear magnetic resonance spectroscopy. The vibrational excitation caused by the absorption of the infrared radiation is quantized and occurs by absorption of infrared radiation energy in the particular region of the spectrum. The position of an infrared absorption band is specified in frequency units by its wave number ($\bar{\nu}$) measured in reciprocal centimeters (cm^{-1}), or by its wavelength (λ), measured in micrometer.

2.1.1. Fourier Transform Infrared (FT-IR) Spectrophotometry

Fourier Transform Infra Red (FT-IR), the preferred method of infrared spectroscopic characterization. An infrared spectrum represents a fingerprint of a sample with absorption peaks which correspond to the frequencies of vibrations between the bonds of the atoms making up the material [2]. In an infrared spectrophotometer, infrared radiation of successively increasing

wavelength was passed through the sample of the compound and the percent transmittance was measured. An infrared spectrum is the graph of percent transmittance versus either increasing wavelength or decreasing frequency. Infrared spectrum shows percent transmittance versus frequency expressed as wave numbers, which have the units of reciprocal of centimetres (cm^{-1}). Each dip in a spectrum called a band or peak represents absorption of infrared radiation at that frequency by the sample. A 100 % transmittance means no absorption and if all the radiation is absorbed the transmittance is 0%. In the spectrum the region from 600 to 1400 cm^{-1} is called the fingerprint region because the pattern of absorption is unique to any particular compound, just as a person's fingerprints are unique. The infrared region constitutes three parts, the near infrared, middle infrared and far infrared. The near infrared region corresponds to energies in the range 37-10 kcal mol^{-1}. It is of little use because of the few organic compounds absorbs in this region. Radiation in the middle infrared region (usually 4000-650 cm^{-1}) has energy in the range 10-1 kcal mol^{-1}, an important region because most of the organic compounds absorbs in this region. The far infrared region has energy in the range 1.0-0.1 kcal mol^{-1}. This region is also of not much use since only little useful absorption occurs here. The spectrum of all the synthesized charged membranes was recorded in the middle infrared region using spectrum GX series49387 FT-IR spectrophotometer.

2.1.1.1. Attenuated total reflection–Fourier transforms infrared spectroscopy (ATR-FTIR)

ATR-FTIR is used to identify the types of chemical bonds or functional groups present in membrane samples. For analysis a sample membrane is pressed against an eternal reflection element (IRE) which may be a block of zinc selenide or germanium [3,4] under vacuum condition (Fig. 2.1.1). IR radiation covering a certain frequency range (corresponding to wave numbers in the infrared spectrum between 4000 and 400 cm^{-1}) is focused onto the end of the IRE where the beam under goes total internal reflection before exiting and arriving at a detector. At each internal reflection the IR beam penetrates

a short distance from the surface to the IRE to the sample, forming an evanescent wave at the interface ATR–FTIR analyses are thus based on the interaction between the evanescent wave and any adsorbed species. ATR–FTIR has been widely used to characterize the chemical composition, physical structure and morphology of clean, unused membranes [5,6].

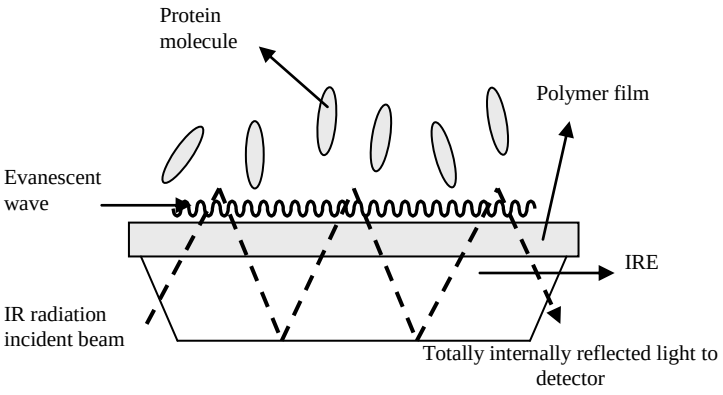

Figure 2.1.1. Diagram illustrating flow-cell operation in ATR–FTIR.

2.1.2. Nuclear magnetic resonance (NMR) spectroscopy

Nuclear magnetic resonance spectroscopy is the technique which exploits the magnetic properties of certain nuclei. Principally proton NMR (^{1}H-NMR) and carbon-13 NMR (^{13}C) spectroscopy has been used to characterize the prepared charged ultrafilter membranes. When placed in a magnetic field, NMR active nuclei (such as ^{1}H or ^{13}C) absorb at a frequency characteristic of the isotope. The resonant frequency, energy of the absorption and the intensity of the signal are proportional to the strength of the magnetic field. As the name indicates, ^{1}H-NMR spectroscopy involves the change of the spin state of nuclear magnetic moment of the proton when the nucleus absorbs electromagnetic radiations in a strong magnetic field [1]. By studying the membranes by ^{1}H-NMR, one can obtain the following information. Initially it gives the relation between the number of signals in the spectrum and the number of different kinds of the hydrogen atoms in the molecule. Thus one can know the different kinds of environments of the hydrogen atoms in the polymer. The area underneath each signal is in the same ratio as the number of hydrogen atoms causing each signal. The principal signal may get splits into smaller peaks i.e., spin-spin splitting may be observed. The type of splitting pattern observed (doublet, triplet, quartet

and so forth) depends on the number of neighboring nonequivalent protons. For many simple compounds, one can predict the splitting pattern with *n+1* rule, where *n* is the number of neighboring protons. Spin-spin splitting thus helps in deducing molecular structure. The spacing between the peaks as a result of spin-spin splitting is denoted by *J* with units of cycles per second or Hertz (Hz). *J* is the coupling constant between two protons and it gives further information on the molecular structure and stereo chemical features. It is also possible to evaluate quantitatively degree of sulphonation by ^{1}H-NMR spectroscopy.

In the ^{1}H-NMR spectra the presence of a sulphonic group causes a significant downfield shift from 7.31 ppm to 8.21 ppm of the hydrogen located in the ortho position at the aromatic ring. By evaluating the ratios between the peak area of the signal corresponding to the hydrogen atoms located next to the sulphonic acid groups (H_E) and the peak areas of the signals corresponding to the other aromatic hydrogen atoms, the extent of sulphonation could be calculated using the Eq. 2.3. In Eq. 2.1, *n* is the number of H_E hydrogen atoms and α-2n is the number of residual hydrogen atoms of aromatic rings. α Denotes total number of hydrogen atoms with different electron density in the aromatic rings and is 8 for poly (ether sulfone) (PES). Degree of sulphonation of PEEK and PES were estimated using the following mathematical expressions [7,8],

$$\frac{n}{(\alpha - 2n)} = \frac{AH_E}{\sum AH}, \qquad (2.1)$$

and with

$$z = \frac{AH_E}{\sum AH}, \qquad (2.2)$$

$$X = \frac{\alpha z}{(1 \div 2z)} \times 100, \qquad (2.3)$$

where *x* = degree of sulphonation (mole %), AH_E = integral of H_E, ΣAH = integrals of the remaining hydrogen atoms.

2.2. Thermal analysis of charged membranes

The group of technique that has been developed to make analytical instrument during heating is given the general name 'thermal analysis'. Thermal analysis comprises a group of techniques in which the physical property of a substance is measured as a function of temperature, while the substance is subjected to a controlled temperature program [9]. In differential thermal analysis, the temperature difference that develops between a sample and an inert reference material is measured, when both are subjected to identical heat-treatments. The related technique of differential scanning calorimetry relies on differences in energy required to maintain the sample and reference at an identical temperature.

2.2.1. Thermal Gravimetric Analysis (TGA)

TGA is a simple analytical technique that measures the weight loss (or weight gain) of a material as a function of temperature. It is used to characterize the polymeric materials to determine changes in weight in relation to change in temperature and thermal stability of membranes.

As materials are heated, they can loose weight from a simple process such as drying, or from chemical reactions that liberate gasses. Some materials can gain weight by reacting with the atmosphere in the testing environment. Since weight loss and gain are disruptive processes to the sample material or batch, knowledge of the magnitude and temperature range of those reactions are necessary in order to design adequate thermal ramps and holds during those critical reaction periods. The measurement is normally carried out in air or in an inert atmosphere, such as Helium or Argon, and the weight is recorded as a function of increasing temperature. The record is the thermo-gravimetric or

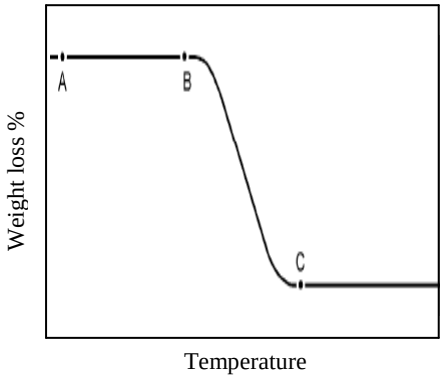

Figure 2.2.1. Formalized TGA curve.

TG curve; the mass should be plotted on the ordinate decreasing downwards and temperature (*T*) or time (*t*) on the abscissa increasing from left to right (Fig. 2.2.1). As many weight loss curves look similar, the weight loss curve may require transformation before results may be interpreted. A derivative weight loss curve can be used to tell the point at which weight loss is most apparent.

TGA is inherently quantitative, and therefore an extremely powerful thermal technique, but gives no direct chemical information. The ability of TGA to generate fundamental quantitative data from almost any class of materials, has led to its widespread use in every field of science and technology. The key information obtained from TGA is listed below:

- Thermal Stability: related materials can be compared at elevated temperatures under the required atmosphere. The TG curve can help to elucidate decomposition mechanisms.
- Kinetic Studies: a variety of methods exist for analyzing the kinetic features of all types of weight loss or gain, either with a view to predictive studies, or to understand the controlling chemistry.
- Material characterization: TG and DTG curves can be used to "fingerprint" materials for identification or quality control.
- Corrosion studies: TG provides an excellent means of studying oxidation, or reaction with other reactive gases or vapours.
- Simulation of industrial processes: the thermo-balance furnace may be thought of as a mini-reactor, with the ability to mimic the conditions in some types of industrial reactor.
- Compositional analysis: by careful choice of temperature programming and gaseous environment, many complex materials or mixtures may be analyzed by selectively decomposing or removing their components. This approach is regularly used to analyze e.g. filler content in polymers, carbon black in oils, ash and carbon in coals, and the moisture content of many substances.

TGA is commonly employed to asses the degradation process and the thermal stability of the membranes were investigated using TGA (Mettler Toledo TGA/SDTA851^{e} with star^{e} software), under nitrogen atmosphere with heating rate of 10 ^{o}C/min from 50 to 600 ^{o}C.

2.2.2. Differential scanning calorimetric analysis (DSC)

Differential scanning calorimetry (DSC) is a thermo-analytical technique in which the difference in the amount of heat required to increase the temperature of a sample and reference are measured as a function of temperature. In DSC, the thermal properties of a sample are compared against a standard reference material, which has no transition in the temperature range of interest, such as powdered alumina (Fig. 2.2.2). Both the sample and reference are maintained at nearly the same temperature throughout the experiment. The basic principle underlying this technique is that, when the sample undergoes a physical transformation such as phase transitions, more (or less) heat will need to flow to it than the reference to maintain both at the same temperature. Whether more or less heat must flow to the sample depends on whether the process is exothermic or endothermic [10]. DSC may also be used to observe more subtle phase changes, such as glass transitions. DSC is widely used in industrial settings as a quality control instrument due to its applicability in evaluating sample purity and for studying polymer curing. Theses measurements provide quantitative and qualitative information about physical and chemical changes that involve endothermic and exothermic process and change in heat capacity.

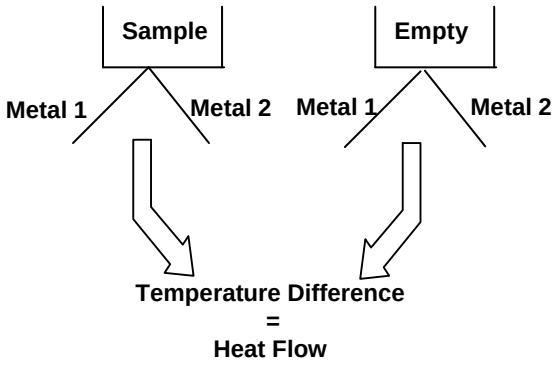

Figure 2.2.2. Representative sample holder within an adiabatic enclosure in DSC analysis.

A plot of the difference in energy supplied to the sample against the average temperature, as the latter is slowly increased through one or more thermal transitions of the sample yields important information about the transition, such as latent heat or a relatively abrupt change in heat capacity. The glass transition process is illustrated in the Fig. 2.2.3 below for a glassy polymer, which does not crystallize and is being slowly heated from below T_g. Here, the drop marked T_g at its midpoint represents the increase in energy supplied to the sample to maintain it at the same temperature as the reference material, due to the relatively rapid increase in the heat capacity of the sample as its temperature is raised through T_g. The addition of heat energy corresponds to this endothermal direction.

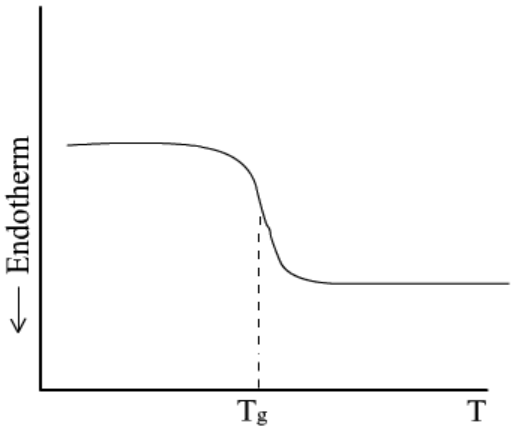

Figure 2.2.3. Typical thermogram of DSC analysis.

A melting process is also illustrated in Fig. 2.2.4 for the case of a highly crystalline polymer, which is slowly heated through its melting temperature (T_m). Again, as the melting temperature is reached, an endothermal peak appears because heat must be preferentially added to the sample to continue this essentially constant temperature process. The peak breadth is primarily related to the size and degree of perfection of the polymer crystals. Note that if the process were reversed so that the sample was being cooled from the melt, the plot would be inverted. In that case, as both are being cooled by ambient conditions, even less heat

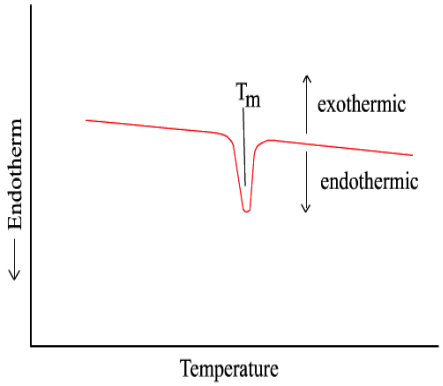

Figure 2.2.4. Typical melting process in DSC analysis.

would need to be supplied to the sample than to the reference material, in order that crystals can form. This corresponds to an exothermal process.

The key information obtained from DSC are Glass transitions, melting and boiling points, crystallisation time and temperature, percent crystallinity, heats of fusion and reactions, sspecific heat capacity, oxidative/thermal stability, rate and degree of cure, rreaction kinetics, purity.

Polymers are unique in the dominance of the glass transition as the decisive factor in their mechanical properties. Polymers are the only material for which the equilibrium ground state is often glassy rather than crystalline. This is because topological and stereo- chemical constraints prevent the formation of crystals in many cases. The glass transition is often called a pseudo-second order transition because of the dominance of kinetics. Slower cooling rates in the DSC, for instance, lead to lower measured values of the glass transition. The DSC of developed membrane was carried out using a Mettler Toledo DSC822^{e} thermal analyzer with star^{e} software.

2.3. Dynamic mechanical analysis (DMA)

Dynamic mechanical analysis (DMA), is useful for observing the viscoelastic nature of polymers. When a polymer is subjected to a forced mechanical vibration at a fixed frequency, temperature and elongation a fraction of the energy is absorbed and a fraction is returned elastically [10]. The use of DMA is in understanding the mechanical response of elastomers. The mechanical properties of the membrane under investigation were carried out at room temperature with different force and frequencies in order to assess their suitability for different processes.

Viscoelastic materials such as polymers typically exist in two distinct states. They exhibit the properties of a glass (high modulus) at low temperatures and those of a rubber (low modulus) at higher temperatures. By scanning the temperature during a DMA experiment this change of state, the glass transition or alpha relaxation, can be observed. DMA technique is more sensitive and yields more easily interpreted data. DMA can also be used

to investigate the frequency (and therefore time) dependent nature of the transition. This is usual, as the degree of dependence is specific to the transition type. In addition, DMA gives modulus values. This analysis of mechanical strength of the membranes was carried out using a Mettler Toledo dynamic mechanical analysis (DMA) 861^{c} instrument with star^{c} software under isothermal conditions.

2.4. Scanning electron microscopy (SEM)

The Scanning electron microscope (SEM) is a scientific instrument that uses a beam of highly energetic electrons to examine objects on a very fine scale rather than light to form an image [5]. Electron microscopes were developed due to the limitations of light microscopes, which are limited by the physics of light to 500x or 1000x magnification and a resolution of 0.2 micrometers. With the use of electron beam one can get the magnification of 10,000x and plus. SEM can yield following information of the sample under study. i) Topography, the surface features of an object or "how it looks", its texture; direct relation between these features and materials properties (hardness, reflectivity etc.). ii) Morphology, the shape and size of the particles making up the object; direct relation between these structures and materials properties (ductility, strength, reactivity etc.). iii) Composition, the elements and compounds that the object is composed of and the relative amounts of them; direct relationship between composition and materials properties (melting point, reactivity, hardness etc.). iv) Crystallographic information, how the atoms are arranged in the object; direct relation between these arrangements and materials properties (conductivity, electrical properties, strength etc.).

SEM images of the charged membranes were recorded using Leo microscope at 15kV accelerating voltage after gold coating.

2.5. Physicochemical and electrochemical characterization of charged membranes

In charged membranes, the fixed anions are in electrical equilibrium with mobile cations in the interstices of the polymer. In contrast, the mobile anions, called co-ions, are more or less completely excluded from the polymer matrix because of their electrical charge, which is identical to that of the fixed ions. This type of exclusion called Donnan-exclusion in the honor of his pioneer work [11]. Due to the exclusion of co-ions, a cationic membrane permits transfer of cations only. Anionic membranes carry positive charges fixed on the polymer matrix. Therefore, they exclude all cations and are permeable to anions only. Thus the selectivity of membrane results from the exclusion of co-ions from the membrane phase. The Donnan-exclusion and thus membrane selectivity depend on: (i) the concentration of the fixed ions; (ii) the valence of co-ions; (iii) the valence of counter-ions; (iv) the concentration of the electrolyte solution; and (v) the affinity of the exchanger with respect to the counter-ions.

Additional important parameters for the characterization of charged membranes are the density of the polymer network, hydrophobic and hydrophilic properties of the matrix polymer, charge density, membrane conductivity, and their morphology. It is difficult to optimize the properties of charged membranes because the parameters determining different properties often have opposing effects. For instance, a high degree of cross-linking improves the mechanical strength of the membrane but also increases the electrical resistance. The properties of charged membranes are determined by two parameters, namely the basic polymer matrix and the nature and concentration of fixed ionic moiety. The basic polymer matrix determines to a large extent the mechanical, chemical and thermal stability of the membrane, while the concentration of the fixed ionic charges determine the permselectivity and electrical resistance of the membrane but they also have significant effect on the mechanical properties of the membrane [12-15].

2.5.1. Contact angle measurement

Contact angle is an invaluable metric for understanding material surface properties like adhesion, wettability, and solid surface free energy. This angle (θ) is made at which a liquid/vapor interface meets the solid surface. It is a quantitative measure of the wetting of a solid by a liquid. The theoretical description of contact arises from the consideration of a thermodynamic equilibrium between the three phases: the liquid phase of the droplet (*L*), the solid phase of the substrate (*S*), and the gas/vapor phase of the ambient (*V*) (which will be a mixture of ambient atmosphere and an equilibrium concentration of the liquid vapor). The *V* phase could also be another (immiscible) liquid phase. At equilibrium, the chemical potential in the three phases should be equal. It is convenient to frame the discussion in terms of the interfacial energies. We denote the solid-vapor interfacial energy (see surface energy) as γ_{SV}, the solid-liquid interfacial energy as γ_{SL} and the liquid-vapor energy (i.e. the surface tension) as simply γ, we can write an equation that must be satisfied in equilibrium (known as the Young Eq. (2.4.))

$$\theta = \gamma_{sv} - \gamma_{sl} - \cos\phi_{\,c} \qquad (2.4)$$

Contact angle can be measured by producing a drop of pure liquid on a solid. The angle formed between the solid/liquid interface and the liquid/vapor interface and which has a vertex where the three interfaces meet is referred to as the contact angle. This angle is specific for any given system. Three interfaces (liquid/solid/vapor) boundary is in actual motion the angles produced are called "Dynamic Contact Angles" and are referred to as 'advancing' and 'receding' angles. When the drop has recently expanded the angle is said to represent the 'advanced' contact angle. If the liquid is very strongly attracted to the solid surface (for example water on a strongly hydrophilic solid) the droplet will completely spread out and the contact angle will be close to 0°, which reflects better wetting, adhesiveness, and higher surface energy. Less strongly hydrophilic solids will have a contact angle up

to 90°. This condition is exemplified by poor wetting, poor adhesiveness and the solid surface free energy is low [16].

Assessment of extent of hydrophilic nature of membranes, contact angle in water of membranes was measured with a tensiometer (DCAT 21, Dataphysics, Filderstadt, Germany) based on energy balance approach to the three-phase equilibrium.

2.5.2. Molecular weight cutoff of membrane

Protein retention in ultrafiltration has traditionally been viewed as a purely size based exclusion phenomena. The rejection characteristic of ultrafilter membranes are usually expressed as a nominal molecular weight cut off. This number refers to the molecular weight (Dalton) of species, which would be expected to have a R_i value of at least 0.9. Molecular weight cutoff (MWCO) profile of retention curve is constructed by measuring the R_i values of chemically similar compounds with varying molecular weights. In other words MWCO is defined as 'molecular weight of protein which is 90% retained by the membrane, it provides minimal information on product retention since membrane with the same MWCO but different pore size distributions can have very different behaviour at the > 99 % retention level needed for ultrafiltration process.

The MWCO of charged ultrafilter membranes were determined by polyethylene glycol (PEG) rejection analysis by plotting the rejection against the molecular weight. The MWCO curve was obtained by plotting the rejection of each solute against the molecular weight. The observed solute rejection (R_i) for a given species i was determined by Eq. 2.5.:

$$R_i\,(\%) = \left(1 - \frac{(C_P)_i}{(C_F)_i}\right) \times 100 \qquad (2.5)$$

$(C_P)_i$ and $(C_F)_i$ are the concentration in permeate and feed solution, respectively. Samples of feed and filtrate are taken under steady state conditions. The concentration of PEG in feed and permeate were analyzed by chromatographic technique.

2.5.3. Water uptake properties of charged membranes

The swelling capacity of a charged membrane determines not only its dimensional stability but also affects its selectivity, electrical resistance and hydraulic permeability. It depends on the nature of the polymeric material, the ion-exchange capacity and the cross-linking density. Usually the swelling of a membrane is expressed in turn of water content or uptake (φ_w) under given experimental conditions and can be defined by weight difference between the wet and dry membrane,

$$\Phi = \frac{(W_h - W_d)}{W_d} \qquad (2.6)$$

Here, W_h *is* the wet membrane weight and W_d is the dry membrane weight.

A sample is equilibrated in deionized water, after removing the surface water from the sample the wet weight of the swollen membrane is determined. Then the sample was dried at elevated temperature until a constant weight was obtained. The water uptake was determined as weight percentage from the weight of the dry and wet sample. Water content in terms of water concentration in the membrane phase can be determined by means of the following equation [17-18],

$$C_w^m = (W_w - W_d)\rho_m \Big/ W_w M_w \qquad (2.7)$$

where C_w^m designates the concentration of water in the membrane, ρ_m the density of wet membrane and M_w the molar mass of water (18 g mol^{-1}).

The membrane porosity τ (volume of free water within membrane per unit volume of wet membrane) can be obtained by following equation:

$$\tau = \Delta V \Big/ (1+\Delta V) \qquad (2.8)$$

where ΔV designates the volume increase of the membrane upon absorption of the water per unit dry membrane volume, which may be estimated by using following equation.

$$\Delta V = (W_w - W_d)\,\rho_d / \rho_w W_d \qquad (2.9)$$

Where ρ_d is the density of dry membrane and ρ_w is the density of water, which enters into the membrane.

2.5.4. Determination of membrane ion-exchange capacities

The ion-exchange capacity of charged membranes is determined by titrating the fixed ions, e.g. $-SO_3^-$ or $-R_4N^+$ group with 0.1N NaOH or HCl, respectively. For these tests, cationic and anionic charged membranes are equilibrated for about 6 hr. in 1N HCl or NaOH respectively, and then rinsed free from chloride or sodium with deionized water. The ion-exchange capacity of the sample is then determined by back titration with 0.1N NaOH or HCl, respectively. Weak base anionic charged membranes are characterized by equilibration in 1N NaCl solution and titrated with standardized 0.1N $AgNO_3$ solution. The sample was dried and the ion-exchange capacity (E_c; mequiv./g) of the membrane is calculated by Eq. 2.10.

$$E_c = ab/w \qquad (2.10)$$

where a is the burette reading of acid, base or silver nitrate, b is the concentration of acid, base or silver nitrate and w is the dry weight of the membrane (gm.).

Further more, Ion-exchange capacity can be used for the determination of fixed-ion concentration (X^m) of the membrane in units of (moles of sites)/ (unit volume of wet membrane) by Eq. 2.11.

$$X^m = \tau(IEC)\rho_d / \Delta V \qquad (2.11)$$

where IEC is expressed in equiv/g of dry membrane and τ and ρ_d expressed as in Eq. (2.10) and (2.11).

2.5.5. Membrane Potential Measurements

It was observed that when a membrane separated two electrolyte solutions, an electric field (diffusion potential) maintain electro-neutrality and brought about the balance of fluxes. The magnitude and sign of potential

depended on the nature of the membrane and the permeating species. If the membrane carried no fixed charges, the potential was the same at the liquid junction potential. Whereas, if the membrane carried some fixed charges, the magnitude of the potential was determined by the concentration of the external solution and its sign by the nature of the fixed charge. However, it is found that many membranes considered completely inert, because of the absence of measurable quantity of fixed charge, have a tendency to generate an electric potential. This was attributed to the adsorption of cations or anions to make them anion or cation selective.

The electrical potential arising across an ionic membrane separating different salt solutions are usually measured by constructing cells of the type as presented in Fig. 2.5.1. The reference electrode may be reversible electrode of the type Ag-AgCl standing in chloride solution or calomel connected to the solutions via KCl-agar bridges. In the former case the total potential measured is made up of two compartments, one the electrode potential and the other the membrane potential. In the case of latter, the cell potential directly gives the membrane potential. These measurements to evaluate membrane potential are not unambiguous [19-20]. These types of measurements have become routine procedures to characterize the selectivity of membranes. The total membrane potential is considered to be composed of two Donnan potentials at the two solution membrane interfaces 1 and 2 and a diffusion potential arising from unequal concentration of the two membrane faces. The membrane surfaces are assumed to be in a state of equilibrium instantaneously established although this seems less true as the concentration gradient and consequent steady diffusion of the electrolyte and solvent become appreciable. Detailed

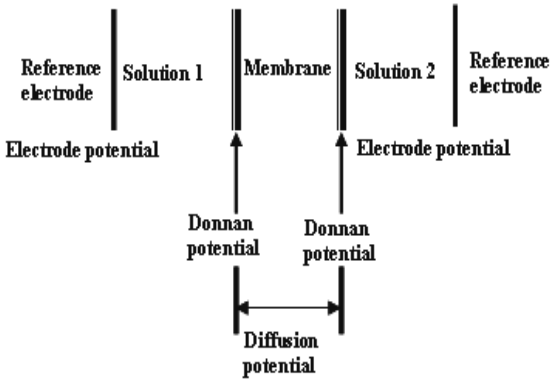

Figure 2.5.1. Schematic diagram for membrane potential measurements

experimental set up used for membrane potential measurements is shown in Fig. 2.6 Selective transport of counter-ion through membrane is quantitatively expressed in terms of permselectivity. The measurement of permselectivity can be done in terms of counter-ion transport number.

Transport number is determined by the Hitorf's method, where concentration of certain ions increases in the feed and decreases in the dilute solution, which was measured by passing known amount of current through the unit during the electro-dialysis. A faster method for the determination of apparent permselectivity is based on membrane potential measurement. The experimental set-up for the membrane potential measurement is shown in Fig. 2.5.2. The advantage of the determination of the potential between two solutions of different concentrations is that the tests are not obscured by concentration polarization effect at the membrane surface.

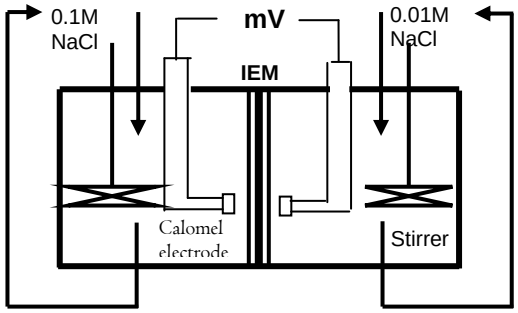

Figure 2.5.2. Schematic experimental set for the determination of membrane permselectivity by membrane potential

Membrane potential data are used to calculate counter ion transport number using Eq. 2.12.

$$E^m = (1 - 2t_i^m)\frac{RT}{nF}\ln\frac{a_1}{a_2} \qquad (2.12)$$

Where E^m is the potential difference between two solutions containing electrolyte solutions, n is electro-valence of electrolyte, t_i^m the transport number a_1 and a_2 are activities of electrolyte solutions, R the gas constant, T temperature and F faraday constant. The superscript 'm' refers to the membrane, respectively.

Ion selectivity of membranes is quantitatively expressed in terms of membrane permselectivity, which measures the ease with which counter-ion migration occurs through membrane, and is defined as [21-23].

$$P = \frac{t_i^{\,M} - t_i}{1 - t_i} \qquad (2.13)$$

Here, P = permselectivity of membrane, t_i^m = counter-ion transport number through the membrane, t_i= counter-ion transport number in the solution phase.

Further, with the knowledge of permselectivity, fixed charge density of the ion-exchange membranes can be obtained using the relation.

$$\phi_x = \frac{2CP}{\sqrt{1 - P^2}} \qquad (2.14)$$

Where 'C' denotes the mean concentration. Thus the permselectivity of membranes relates the transport of electric charges by specific counter-ion to the total transport of electric charges through the membrane. An ideal cation selective membrane would transmit positively charged ions only. The permselectivity approached 'zero' when the transference number within the membrane is the same as in the electrolyte solution. Due to the 'Donan-Exclusion' the permselectivity of membrane depends upon the concentration of electrolyte in the solution and on the ion exchange capacity of membranes.

2.6. Membrane permeability measurements

To investigate the impact of membrane forming materials, their charged nature and optimum condition of gelation on the membrane performance and throughput, volumetric fluxes (J) through the membranes were measured under varied applied pressure (membrane hydrodynamic permeability) and electrical gradient (electro-osmotic permeability), separately in equilibration with NaCl solution of 0.001 mol dm^{-3} concentration [24].

2.6.1. Electro-osmotic permeability measurements

If electric field is applied to such charged surfaces, force is exerted on both solutions part of double layer and the charge surface. At immobile surface the solution part of double layer will respond to shear, the part close

to the surface remaining stationary but the reminder part of solution will move under the influence of field carrying solvent with it. This process is called as 'electro-osmosis'. Solvent is transported either by an association with the transported ion, such as hydration sphere, or by hydrodynamic pumping due to the movement of the ions and associated solvent molecules. This solvent transport accompanying the ion transport through the membrane is termed as electro-osmosis. The application of an electric field to a membrane causes not only transport of ions but also transport of liquid existing in the pores of the membrane [25]. This solvent transport occurs due to solvation of ions through a membrane under applied potential can be called in a phenomenological way electro-osmosis. Usually this transport takes place in the direction in which the counter-ions moves. As counter-ions experience less resistance due to solvent movement also in the same direction, they move faster than co-ions. True transport numbers of counter-ions account for increased ion transport due to convection.

Electro-osmotic permeability of charged membranes was measured in a two-compartment membrane cell [26] with effective membrane area of 24.0 cm^2, in equilibration with 0.001M NaCl solutions (Fig. 2.6.1). Both compartments were kept in a state of constant agitation by means of magnetic and mechanical stirrer. A known potential difference was imposed across the membrane with the help of electronically operated power supply using Ag/AgCl electrodes and ensuing volumetric flux was measured by observing movement of liquid in a horizontally fixed capillary tube of known radius. The current flowing

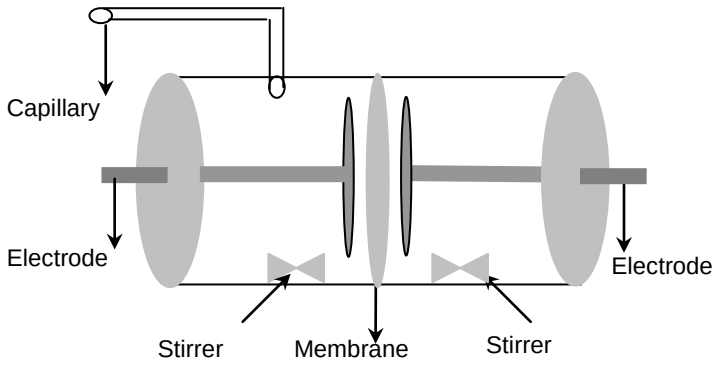

Figure 2.6.1. Cell used for electro-osmotic flux measurements

through the system was also measured using a digital ammeter connected in series. Several measurements were performed in order to obtain reproducible values. The electro-osmotic permeability of membrane can be defined as

$$\left(\frac{J}{\Delta I}\right) = L_{12} \qquad (2.15)$$

Where L_{12} is electro-osmotic permeability of the charged membranes (Amp^{-1} cm s^{-1}), J is the pure water flux (l $m^{-2}h^{-1}$) and ΔE is applied potential gradient across the membrane. Knowledge of the electro-kinetic properties such as zeta potential of a particular membrane will be proved to be major contributing factor behind the decision to implement that membrane for a specific separation process, as the surface charge on synthetic membrane has significant effect on its separation properties and fouling tendency. The zeta potential (ξ) can be obtained from electro-osmotic permeability (L_i) using Smoluchowski equation.

$$J/I = \varepsilon_0 \varepsilon_r \xi / \eta \kappa \qquad (2.16)$$

Where ε_0 is the permittivity of vacuum, ε_r the relative dielectric constant of the electrolyte, η the electrolyte viscosity, and κ is the conductivity of the electrolyte. In general, the zeta potential of the membranes is supposed to represent the charge characteristics of membrane-solution interfacial zone due to presence of charges at membrane surfaces. Furthermore, values of zeta potentials of these membranes suggest their capability for charge based selection/rejection.

2.6.2. Hydrodynamic permeability

Hydrodynamic permeability is the volume of liquid passed through one unit area of membrane surface for one time unit of pressure difference.

Water can penetrate through either gel areas or intergel areas in a membrane. The intergel areas are less cross-linked, and the water flow would meet less resistance in these areas. However, volumetric fraction of intergel

areas is small; therefore, it is not possible to predict the contribution of gel areas and intergel areas in the total hydraulic permeability.

The membrane permeability is typically evaluated from the water (buffer) volumetric flux J_v (l m $^{-2}$h^{-1}) through the membrane as a function of the trans membrane pressure based on Darcy's law;

$$J_v = \frac{V}{S\,t\,\Delta P} \qquad (2.17)$$

where V is the volume of fluid transported (m^3), S is the membrane active surface area (m^2), t is the time (h) span of transport collection, and ΔP is applied hydrostatic pressure across the membrane. The volume of fluid transported through the membranes linearly increased with time and pressure [27]. Charged nature of the membrane influences the membrane flux because the increase in membrane compactness or decrease in its hydrophilic characteristics with decrease in functional nature.

To investigate the impact of the membrane forming materials, their charged nature, optimum casting and gelation conditions, performance and throughput and volumetric fluxes of both membranes was evaluated by under applied pressure and electric gradient. In all cases, straight line passed through origin was obtained. Hydrodynamic permeability (L_{12}) of the membrane was evaluated directly from the slope of the volumetric flux (J_v; volume flow rate per membrane area) versus pressure (ΔP) data:

$$L_{11} = J_v \big/ \Delta P \qquad (2.18)$$

Values of L_{11} were used with advantage for the estimation of apparent pore radius (r_p) using Eq. (2.19).

$$L_{11} = \frac{r_p^2}{8\eta\left(\delta/\lambda\right)} \qquad (2.19)$$

where L_{11} is the hydrodynamic permeability of the charged membrane (cm^3 Ncm^{-2} s^{-1}), δ denotes membrane thickness, η the coefficient of viscosity of the permeate and water content (dimensionless) of the membrane.

2.7. Electrical resistance of charged membranes

The electrical resistance of charged membranes is one of the factors that determine the energy requirements of electro-dialysis processes. It may be noted that true electrical resistance is measured by AC or electrochemical impedance at certain frequency. It is however, in most practical cases considerably lower than the resistance of the dilute solutions, since the ion concentration in the membrane is relatively high. The specific membrane resistance is given as Ω cm^{-1}. From the engineering point of view, the membrane area resistance in Ω cm^2 is more convenient. As reported, membrane resistance is measured with the help of the cell composed of two black graphite electrodes fixed on Plexiglas plates with known active area of electrodes as well as membrane [28]. Both electrodes were not in direct contact with membrane. Membrane resistance (R^m) is estimated by subtraction of electrolyte resistance (R_{sol}) without membrane from membrane resistance equilibrated in electrolyte solutions (R_{cell}) [$R^m = R_{cell} - R_{sol}$].

The effective membrane resistance determined experimentally as a function of solution concentration in equilibrium with the membrane, could be used for the estimation of membrane specific conductivity. The specific conductivity κ^m of the membrane in given by the eq. 2.20.

$$\kappa^m = \frac{\Delta x}{A R^m}, \qquad (2.20)$$

where Δx is the thickness of the wet membrane, A it's area and $1/R^m$ its electrical conductivity.

2.8. Protein concentration analysis

2.8.1. High Performance Liquid Chromatography (HPLC)

HPLC is widely used analytical technique in biochemistry and analytical chemistry to separate, identify, and quantify compounds. HPLC utilizes a liquid mobile phase to separate the components of a mixture.

These components (or analytes) are first dissolved in a solvent, and then forced to flow through a chromatographic column under a high pressure (up to 400 atmospheres), that makes it much faster (Fig. 2.8.1). In the column, the mixture is resolved into its components. The interaction of the solute with mobile and stationary phases can be manipulated through different choices of both solvents and stationary phases and a detector that shows the retention times of the molecules. Retention time varies depending on the interactions between the stationary phase, the molecules being analyzed, and the solvent(s) used. As a result, HPLC acquires a high degree of versatility not found in other chromatographic systems and it has the ability to easily separate a wide variety of chemical mixtures. It also allows you to use a very much smaller particle size for the column packing material which gives a much greater surface area for interactions between the stationary phase and the molecules flowing past it. This allows a much better separation of the components of the mixture. The other major improvement over column chromatography concerns the detection methods which can be used. These methods are highly automated and extremely sensitive [29].

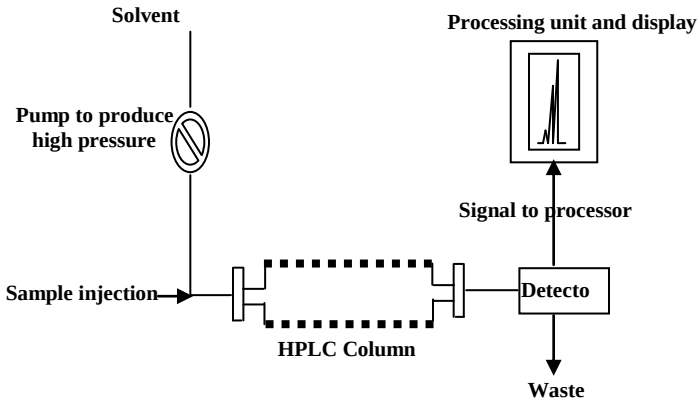

Figure 2.8.1. Schematic of HPLC instrument.

HPLC as compared with the classical technique is characterized by:

- Small diameter (2-5 mm), reusable stainless steel columns;
- Column packings with very small (3, 5 and 10 µm) particles;
- Relatively high inlet pressures and controlled flow of the mobile phase;
- Precise sample introduction without the need for large samples;
- Special continuous flow detectors capable of handling small flow rates and detecting very small amounts;
- Automated standardized instruments;
- Rapid analysis;
- High-resolution.

Single and mixed protein concentration was determined by high performance liquid chromatography (HPLC) (Prominence, Shimadzu HPLC) using BioSep-SEP-S2000 (Phenomenex) column with geometry 300 mm × 7.80 mm. The used mobile phase was a phosphate buffer (NaH_2PO_4/Na_2HPO_4; 5.0 mM, pH 7.0); the wavelength determination for both proteins was 280 nm. Flow rate of the mobile phase was adjusted to 1.0 mL/min. and oven temperature was set on 30.0 ^{0}C. Retention time for Casein, Bovine Serum Albumin and Lysozyme was observed at 10.23, 12.58 and 6.14 min respectively. Determination of the proteins concentrations was achieved up to ± 0.001 mg/ml.

2.8.2. Ultraviolet visible (UV) Spectrophotometry

Change in concentration of protein solution is measured with the help of ultraviolet-visible (UV) spectrophotometry. The method is most often used in a quantitative way to determine concentrations of an absorbing species in solution, using the Beer-Lambert law:

$$A = -\log_{10}\left(I/I_o\right) = \varepsilon c l \qquad (2.21)$$

where A is the measured absorbance, I_0 is the intensity of the incident light at a given wavelength, I is the transmitted intensity, l the path length through

the sample, and c the concentration of the absorbing species. The instrument used in UV spectroscopy is called a UV/vis spectrophotometer. It measures the intensity of light passing through a sample (I), and compares it to the intensity of light before it passes through the sample (I_o). The ratio I/I_o are called the transmittance, and are usually expressed in percentage (%T). The absorbance, A, is based on the transmittance:

$$A = -\log(\%T) \qquad (2.22)$$

Considering the change in absorbance by solution after every 1h, concentration change was calculated with the help of reference graphs. The concentration of Bovine Serum Albumin and lysozyme was measured by ultraviolet spectroscopy at 280 nm and that of haemoglobin is measured at 420 nm.

2.9. Adsorption on protein on membrane surface

The contact of synthetic material, particularly polymers, with biological environment usually induces non-specific protein adsorption, which induces negative affect on membrane performance [30]. Protein adsorption property of ultrafilter membrane is used as an indicator of the membrane performance [31].

For determination of membrane performance as a membrane adsorption, different membrane samples were cut into small pieces and introduced in a small beaker containing 25 ml protein solution of different initial concentration and pH. These suspensions were kept for 6 hr shaken condition at 25 ^{0}C under shaken condition. The concentrations of the supernatants were determined spectro-photometrically for estimation of adsorption and protein binding capacity. To examine the interactions between protein and charged surfaces, protein adsorption and binding capacity was determined in batch mode at different pH of protein solution. Protein adsorption % was estimated by the ratio of amount of protein adsorbed and amount of protein taken for equilibration. Concentration of

protein in feed and after adsorption was estimated by high performance liquid chromatography.

2.10. Observed protein transmission

In an ultrafiltration process, the transmission of solute or particular protein through a membrane can be expressed by the 'observed protein transmission' (ζ_{obs}), which is also referred to as the 'apparent sieving coefficient' (S_a). ζ_{obs} was estimated by the ratio of protein concentration in the feed side to the permeate side.

$$\zeta_{obs} = \frac{(C_P)_i}{(C_F)_i} \qquad (2.23)$$

where C_p is the protein concentration in the permeate (kg/m^3) and C_b is the protein concentration in the bulk feed (kg/m^3).

For fractionation of binary mixture of solutes, it is desirable to achieve maximum transmission of one solute and minimum transmission of the other. Efficiency of solute transmission for a binary mixture is expressed in terms of the selectivity parameter (SP) or separation factor (SF) which is ratio of transmission of individual proteins from their mixture [32].

$$SP\,or\,SF = \frac{(\zeta_{obs})_1}{(\zeta_{obs})_2} \qquad . \qquad (2.24)$$

Where $(\zeta_{obs})_1$ is observed protein transmission of solute 1 and $(\zeta_{obs})_2$ is observed protein transmission of solute 2. The concentration of feed and permeate was confirmed by UV-Visible spectrophotometer.

2.11. Electro-ultrafiltration

Electro-ultrafiltration is used for separation of charged molecules or ions under coupled derived forces (electric and pressure gradient). As a particle in suspensions carry an electric charge, it is possible by means of suitable superposition of ultrafiltration process with applied electric field. This process is a developed to combat residual cake formation at the

membrane surface by use of an applied electric field [33]. The following effects have to be taken into consideration when an electric field is applied in ultrafiltration process.

Ultrafiltration experiments, with or without applied potential gradient, using desired protein solution and their mixture, were conducted in dead-end and cross-flow permeation modes using plate and frame model. The experimental cell was made of acrylic with compressed air as the driving force having volume of 200 cm^3. Effective membrane area was 65 cm^2. The experiments were conducted in batch mode of operation under stirred conditions using magnetic stirrer to minimize the effects of concentration polarization. There was provision for applying desired potential across the membrane by using two platinum electrodes on its either side. Desired electric field was applied through the platinum electrodes using a regulated digital power supply (Aplab, India, model) so that electrode in the permeate side was the cathode, while simultaneous pressure was controlled using air compressor made of stainless steel. Effective pressure in the ultrafiltration cell was measured by a pressure meter fitted on the top of cell with a safety valve. Before each measurement, the membrane was soaked in distilled water for 2 h then equilibrated in the experimental solution. The pressure was varied in between 2 to 4 × 10^{-11} N cm^{-2}, while applied electrical gradient was varied between 0.67 and 2.00 V cm^{-1}. To prevent gas evolution at the electrodes by electrolysis and heat generation, the ionic strength of the buffer solution and applied electrical gradient were kept relatively low. Also micro-filters were separated two electrodes and restrict the approach of proteins on the electrodes. Permeate volume was measured with respect to time at each applied pressure with accuracy of 0.01 cm^3. Concentration of protein in the permeate side was determined by high performance liquid chromatography. At least three protein samples were collected at regular intervals for subsequent protein analysis. After completion of the experiments membrane was washed thoroughly with double distilled water and original membrane permeability was reproduced to ensure the absence of any adsorption or

fouling. Denaturation or degradation of protein was studied by recording the retention time in the chromatogram before and after the experiments.

2.12. Electro-chemical membrane reactor

The system was comprised of an electrochemical membrane reactor; two tanks; two peristaltic pumps and an adjustable DC power supply (Fig 2.12.1). The electrochemical membrane reactor made by PTFE was divided into an anode and cathode compartment by an anion-exchange membrane. The thickness of the two compartments (anolyte and catholyte) was 5 mm, respectively. The effective membrane area was 65 cm^2. Two electrodes (anode and cathode) connected to the DC power supply were made of platinum. The constant potential gradient applied to the reactor was controlled by the DC power supply. Two storage tanks and two pumps were used to continuously deliver anolyte and catholyte into the reactor with the flow rate of about 0.006 m^3/h, respectively in order to create high turbulence in both the compartments of reactor. Experiments were conducted in batch mode of operation i.e. same volume of solution was re-circulated in the respective compartment. Magnetic stirrers were used to ensure the complete mixing of

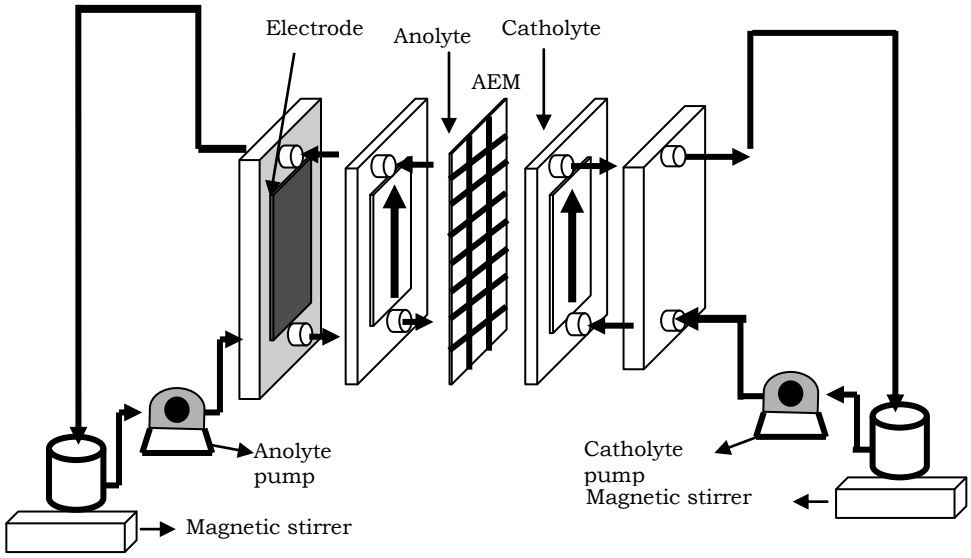

Figure 2.12.1. The set-up of electro-chemical membrane reactor.

the solution in both tanks. The whole set-up was placed in environment at room temperature without additional temperature controller. Initially, known volume of distilled water was fed through the anolyte while known volume and concentration of sodium lactate solution was recirculated through catholyte. The pH of both compartments and concentration of the anolyte were recorded with respect to time. During progress of the experiment current was also recorded at different time interval. Concentration in the anolyte was determined using UV-visible spectrophotometer with Randox lactate enzyme (Ranchem, India). Concentration determination accuracy was up to 0. 001 M.

References

[1] Kalsi PS. Spectroscopy of organic compounds, second ed. New Age International Limited Publication, 1996.

[2] Oldani M, Schock G. J Membr Sci 1989;43:243.

[3] Campbell P, Srinivasan R, Knoell T, Phipps D, Ishida K, Safarik J, Cormack T, Ridgway H. Biotechnol Bioeng 1999;64:527.

[4] Mulder M. Basic Principles of Membrane Technology, Kluwer Academic Publishers, Netherlands, 1996.

[5] Fontyn M, Bijsterbosch BH, Van't Riet K. J Membr Sci 1988;36:141.

[6] Shahi VK, Murugesh AP, Makwana BS, Thampy SK, Rangarajan R. Indian J Chem 2000;39:1264.

[7] Nagarale RK, Shahi VK, Thampy SK, Rangarajan R. React Fuct Poly 2004;61:131.

[8] Bhadeshi HKDH. Thermal Analysis Techniques, Material Science and Metallurgy, University of Cambridge.

[9] Strathmann H, in Ho WSD, Sirkar KK, (Eds.). Membrane Handbook, Van Nostrand Reinhold, New York 1992. Chapter 1.

[10] Shahi VK, Makawana BS, Thampy SK, Rangarajan R. Indian J Chem 1999;38A:124.

[11] Fontyn M, Bijsterbosch BH, Van't Riet K. J Membr Sci 1988;36:141.

[12] Shahi VK, Makawana BS, Thampy SK, Rangarajan R. Indian J Chem 1999;38A:124.

[13] Elatter A, Elmidaoni A, Pismenskia N, Gavach C, Pourcelly G. J Membr Sci 1998;143:249.

[14] Nakanishi T, Akiyama T, Seike T, Satoh M, Komiyama J. J Membr Sci 1991;64:217.

[15] Koter S, Piotrowski P, Kerres J. J Membr Sci 1999;153:83.

[16] Niency BV, Membrane processes, (Ed.) thired, John Villy Publications, 1991.

[17] Lehmani A, Turq P, Perie M, Perie J, Simonin JP. J Electranal Chem 1997;428:81.

[18] Shahi VK, Trivedi GS, Thampy SK, Rangarajan R. J Colloid Inter Sci 2003;262:566.

[19] Gottlieb MH, Neihof R, Sollner K. J Phys Chem 1957;61:154.

[20] Spiegler KS, Wyllie MRJ, 'Physical technique in biological research , Vol. 2, P. 301, Academic press, New York, 1956.

[21] Shahi VK, Thampy SK, Rangarajan R. J Membr Sci 1999;158:77.

[22] Singh K, Shahi VK. J Membr Sci 1990;49:223.

[23] Singh K, Shahi VK. J Membr Sci 1998;140:51.

[24] Bargeman, G., Houwing, J., Recio, I., Koops, R.H., Horst, C.v.d., 2002. Electro-membrane filtration for the selective isolation of bioactive peptides.

[25] Nadh Jagannadh S, Muralidhara HS. Ind Eng Chem Res 1996;35:1133.

[26] Nagarale RK, Gohil GS, Shahi VK, Rangarajan R. J Colloid Interf Sci 2005;287:198.

[27] Breslau BR, Testa AJ, Milnes BA, Medjanis G, in: Cooper, A. R. (Ed.), Ultrafiltration Membranes and Applications, Plenum Press: New York, 1980.

[28] Saxena A, Kumar A, Shahi VK. J Colloid Interface Sci 2006;303:484.

[29] Winston Ho WS, Sirkar KK. Membrane Handbook, University of Newark, New jersey.

[30] Wu Y, Zheng YL, Yang WL, Wang CC, Hu JH, Fu SK. Carbohydr Polym 2005;59:165.

[31] Enevoldsen AD, Hansen EB, Jonsson G. J Membr Sci 2007;299:28.

[32] Helfferich F. Ion-exchange. New York: McGraw-Hill, 1962.

[33] Wei J, Helm GS, Corner-Walker N, Hou X. Desalination 2006;192:25.

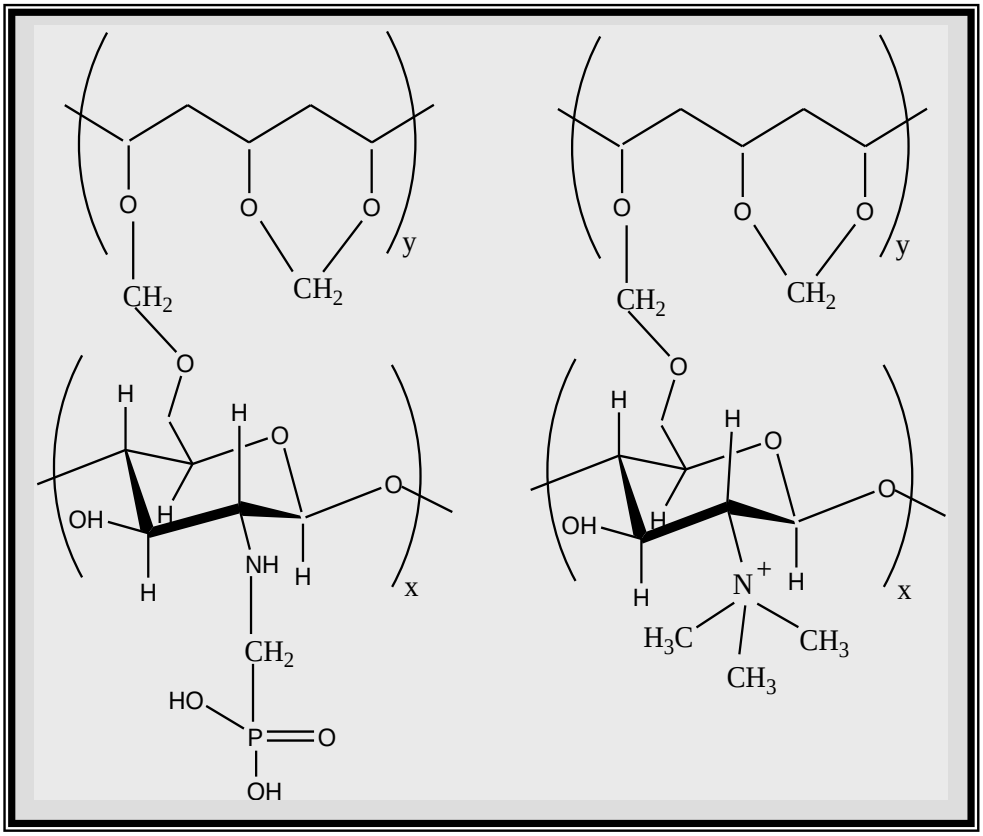

CHAPTER III

MODIFIED CHITOSAN BASED MEMBRANES FOR SIZE AND CHARGE BASED SEPARATION

3.1. *N*-methylene phosphonic and quaternized chitosan composite membranes for separations

With the rapid development of modern industry, environmental contamination has become more and more severe in that numerous industrial wastes have ruthlessly polluted the natural environment that is very suitable for the habitation of human being in the past, thus the treatment of industrial wastewater and the recovery of chemicals that are going to waste becoming extremely important issues. As a result, with the drive to treat such environmentally harmful substances, innovative green technologies to meet this demand have attracted many researchers. Separation of Ca^{2+} and Mg^{2+} from Na^{+} also a serious problem for the removal of hardness from ground water, boiler feed water, production of pure salt etc. Many technologies such as ion-exchange resin [1], chelation of bi-valent ions [2,3] ultrafiltration or nanofiltration [4,5], electrodialysis [6,7] etc were used by different scientists to solve this problem. But use hazaourdous chemicals and solvents during the preparation of membranes or resin are the serious problems. Thus there is urgent need to develop membrane preparation methodology in eco-friendly manner using renewable biomass for the separation of mono- and bi-valent electrolyte.

Chitosan is an important biomass prepared by the deacetylation of chitin mainly obtained from crab and shrimp shell [8] and is an amino polysaccharide that is useful in chemical modifications because it has reactive amino and hydroxyl group. Chitin and chitosan are generally discarded as industrial waste around the world [9], so chitosan can be considered to be an extremely low cost, nonhazardous, and environmentally benign polymer. Reports are available, where chitosan has been used as membrane forming material in pervaporation for the dehydration of alcohols, because of its hydrophilic nature and very high affinity towards water [10-13]. However, chitosan membranes are highly swollen in water and alcohol solutions, and the swollen membranes usually lose their permselectivity and show poor long-term stability of operation. Great efforts are therefore

attempting to improve the stability and mechanical properties of chitosan-based membranes, such as bringing cross-linked structure to membranes [14-16], blending chitosan with other polymers [17,18], casting chitosan on another polymer substrate to form composite membrane [15], and adding inorganic reinforcements into chitosan membranes [19]. However, the reduction in permeation flux is always accompanied with these modifications. Furthermore, till date no report is available modified chitosan based nanoporous charged membranes prepared in aqueous medium and gelated in methanol in order to tailor the pore structure.

In first part of chapter III, we are reporting modified chitosan based charged nanoporous membrane for the separation of mono- and bi-valent ions depending on their hydrated ionic radius and hydrophilic nature. Modifications of chitosan were carried out by either introducing $–PO_3H_2$ or by $–N^+(CH_3)_3$ for preparing positively or negatively charged surfaces. N-methylene phosphonic chitosan (NMPC), quaternized chitosan (QC) or blend membranes of different composition were prepared by cross-linking them with poly (vinyl alcohol) and they were characterized by measuring their physicochemical, electrochemical and permeation characteristics.

3.1.1. Materials and preparation of N-methylene phosphonic and quaternized chitosan composite membranes

Chitosan (100% deacetylation and 20×10^5 g/mol molecular weight), poly (vinyl alcohol) (PVA; Mw: 125,000) and phosphorous acid (99% purity) were received from Sigma Aldrich Chemicals and used as obtained. Methyl iodide, acetone, methanol, formaldehyde (35% w/v) solution, sodium chloride, etc. of AR grade were obtained from Rankem, India, and were used without further purification.

Synthesis of N-methylene phosphonic chitosan (NMPC), chitosan solution 2% (w/v) in glacial acetic acid 1% (v/v) was prepared. One part (by

weight) of chitosan was used and one part of phosphorous acid (by weight) dissolved in water was added drop wise with continuous stirring for an hour. Then the temperature of the reaction vessel was raised to 70 ^{0}C with reflux and 1 part of formaldehyde 36.5% (by weight) was added drop wise for 1 h. Heating was protected at the same temperature for 6 h. Then approximately 75% (v/v) solvent was removed under vacuum. Thus obtained viscous solution was precipitated with acetone, and precipitate was dried under vacuum at 50 ^{0}C. For the synthesis of quaternized chitosan (QC), 2.5% (w/v) chitosan was dissolved in 42% methanol and mixture was kept under constant stirring for 1h at 30 ^{0}C. Then 5% NaCl (w/v) and 5% (v/v) CH_3I was added at the interval of 4 h in proportion of 2:1:1 under constant stirring and reaction mixture was refluxed at 70 ^{0}C for 12 h. Quaternized chitosan was then precipitated with acetone, and precipitate was washed, dried under vacuum at 50 ^{0}C.

NMPC, QC and PC/QC composite membranes with PVA of different compositions were prepared by dissolving desired amount of PVA (50% w/w in all cases), NMPC and QC (0-50% w/w) in known amount of water, separately. Thus obtained solutions were mixed drop-wise under constant stirring for 2 h. Air bubbles were removed by applying vacuum to obtain a clear solution, which was cast on a clean glass plate covered with poly(ethylene) (HDPE) sheet in the form of thin film with desired thickness and was partially dried at 60 ^{0}C for 1h. Then these films were gelated in the methanol at room temperature. Obtained films were then immersed in a solution containing formaldehyde (54.1 g), sodium sulfate (150.0 g), sulfuric acid (125.0 g), and water (470.0 g) for 2 h at 60 ^{0}C for effecting cross-linkage in the membrane by formal reaction. Before being subjected to physiochemical and electrochemical studies, the resulting membranes were conditioned in 0.10 M HCl and 0.10 M NaOH solutions alternately several times and stored in distilled water. The membranes thus prepared were designated as NMPC, QC or PC/QC-X, where X is the NMPC content (%, w/w) in the membrane phase.

3.1.2. Results and discussion for *N*-methylene phosphonic and quaternized chitosan composite membranes

3.1.2.1. FT IR results

Modification of chitosan (phosphorylation and quaternization) was confirmed by FTIR spectra presented in Fig. 3.1.1 for NMPC, QC and PC/QC-30 membranes. The infrared spectrum of the NMPC derivatives shows the same position and intensity near 1650 cm^{-1} band due to amide carboxyl group (-$NHCOCH_2$). The absorption band near 1500 cm^{-1}, attributed to the bending vibration of the amino group in chitosan. While the ν P–OH shows a slight shift around 1070 cm^{-1} for NMPC membrane which was suppressed due to it's blending in QC for PC/QC membrane [20]. Also absorption band near 2080 cm^{-1} may by assign to qauternized amino groups. Furthermore, NMPC/PVA composite membrane exhibited the broad peak around 3400 cm^{-1}, confirms the formation of composite membranes of modified chitosan and PVA by H bonding. Fig. 3.1.2 (A&B) represents the schematic structure of the cross-linked structure of NMPC/PVA and QC/PVA composite.

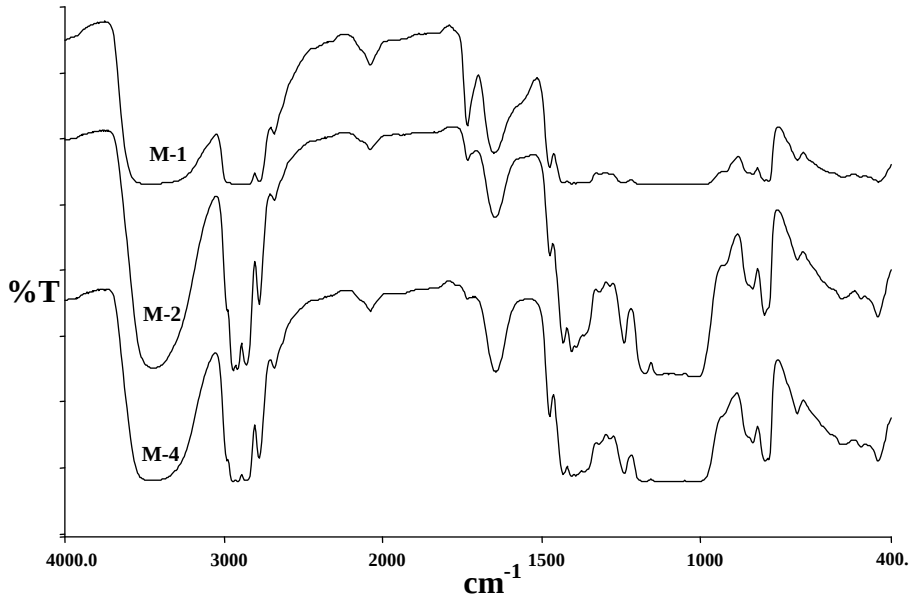

Figure 3.1.1. FTIR spectra of the different membranes: M_1- QC; M_2 – NMPC; M_4 – PC/QC-30.

All these bonds exhibited affinity toward water, which leads hydration of polymer matrix with enhanced water retention NMPC/PVA composite biomaterial, which was used for the membrane preparations with known composition. This is basically weak base-strong acid composite material and strong base material confirmed the presences of functional groups such as – PO_3H_2 and – $N^+(CH_3)_3$. Also, it was expected that due to blending of strong acid and strong base material resultant composite would result zwitterionic ionic structure at the membranes surfaces.

3.1.2.2. Viscosity measurements and interactions studies

Viscosity measurements for NMPC, QC and their mixed solutions were carried out in order to understand solute-solvent interaction and interaction between NMPC and QC. The intrinsic viscosity [η] of the modified chitosan solutions and their blend was obtained by extrapolating the reduced viscosity to zero concentration (with the polymer concentration in g/ml) [21]. Table 3.1.1 shows the intrinsic viscosity [η] and viscosity average molecular weight M_v values of polymers and their blend. Viscosity average molecular weight M_v of the modified chitosan were found to be lesser when compared to the molecular weight of the native chitosan showing breaking of polymeric units while functionalizing. The intrinsic viscosity and viscosity average molecular weight were found to higher for QC, least for NMPC whereas for the blend, values were in between, showing compatibility of both the polymers in the mixture.

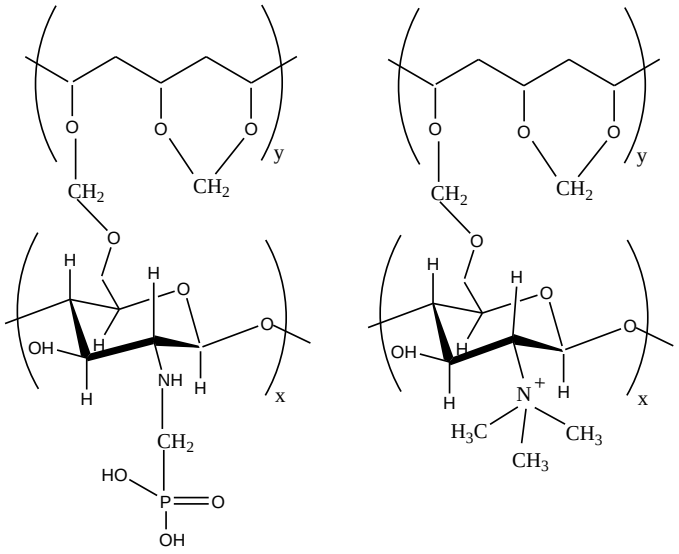

Figure 3.1.2. Schematic structure of NMPC/PVA and QC/PVA composites.

Interaction parameter x measures the extent with which the polymer interacts with the solvent. For polymer solvent system x was obtained from free energy per unit mole of solution and free energy of the solvent values [22]. Interaction parameter x decreases slightly with increase in concentration of the substrate and follow the reverse trend i.e. QC>NMPC+QC>NMPC. Polymer-water interaction at infinite dilution χ_0 for all the systems studied was determined by linear fitting of x values against concentration. In present case χ_0 values obtained are greater than 0.5 (Table 3.1.2), showing some interaction between polymer and water. Values are in the order QC>NMPC+QC >NMPC indicating the weakest solute-solvent interaction in case of QC, strongest in NMPC, and moderate in case of mixture of both confirming the results obtained qualitatively. Furthermore, χ_0 also suggest the weak electrostatic interactions between NMPC and QC in the solution phase.

Table 3.1.1. Intrinsic viscosity, viscosity average molecular weight and interaction parameter and relaxation time for different polymers at 298.15 K.

Polymeric species	[η] (ml/g)	$10^{-4}M_V$ (g/mol)	χ_0
QC	169.9	2.64	1.195
NMPC+QC	155.0	2.34	0.895
NMPC	107.6	1.45	0.654

3.1.2.3. TGA and DSC analysis

Thermal stability of the membranes was illustrated by the TGA analysis. The TGA curves measured under flowing nitrogen are shown in Fig. 3.1.3 for cross-linked PVA composite membranes with NMPC, QC and PC/QC-30 separately. The two stage TGA curves were observed for NMPC, QC and PC/QC-30 membranes. The first weight loss occurred below 100 ^{0}C for all three membranes and was attributed to the loss of absorbed water molecules in the membrane matrix. Second weight loss for membrane forming material started at about 350 ^{0}C for NMPC while that for QC and PC/QC-30 membranes at about 250 ^{0}C, which indicates the loss in the thermal stability of the modified biomaterial due to the blending of QC with

NMPC. Complete weight losses for all membrane were attained in the final stage of the sample decomposition starting at around 400 ^{0}C. Loss of PVA was also accompanied with thermal degradation of membrane forming material in the second stage. Furthermore, degradation of QC and PC/QC-30 membranes started around 250 ^{0}C while that for NMPC was at 300 ^{0}C.

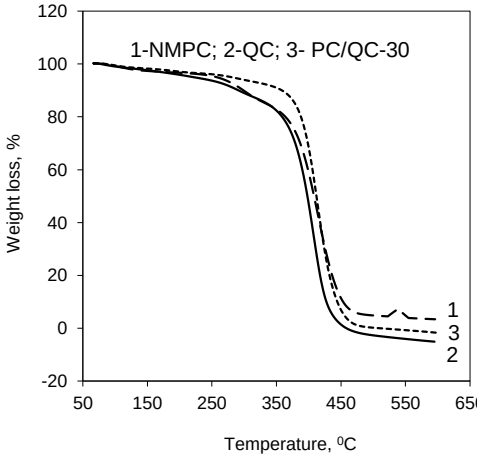

Figure 3.1.3. TGA curves of different membranes.

The DSC analysis of these membranes was carried out in the nitrogen atmosphere with a heating rate 5 ^{0}C /min, and resulting curves for NMPC, QC and PC/QC-30 membranes are presented in Fig. 3.1.4. These membranes exhibited T_g value around 127, 118, and 111 ^{0}C, respectively. This difference in the T_g values of phosphorylated and quaternized chitosan and their blend membranes may be attributed to thermal stability of chitosan matrix containing $–PO_3H_2$ or $–N^+(CH_3)_3$ functional groups. Moreover, all these membranes seem to be thermal stable.

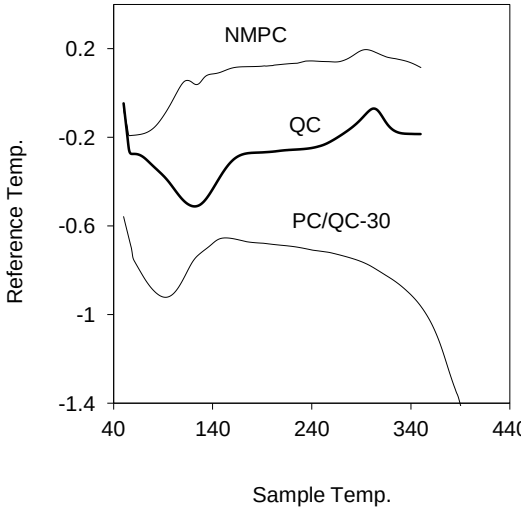

Figure 3.1. 4. DSC analysis of NMPC, QC and PC/QC-30 membranes.

3.1.2.4. IEC and water content properties

Ion-exchange capacity indicates the density of ionizable hydrophilic groups in the membrane matrix, which are responsible for their charged nature. In, general, membranes having the same degree of cross-linking and composition absorb the same amount of water, where density of ionizable groups is the same throughout the membrane matrix [23,24]. The IEC values

for acidic and basic functional groups of all synthesized membranes are presented in Table 1 in H^+ and/or OH^- form. It can be seen that the NMPC membrane exhibited quite higher IEC values (0.625 meq./g) in compare with QC membrane (0.275 meq./g). As per nature of their functional groups these membranes showed only acidic and basic IEC values, respectively. With the increase in the content of QC in its blend with NMPC, acidic IEC value progressively decreased while basic IEC values increased. These data reveals that PC/QC composite membranes showed both types of dissociable functional groups ($-PO_3H_2$ & $-N^+(CH_3)_3$), which were free for exchange of counter-ions and thus these composite membranes behaved as zwitterionic while NMPC and QC membranes showed cation and anion-exchange capacity, respectively. In addition one cannot completely ignore partial cross-linking between both types of functional groups in case of PC/QC composite membranes. Furthermore, relatively low IEC values of these membranes suggested that these membranes are mild in charged nature.

Water content of the membrane was determined by means of Eq. (2.6) [25,26]. ΔV values for membrane with different compositions are presented in Table 3.1.2. It can be seen that NMPC membrane showed 1.33, ΔV value while QC membrane 2.05. Also ΔV values for PC/QC membranes were progressively decreased with the increase in QC content in the membrane matrix. Lower values of ΔV for PC/QC composite membranes may be because of either less exchangeable functional groups as evident from IEC values of these membranes or partial interaction between NMPC and QC in the blend membrane casting solutions. On the basis of IEC values and thermodynamic studies in mixed solutions of NMPC and QC, it seems both of the above-mentioned factors contributed together and resulted relatively tight/dense membrane matrix in case of PC/QC composite membranes. Information regarding membrane void volume also can be have from the membrane void porosity (τ, volume of free water within membrane per unit volume of wet membrane) data obtained by Eq. (2.8) [25,26].

Table 3.1.2. Physicochemical properties of different chitosan composite membranes.

Membranes	IEC (meq/g)		τ	Φ	X^m (mol dm^{-3})
	H^+ form	OH^- form			
NMPC	0.625	-	0.570	1.20	0.254
QC	-	0.275	0.672	1.84	0.086
PC/QC-40	0.567	0.050	0.624	1.49	0.034
PC/QC-30	0.438	0.118	0.561	1.15	0.049
PC/QC-20	0.328	0.172	0.514	0.95	0.083
PC/QC-10	0.147	0.205	0.397	0.59	0.347

τ Values for different membranes are also presented in Table 3.1.2, which was used for the determination of fixed ion concentration (X^m) of the membrane in units of (moles of sites)/(unit volume of wet membrane) which is related to the ion-exchange capacity by Eq. 2.11. Where IEC is expressed in equivalents per gram of dry membrane. X^m data presented in Table 3.1.2 reveals that NMPC membrane was moderately charged (0.254 mol dm^{-3}) while QC membrane was comparatively lower charged (0.086 mol dm^{-3}). PC/QC membranes exhibited much lower charge then their individual components may be because of partial electrostatic interactions between positively charged $–PO_3H_2$ and negatively charged $–N^+(CH_3)_3$ groups resulting lesser number of dissociable functional groups. This observation was also verified by the estimation of interaction parameter on the basis of viscosity measurements of NMPC, QC and NMPC-QC mixed solutions. Furthermore, moderate positive, negative and zwitterionic charge on these nanoporous charged membranes might extend their potential applications for the separation of mono- and bi-valent electrolytic solutions.

3.1.2.5. Membrane permselectivity studies

Membrane permselectivity values for different types of membranes were estimated from membrane potential and thus counter-ion transport number $\left(t_i^m\right)$ values in order to assess selectivity of synthesized membrane for different ions. Membrane potential measurements were performed using different membranes and electrolyte (NaCl, $CaCl_2$ and $MgCl_2$) solutions.

Membrane potential arises due to the tendency of oppositely charged ions to migrate with different mobilities across the membrane and its magnitude depends on the charged nature of membrane in addition to the nature and concentration of equilibrating electrolyte solutions. Measured values of membrane potential clearly showed that NMPC and PC/QC membranes endowed with cation selectivity since membrane potential was negative with respect to higher concentration side, which was taken as positive in the voltammeter thus only cations were accelerated. In case of QC membrane opposite trend was observed and indicated its anion selectivity. Membrane permselectivity (*P*) was estimated by following Eq. 2.13.

The permselectivity values along with counter-ion transport number for different membrane a function of NMPC content in the membrane matrix are presented in Fig. 3.1.5 (A&B) in equilibration with electrolytic solutions of 0.055 mol dm^{-3} concentrations.

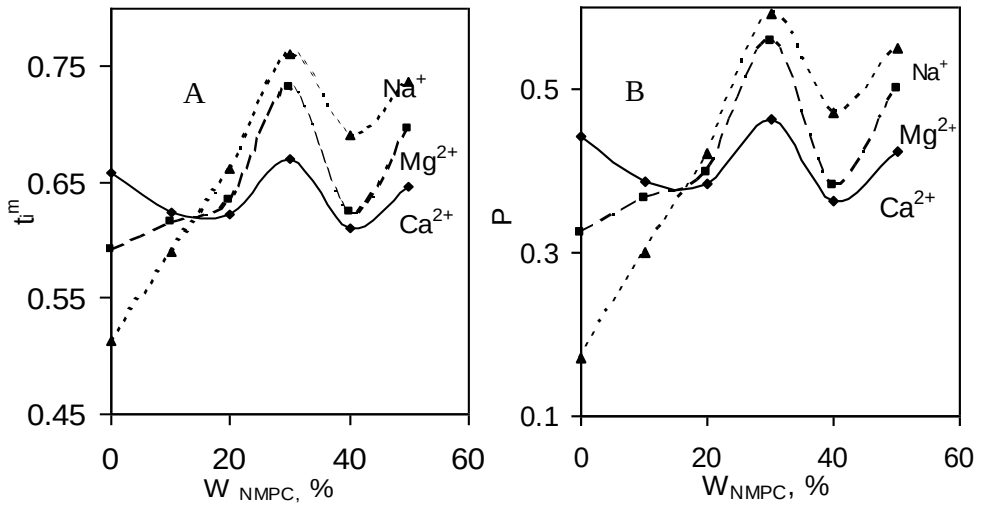

Figure 3.1.5. **Variation of: (A) counter-ion transport number (t_i^m); (B) membrane permselectivity (*P*) with NMPC content in the chitosan composite membranes for different counter-ions.**

QC membranes (W_{NMPC}=0) exhibited quite low selectivity for cation due to its negatively charged or anion selective nature, while cation selectivities for different ions were increased progressively with in increase in NMPC content up to W_{NMPC}=30. Highest permselectivity value for PC/QC-30 membrane may

be observed because of tight/dense nature of this membrane due to cross-linking or electrostatic interactions between both types of functional groups present in the composite membrane. This observation also may be explained by the change in pore texture of PC/QC membranes, which resulted increase in Donnan exclusion and thus increase in permselectivity.

3.1.2.6. Membrane conductivity and counter-ion diffusion coefficient in the membrane phase

For nanoporous charged membranes, conductivity studies are an important tool in order to understand ionic migration mechanism across it. Membrane conductivity was measured for different membranes as a function of NMPC content in the membrane matrix in equilibration with electrolyte (NaCl, $CaCl_2$ and $MgCl_2$) solutions of 0.01 mol dm^{-3} concentrations. Variation of specific membrane conductivity (κ^m) with W_{NMPC} (weight content of NMPC in the membrane matrix) is shown in Fig. 3.1.6. QC membrane exhibited low conductivity in comparison with NMPC membrane because of low concentration of charged functional groups in the membrane matrix. Also low conductivity exhibited by PC/QC membranes may be explained by the charge neutralization due to partial cross-linking or electrostatic interactions between them.

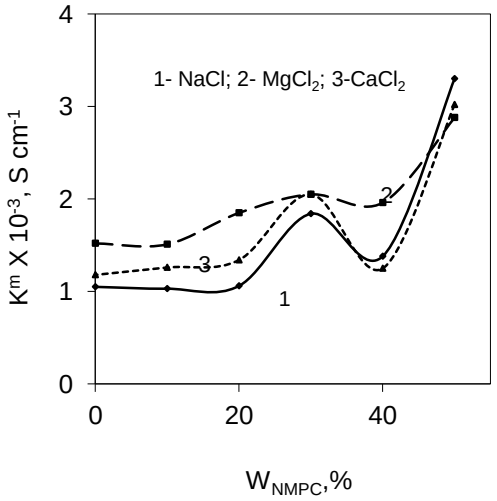

Figure 3.1.6. Variation of κ^m with NMPC content in the chitosan composite membranes in equilibration with different electrolyte solutions of 0.01 mol dm^{-3} concentrations.

We can have further information regarding counter-ion diffusion coefficient in the membrane phase by membrane conductivity data. According to the model developed by Zabolotsky and Nikonenko [27], the charged membranes may be considered as a micro-heterogeneous system with a combination of a gel phase with relative uniform distribution of functional groups and a hydrophilic part of the polymer matrix chains, on the one hand, and an electro-neutral solutions filling the interstices between the elements of gel phase, named the integral phase, on the other hand. It was shown [28] that the micro heterogeneous structure of the membrane material is the main factor determining the concentration dependence of membrane transport properties such as electrical conductivity, diffusion permeability and transport numbers. As a representative case, the variation of specific membrane conductivity (κ^m) with the NaCl concentration is shown in Fig. 3.1.7 for NMPC, PC/QC-30, PC/QC-10 and QC membranes. The solid line represents solution specific conductivity. Near the iso-conductance point κ_{iso}^m the conductivity of the membrane phase (κ^m) and the solution phase (κ) become equal. κ_{iso}^m Was obtained from the intercept of the curve drawn for membrane conductivity and solution conductivity for different membranes and electrolytic systems and their values are presented in Table 3.1.3 along with C_{iso} (electrolyte concentration corresponding to κ_{iso}^m) values. Both these values were highest for NMPC membrane and lowest for QC membrane for

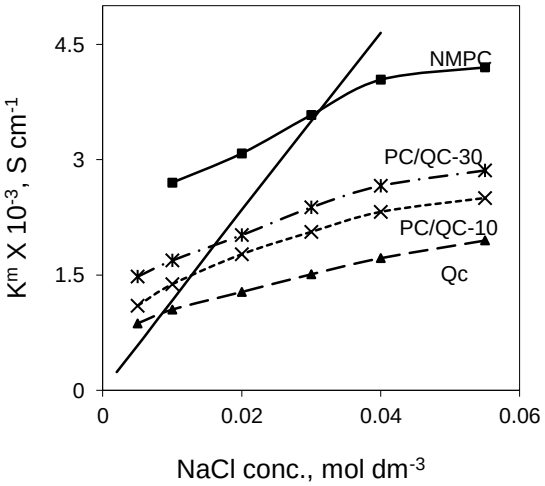

Figure 3.1.7. Variation of κ^m with NaCl concentration for chitosan composite membranes. Solid line indicates solution conductivity.

each type of electrolyte. For the composite membrane these values were decrease with the decrease in NMPC content in the membrane matrix.

The diffusion coefficient $\left(D_i^m\right)$ of the counter-ions in the membrane phase also can be calculated from the magnitude of the membrane conductivity at the iso-conductance point using Eq. 3.1.

$$D_i^m = \frac{RT}{F^2}\frac{\kappa_{iso}^m}{Q} \qquad (3.1.)$$

where Q *is* the ion-exchange capacity of the joint gel phase (equiv/cm^3). Estimated values for D_i^m for different types if ions across various membranes are presented in Fig. 3.1.8 as a function of W_{NMPC}. Diffusion coefficient for counter-ions in NMPC and QC membranes are lowest for each of ions. For PC/QC-30 membrane, highest D_i^m values was observed, which also extend the possible applications of these membranes for electrolyte separations. In case of PC/QC membranes, there is a possibility of interactions between the oppositely charged functional groups and thus either formation of zwitterionic types of structure as concluded on the basis of ion-exchange capacity and solution viscosities studies. This results relatively tight/dense membrane and may be able to discriminate between different types of based on their ionic radius. D_i^m values for different

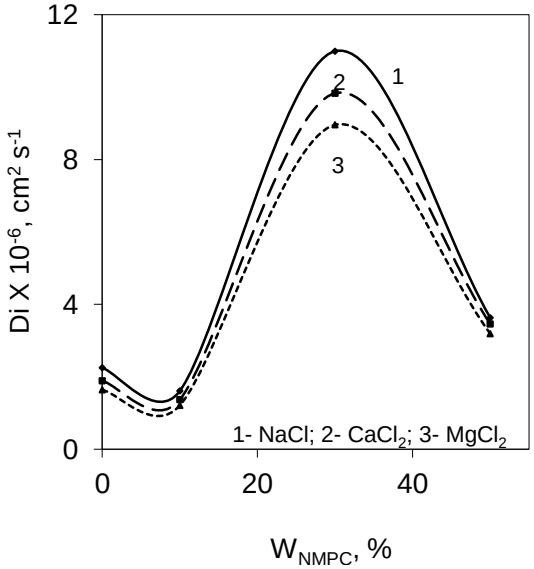

Figure 3.1.8. Dependence of counter-ion diffusion coefficient values on the NMPC content in the chitosan composite membranes for different electrolyte solutions of with 0.01mol dm^{-3} concentration.

electrolyte in case of PC/QC-30 membrane follow the trend NaCl > $CaCl_2$ > $MgCl_2$, which also suggest the applicability of this membrane for electrolyte separations because of their varied diffusional migration.

Table 3.1.3. Iso-concentration (C_{iso}) and iso-conductnace (κ_{iso}^{m}) values for different chitosan composite membranes in equilibration with electrolyte solution of 0.01mol dm^{-3} concentration.

Membranes	NaCl		$CaCl_2$		$MgCl_2$	
	C_{iso} (mol dm^{-3})	$\kappa_{iso}^{m} \times 10^{-3}$ (S cm^{-1})	C_{iso} (mol dm^{-3})	$\kappa_{iso}^{m} \times 10^{-3}$ (S cm^{-1})	C_{iso} (mol dm^{-3})	κ_{iso}^{m} X10^{-3} (S cm^{-1})
NMPC	0.031	3.65	0.027	3.48	0.025	3.21
PC/QC-30	0.016	2.00	0.013	1.79	0.011	1.63
PC/QC-10	0.013	1.50	0.012	1.28	0.011	1.13
QC	0.008	1.00	0.006	0.84	0.055	0.73

3.1.2.7. Membrane permeation studies

To investigate the impact of the membrane forming material and their charged nature on membrane performances, pure water flux was measured and data are presented in Fig. 3.1.9 against applied pressure for NMPC, QC and PC/QC-30 membranes. In the absence of compaction or fouling, the pure water flux should increase linearly with pressure (i.e., constant permeability). The relationship between flux and pressure is linear for all studied membranes in applied pressure range. It is very interesting to find that the composition of the prepared membranes highly influence pure water flux, which follows the NMPC > PC/QC-30 > QC trend. Reason of this trend might be related with increase in membrane compactness or decrease in their hydrophilic

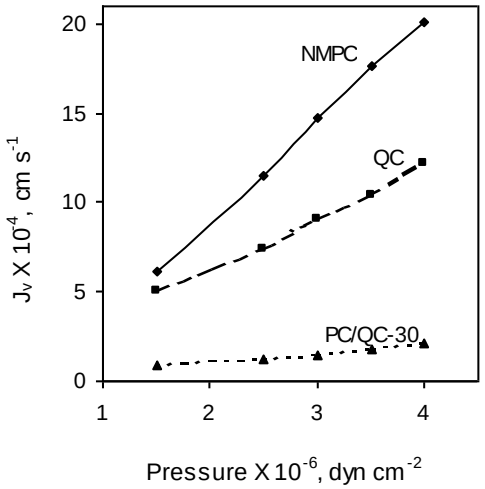

Figure 3.1.9. **Variation of J_v values with applied pressure for different chitosan composite membranes.**

characteristics by decrease in NMPC content in the membrane matrix. Further idea about compactness of membranes we can have from equivalent pore radius of the membrane data. For a microscopic membrane, the pressure driven water permeability can be expressed in term of equivalent pore radius (r_p) from Hagen–Poiseuille equation [29,30]. r_p values estimated from Eq. 2.19 are presented in Table 3.1.4. NMPC and QC membranes exhibited r_p values 41.4 and 40.3 nm, respectively while for PC/QC-30 membrane it was found to be 15.9 nm. This observation also in agreement with conclusion made on the basis of IEC, water content and membrane conductivity studies that PC/QC composite membranes are compact in nature in comparison to individual NMPC or QC membranes and also posses moderate charge on the membrane interfaces. Thus this membrane especially PC/QC-30 can be used for the separation of electrolyte based on their size and hydrophilic/hydrophobic nature.

Table 3.1.4. Hydrodynamic permeability (L_p) and equivalent pore radius (r_p) values for QC, NMPC and PC/QC-30 membranes.

Membranes	$L_p \times 10^{-10}$ ($cm^3\ s^{-1}\ dyn^{-1}$)	r_p (nm)
NMPC	5.6	41.4
PC/QC-30	0.5	15.9
QC	2.9	40.3

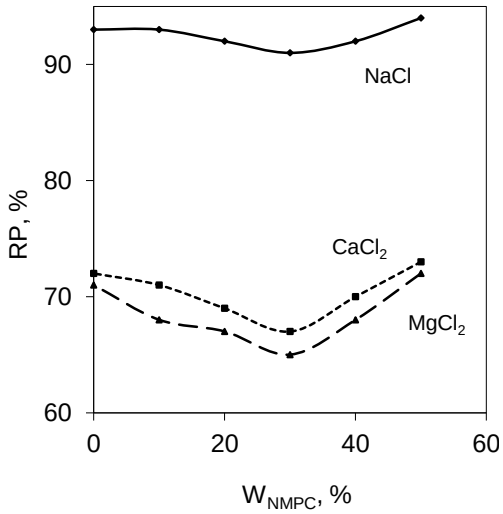

Figure 3.1.10. **Variation of relative salt permeability (RP) values with NMPC content in the chitosan composite membranes for different electrolyte**

Pressure driven membrane permeation studies using different electrolytic solutions (NaCl, $CaCl_2$ and $MgCl_2$) of 0.01 mol dm^{-3} concentration in order to record relative ionic permeability across synthesized membranes. Fig. 3.1.10 presents measured relative permeability of each ion (Na^+, Ca^{2+}

and Mg^{2+}) during the dead end test run against W_{NMPC}. The relative permeability, *RP*, of the ions was calculated as: $RP = (C_f / C_i) \times 100$, where C_f is the ion concentration in filtrate and C_i is the ion concentration in the solution being filtered. RP values for Na^+ were found to be higher than 90% for all types of membranes, while for Ca^{2+} and Mg^{2+} ions RP values were in between 65-70%. Furthermore, PC/QC-30 membrane exhibited lowest RP values among all PC/QC membrane, which indicates its suitability for separation of Na^+ from Ca^{2+} and Mg^{2+} ions. Relative permeability values for different types across composite membrane showed the following trend: $Na^+ > Ca^{2+} > Mg^{2+}$, which was also in agreement of their hydration radius. Hydration radius for Na^+, Ca^{2+} and Mg^{2+} ions are 0.178, 0.260 and 0.300 nm, respectively [31]. This indicates larger hydrated ions were highly retained by the membrane especially PC/QC-30 membrane because of its relative compact structure, low equivalent pore radius and above all formation of either zwitterionic structure due to blending of acidic and basic functionalized chitosan or charge neutralization because of electrostatic interactions between phosphonic and quaternary ammonium groups.

3.1.3. Conclusions for *N*-methylene phosphonic and quaternized chitosan composite membranes

Modifications of chitosan were carried out by either introducing phosphonic acid group or by quaternization of existing primary ammonium groups in order to make it water soluble functionalizd material. Using these material charged nanoporous composite membranes of different compositions of NMPC and QC were prepared by taking required modified material and poly(vinyl alcohol) 50% (w/w) in aqueous media and latter these membrane were gelated in methanol at 10 ^{0}C for tailoring pore structure in the membrane matrix. Characterization of FTIR and ion-exchange capacity studies confirmed the introduction phosphonic acid groups and quaternary ammonium groups resulting and formation cross-linking or covalent bonding with PVA resulting composite membrane. Thermodynamic properties of dilute aqueous solutions of NMPC, QC and their mixture were also studied and

concluded that both individual materials have good hydrophilic interactions with water and mixed solution exhibited electrostatic interactions between negatively charged $–PO_3H_2$ and positively charged $–N^+(CH_3)_3$ groups resulting charge neutralization. Adequate thermal stability NMPC, QC and PC/QC membranes were revealed thermal analysis while nature of their ionic selectivity was studied by estimating permselectivity values. Membrane conductivity studies reveal that PC/QC-30 was relatively tight/dense membrane and may be able to discriminate between different types of based on their ionic radius. D_i^m values for different electrolyte in case of PC/QC-30 membrane follow the trend NaCl > $CaCl_2$ > $MgCl_2$, which also suggest the applicability of this membrane for electrolyte separations because of their varied diffusional migration. Membrane permeation studies also confirmed lowest equivalent pore radius for PC/QC-30 membrane and relative permeability of these membranes for different types of ions suggest the suitability of PC/QC-30 membrane for the separation of Na^+ from Ca^{2+} and Mg^{2+}.

Furthermore, chitosan provides a low-cast material and, in future work, a way of increasing its stability and ionic conductivity should be investigated for the purpose of tailoring charged nanoporous structure for solving diversified types of separation problems. The utilization of biopolymer composite such as NMPC/PVA, QC/PVA or NMPC-QC/PVA is also novel and challenging, as it is inexpensive, non-hazardous, and environmentally benign. Besides their ion-conducting properties, and water retention capability, this biopolymer composite material may have the potential for application in bio-electrochemical devices, ion chromatography and biosensors.

3.2. Separation of proteins using modified chitosan-silica cross-linked charged ultrafilter membranes under coupled driving forces

Chitosan is a safe and friendly biomass and during last decade its several specific applications were developed such as: technological advance material; material for biochemical significance (blood coagulation, wound healing, bone regeneration etc); inhibition of biosynthesis; molecular biology; and biopolymer [32,33]. As an amino polysaccharide, it is a promising hydrophilic membrane material that contains many reactive amino and hydroxyl groups. Because of its hydrophilic nature and high affinity for water chitosan based membranes were used for pervaporation [12,13], drug delivery [32,34,35], ultrafiltration of bio-product [36,37] and protein adsorption/separation [38,33]. However, chitosan membranes are highly swollen in water, therefore losses physical structure. Efforts were made to prepare chitosan-polymer blend [39,8] or chitosan-inorganic composite membrane [40], in order to have control on dimensional stability and selectivity of the membranes. Organic-inorganic composite nanostructured membranes are viewed as of next generation membranes. They showed the attractive properties of mechanical and thermal stable inorganic backbone and the specific chemical reactivity and flexibility of the organo-functional groups [40-42]. Till date no report is available of hydrophilic modified chitosan-inorganic composite membrane prepared in aqueous media and gelated in methanol in order to tailor the pore structure. Thus functionalized chitosan-inorganic composite membranes will be a grate alternative as charged nanoporous membranes for efficient and selective isolation/separation of bioproduct.

In recent years, ultrafiltration (UF) of protein solution is gradually emerging as a powerful bio-separation process for diversified fields as biotechnology, biomedicine, dairy and food industry [43-47]. However, the effectiveness and efficiency of the UF are strongly dependent on operating parameters such as pH, salt concentration; permeate flux, membrane fouling and system hydrodynamics [48-51]. Additionally, UF is a size based separation process, and it is difficult to achieve high selectivity with high throughput. To solve these problems, charged porous (UF) membranes were

used for protein separation and electrostatic interactions between charged proteins and membranes were also studied [51-54]. Many processes with electric gradient as driving force such as electrophoresis, gel electrophoresis, capillary electrophoresis, etc [55-57] were also developed for commercial practice of protein separation. In all these processes, either pressure or electric gradient was imposed to achieve protein separation. In literature electro-ultrafiltration (UF under electric field) is also reported to achieve fractionation/separation of protein with enhanced throughput using uncharged UF membranes [44,48]. But no report is available, in which UF with charged membrane was performed under coupled driving forces using positively or negatively charged membranes for achieving enhanced selectivity (purity) and membrane throughput.

Herein, first time we are reporting hydrophilic modified chitosan-silica composite charged UF membranes for protein separation under coupled driving forces (pressure and electric gradient) for achieving high selectivity and maximum membrane throughput because of three selective parameters (*i.e.* charge on the membrane matrix, nature of charge and molecular size of the protein). Whereas, in aforementioned method, only one selective parameter either charge or molecular size was considered for their fractionation/separation. Positively and negatively charged chitosan-silica composite membranes were employed to achieve pH sensitive protein separation under coupled driving forces using binary mixture of bovine serum albumin (BSA) and lysozyme (LYS) as a model case.

3.2.1. Materials and preparation of chitosan-silica cross-linked charged ultrafilter membranes

Chitosan (100% deacetylation), poly (vinyl alcohol) (PVA; Mw: 125,000 Daltons), phosphorous acid (99% purity), tetraethylorthosilicate (TEOS) were received from Sigma Aldrich chemicals and used without further purification. CH_3I, NaCl, HCHO, glacial CH_3COOH, CH_3OH, H_2SO_4, HCl, NaOH, NaH_2PO_4, Na_2HPO_4 (AR grade, S.D. Fine Chemicals, India) were used as received.

Bovine serum albumin (mol wt 67000 Daltons), lysozyme (mol. wt. 14600 Daltons) were received from HiMedia Laboratories Pvt. Ltd. India. Double-distilled water was used in all experiments.

Syntheses of *N*-methylene phosphonic chitosan and quaternized chitosan were achieved by the method reported earlier [37]. Chitosan solution 2% (w/v) in glacial acetic acid 1% (v/v) was prepared. One part (by weight) of chitosan was used and 1 part of phosphorous acid (by weight) dissolved in water was added drop wise with continuous stirring for an hour. Then the temperature of the reaction vessel was raised to 70 ^{o}C with reflux and 1 part of formaldehyde 36.5% (by weight) was added drop wise for 1 h heating was maintained at the same temperature for 6 h. Then approximately 75% (v/v) of the solvent was removed under vacuum. The viscous solution thus obtained was precipitated with acetone, and the precipitate was dried under vacuum at 50 ^{o}C. For the synthesis of quaternized chitosan (QC), 2.5% (w/v) chitosan was dissolved in 42% methanol and the mixture was kept under constant stirring for 1 h at 30 ^{o}C. Then 5% NaCl (w/v) and 5% (v/v) CH_3I was added at intervals of 4 h in 2:1:1 proportion under constant stirring and the reaction mixture was refluxed at 70 ^{o}C for 12 h. Quaternized chitosan was then precipitated with acetone and the precipitate was washed and then dried under vacuum at 50 ^{o}C.

PC-silica and QC-silica composite membranes were prepared by dissolving 20 g PVA (50% w/w in all cases; used as a plasticizer) and 16 g of PC or QC (40% w/w) in 100 cm^3 of water. Mixed solution was stirred for 2 h, then 4 g of TEOS (10% w/w) was drop wise added under constant stirring. The pH of mixed solution was adjusted to 2.0 using dil. HCl. Resultant clear solution was again stirred for 1 h and air bubbles were removed by applying vacuum. Solution was cast in the form of thin film of desired thickness on the glass plate covered with poly (ethylene) (HDPE) sheet, and partially dried for 1.5 h at 30 ^{o}C. Then these films were gelated in the methanol at room temperature. Thus obtained thin films were immersed in a solution containing formaldehyde (54.1 g), sodium sulfate (150.0 g), sulfuric acid

(125.0 g), and water (470.0 g) for 1 h at 80 °C to affect cross-linkage in the membrane by formal reaction. Before being subjected to physicochemical and electrochemical characterizations, the resulting membranes were conditioned in 0.10 M HCl and 0.10 M NaOH solutions alternatively several times and stored in the distilled water. The membranes thus obtained were named as PC-Si or QC-Si.

3.2.2. Theoretical aspects for ultrafiltration experiments under applied potential gradient

The flux aroused in the ultrafiltration process can be described as

$$J_v = \frac{dV}{A\,dt} = \frac{\Delta P}{viscosity \times resistance} \qquad (3.2)$$

However average filtrate flux can be defined as

$$\overline{J_v} = \frac{V_F}{At} \qquad (3.3)$$

The observed protein transmission and selectivity parameter (SP) of the UF also can be defined as

$$\zeta_{obs} = \frac{C_{filtrate}}{C_{feed}} \qquad (3.4)$$ while,

$$SP = \frac{(\zeta_{obs})_i}{(\zeta_{obs})_j} \qquad (3.5)$$

Under the two types of driving forces (pressure and electrical potential), the best process conditions for the separation of proteins according to their charge are high applied electric field, high zeta potentials of protein molecules (achievable by pH and ionic strength of the protein solution) and membrane interface, and low filtrate velocity (at low applied pressure gradient). A limit of the applied electrical gradient is to be fixing by the electrical current flowing in the circuit, high electrical current cause the electrolysis. The effective electrical field (E_{eff}) as a force on the protein molecule can be calculated by

following equation, assuming the conductivity remains constant within the filter chamber:

$$E_{eff} = \frac{I}{\kappa A} \qquad (3.6)$$

The effective electric field is not equal to the applied electric field (E). The applied electric field was determined by the applied voltage divided by the electrode distance ($E = U/d$). As the voltage not only drops in the membrane or in the filter chamber but also at the electrodes, thus E was always greater than E_{eff}. Also the zeta potential is depends on the surface charge nature of the membrane matrix. The filtrate velocity should be high or low needed for the selectivity. This becomes clear using extended Nernst-Planck equation for the transport of the substance:

$$J_i = k_i \nu c_i - D_i \frac{\partial c_i}{\partial x} + F z_i c_i u_i E \qquad (3.7)$$

The three terms describe the convective, diffusive and electrophoretic transport through the any medium; say membrane in this case. If the convective flow and electrophoretic transport are in opposite directions, a fractionation process can be improved through the use of small fluid velocities as only the electrophorectic influence exceeds the convective transport. In the case relatively dense membrane, convective transport will be approaching towards zero and total volumetric flux obtained under the simultaneously active forces (pressure and electric gradient in this case) can be written as follows in the form of phenomenological equation based on non-equilibrium thermodynamic principle.

$$\left(J_v\right)_{coup} = L_{11}\Delta P + L_{12} E \qquad (3.8)$$

In case, when $E = 0$;

$$\left(\frac{J_v}{\Delta P}\right)_{E=0} = L_{11} \qquad (3.9)$$; and when ΔP = 0, then

$$\left(\frac{J_v}{E}\right)_{\Delta P=0} = L_{12} \qquad (3.10)$$

The term (J_v/E) of Eq. 3.10 is known as electro-osmotic permeability. Usually, measurement of E_{eff} at the membrane interface is difficult, thus it is convenient to use current (I) for estimating electro-osmotic flux ($L_{12} = (J_v/I)$. In case of coupling of forces, $(J_v)_{E=0} < (J_v)_{coup} > (J_v)_{\Delta P=0}$. Furthermore, we can use L_{12} for the estimation of zeta potential at the membrane interface by Eq. 2.16. Also, L_{11} can be used with advantage for the estimation of apparent pore radius of the membrane using Hagen-Poiseuille equation (Eq. 2.19).

3.2.3. Results and discussion for separation of proteins using modified chitosan-silica cross-linked charged ultrafilter membranes under coupled driving forces

Modifications of chitosan were carried out for making it more hydrophilic in nature by introducing phosphonic acid or quaternized ammonium groups. Water-soluble functionalized chitosan was used for developing it silica composite membrane cross-linked with PVA in the aqueous medium. Generally, membranes are being made in non-aqueous medium, but in this case we prepared the composite membranes in aqueous medium and gelated in non-aqueous medium (methanol) in order to tailor their pore dimensions and structure. Functionalization of chitosan and necessary cross-linking for PC-Si and QC-Si composite membranes were confirmed by FT IR spectra (Fig. 3.2.1.) The infrared spectrum of QC-Si membrane showed the absorption band near to 2080 cm^{-1} due to quaternized amino group. QC-Si composite cross-linked with PVA membrane exhibited

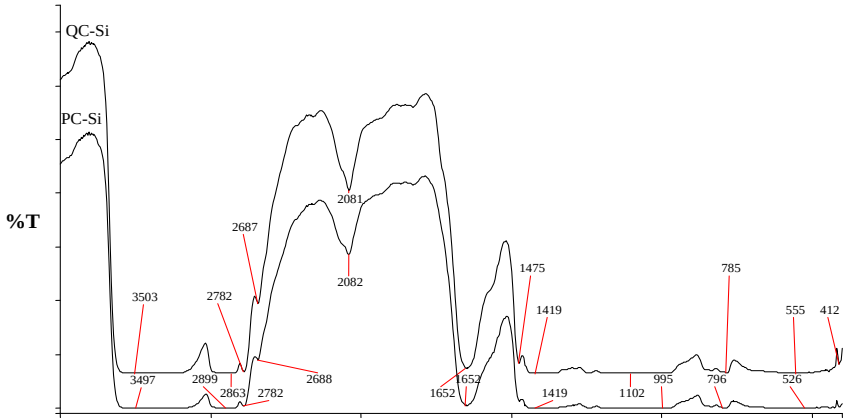

Figure 3.2.1. FTIR spectra of QC-Si and PC-Si membranes.

a broad peak near to 3503 cm^{-1}, which confirmed the formation of composite membrane of quaternized chitosan and PVA by hydrogen bonding. For PC-Si membrane, the absorption band near 1650 cm^{-1} was attributed to the amide carboxyl group (-$NHCOCH_2$). Also absorption band near to 1400-1500 cm^{-1} was observed due to the bending vibration of the amino group in the chitosan. Furthermore, PC-Si composite membrane cross-linked with PVA exhibited a broad peak around 3400 cm^{-1}, which confirms the formation of composite membrane because of hydrogen bonding. In composite membrane silane group of TEOS attach covalently, which confirms the broaden band at 1100-1000 cm^{-1} owing to the absorption from the Si-O-C and Si-O-Si symmetric stretching. Fig. 3.3.2 (A&B) represents the schematic structures for cross-linked PC-Si and QC-Si composite membranes, respectively. These composites of modified chitosan exhibited affinity towards water, which leads to hydration of polymer matrix with enhanced water retention. Basically, these are strong acid and base composite material and are expected to exhibited surface charge properties due to the presence of functional groups.

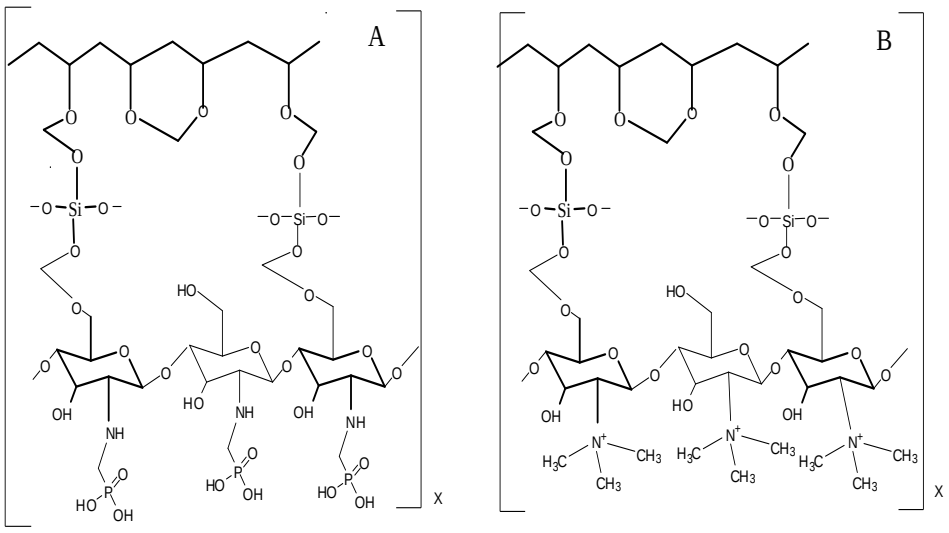

Figure 3.2.2. Schematic structure of: (A) PC-Si; (B) QC-Si composite membranes.

3.2.3.1. Physicochemical and electrochemical properties

Thermal stability of the membranes was illustrated by the TGA analysis, and relevant TGA curves obtained under flowing nitrogen for PC-Si and QC-Si composite membranes are presented in Fig. 3.2.3. The three-stage TGA curves were observed for both cases. First weight loss occurred below 100 °C for both membranes were attributed to loss of adsorbed water molecules in the membrane matrix. The second stage started at around 250 °C for both cases, indicate loss of membrane forming material due to thermal oxidation. In the third stage, complete weight loss was observed around 400 °C for both membranes. The DSC analysis of these

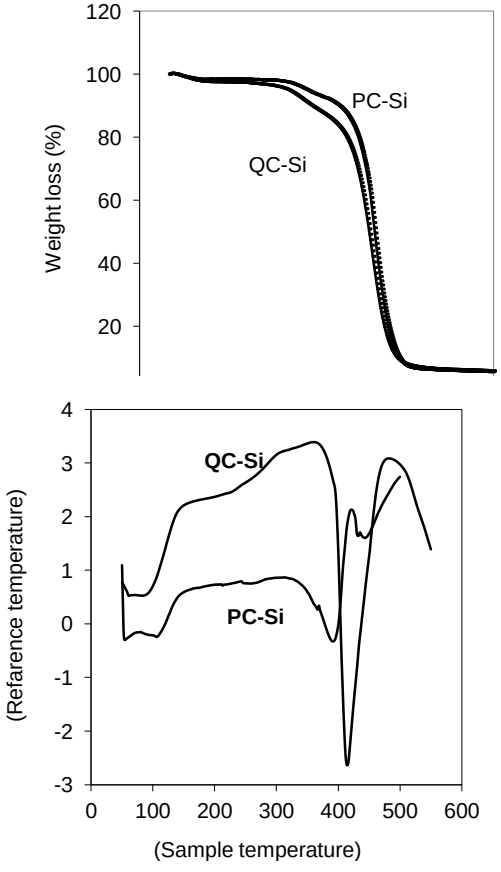

Figure 3.2.4. DSC curves for PC-Si and QC-Si membranes.

membranes was also carried out under nitrogen with a heating rate of 5 °C/min, and first T_g values were obtained around 125 and 104 °C for PC-Si and QC-Si membranes, respectively (Fig. 3.2.4). Second *Tg* value for PC-Si was at 398 °C, while that for QC-Si was at 410 °C. This difference in the T_g values of phosphorylated and quaternized chitosan composite membranes may be attributed to thermal stability of functionalized chitosans.

Dynamic mechanical analysis (DMA) for PC-Si and QC-Si membranes was recorded under 10 N constant applied forces at a constant temperature (100°C) and frequency (10 Hz) (Fig. 3.2.5). The membrane exhibited good mechanical stability under these experimental conditions, and no breaking of the polymeric film was observed. However, PC-Si membrane showed elongation but no elongation was observed for QC-Si membrane. Both membranes were also characterized by measuring their water content, ion-exchange capacity, contact angle, membrane conductivity and counter-ion transport numbers in the membrane phase. The relevant data are presented in Table 3.2.1. Water content (θ) value in the membrane phase was estimated using Eq. 2.6, which was quite high for PC-Si membrane. θ value was used for the estimation of membrane void porosity (τ, volume of free water within membrane per unit volume of wet membrane) using Eq. 2.8 [26], and the data is also presented in Table 3.2.1. From both the information, it seems PC-Si membranes showed higher porosity in comparison with QC-Si membrane. Ion-exchange capacity (IEC) values presented in Table 3.2.1, reveal that both membrane possessed about same molality of exchangeable functional groups (-PO_3H_2 or –$(CH_3)_3N^+$) in the membrane matrix. In general, membranes having the same degree of cross-linking and composition absorb the same amount of water, where

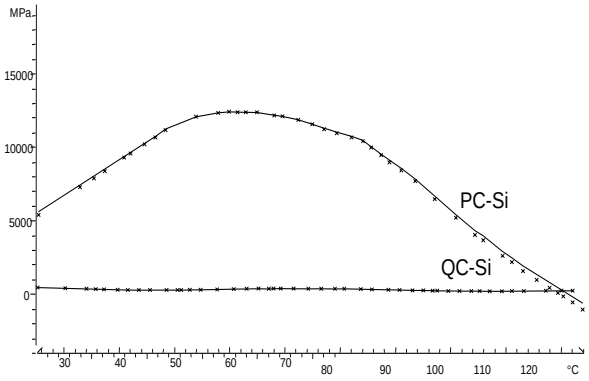

Figure 3.2.5. DMA curves for PC-Si and QC-Si membranes.

density of ionizable groups is the same through out the membrane matrix [31,32]. Contact angles in water were measured with a tensiometer (DCAT 21, Dataphysics, Filderstadt, Germany) based on energy balance approach to the three phase equilibrium. Contact angle values also suggest the same extent of hydrophilic nature of both membranes. Quite high contact angle value (close to 90^{o}) will be favourable for the use of these membranes for protein separations. Furthermore, IEC value in conjunction with τ value was used to estimate the surface charge density (X^m) in the membrane matrix [43]. The X^m values suggest mild charged nature for both

Table 3.2.1. Physicochemical and electrochemical properties of PC-Si and QC-Si membranes.

Properties	Membranes	
	PC-Si	QC-Si
Membrane thickness (mm)	0.21	0.27
Water content (%)	48.76	26.85
IEC (mequiv./gm)	0.282	0.299
Contact angle	76.70^{o}	77.34^{o}
Membrane conductivity (mS cm^{-1})	2.25	1.13
Counter-ion transport number	0.76	0.75
Membrane porosity	0.330	0.212
Surface charge concentration (m mol dm^{-3})	0.189	0.157

[a] *measured in the equilibration with 0.001 mol dm^{-3} NaCl solution.*
[b] *estimated from membrane potential measurements using NaCl solutions of 0.01/0.001 mol dm^{-3} concentration across the membrane.*

membranes; however charge density of PC-Si membrane was slightly higher than QC-Si composite membrane. Mild charged nature of the composite membranes was also revealed by membrane conductivity (κ^m) and counter-ion transport number in the membrane phase (t_i^m) data, latter suggested that

PC-Si behaved as cation selective while QC-Si behaved as anion selective membrane. Also t_i^m values were higher in comparison to transport of the counter-ions in the solution phase (for NaCl solution of 0.055 mol dm^{-3} concentration, Na^+ transport number is 0.392, while for Cl^- it is equal to 0.618). Based on these characterizations we can conclude that both types of modified chitosan composite membranes are hydrophilic in nature, having mild porosity and charged nature.

3.2.3.2. BSA adsorption on the membranes

Porous charged membranes had higher dynamic i.e. practical binding capacity for proteins and exhibited a higher through put for protein recovery. Introduction of a high density of functional groups in the membrane is required, while maintaining high selectivity for the protein adsorption/separation [24]. In order to examine the interactions between positively or negatively charged modified chitosan composite membrane, BSA binding capacity for the PC-Si and QC-Si membranes was determined in batch mode at different pH of BSA solution with 5 mg/ml concentration for 6h adsorption, and relevant data is presented in Fig. 3.2.6. BSA binding capacity was highly dependent on pH of the solution as well nature of the charge on the membrane matrix. For PC-Si membrane, binding capacity decreased progressively with the increase in the pH of the solution, while opposite trend was observed for QC-Si composite membrane. At low pH, BSA carries positive charges (BSA^+) and its adsorption on negatively charged matrix was favored due to mutual electrostatic attraction, while opposite case will be happened at higher pH where BSA

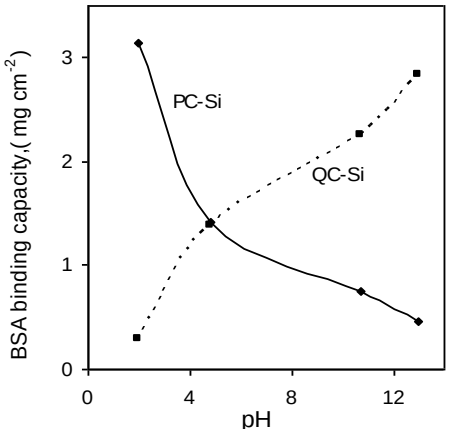

Figure 3.2.6. Comparison of binding capacity for PC-Si and QC-Si membranes with BSA at different solution pH and 5 mg/ml concentration for 6h adsorption.

carries negative charge (BSA^-). At iso-electric point of BSA (pH: 4.8), it exist in the zwitterionic form, and interestingly at this pH both membrane showed similar BSA binding capacity. Thus pH of the protein solution is an important parameter by varying which one can obtain its high adsorption and thus transport/separation across charged functionalized chitosan ultrafilter membrane.

3.2.3.3. Membrane permeation studies

In general membranes were prepared in non-aqueous media and gelated in water media for tailoring their pore dimensions. In this case membranes were prepared in water and gelated in methanol. To investigate the impact of the membrane forming biomaterials, their charged nature, optimum casting and gelation conditions, performance of both membranes was evaluated by their volumetric flux under applied pressure and electric gradient. In all cases, straight line passed through origin was obtained. Phenomenological coefficients L_{11} and L_{12} were estimated from the slope of these straight lines and are presented Table 3.2.2 The L_{11} values were used with advantage for the estimation of apparent pore radius (r_p) using Eq. (2.19). It can be seen that although pressure driven permeability value (L_{11}) for PC-Si membrane is high, its low apparent pore radius is due to low thickness (d) and high water content (θ) values in comparison to QC-Si composite membrane. It was very interesting to find that nature and extent of charge in the membrane matrix influences their flux. Also surface charge on a membrane has significant influence on its separation properties. Knowledge of the electro kinetic properties such as zeta potential of a particular membrane will be proved to be major contributing factor behind the decision to implement that membrane for a specific separation process, as the surface charge on synthetic membrane has significant effect on its separation properties [58,59], and fouling tendency [60,61]. The zeta potential (ζ) can be obtained from electro-osmotic permeability (L_{12}) values presented in Table

3.2.2, using Smoluchowski equation (Eq. 2.16). In general the zeta potential of the membrane is supposed to represent the chemical nature of the membrane forming material. It depends on the nature and concentration of functional groups attached to the membrane matrix. PC-Si membrane exhibited slightly high zeta potential value (2.88 mV) in comparison to QC-Si (2.69 mV).

Table 3.2.2. Hydrodynamic permeability (L_{11}), equivalent pore radius (r_p), electro-osmotic permeability (L_{12}), and membrane zeta potential (ξ) values for PC-Si and QC-Si membranes.

Membrane	$L_{11} \times 10^{-10}$ ($cm^3\ dyn^{-1}\ s^{-1}$)	r_p[a] (nm)	$L_{12} \times 10^{-6}$ ($Amp^{-1}\ cm\ s^{-1}$)	ξ [b] (mV)
PC-Si	1.48	2.02	1.70	2.88
QC-Si	0.97	2.49	1.54	2.69

[a] estimated from water permeability data; [b] estimated from electro-osmotic data in equilibration with 0.001 mM NaCl solution.

Mild charged nature for the both membranes are responsible for the observed zeta potential, and it is evident from X^m values presented in Table 3.2.1 that PC-Si composite membrane is relatively highly charged. Furthermore, moderate values of zeta potentials of these membranes suggest their capability for charge based selection/rejection.

3.2.3.4. Transmission of BSA under coupled driving forces

BSA transmissions across both types of membranes and its effect on the pH of the feed protein solution were studied under coupled driving forces (pressure and electric gradient) in order to investigate the effect of nature of charge on the protein molecule (BSA), membrane matrix and direction of

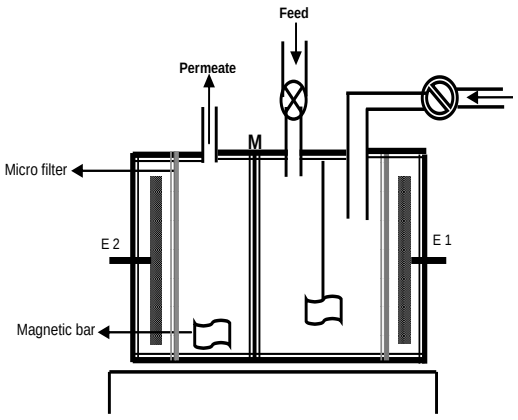

Figure 3.2.7. Experimental cell for protein separation under coupled driving forces.

electric polarity applied. Experimental cell for protein separation under coupled driving forces is presented in Fig. 3.2.7. Schematic diagram for the different modes of protein transmission such as protein transmission using uncharged ultrafilter membrane without any electric gradient is presented in Fig. 3.2.8(A). While Fig. 3.2.8(B) represents protein transmission under coupled driving forces using negatively charged ultrafilter membrane (PC-Si) and same for positively charged membrane (QC-Si) is depicted in Fig. 3.2.8 (C). Polarity of the electric gradient was fixed in such a way that positively charged protein (BSA^+, pH<p*I*) was facilitated to migrate through negatively charged membrane, while negatively charged protein (BSA^-, pH > p*I*) was facilitated to migrate through positively charged membrane. Under these mode of operation, three screening parameters such as pore size and nature of the charge on the membrane, and electric gradient not only enhance the protein transmission but membrane throughput will also increased due to the electrophoretic migration of the solvent along with protein. Fig. 3.2.9 presents volumetric

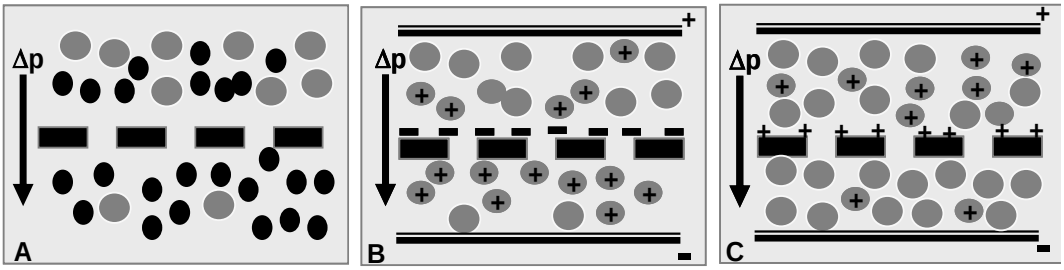

Figure 3.2.8. Diagram for: (A) UF through charged membrane; (B) UF under coupled driving forces using PC-Si membrane; and (C) UF under coupled driving forces using QC-Si membrane.

flux of BSA solutions of pH: 2.0 and 13.0 across the PC-Si and QC-Si membrane, respectively, under varied applied pressure without or with applied electric gradient.

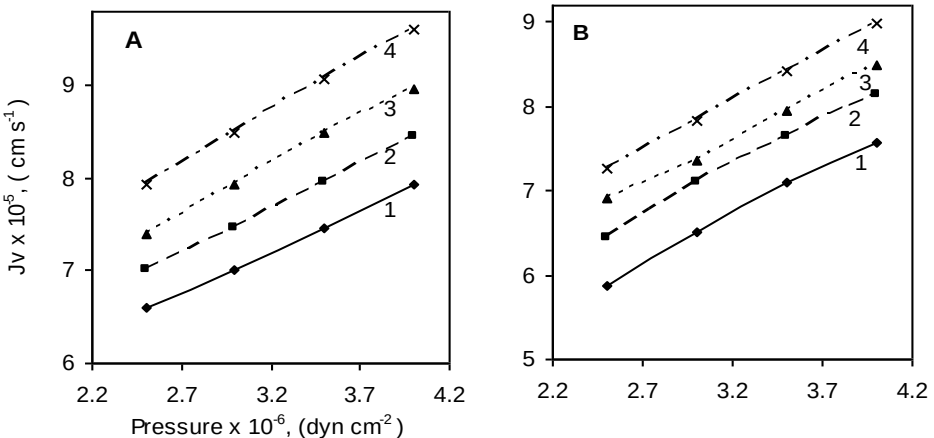

Figure 3.2.9. Variation of volumetric flux of BSA solution (5 mg/ml) with applied pressure for: (A) PC-Si membrane at pH: 2.0; (B) QC-Si membrane at pH: 13.0, at different applied electric gradient: 1-0 V cm^{-1}; 2-0.67 V cm^{-1}; 3-1.33 V cm^{-1}; 4-2.00 V cm^{-1}.

It can be seen that without any electric gradient (at 0 V cm^{-1}) and under constant pressure, flux values were lowest for both membranes, which were progressively increased with the increase in electric gradient. It was also observed that at pH: 2, PC-Si membrane exhibited highest flux, while QC-Si membrane showed highest flux at pH: 13.0. The filtrate flux is an important parameter of amelioration when evaluating the separation/fractionation process. After bio-production, the targeted product should be quickly separated because enzyme activity reduced with time [16]. Here it can be seen that filtration velocity was accelerated by coupling of driving forces, pressure and electric gradient, for both type of membranes. Volumetric flux data with respect pH of the feed solution is also presented in Fig. 3.2.10 for both membranes under 3.0 × 10^{-6} dyn cm^{-2} applied pressure and 1.33 V cm^{-1} applied potential gradient. Filtrate flux was highly dependent on pH of the feed BSA solution. PC-Si membrane showed highest filtrate flux at pH: 2 (BSA^{+}) and flux was decreased with the increase in the solution pH (BSA^{-}),

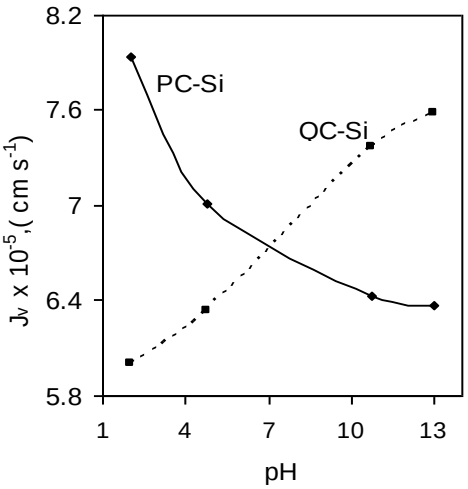

Figure 3.2.10. Volumetric flux data for composite membranes at different pH of 5.0 mg/ml BSA solution under 3.0 X 10^{-6} dyn cm^{-2} applied pressure and 1.33 V cm^{-2} applied electric gradients.

while opposite trend was observed for QC-Si membrane under similar experimental conditions. Interestingly, membranes showed almost same filtrate flux, when pH of the BSA solution was equal to its p*I* (pH: 4.8) and BSA existed in BSA^0. The region beyond this behaviour is again controlled migration BSA molecules to the anode or cathode side depending on its pH, which was not possible without an electric field. Also alteration in the filtrate flux under different experimental conditions may be attributed to the combined electro-phoretic and electro-osmotic effects.

For the protein separation/fractionation, transmission or selectivity of the targeted protein molecules is also an important parameter in addition to the throughput. Observed protein transmission (ζ_{obs}) was estimated from the ratio of protein concentration in the feed side to the concentrate side. Representative curves for ζ_{obs} against applied pressure and varied electric gradient is presented in Fig. 3.2.11 (A), which also indicate the dependency of BSA transmission on the applied electric gradient. It can be seen that coupled driving forces under suitable experimental conditions, not only influences the filtrate flux but it also enhanced the BSA flux for both types of membranes. Fig. 3.2.11 (B) presents ζ_{obs} values with respect pH of the feed solution both membranes under 3.0×10^{-6} dyn cm^{-2} applied pressures and 2.00 V cm^{-1} applied electric gradient. Similar to the filtrate flux values, ζ_{obs} value for BSA^+ was very high across PC-Si composite membranes, while for QC-Si membrane it was very low. Progressive alteration in the ζ_{obs} value with the pH of the BSA feed solution was due to the nature of charge on the BSA. Furthermore, BSA transmissions for both membranes were identical at pH: 7.

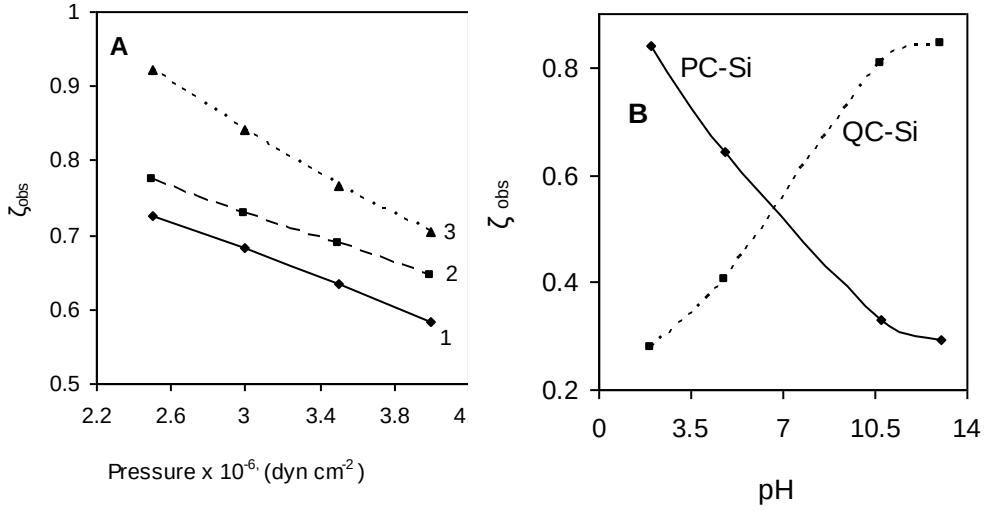

Figure 3.2.11. Variation of observed BSA transmission (ζ_{obs}) with: (A) applied pressure through PC-Si membrane in equilibration with 5 mg/ml BSA solution at pH 2 for: 1- 0 V cm^{-1}; 2-1.33 V cm^{-1}; and 3- 2.00 V cm^{-1}, (B) pH of 5 mg/ml BSA solution at 3.0 X 10^{-6} dyn cm^{-2} applied pressure and 2.0 V cm^{-1} electric gradient.

Thus in this study, there are three parameters such as applied pressure, electric gradient and the nature of the charge on the membrane matrix govern the filtrate flux and BSA transmission across the membranes, which had about same pore diameter. Here it is important to record that, fouling was noticeably absent in all cases with less than 1% reduction in the membrane permeability after repeated use, due to applied electric gradient.

3.2.3.5. Protein transmission and selectivity in the mixture of BSA and LYS

The selective separation of BSA and LYS from them equi-gram mixed solution was carried out at different pH ranging between 2.0-13.0, where both existed in different ionic forms across both membranes. Representative ζ_{obs} values for BSA and LYS separately, when mixed protein solution was used as feed, is presented against pH in Fig. 3.2.12 (A&B) for PC-Si and QC-Si membranes, respectively under 3.0 × 10^{-6} dyn cm^{-2} applied pressure without or with 2.0 V cm^{-1} applied electric gradient.

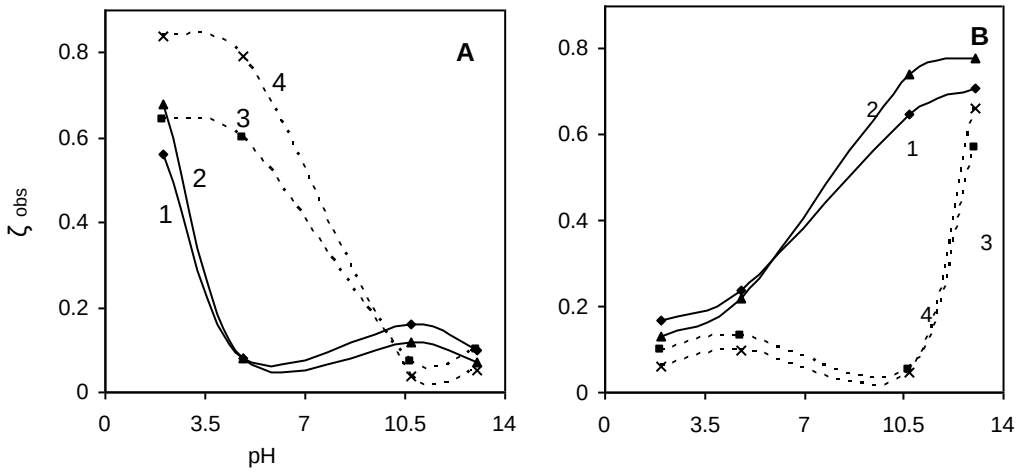

Figure 3.2.12. ζ_{obs} values for BSA (solid line) and LYS (dotted line) separately through: (A) PC-Si; (B) QC-Si membrane in equilibration with BSA, LYS mixed solution (5 mg/ml each) under 3.0 X 10^{-6} dyn cm^{-2} applied pressure gradient and: 1 & 3- without any applied potential, 2 & 4- with 2.0 V cm^{-1} applied electric gradient.

For both protein, BSA and LYS, transmission was strongly dependent on the nature of the charge on the transmitting species (pH), nature of the membrane and electric gradient. At pH: 2.0, BSA and LYS both existed in positively charged species (BSA^+ or LYS^+) and thus showed very high ζ_{obs} value across PC-Si membrane, while it was extremely low (less than 0.2) for QC-Si membrane.

At pH: 4.8, transmission of BSA across both type of charged membranes were very low because of uncharged nature of permeating species (p*I* : 4.8). Transmission of the LYS^+ (pH: 4.8) across the PC-Si was extremely high due to electrostatic attraction between migrating species and membrane interface, while for QC-Si membrane it was extremely low because of Donnan-exclusion due to same charged nature of transmitting species and membrane interface. QC-Si membrane allowed high transmission of BSA^- (pH: 10.7), while transmission of LYS^0 (p*I* : 10.7). At pH: 13.0, transmission of BSA^- or LYS^- was very low across the PC-Si membrane, while across the QC-Si, it was very high due to electrostatic repulsion/attraction depending on the charged nature of transmitting protein species and the membrane interface.

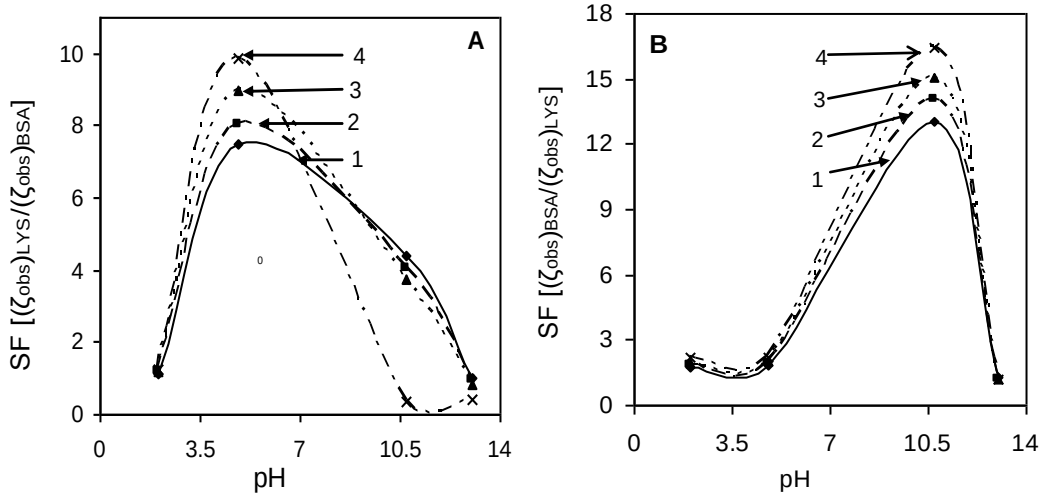

Figure 3.2.13. Separation factor as function of pH for the BSA and LYS mixed solution (5 mg/ml each) through: (A) PC-Si; (B) QC-Si membrane 3.0 X 10^{-6} dyn cm^{-2} applied pressure and: 1- without any electric gradient; 2- 0.67 V cm^{-1}; 3- 1.33 V cm^{-1}; 4-2.00 V cm^{-1}.

Thus it is possible to separate LYS from the mixture of BSA-LYS at pH: 4.8 (p*I* of BSA) using negatively charged PC-Si membrane or BSA from the mixture of BSA-LYS at pH: 10.7 (p*I* of LYS) using positively charged PC-Si membrane with high selectivity. Also in all cases due to coupling of driving forces, filtrate flux and protein transmission was enhanced.

Further idea about protein separation and selectivity, we can have from separation factor (SF) defined as the ratio of transmission of individual proteins from their mixture. Estimated SF values for PC-Si and QC-Si composite membranes are presented in Fig. 3.2.13. (A&B), respectively as a function of pH of the mixed protein feed solution. For PC-Si membrane, SF values under different electric gradient was in between 8 to 10 at pH; 4.8, while it was varied 12-15 for QC-Si at pH: 10.7. Furthermore, applied electric gradient further progressively enhanced the SF values, suggested highly selective separation of protein under coupled driving forces. However, applied electric gradient was so small that no denaturation of protein is possible under given experimental conditions [16]. Thus it is possible to develop a rapid and highly selective protein separation method using modified biomaterial as charged membranes (functionalized Chitosan) under coupled driving forces (pressure and electric gradient). In this process no appreciable membrane fouling or protein denaturation was observed, while by focusing one component at its iso-electric point, other component in the charged state (depending on pH) may be effectively separated. In this case the difference in the *pI* values of LYS and BSA was quite high, but in general cases where *pI* values were near by, this process also can be efficiently used by varying the pore size of the membrane according to the molecular weight of the protein to be separated and with fine variations in their pH. Two screening parameters such as *pI* values and molecular size were taken in account for achieving high degree of selectivity.

3.2.4. Conclusions of chitosan-silica cross-linked charged ultrafilter membranes

Functionalizations of chitosan were carried out by either introducing phosphonic acid group or by quaternization of existing primary ammonium groups for making it water soluble biopolymer material. Negatively charged PC-Si and positively charged QC-Si membranes were prepared using TEOS and PVA as plasticizer by acid catalyzed sol-gel reaction in aqueous media. These membranes were gelated in the methanol under optimized conditions for tailoring the pore structure of the membrane matrix. FTIR spectra and ion-exchange capacity study of these membranes confirmed the introduction of highly acidic $–PO_3H_2$ or basic $–N^+(CH_3)_3$ groups, resulting in formation of cross-linking or covalent bonding with silica and PVA. Electrochemical characteristics such as membrane conductivity; surface charge density and counter-ion transport number of these membranes also revealed mild charged nature of the membrane matrix. These membranes were employed for the separation of proteins from their mixture under coupled driving forces. It was concluded that separation of LYS from the mixture of BSA-LYS at pH: 4.8 (p*I* of BSA) using negatively charged PC-Si membrane or BSA from the mixture of BSA-LYS at pH: 10.7 (p*I* of LYS) using positively charged PC-Si membrane, was possible with high selectivity. Also in all cases due to coupling of driving forces, filtrate flux and protein transmission was enhanced. Furthermore, applied electric gradient further progressively enhanced the SF values, suggested highly selective separation of protein under coupled driving forces.

In the present work product yield defined as transmission through the membrane could be highly raised due to coupling of driving forces and three screening parameters such as: charge on the protein; charge on the membrane matrix and superimposed electric gradient. Thus this is a novel process using modified biopolymer membrane for improving product purity, and filtration velocity (throughput). Both, the electrophoretic migration of molecules and the positive effect of electro-osmosis, lead to increase in

product purity. Also, an additional driving force (electric field) could raise filtration velocity even when the increase in applied pressure had reached to its limit. Reported process is a promising tool to make downstream processing faster and product purer in certain fields of application. It is an alternative for ultrafiltration, chromatographic or conventional electrophoresis processes to fractionate protein. Above all, hydrophilic modified biopolymer membrane prepared in the aqueous media was used in this process. It was inexpensive, non-hazardous, and environmentally benign.

References

[1] Juang RS, Wang YC. Ind Eng Chem Res 2003;42:1949.

[2] Juang RS, Liang JF. J Membr Sci 1993;82:175.

[3] Tomida T, Hamaguchi K, Tunashima S, Katoh M, Masuda S. Ind Eng Chem Res 2001;40:3557.

[4] Kawano K, Hamaguchi K, Masuda S, Tomida T. Ind Eng Chem Res 2002;41;5079.

[5] Teixeira MR, Rosa MJ, Nystrom M. J Membr Sci 2005;265;160.

[6] Balster J, Krupenko O, Pünt I, Stamatialis DF, Wessling M. J Membr Sci 2005;263:137.

[7] Sata T, Yamaguchi T, Kawamura KK, Matsusaki K. J Chem Soc Faraday Trans. 1997;93:457.

[8] Uragami T, Yamamoto S, Miyata T. Biomacromolecules 2003;4:137.

[9] Yamada M, Honma I. Angew Chem Int Ed 2004;43:3688.

[10] Uragami T, Polysaccharides, Structural Diversity and Functional Versatility. Marcel Dekker: New York, 1998; p. 887.

[11] Uragami T, Takigawa K. Polymer 1990;31:668.

[12] Liu YL, Hsu CY, Su YH, Lai JY. Biomacromolecules 2005;6:368.

[13] Anjali Devi D, Smitha B, Sridhar S, Aminabhavi TM. J Membr Sci 2005;262:91.

[14] Ge J, Cui Y, Yan Y, Jiang W. J Membr Sci 2000;165:75.

[15] Huang RYM, Pal R, Moon GY. J Membr Sci 1999;160:17.

[16] Liu YL, Su YH, Lai JY. Polymer 2004;45:6831.

[17] Jiraratananon R, Chanachai A, Huang RYM. J Membr Sci 2002;199:211.

[18] Toti US, Aminabhavi TM. J Appl Polym Sci 2002;85:2014.

[19] Okumus E, Gurkan T, Yilmaz L. J Membr Sci 2003;223:23.

[20] Binsu VV, Nagarale RK, Shahi VK, Ghosh PK. Rect Funt Polym 2006;66:1619.

[21] Schoff CK, Kamarchik P, *in: "Kirk-Othmer Encyclopedia of Chemical Technology",* 4th edition, J.I. Kroschwitz, M. Howe-Grant, L. Humphreys, L. Altieri, J. Lee, J. *Eds., John Wiley & Sons*, New York 1997, vol. 21, p. 347.

[22] Kalyanasundaram S, Hemalatha J. J Polym Mater1997;14:285.

[23] Nagarale RK, Shahi VK, Schubert R, Rangarajan R, Mehnert R. J Colloid Interface Sci 2004;270:446.

[24] Koter S, Piotrowski P, Kerrs J. J Membr Sci 1999;153:83.

[25] Capeci SW, Pintauro PN, Bennion DN. J Electrochem Soc1989;136: 10.

[26] Nagarale RK, Gohil GS, Shahi VK, Rangarajan R. J Colloid Interface Sci 2005;287:198.

[27] Zabolotsky VI, Nikonenko VV. J Membr Sci 1993;79:181.

[28] Elatter A, Elmidaoni A, Pismenskia N, Gavach C, Pourcelly G. J Membr Sci1998;143:241.

[29] Garcia-Aleman J, Dickson J, Mika A. J Membr Sci 2004;240:237.

[30] Shahi VK, Trivedi GS, Thampy SK, Rangarajan R. J Colloid Interface Sci 2003;362:566.

[31] Kiriukhin MY, Collins KD. Biophys Chem 2002;99:155.

[32] Ravi Kumar MNV, Muzzarelli RAA, Muzzarelli C, Sashiwa H, Domb J. Chem Rev 2004;104:6017.

[33] Yi H, QL Wu, Bentley WE, Ghodssi R, Rubloff GW, Culver JN, Payne GF. Biomacromolecules, 2005;6:2881.

[34] Hejazi R, Amiji M. J Controlled Release 2003;89:151.

[35] Prego C, Torres D, Fernandez-Megia E, Novoa-Carballal R, Quinoa E, Alonso MJ. J Controlled Release 2006;111:299.

[36] Matsuoka Y, Kanda N, Lee YM, Higuchi A. J Membr Sci 2006;280: 116.

[37] Saxena A, Kumar A, Shahi VK. J Colloid Interface Sci 2006;303: 484.

[38] Machado RL, Arruda EJ, Santana CC, Bueno SMA. Process Biochemistry 2006;41:2252.

[39] Wan Y, Wu H, Yu A, Wen D. Biomacromolecules 2006;7:1362.

[40] Uragami T, Katayama T, Miyata T, Tamura H, Shiraiwa T, Higuchi A. Biomacromolecules 2004;5:1567.

[41] Nagarale RK, Gohil GS, Shahi VK, Rangarajan R Macromolecules 2004;37:10023.

[42] Binsu VV, Nagarale RK, Shahi VK. J Mater Chem 2005;15:4823.

[43] Saxena A, Shahi VK. J Membr Sci 2007;299:211.

[44] Kappler T, Posten C. J Biotechnology 2007;128:895.

[45] Ghosh R, Cui ZF. J Membr Sci 1998;139:17.

[46] Feins M, Sirkar KK. Biotechnol Bioeng 2004;86:603.

[47] Maruyama S, Katoh T, Nakajima M, Nabetani H. Biotechnol Bioeng 2001;75:233.

[48] Iritani E, Mukai Y, Kiyotomo Y. J Membr Sci 2000;164:51.

[49] Wan Y, Ghosh R, Cui Z. Biotechnol Prog 2004;20:1103.

[50] Muller CH, Agarwal GP, Melin Th, Wintgens Th. J Membr Sci 2003;227:51.

[51] Ghosh R. Biotechnol Bioeng 2001;74:1.

[52] Ebersold MF, Zydney AL. Biotecnol Prog 2004;20:543.

[53] Burns DB, Zydney AL. J Membr Sci 2000;172:39.

[54] Cheang B, Zydney AL. Biotechnol Bioeng 2003;83:201.

[55] Carlsson N, Sanandaji N, Voinova M, Akerman B. Langmuir 2006;22:4408.

[56] Roche ME, Oda RP, Landers JP. Biotechnol Prog 1997;13:659.

[57] Lilley KS, Razzaq A, Dupree P. Current Opinion Chem Bio 2001;6: 46.

[58] Wang DIC, Sinskey AJ, Sonoyama T. Biotechnol Bioeng 1969;11: 987.

[59] Dukhin SS. Derjaguin BW in Matijevic, E. (Ed.) Surface and Colloid Science, Vol. 7, Wiley, New York, 1974, p. 118 and 127.

[60] Larsson K. Desalination 1980;35:105.

[61] Breslau BR, Testa AJ, Milnes BA, Medjanis G, in Cooper, A.R. (Ed.), Ultrafiltration Membranes and Applications, Plenum Press, New York, 1980, p. 109.

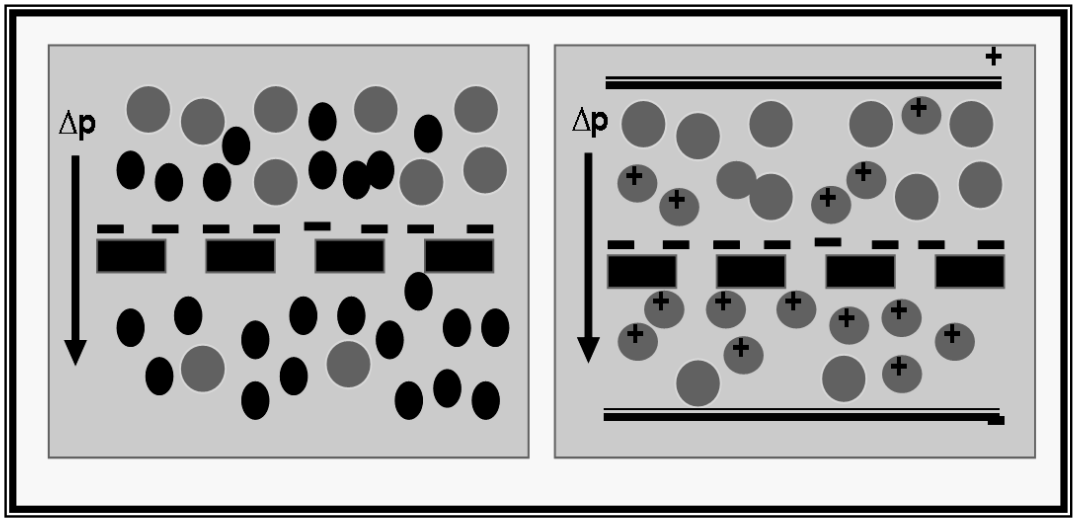

CHAPTER IV

pH CONTROLLED SELECTIVE TRANSPORT OF PROTEINS THROUGH CHARGED ULTRAFILTER MEMBRANES

4.1. Sulfonated poly(ether sulfone) based charged ultrafilter membranes

It is often a requirement in the chemical and biochemical sciences to separate a component from mixture based on its molecular size or charge on individual component. The increasing complexity of chemical and in particular, biochemical, or biological systems has required more sophisticated, selective and efficient technique to resolve/separate individual components. Ultrafiltration is an efficient and scalable bio-separation technique has been extensively studied in recent years and has shown grate potential for use in downstream processing of biological substances (*e.g.,* protein concentration/fractionation). Although protein concentration using ultrafiltration has become a routine and successful operation in biotechnology, fractionation of proteins using ultrafiltration is still a technological challenge and its effectiveness and efficiency are strongly dependent on operating parameters such as pH, salt concentration, permeate flux, and system hydrodynamics [1-9]. Additionally, ultrafiltration is size based separation processes and it is difficult to achieve high selectivity with high throughput. Zydney and co-workers have studied electrostatic interactions between charged proteins and charged membranes [10-14] and demonstrated that pH values and ionic strengths have profound effects on protein separation [13-15]. Several investigators were proposed nanotubular membranes [16-19], self-assembled monolyares [20,21], where pore size can be adjusted so that it can be applied to the size based protein separations. Use of porous ion-exchange membranes for protein separations is also reported by several researchers [22-24].

Electric field driven migration in the porous gels is also commonly used to separate proteins based on their charged nature [25,26]. Many electrophoretic processes have been developed under various electrical field conditions from constant applied voltages or currents to single- or multiple-dimensional pulsed electrical fields for the separation of biomolecules [27]. In addition capillary electrophoresis was also developed for solving separation/fractionation problems of proteins [28-30]. In all these aforementioned processes only one property of given molecule either its molecular size or charge and iso-electric point was used to achieve its separation under only one driving force either pressure gradient or electrical gradient. All processes involve only one selectivity parameter (either molecular size or charge) and one driving force, which result less selectivity and membrane throughput. No report is available, in which, nature of charge on the protein, its molecular size, nature and extend of charge on the membrane matrix was used to increase the selectivity of separation with high membrane throughput under coupled driving forces (pressure and potential gradient).

Herein, I am reporting negatively charged ultrafilter membrane for studying the transmission of proteins in different environments under simultaneous action of driving forces for achieving high selectivity and maximum membrane throughput because of three selectivity parameters (*i.e.* charge on the membrane matrix, nature of charge and molecular size of the protein) and dual driving forces. These charged ultrafilter membranes were characterized to investigate their physicochemical, electrochemical properties and protein binding capacity.

4.1.1. Preparation of sulfonated poly(ether sulfone) based charged ultrafilter membrane

Udel poly(ether sulfone) (PES) was obtained from Aldrich Chemicals, dimethylformamide, H_2SO_4, HCl, NaOH, NaH_2PO_4, Na_2HPO_4 (AR grade, S.D. Fine Chemicals, India) were used as received. Bovine serum albumin (BSA,

mol wt 67000 Daltons), lysozyme (LYS, mol. wt. 14600 Daltons) were received from HiMedia Laboratories Pvt. Ltd. India. Double distilled water was used for the preparation of all the solutions.

For the sulfonation of PES, 5 g of PES was dissolved in 100 ml of H_2SO_4 and the solution was kept at 50 ^{0}C in water bath for desired time (10, 15 and 24 hr. in this case) in order to achieve different degree of sulfonation. Afterward reaction was terminated by addition of five folds of water in the reaction mixture. Precipitate was collected, washed thoroughly with water and dried at 50 ^{0}C. Membranes were prepared by dissolving a known amount of sulfonated poly (ether sulfone) (SPES) in dimethylformamide with 40% (w/v) composition under constant stirring. Resulting solution was cast in the form of thin film on a cleaned glass plate and dried at 30 ^{0}C for 2 hr. Then these membrane films were gelated in water at 10 ^{0}C. These membranes were stored in wet condition and subjected to physicochemical and electrochemical studies. Different SPES based ultrafilter membranes were designated as M_x, where X is the time in hour allowed for the sulfonation reaction, while subscript 0 denotes material without any sulfonation.

4.1.2. Results and discussion for SPES based charged ultrafilter membrane

In order to achieve different functional charge density, membranes were prepared using varying degree of sulfonation of PES, by varying time span of sulfonation reaction (10, 15 and 24 hr in this case). Extent of sulfonation of PES with concentrate sulfuric acid was confirmed by ^{1}H-NMR spectroscopy. In the ^{1}H-NMR spectra, the presence of sulfonic acid group causes a

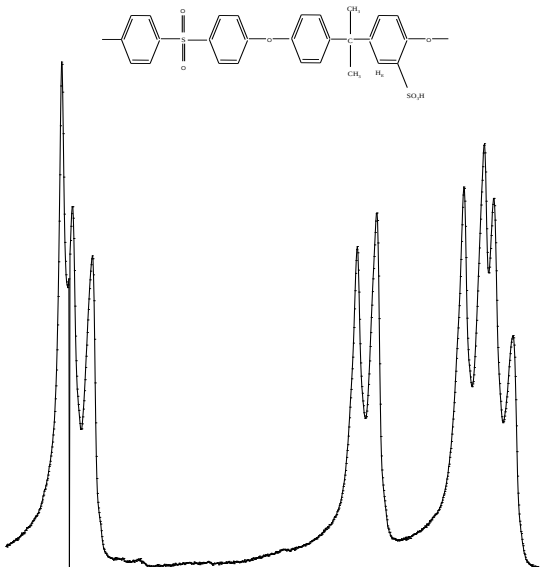

Figure 4.1.1 ^{1}HNMR Spectra of SPS.

significant downfield shift from 7.31 ppm to 8.21 ppm of the hydrogen located in the ortho position at the aromatic ring as shown in Fig. 4.1.1. By evaluating the ratios between the peak area of the signal corresponding to the hydrogen atoms located next to the sulfonic acid groups (H_E) and the peak areas of the signals corresponding to the other aromatic hydrogen atoms [31,32] degree of sulfonation was estimated. Further, sulfonation was also confirmed by FT-IR spectra, and CHNS analysis for different membrane forming material. Strong characteristic peaks for FT-IR spectra (Fig. 4.1.2) at around 1023 and 1105 cm^{-1} were observed for all sulfonated polymers, which were assigned to symmetric and asymmetric stretching of sulfonate group. Degree of sulfonation values for PES from ^{1}H-NMR measurements and C, H, N, S analysis data for different membrane forming materials are presented in the Table 4.1.1. From the increasing percentage of sulfur content in the polymer matrix and degree of sulfonation values, it was concluded that different extent of mild sulfonation of PES was achieved.

Table 4.1.1 Degree of sulfonation and % of S fo different membrane forming material**.**

Membrane forming material	Degree of sulfonation	% of S
M_{10}	70.2	8.03
M_{15}	73.0	8.88
M_{24}	75.3	9.06

[a] estimated from ^{1}H NMR.
[b] obtained from CHNS analysis.

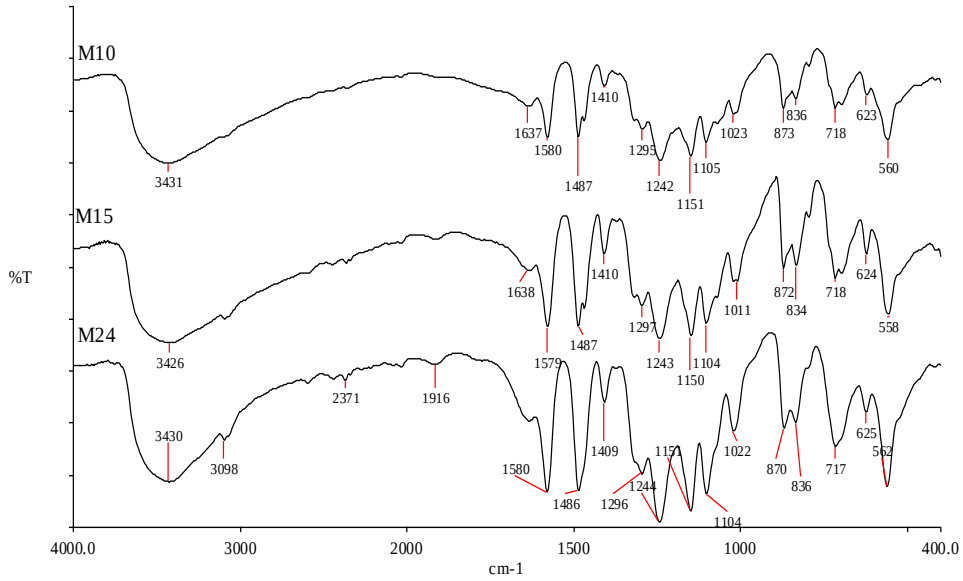

Figure 4.1.2. FTIR spectra of M_{10}; M_{15} and M_{24} membranes.

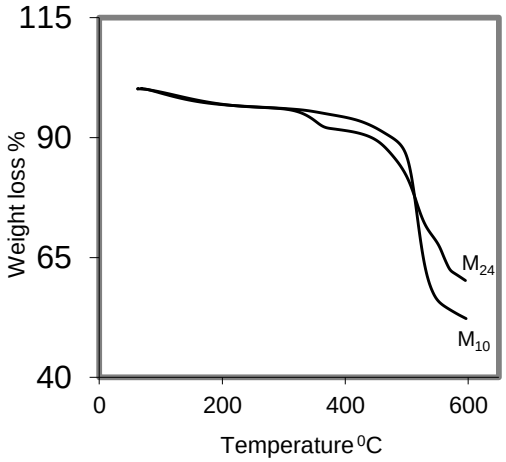

Figure 4.1.3. TGA curves of M_{10} and M_{24} membranes.

Thermal stability of prepared membranes was illustrated by TGA analysis and representative TGA curves for M_{10} and M_{24} membranes are presented in Fig. 4.1.3. All membranes exhibited two stage thermal degradation (bound water loss and polymer loss, respectively), but for membrane with high degree of sulfonation, second stage started earlier (about at 300 ^{0}C for M_{24} while about 400 ^{0}C for M_{10} membrane). Degradation in this region aroused due to oxidative desulphurization, which were pronounced for the membranes with high degree of sulfonation. The DSC analysis of these membranes was also carried out and resulting curves are presented in Fig. 4.1.4. M_{10}, M_{15} and M_{24} membranes exhibited 76.14, 98.60 and 99.80, respectively T_g values. This difference in T_g values for difference membranes may be attributed to extent of sulfonation.

Table 4.1.2. Physicochemical and electrochemical properties of membranes

Membrane	IEC (mequiv./g)	Water content (%)	φ	κ^m (mS cm^{-1})[a]	t_+^m [b]	X^m (m mol dm^{-3})
M_0	0.06	27.44	0.35	0.61	0.57	0.04
M_{10}	0.18	38.62	0.37	1.09	0.82	0.12
M_{15}	0.25	45.20	0.38	1.24	0.84	0.16
M_{24}	0.28	47.65	0.39	1.71	0.88	0.28

[a] measured in the equilibration with 0.001 mol dm^{-3} NaCl solution.
[b]estimated from membrane potential measurements using NaCl solutions of 0.01/0.001 mol dm^{-3} concentration across the membrane.

4.1.2.1. Physicochemical and electrochemical properties

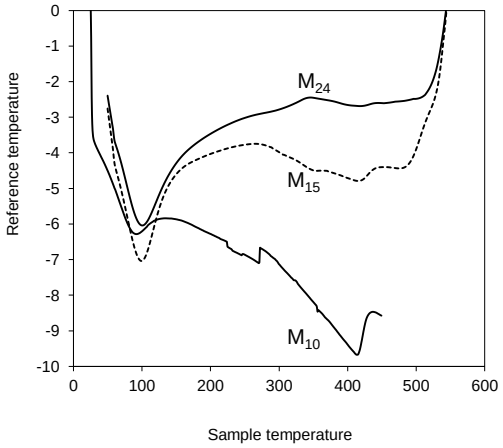

Figure 4.1.4. DSC analysis of M_{10}; M_{15} and M_{24} membranes.

Prepared membranes were characterized by measuring their physicochemical properties such as ion-exchange capacity, water content etc. Ion-exchange capacity indicates the density of ionizable hydrophilic groups in the membrane matrix, which are responsible for their charged nature. In general, membranes having the same degree of cross-linking and composition absorb the same amount of water, where density of ionizable groups is the same throughout the membrane matrix [33,34]. The IEC values presented in Table 4.1.2, reveal that membranes ion-exchange capability increased with increase in degree of sulfonation or time allowed for the sulfonation reaction. Furthermore, relatively low IEC values of these membranes suggested that these membranes are mild in charged nature.

Water content of the membrane was determined by means of Eq. 2.6 and relevant data are presented Table 4.1.2. It can be seen that with the increase in extent of functionalization for different membranes, their water content values were increased because of increase in hydrophilic nature of

membrane forming material. Information regarding membrane void volume also can be have from the membrane void porosity (τ, volume of free water within membrane per unit volume of wet membrane) data was obtained by Eq. 2.8 [35,36]. ΔV may be estimated by Eq. 2.9. φ Values for different membranes are also presented in Table 4.1.2, which was used for the determination of fixed ion concentration (X^m) of the membrane in units of (moles of sites)/(unit volume of wet membrane) which is related to the ion-exchange capacity by Eq. 2.11. X^m data presented in Table 4.1.2 reveals extremely low charge density for PES membrane without any sulfonation (M_0) (X^m = 0.037 m mol dm^{-3}), while M_{24} membrane exhibited 0.283 m mol dm^{-3} fixed ion concentration. These values indicate that membranes were moderately charged, while their degree of sulfonation and fixed ion concentration increased with the time allowed for the sulfonation reaction. Furthermore, moderate negatively charged ultrafilter membranes subjected for electrochemical characterization by measuring membrane conductivity (κ^m) and counter-ion transport number in the membrane phase (t_+^m).

Membrane conductivity, which bears important information about ionic migration across the membrane, was measured for different membranes in equilibration with NaCl solution of 0.01 mol dm^{-3} concentration and relevant data are presented in Table 4.1.2. All membrane exhibited relatively low conductivity because of their porous nature. Also an increase in the degree of sulfonation in the membrane matrix, concentration of charged functional groups in it increases and resulted in the increase in membrane conductivity. Counter-ion transport number $\left(t_i^m\right)$ in the membrane matrix, is also an important parameter to assess selectivity of synthesized membrane, was estimated from membrane potential measurements in equilibration with NaCl solutions of 0.0055 mol dm^{-3} mean concentration. All membranes showed mild selectivity for Na^+, and membrane selectivity increased with the degree of sulfonation for membrane forming material. Furthermore, these values exhibited good correlation with X^m obtained from the IEC measurements.

4.1.2.2. BSA adsorption characteristics

To examine the interactions between protein and mild negatively charged surfaces, BSA adsorption and binding capacity was determined in batch mode at different pH of protein solution. BSA adsorption % was estimated by the ratio of amount of BSA adsorbed and amount of BSA taken for equilibration. Relevant data for BSA adsorption at different pH are presented in Fig. 4.1.5(A) with respect to fixed ion concentration of the membrane interface. At pH: 4.8 and 10.7, adsorption was about independent of the functional nature of the membrane. In this case membrane matrix bears negatively charged interfaces, and net charge on the BSA was either zero or negative at both the pH range, thus adsorption of the BSA was not electro-statically favoured. But at pH: 2, BSA carries positive charge and its adsorption on negatively charged matrix was favored due to mutual electrostatic attraction, in which BSA adsorption increased with the increase in membrane charged nature. Similar trend was also observed in the case of BSA binding capacity data presented in Fig. 4.1.5 (B), in which highly charged membrane M_{24} hold more protein molecules than those, which are relatively less charged (M_{10} & M_{15}) at the given pH.

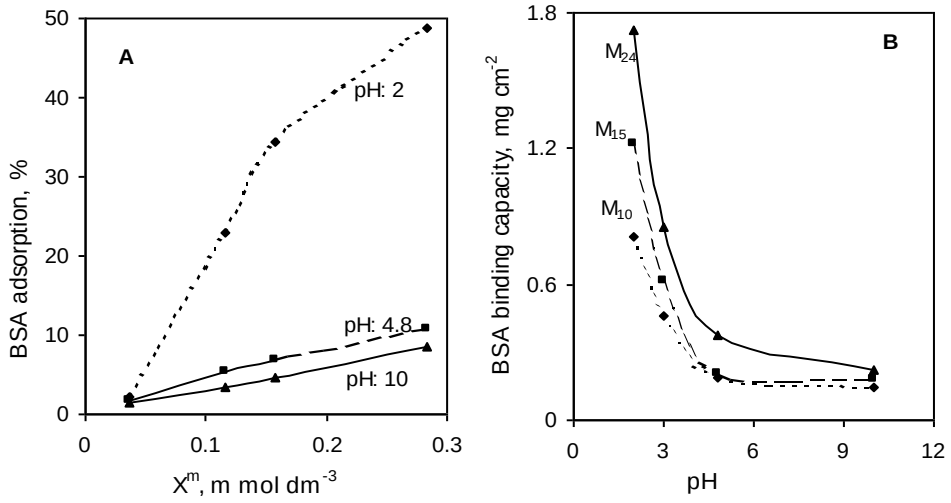

Figure 4.1.5. Comparison of BSA: (A) adsorption; (B) binding capacity at different solution pH and fixed charge density (X^m) of membranes using 5-mg/ml concentration of BSA.

4.1.2.3. Membrane permeation studies

To investigate the impact of membrane forming materials, their charged nature and optimum condition of gelation on the membrane performance and throughput, volumetric fluxes through the membranes were measured under varied applied pressure and electrical gradient, separately in equilibration with NaCl solution of 0.001 mol dm^{-3} concentration and relevant data for electro-osmotic flux and hydrodynamic flux are presented in Fig. 4.1.6 (A & B), respectively.

Electro-osmotic permeability (J_v/I) was determined from the slop of straight lines presented in Fig. 4.1.6 (A), and was used for estimation of zeta potential. Surface charge on a membrane has a significant influence on its separation properties. Knowledge of the electrokinetic properties such as zeta potential of a particular membrane type could prove to be a major contributing factor behind the decision to implement that membrane for a specific separation process, as the surface charge on a synthetic membrane has a significant influence on its separation properties [37,38] and fouling tendency [39,40]. The surface charge density of a porous membrane is related to the zeta potential of the membrane. The widely used techniques are measurements of electro-osmotic permeability and Smoluchowski Eq. 2.16 was used for the estimation of Zeta potential (ξ) [41,42]. The Smoluchowski

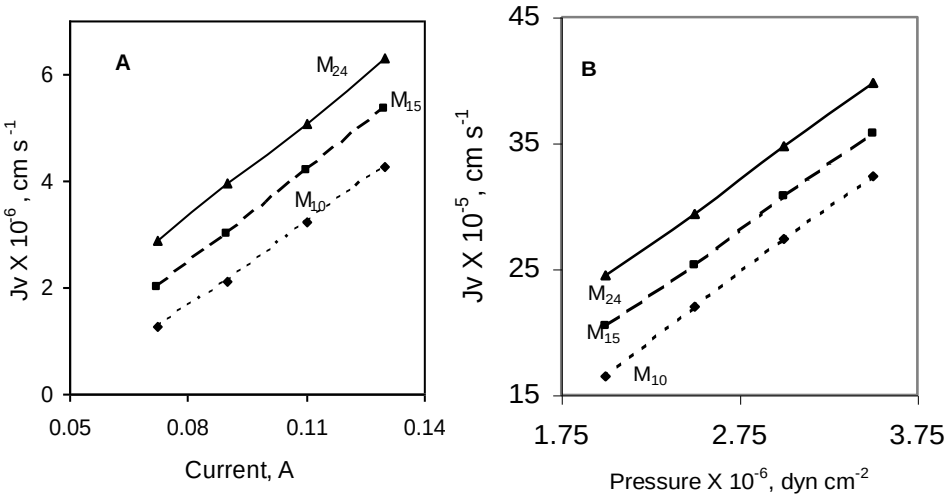

Figure 4.1.6. Variation of volumetric flux through different membranes: (A) under applied current; (B) under applied pressure gradient.

equation is known to be limited in its applicability to small pore size and electrolyte strength less than 10^{-3} M. In general the zeta potential of the membranes is supposed to represent the chemical nature of the membrane material. If the groups are strongly acidic (sulfonic acid group in the present case) the dissociation takes place at once and the zeta potential can be expected to be strongly negative. Zeta potential values for different membranes increased with the increase in the fixed ion concentration in the membrane phase (Table 4.1.3), revels the quite charged nature of the membrane interfaces. Further, relatively moderate zeta potential values indicate membrane capability for charge based selection/rejection.

The relationship between flux (J_v) and pressure was linear for all studied membranes in the applied pressure range (Fig. 4.1.6(B)). It is very interesting to find that charged nature of the membrane influences flux. The reason might be related to the increase in membrane compactness or decrease in its hydrophilic characteristics with decrease in degree of sulfonation or functional nature. Further idea about compactness of the membrane we can have from apparent pore radius (r_p) values from Hagen–Poiseuille Eq. 2.18 [31,43]. In this case hydrodynamic permeability was measured using NaCl solution of 1.0 mM concentration in the absence of any applied electrical gradient. r_p values estimated from Eq. (2.23) are presented in Table 4.1.3. M_{10}, M_{15} and

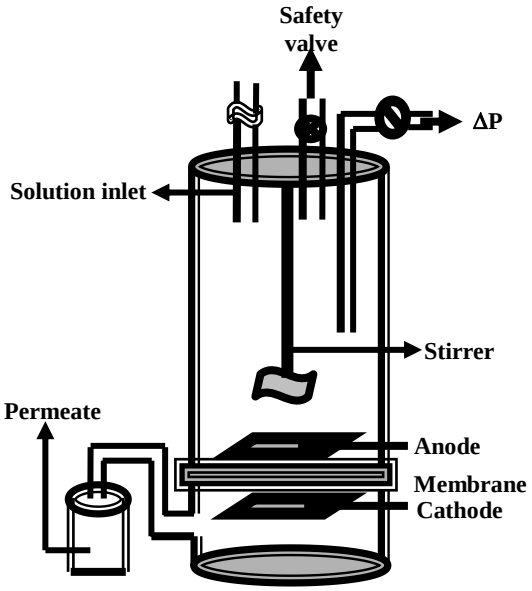

Figure 4.1.7. Experimental cell for ultrafiltration under applied electrical gradient.

M_{24} membranes resulted 2.11, 1.70, and 1.52 nm, r_p values, respectively. This observation shows that compactness of membranes was increased with increase in degree of sulfonation.

4.1.2.4. Ultrafiltration experiments under applied potential gradient

Ultrafiltration experiments, with or without applied potential gradient, using desired solution of BSA or LYS were conducted in dead-end and cross-flow permeation modes using plate and frame model. The experimental cell shown in Fig. 4.1.7. In these experiments using M_{10}, M_{15} and M_{24} membranes and BSA solution of 5.0 mg/ml concentration was carried out at pH: 2.0; 4.8; and 10.7, separately without and with different applied potential gradient in order to investigate the transmission characteristics of protein in various experimental conditions. Schematic diagram for the mode of ultrafiltration experiments were conducted without any applied potential gradient is presented in Fig. 4.1.8(A). While Fig. 4.1.8(B) represents ultrafiltartion experiment with applied potential gradient and electrical polarity. Polarity of

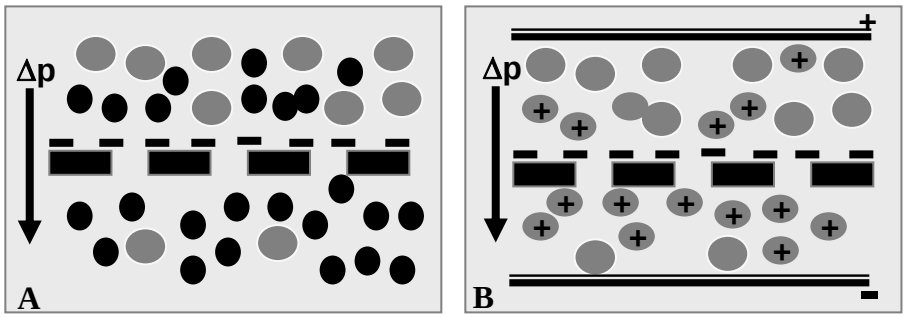

Figure 4.1.8. Schematic presentation of: (A) ultrafiltration; and (B) ultrafiltration under applied potential gradient.

the applied potential was fixed so that electrode in the feed side became anode and towards permeate side became cathode so that only positively charged BSA (BSA^+) are facilitated to cross through the negatively charged membrane under the influence of coupled driving forces (pressure and potential difference). In other cases negatively charged BSA (BSA^-) or

zwitterion BSA (BSA^0) are suppose to be exhibit very low transmission under given polarity and charged nature of the membrane.

Table 4.1.3. Permeation characteristics of membranes

Membrane	L_{11} X 10^{-10} (cm^3 dyn^{-1} s^{-1})	r_p[a] (nm)	J_{12}/I X 10^{-7} (Amp^{-1} cm s^{-1})	ξ [b] (mV)
M_{10}	1.06	2.11	5.19	0.88
M_{15}	1.02	1.70	5.62	0.95
M_{24}	1.02	1.52	5.93	1.01

Fig. 4.1.9(A) presents volumetric flux of BSA solution of varied pH as a function of applied pressure without any applied potential gradient for M_{24} membrane, in representative case. It can be seen that for pH: 2 highest solvent fluxes were observed because of high migration of positive ions across

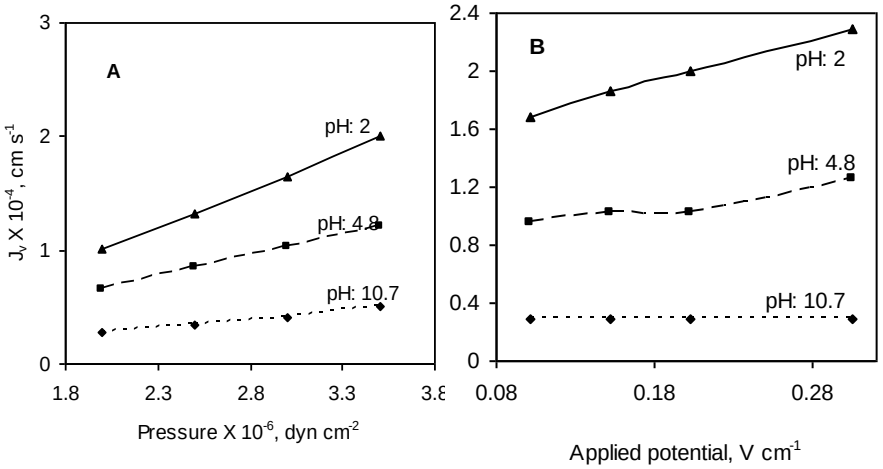

Figure 4.1.9. Volumetric flux of M_{24} membrane in equilibration with 5 mg/ml BSA solutions of different pH: (A) under varied pressure and without potential gradient; (B) under 3 X 10^{-6} dyn cm^{-2} pressure and varied potential gradient.

the membrane, while in other cases relatively low flux may be attributed to less transmission of uncharged or negatively charged ions because of the charged membrane matrix. In order to investigate the effect of BSA transmission on the solvent flux, same experiments were conducted using only buffer solution of desired pH but same trend was reproduced. Similar

conditions were also aroused for Fig. 4.1.9(B) in which flux is presented as a function of applied potential gradient and 3 X 10^{-6} dyn cm^{-2} applied pressure. It was interesting to record that at constant applied pressure, flux also increased with increase in the potential gradient, which was more predominant in the case of BSA^{+}. This may be attributed higher BSA^{+} electrophoretic migration along with solvent molecules. It was also observed that contribution of electrophoretic transmission of BSA^{+} was higher than in the comparison of BSA^{-} or BSA^{0}. Additionally, (Fig. 4.1.10(A)) reveals that flux was not only depends on applied pressure or potential gradient but it also depend on fixed ion concentration on the membrane matrix (X^m). Thus in the present studies, there are three parameters such as applied pressure, potential gradient, and extent of the charge on the membrane matrix, which governs the mass and protein migration across the membrane, where membranes were having more or less same apparent pore diameter (Table 4.1.3). Here it is important to record that, fouling was noticeably absent in all the cases with less than 2% reduction in the membrane permeability after repeated use.

4.1.2.5. Protein transmission and separation factor

Observed protein transmission (ζ_{obs}) was estimated by the ratio of protein concentration in the feed side to the permeate side. ζ_{obs} for BSA solution is presented in Fig. 4.1.10 (B&C) under 3 X 10^{-6} dyn cm^{-2} applied pressure without and with and 0.203 V cm^{-1} applied potential gradient for pH: 2.0 and 10.7, respectively as function of membrane charge density.

Effect of charged nature of the membrane matrix and influence of applied electrical gradient on protein transmission was further investigated by plotting ζ_{obs} against charge density of the membrane (X^m) (Fig. 4.1.10(B&C)) for BSA solution at pH 2.0 and 10.7, respectively. At both pH (BSA^{+} or BSA^{-}) in the absence of any applied potential, ζ_{obs} values decreased with the increase in the X^m or zeta potential of membrane-solution interfacial Zone. But under coupled action of pressure and potential gradient, ζ_{obs} values increased with the membrane charge density for pH 2.0 (BSA^{+}), also same

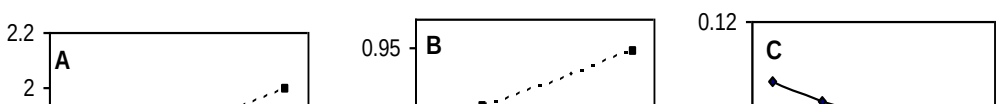

trend was observed for solution at pH 10.7 (BSA^-). But magnitude of ζ_{obs} for BSA^+ was about more than eight times grater than that obtained for BSA^-.

Figure 4.1.10. (A) Volumetric flux; (B) and (C) observed BSA transmission (ζ_{obs}) values as function of fixed charge density of membranes in equilibration with 5 mg/ml BSA solution at under 3 X 10^{-6} dyn cm^{-2} applied pressure for: (A) pH – 2; (B) pH – 2; and (C) pH – 10.7, without or with potential gradient. Solid line - without applied potential gradient and Dotted line - with 0.203 V cm^{-1} applied potential gradient.

In the previous case, charge on the BSA molecule as well as membrane interface, and polarity of potential gradient, all are facilitating the transmission of BSA^+ through the membrane, while in the latter case similar charges on the BSA molecule and membrane interface opposing each other and was responsible for the observed significant reduction in the protein transmission. Here we may conclude that it possible to govern the transmission of protein by varying nature of the charge on it (pH), nature and extent of the charge on the membrane matrix, polarity of the applied potential gradient with an ultrafilter membrane of given pore dimension. Also for both cases ζ_{obs} under constant applied electrical and pressure gradient was higher than without any electrical gradient and exhibited opposite trend. Coupling of the driving forces always resulted more membrane throughput (protein transmission).

ζ_{obs} for BSA solution is presented in Fig. 4.1.11(A&B) under 3 x 10^{-6} dyn cm^{-2} applied pressure without and with 0.203 V cm^{-1} applied potential gradient, respectively as a function of solution pH for M_{10} and M_{24} membrane. ζ_{obs} values for M_{24} membrane was lower than those for M_{10} membrane, when only pressure difference was applied as driving force, but opposite trend was

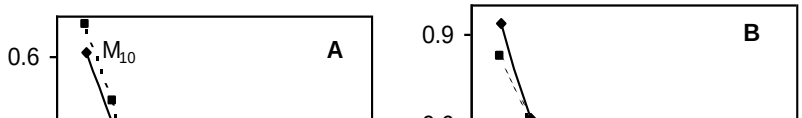

observed when pressure and potential difference, both simultaneous were applied as driving forces.

Figure 4.1.11. Observed BSA transmission (ζ_{obs}) values as function of pH through M_{10} and M_{24} membranes for 5 mg/ml BSA solution: (A) under 3 X 10^{-6} dyn cm^{-2} pressure; (B) under 3 X 10^{-6} dyn cm^{-2} pressure and 0.203 V cm^{-1} applied potential gradient. M_{24}-solid line; M_{10}- dotted line.

This indicates charged nature of the ultrafilter membrane is one of the facilitative parameter for the separation of protein under coupled driving forces, where BSA showed high transmission at constant pH. Further, data presented in (Fig. 4.1.11) reveal that pH of the protein solution also one of the sensitive parameter for achieving higher extent of its transmission through the membrane. In this case, where membrane was negatively charged, highest transmission for BSA^{+} (pH: 2.0) was observed. While in other two cases (pH: 4.8 & 10.7), ζ_{obs} closures to zero indicate negligible protein transmission through the charged membranes.

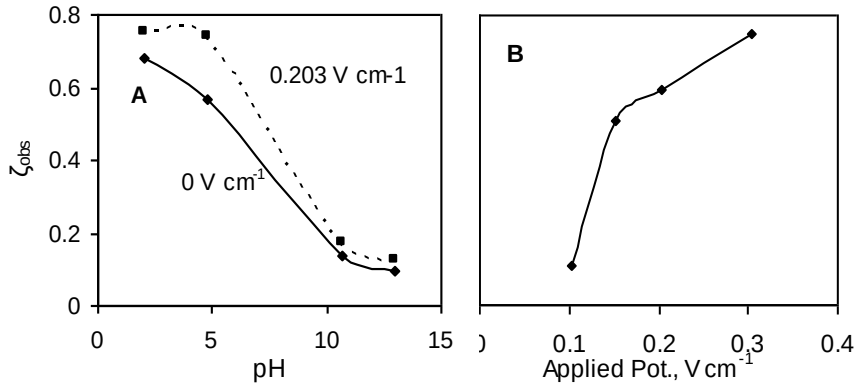

Figure 4.1.12. Observed LYS transmission (ζ_{obs}) values for M_{24} membrane as function of: (A) pH; (B) at pH 4.8, of 5 mg/ml LYS solution in 3 X 10^{-6} dyn cm^{-2} pressure and different applied potential gradient.

Ultrafiltration experiments under coupled driving forces were also conducted using LYS solutions at different pH ranging between 13.0-2.0, where it existed in different ionic forms. Representative data of ζ_{obs} values for M_{24} membrane are presented in Fig. 4.1.12 for different experimental conditions. In this case also observed protein transmission was strongly dependent on the nature of the charge on the transmitting species (pH) and applied potential gradient coupled with the constant applied pressure. Iso-elecetric point of lysozyme is 10.7; hence at pH 2.0 and 4.8 LYS exhibited LYS^+ form. Observed transmission of LYS^+ was close to eight while it was close to zero for LYS^0 and LYS^- (pH: 10.7 or more). Now we will introduce separation factor defined as ratio of LYS to BSA transmission i.e. $(\zeta_{obs})_{LYS}/(\zeta_{obs})_{BSA}$. Variation of separation factors is presented in (Fig. 4.1.13) as function of pH of the protein solutions. At pH 4.8 (iso-electric point of BSA), highest separation factor was achieved. At this pH, transmission of BSA^0 was very less in comparison to extremely high transmission of LYS^+. On other pH range both proteins showed very less transmission across the membrane under given experimental conditions. Interestingly, separation factor values increased with the increase in applied potential difference under the constant action of 3 X 10^{-6} dyn cm^{-2} pressure difference. After studying the variation of ζ_{obs} for BSA and LYS and their separation factor with pH, one can guess the feasible, efficient and selective separation of both proteins using these membranes under coupled driving forces.

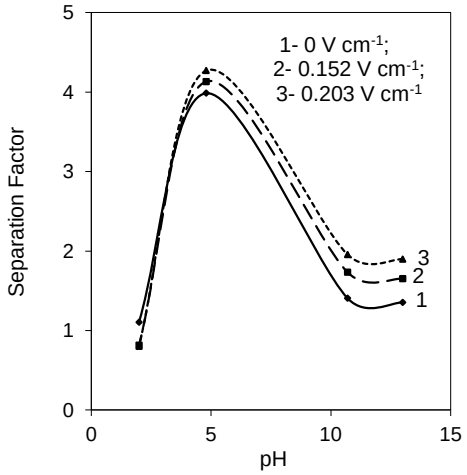

Figure 4.1.13. Separation factor as function of pH for in 3 X 10^{-6} dyn cm^{-2} pressure and different applied potential gradient for M_{24} membranes.

4.1.3. Conclusions for sulfonated poly (ether sulfone) based charged ultrafilter membranes

In this work we prepared negatively charged ultrafilter membranes by different degree of sulfonation of poly (ether sulfone). These membranes showed different extent of charge density on the membrane matrix. Adsorption study at various pH of the protein solution was performed and it was observed that protein binding capacity of the membranes was strongly dependent on the pH of the protein solution as well as extent of charge on the membrane matrix. Using these membranes, transmission characteristics of BSA and LYS were investigated under single or coupled driving forces *i.e.* pressure difference and applied potential gradient. It was found that membrane flux and observed protein transmission through the membrane increased under the simultaneous action of driving forces. pH of the protein solution (*i.e.* their iso-electric points), and extent of the charge on the membrane matrix have strong influence on the observed transmission of the protein. It was concluded that transmission of protein can be governed by varying nature of the charge on it (pH), nature and extent of the charge on the membrane matrix, polarity of the applied potential gradient with an ultrafilter membrane of given pore dimensions. Coupling of the driving forces always resulted more membrane throughput with relatively high selectivity. Based upon these results, it is possible to achieve selective and efficient transport/separation of BSA-LYS at pH 4.8. Furthermore, this study established the basis for the development of new process and hydrophilic modified ultrafilter membrane for the fractionation of proteins depending their iso-electric points. In this processes, charge on the protein, nature and extent of the charge on the membrane interfaces, polarity of the potential gradient all are governing the transport of given protein across the membrane, which will result high selectivity and membrane throughput. As spin off charged nature of the membrane matrix and bipolar electrical environment avoids the fouling of the membrane, which was the common phenomenon for the protein fractionation by ultrafiltration membrane.

4.2. Organic-inorganic hybrid charged ultrafilter membranes for proteins separation

In biotechnology, separation of biochemical from mixture based on its charge and molecular size of individual component is often required. The increasing complexity of chemical and in particular, biochemical, or biological systems has required more sophisticated, selective and efficient technique to resolve/separate individual components [44]. Separation or isolation of individual protein from a mixture is also most cost intensive part during downstream processing for bio-production of proteins. Therefore, selectivity and rate of separation procedure are main factors to make process most attractive and cost effective. Chromatography steps are highly selective but too expensive [45]. Membrane fractionation particularly ultrafiltration (UF) is a promising tool for biotechnological down stream processing, but it seen to be not being very much selective when separating similar sized proteins. UF is a pressure-driven separation process, in which membranes with 1-100 nm pore size being used [46]. Zydney and co-workers have made a grate contribution in investigating the effect of electrostatic interaction on protein transport in the membrane system [12]. Many processes with electric gradient as driving force such as electrophoresis, gel electrophoresis, capillary electrophoresis, etc were also developed for commercial practice of protein separation [26]. In all these processes, either pressure or electric gradient was imposed to achieve protein separation. In literature, electro-ultrafiltration (UF under electric field) is also reported to achieve fractionation/separation of protein with enhanced throughput using uncharged UF membranes [47]. But no report is available, in which UF was performed under coupled driving forces using positively or negatively charged membranes for achieving enhanced selectivity (purity) and membrane throughput. Due to coupling of driving forces across the suitable charged membrane will lead a rapid and selective protein separation process due to high membrane throughput, which is very urgent for the fast down stream processes. In addition, choosing membrane-forming material with which a

given protein can have high degree of interaction can enhance selectivity of the process.

Organic-inorganic nanostructured composites constitute an emerging research field, which has opened the possibility of tailoring new materials because they combine in a single solid both the attractive properties of a mechanically and thermally stable inorganic backbone and the specific chemical reactivity and flexibility of the organo functional groups. Up to now, the cation-exchange organic–inorganic hybrid materials have been frequently reported, in the hope of replacing the expensive perfluorocarbon cation-exchange materials such as Nafion [49-52,42]. Use of these type of material as anion-exchange membranes have been also investigated [35,53]. However, unfortunately no report is available regarding the application of organic-inorganic hybrid nanostructured charged membrane with desired pore size for protein separation either by UF or under coupled driving forces. Due to presence of hydrophilic nature of silica in the membrane forming material and high water content even at elevated temperature, these types of membranes will show improved interactions with protein depending on their charge and thus exhibit more protein transmission across it.

Herein, we are reporting preparation of organic-inorganic hybrid charged membrane by sol-gel process in aqueous media and gelation of these membranes in non-aqueous media for tailoring pore texture. Both type of charged membranes were used for developing a rapid and highly selective protein separation method under coupled driving forces (pressure and electric gradient) for achieving high selectivity and maximum membrane throughput because of three selective parameters (*i.e.* charge on the membrane matrix, nature of charge and molecular size of the protein). Whereas, in aforementioned method, only one selective parameter either charge or molecular size was considered for their fractionation/separation. Positively and negatively charged organic-inorganic hybrid membranes were employed to achieve pH sensitive protein separation under coupled driving

forces using binary mixture of bovine serum albumin and lysozyme as a model case.

4.2.1. Materials and preparation of organic-inorganic hybrid charged ultrafilter membranes

Poly (vinyl alcohol) (PVA) (Mw: 125,000 Daltons), hydrochloric acid, ammonia (Sp gr 0.98), hydrogen peroxide solution (37-40% w/v), sodium hydroxide, sodium chloride, ammonium persulfate, dimethyl sulfate, methanol, formaldehyde, sodium azide, sodium sulfate, Sodium hydrogen phosphate, disodium hydrogen phosphate and sulfuric acid of AR grade were obtained from S. D. Fine Chemicals, Mumbai, India. Mercaptopropylmethyldimethoxysilane (MPDMS), tetraethylorthosilicate (TEOS), 4-vinylpyridine (4-VP) and divinylbenzene (DVB) are obtained from Aldrich Chemicals and used as obtained. Bovine serum albumin (BSA; Mw: 67,000 Daltons) and lysozyme (LYS; Mw: 14,600 Daltons) were received from HiMedia Laboratories Pvt. Ltd. India. Double-distilled water was used in all experiments.

Organic–inorganic hybrid positively charged membranes (PCM) and negatively charged membranes (NCM) based on poly (vinyl alcohol)/SiO_2 were prepared via sol-gel. For the preparation of PCM, five grams of PVA was dissolved in 100 ml of hot (at 70 ^{o}C) deionized water under constant stirred condition to obtain a homogeneous clear solution. Then, two grams of TEOS and five grams of MPDMS were added drop wise under constant stirring for 2 hr. The pH of clear homogeneous solution was adjusted to 2.0 using 1M HCl. Resultant clear solution again stirred for 1 h and air bubbles were removed from the solution by applying vacuum. The obtained milky coloured gels were cast on a cleaned glass plate covered with poly (ethylene) (HDPE) sheet of desired thickness and partially dried for 2 h at ambient temperature (30 ^{o}C). Then dried film gelated by immersing it in methanol at 10 ^{o}C. Thus, obtained thin films were immersed in a solution containing formaldehyde (54.1 g), sodium sulfate (150.0 g), sulfuric acid (125.0 g), and water (470.0 g) for 1 h at 80 ^{o}C for effecting cross-linkage in the membrane by formal reaction. The

obtained membranes were subjected to oxidation for the conversion of mercapto group in to the sulfonic acid group with the treatment of hydrogen peroxide.

For the preparation of NCM, five grams of PVA was dissolved in 100 ml of hot (70 ^{o}C) deionized water under constant stirred condition to obtain a homogeneous clear solution. Then the required quantity of the 4-vinylpyridine (monomer), divinylbenzene (4% w/w), and ammonium persulfate (4% w/w) was added and temperature was maintained at 70 ^{o}C. The mixture was kept for under stirred condition for 1 h to get the semi-interpenetrating polymer network. Further equivalent amount of the dimethyl sulfate with respect to 4-vinylpyridine was added to quaternize the pyridinium group. The mixture was stirred for 2 h at room temperature to obtain a clear homogeneous solution. Then 2 ml of TEOS was added drop wise at room temperature and the mixture was kept under stirred condition for 24 h to get a gel. The resulting gel was cast on a clean glass plate with the desired thickness covered with poly (ethylene) (HDPE) sheet of desired thickness and partially dried 1.5 h at ambient temperature (30 ^{o}C). Then dried film gelated by immersing it in methanol at 10 ^{o}C. Thus, obtained thin films were subjected for effective cross-linkage by formal reaction by immersion in a solution containing formaldehyde (54.1 g), sodium sulfate (150.0 g), sulfuric acid (125.0 g), and water (470.0 g) for 1 h at 80 ^{o}C.

Before being subjected to physicochemical and electrochemical characterizations, the resulting membranes were conditioned in 0.10 M HCl and 0.10 M NaOH solutions alternatively several times and stored in the distilled water.

4.2.2. Results and discussion for organic-inorganic hybrid charged membranes

Organic–inorganic hybrid nano-structured PCM and NCM were prepared by molecular or nanometer level dispersion between inorganic and organic polymers by covalent or hydrogen bonding by sol-gel and based on poly (vinyl alcohol)/SiO_2. PVA grafted with the mercapto groups or poly (4-vinylpyridine) results in good flexibility and silica of the inorganic part provides better thermal and mechanical stabilities. In the sol-gel process, the reaction of silica precursor and water in the presence of acid or base forms one-phase solution that goes through a solution-to-gel transition and forms a rigid two-phase system comprising solid silica (SiO_2) and solvent filled pores. The condensation and polymerization reaction of the silica precursor is a bimolecular nucleophilic substitution reaction, preceded by rapid protonation of the OR or OH substituents bonded directly to silicon atom. With time, sufficient numbers of interconnected Si – O – Si bonds are formed in a region and they interact cooperatively to form colloidal particles or sol. Subsequently, colloidal particles link together to form a three-dimensional network or a gel. The gel was cast on the suitable support and gelated in methanol certain level after drying. In composite film NCM, negatively charged -SO_3H groups were introduced by oxidation of the existing -SH group in MPDMS in acidic condition, on the contrary PCM possesses anion exchange group ($–N^+(CH_3)_3$). Further membranes were cross-linked with HCHO-H_2SO_4. The purpose of gelation in non-aqueous medium is to modify

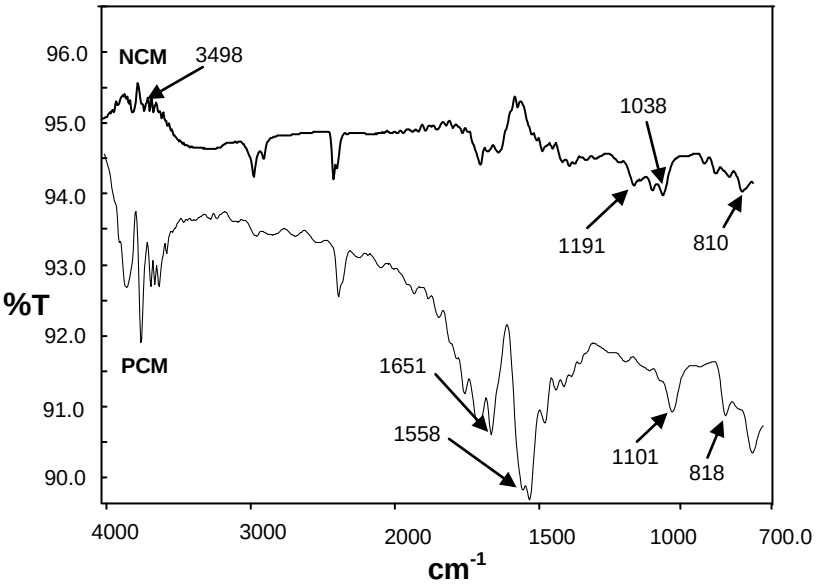

Figure 4.2.1. FTIR spectra for PCM and NCM.

the pore dimension and structure of membrane. Fig. 4.2.1 shows IR spectrum of NCM ad PCM, which show the characteristic bands at around 800 cm^{-1} and 1100-1200 cm^{-1} due to symmetric and asymmetric Si-O-Si stretching respectively. These bands are characteristic bands of PVA-SiO_2 hybrid membranes. In the NCM, presence of broadband in the region of 1030-1090 cm^{-1} confirmed $–SO_3H$ group. The broad absorption band observed at around 3400 cm^{-1}, indicated that there was significant number of -OH groups due to the non-condensed SiOH and/or unreacted –OH groups of the PVA. We suppose that these -OH groups provide the sites for hydrogen bonding between polymer and water, and provide high water retention capacity at elevated temperatures [54]. In the PCM, presence of band at 1558 cm^{-1} is due to C-N stretching, which confirmed $–N^+(CH_3)_3$ group. The absorption band was observed at 1651 cm^{-1} due to the presence of corresponding aromatic groups in PCM [38].

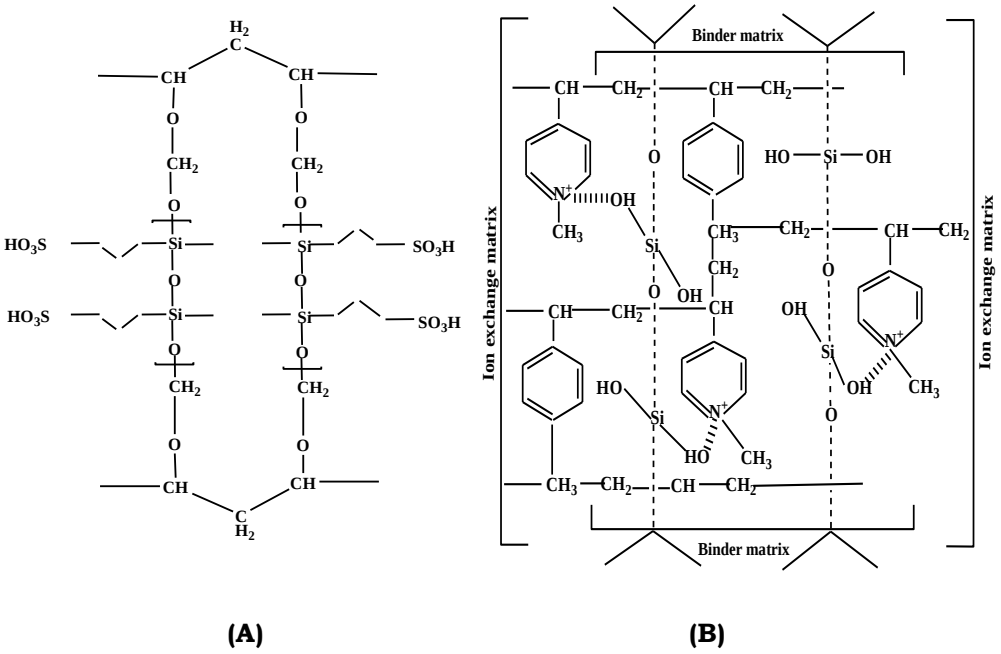

Figure 4.2.2. Schematic structure of: (A) NCM (sulfonated organic-inorganic nanocomposite); and (B) PCM (quaternised semi-interpenetrating (IPN) type organic-inorganic nanocomposite).

Schematic structures of NCM and PCM are presented in Fig. 4.2.2 (A&B), respectively. These nano-composite charged membranes exhibited affinity towards water due to attached silica and grafted functional groups, which leads to hydration of polymer matrix with enhanced water retention capability. Both type of membrane forming materials are moderated acidic or basic in nature and exhibited negative or positive charge depending on functional groups.

4.2.2.1 Physicochemical and electrochemical properties of NCM and PCM

Thermal stability of hybrid membranes was investigated by TGA, and corresponding curves obtained under flowing nitrogen for both PCM and NCM were presented in Fig 4.2.3. The three-stage TGA curves were obtained for both membranes due to three main degradation stages, arising from the processes of thermal desoluation, thermal defunctionalization (desulfonation or decomposition of quaternary amino groups), and thermal oxidation of the polymer matrix. The first weight loss occurred around 100 °C for both membranes were attributed to the loss of absorbed water molecules in the membrane matrix. The second weight loss region (250-400 °C) corresponds to the loss of -SO_3H or quaternary amino group. In the third weight loss region (400-500 °C), the polymer residues were further degraded, which corresponds to the decomposition of the main chains of the PVA. The DSC analysis was also carried out in the nitrogen atmosphere with a heating rate of 5 °C/min, and the resulting curves for PCM and NCM were presented in Fig 4.2.4. PEM exhibited *T*g value around 104 °C while NCM showed *T*g value around 113 °C, indicating comparable *Tg* values for both membranes. NCM and PCM prepared with condensation polymerization of silica precursors by the base catalyst were white and brownish is colors, respectively. Fig. 4.2.5 (A-C) shows SEMs of surface of PCM, NCM and cross-section of PCM, respectively. The effect of nature functional groups is clearly observed in these SEMs. In

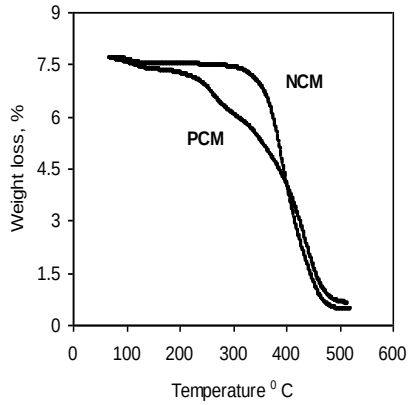

Figure 4.2.3. TGA curves for PCM and NCM membranes.

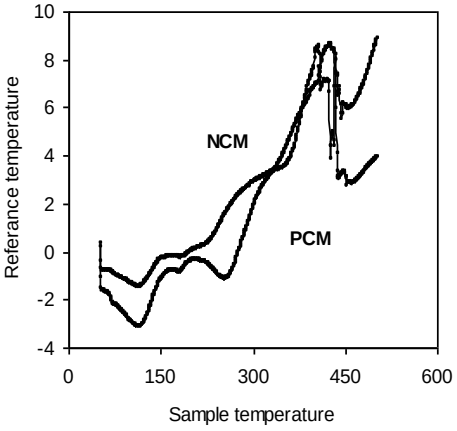

Figure 4.2.4. DSC curve for PCM and NCM membranes.

Fig. 4.2.5 (C), presence of quaternary amino groups is clearly visible from the SEM of cross-section of PCM. Surfaces of both membranes were quite smooth and no phase separation of the membrane surface could be observed suggesting that the prepared polymeric thin films were homogeneous and quite dense in nature.

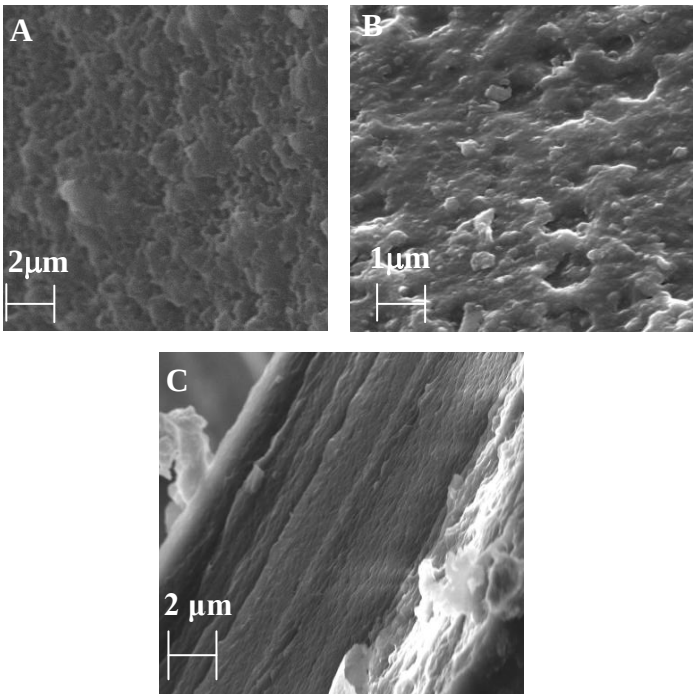

Figure 4.2.5. SEM images of: A) PCM; B) NCM; and C) Cross-section image of PCM.

NCM and PCM were also characterized by measuring their electrochemical properties like ion exchange capacity, membrane conductivity and counter ion transport number, and contact angle in the membrane phase. The corresponding data were presented in Table 4.2.1 Water content values in membrane phase were estimated using Eq. 2.6, was quite high for NCM due to more hydrophilic mature of membrane. Water content value was used for the estimation of membrane void porosity (τ, volume of free water within membrane per unit volume of wet membrane) [38]. Thus, NCM showed higher void porosity in comparison with PCM. IEC values for both membranes presented in Table 4.2.1, reveal higher exchange capacity of NCM in compare with PCM. Furthermore, moderate IEC value (0.4-0.6 mequiv g^{-1}) of these membranes indicated their charged nature due to presence of functional groups rather than their highly ion-exchange characteristics. Furthermore, IEC value in conjunction with τ value was used to estimate the surface charge density (X^m) in the membrane matrix [51]. The X^m values also suggest

mild charged nature for both membranes; however, charge density of NCM membrane was slightly higher than PCM composite membrane. Contact angle values indicate the wettability or hydrophilic nature of membranes. Quite high contact angle value (≈ 90°) will be favourable for the use of these membranes for protein separations. Mild charged nature of the composite membranes was also revealed by membrane conductivity (κ^m) and counter-ion transport number in the membrane phase (t_i^m) data.

Table 4.2.1. Physico-chemical properties of membranes.

S. No	Properties of membranes	Membranes	
		NCM	PCM
1.	Membrane thickness (δ; mm)	0.24	0.27
2.	Water content (%)	48.46	36.66
3.	IEC (equiv./gm)	0.593	0.461
4.	Contact angle	80.70^0	69.61^0
5.	Membrane conductivity (mS cm^{-1})	3.37	3.01
6.	Counter-ion transport number	0.727	0.621
7.	Membrane porosity	0.326	0.301
8.	Surface charge concentration (m mol dm^{-3})	0.399	0.269

[a] *measured in the equilibration with 0.001 mol dm^{-3} NaCl solution.*
[b] *estimated from membrane potential measurements using NaCl solutions of 0.01/0.001 modm^{-3} concentration across the membrane.*

It was observed cation migration was accelerated across NCM due to negatively charged nature, while anion transport was accelerated across PCM due to its positively charged nature. Based on these characterizations we can conclude that both types of organic-inorganic hybrid membranes are hydrophilic in nature, having mild porosity and charged nature.

4.2.2.2. BSA adsorption on the organic-inorganic hybrid charged membranes

Protein adsorption phenomena have recognized as the

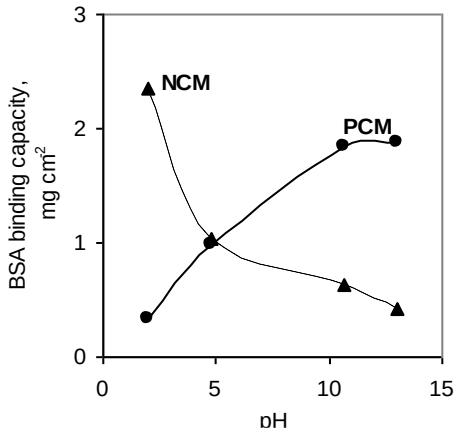

Figure 4.2.6. Binding capacity of BSA solution (5.0 mg/ml) with NCM and PCM at different pH for 6 h adsorption.

initial step of membrane fouling in many bioprocesses and it is widespread phenomenon afflict a variety of medical, biotechnological and industrial membrane operating systems [54.55,56]. Furthermore, protein adsorption property of membrane is used as an indicator of the membrane performance [57,58,59,60]. Main factor of influencing protein adsorption is the interaction between protein molecule and materials of operation surface. Many experimental methods have been used to characterize protein adsorption properties of the membranes. The static adsorption method has been generally used. In this method, the adsorption of components that is in contact with a membrane under atmospheric pressure was performed by simply submerging the membranes into a protein solution. The adsorption was influenced by pH of the solution because the charge of a macromolecule is highly dependent on the pH value.

Charged mild porous membranes had higher dynamic, i.e., practical binding capacity for proteins for their higher recovery. Membrane charged nature played a vital role and generally, higher charge density required for providing high binding sites. In order to examine the interaction between BSA with different charged nature (at different pH) and charged NCM or PCM, BSA binding capacity was investigated in batch mode with varied pH range of protein solution with concentration of 5 mg/ml for 6 h adsorption in continuous shaken condition; corresponding data is presented in Fig 4.2.6. BSA binding capacity was highly dependent on pH of the solution as well as nature of the charge on membrane matrix. For NCM, binding capacity decreases gradually with the pH of solution and attained limiting value at pH: 4.8, which is *pI* of BSA. Below the iso-electric point, BSA carries positive charge (BSA^{+}), and its adsorption on negatively charged surface was facilitating owing to electrostatic interaction, while above *pI*, very low binding capacity with NCM was observed due to negatively charged (BSA^{-}) nature. For PCM reverse trend was observed depending on charged nature of membrane interfaces and adsorbing species. Thus, pH of the protein solution is an important parameter by altering which one can obtain its high adsorption

and thus transport/separation across charged organic-inorganic nanocomposite membranes.

4.2.2.3. Membrane permeation characteristics

Organic-inorganic nanocomposite charged membranes were prepared in aqueous media via sol-gel by phase inversion route and gelated in non-aqueous media (methanol) for tailoring their pore dimensions. To investigate the impact of the membrane forming materials, their charged nature, optimum casting and gelation conditions, performance and throughput and volumetric fluxes of both membranes was evaluated by under applied pressure and electric gradient. In all cases, straight line passed through origin was obtained. Hydrodynamic permeability (L_{11}) of the membrane was evaluated directly from the slope of the volumetric flux (J_v; volume flow rate per membrane area) versus pressure (ΔP) data (Eq. 2.17). Values of were used with advantage for the estimation of apperent pore radius (r_p) using Eq. 2.19. L_{11} values for both membranes were presented in Table 4.2.2.

L_{11} value for NCM was slightly higher than that for PCM in spite of similar pore tailoring condition (gelation) may be because higher hydrophilic nature of its membrane forming material or higher concentration of $-SO_3H$ groups on the membrane matrix. r_p values estimated from Eq. 2.19, are also presented in Table 4.2.2 NCM and PCM. NCM shows comparatively higher R_p value (18.8 nm) in comparison to PCM (11.0 nm). Thus, higher volumetric flux observed in the case of NCM under constant applied pressure in comparison to PCM may be explained due large apparent pore radius in the previous case. Formation of pores in the membrane interfaces not only depending on the gelation condition by phase inversion but it also depends on the membrane forming material and its hydrophilic or hydrophobic nature. Fig. 4.2.7 depicts variation of r_p value with the surface charge concertino (X^m) for NCM and PCM. For both type of membranes r_p values

reduced significantly with the increase in X^m. Under similar pore forming conditions, slightly hydrophobic membrane forming material formed quite loose membrane whereas hydrophilic material formed quite dense membrane. Thus, it was possible to have a fine control over pore dimension by varying degree of functionalization of the membrane forming material and optimized conditions for the phase inversion.

Table 4.2.2. Hydrodynamic permeability (L_{11}), equivalent pore radius (r_p), electro-osmotic permeability (Jv/I), and membrane zeta potential (ξ) values for NCM and PCM membranes.

Membrane	$L_{11} \times 10^{-6}$ ($cm^3\ N^{-1}\ s^{-1}$)	r_p[a] (nm)	$Jv/I \times 10^{-3}$ ($Amp^{-1}\ cm\ s^{-1}$)	ξ[b] (mV)
NCM	1.51	18.8	0.468	7.92
PCM	1.13	11.0	0.312	5.28

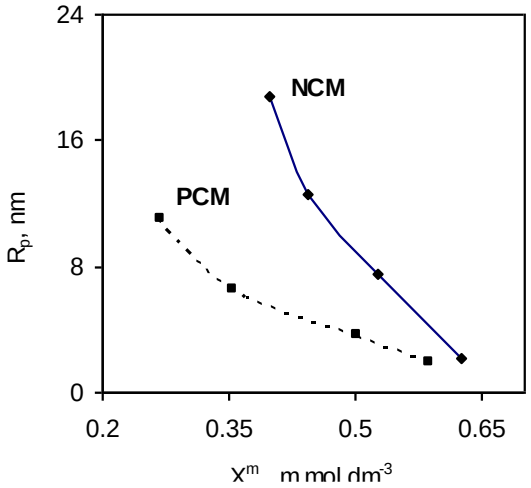

Figure 4.2.7. Variation of membrane pore radius (r_p) with surface charge concentration (X^m) of the NCM and PCM.

Surface charge on a membrane has significant influence on the separation properties and membrane throughput. Knowledge of the electrokinetic properties such as zeta potential of a particular membrane will be proved major contributing factor behind the decision to implement that membrane for specific separation process. The surface charge on synthetic membrane has significant effect on its separation properties [39,40] and fouling tendency [41,42]. By measuring electroosmotic potential (J_v/I) and using Smoluchowski equation, [43,44] zeta potential (ξ) can be estimated by Eq. 2.16. Zeta potential values for NCM and PCM are also presented in Table 4.2.2 along with J_v/I values, which wad determined from the slope of J_v *vs* I plots. In general, the zeta potential of the membranes is supposed to represent the charge characteristics of membrane-solution interfacial zone due to presence of charges at membrane surfaces. NCM

showed relatively high ξ values because of presence of strongly acidic (-SO_3H) groups. It can be seen that ξ depends on the charged nature of the membrane and concentration of fixed ionic groups. Further, zeta potential values for both membranes (NCM and PCM) suggested their mild charged nature and suitability for charged based separation of proteins.

4.2.2.4. Transmission of protein under coupled driving forces

BSA transmission across both types of membranes and its effect in the pH of the feed protein solution were studied under coupled driving forces (pressure and electrical gradient) in order to investigate the effect of nature of charge on the BSA molecule, membrane matrix and direct electrical polarity applied. Schematic diagrams for the different experimental modes such as transmission of BSA^+ ($pH < pI$), BSA^0 ($pH = pI$) or BSA^- ($pH > pI$) across NCM and PCM under pressure and electrical gradients are shown in Fig. 4.2.8 (A&B). Polarity of the electric gradient was fixed in such way that BSA^+ was facilitated to migrate through NCM, while BSA^- was facilitated to migrate through PCM. Under these modes of operation, three screening parameters such as pore size and nature of charge on the membrane matrix, and electric

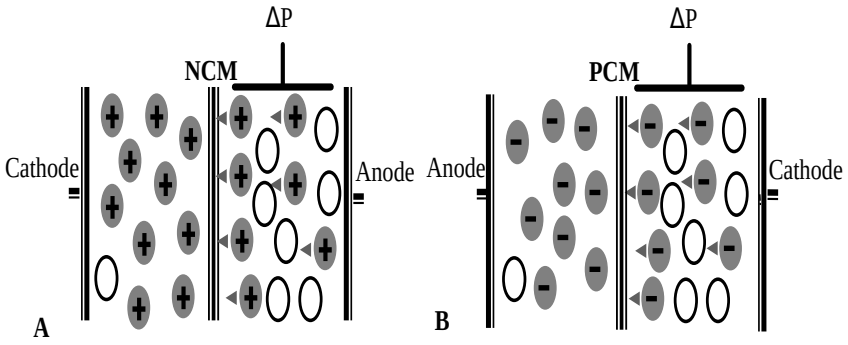

Figure 4.2.8. Schematic diagram for: (A) protein separation using NCM, and (B) protein separation using PCM, under coupled driving forces.

gradient only enhance of the protein transmission but purity of separation. Membrane throughput will also increase due coupled driving forces, electrophoretic migration of protein molecules and rejection or selection of protein molecules based on their charge and charge on the membrane

interfaces. Fig. 4.2.9 presents volumetric flux of BSA solutions of pH: 2.0 and 13.0 across NCM and PCM, respectively under varied applied pressure and without or with varied electric gradient. Without any applied electric gradient

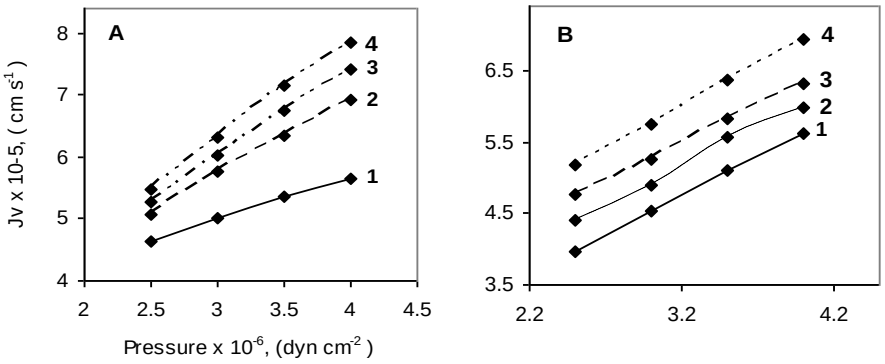

Figure 4.2.9. Variation of volumetric flux of BSA solution (5 mg/ml) with applied pressure for: (A) NCM at pH: 2.0; (B) PCM at pH: 13.0, at different applied electric gradient: 1- 0 V cm^{-1}; 2- 0.67 V cm^{-1}; 3- 1.33 V cm^{-1}; 4- 2.00 V cm^{-1}.

(0 V cm^{-1}) flux increased with the increase in applied pressure difference for both cases. In was also observed that at pH: 2.0, NCM membrane showed highest flux, while PCM showed highest flux at pH: 13.0. The filtrate flux is an important parameter to asses the suitability of separation/fractionation process. During separation/fractionation of bio-product, time involve for the bioprocess should be very low for the recovery of targeted product because enzyme activity of bio-product reduced with time.

Herein, filtration velocity was accelerated by coupling of driving forces, and increased with the increase gradient of additional driving force (electric gradient). Volumetric flux of BSA and LYS solution at different was also studied across NCM and PCM and it was found that J_v values were highly dependent on pH of protein solution. Variation of J_v with

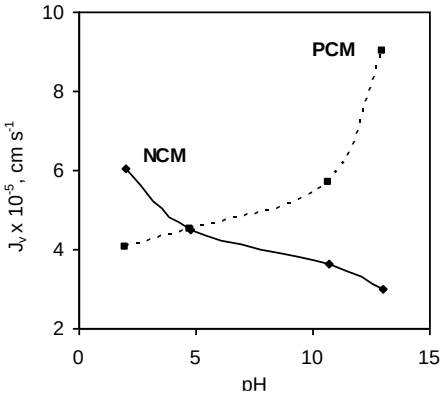

Figure 4.2.10. Variation of volumetric flux with pH of BSA (5 mg/ml) under 3.0 × 10^{-6} dyn/cm^2 applied pressure and 1.13 V cm^{-1} electric gradient across NCM and PCM.

pH of BSA (5 mg/ml) under 3.0×10^{-6} dyn/cm^2 applied pressure and 1.13 V cm^{-1} electric gradient for NCM and PCM was also presented in Fig. 4.2.10 representative case. NCM showed highest flux at pH: 2.0 (BSA^+) and flux decreased rapidly up to its p*I* (pH: 4.8) than slowly with the pH across NCM. While opposite trend was observed for transmission of BSA across PCM. J_v value for BSA^+ was very low and beyond p*I*, its increased rapidly and showed highest value at pH: 13.0. Also opposite trend was observed for PCM under similar experimental conditions. Interestingly, both membranes showed same J_v values for BSA^0 (pH: 4.8). Thus, filtrate flux can control by varying pH of the solution in addition to applied pressure difference and electric gradient.

For the separation/fractionation of protein, observed protein transmission (ζ_{obs}) is an important parameter in addition to flux. ζ_{obs} values was estimated from the ratio of protein concentration in the filtrate ($C_{filtrate}$) side to the feed side (C_{feed}) (Eq. 2.22).

Representative curves for ζ_{obs} against applied pressure and varied electric gradient is presented in Fig. 4.2.11(A), which also indicate dependent of BSA transmission on both driving forces. Under constant applied pressure, ζ_{obs} increased with the increase in applied electric gradient, thus coupling of driving forces enhanced membrane throughput and selectivity both. Fig. 4.2.11(B) depicts ζ_{obs} values with pH for both type of membrane under 3.5×10^{-6} dyn/cm^2 applied pressure and 1.13 V cm^{-1} electric gradient. Similar to the filtrate flux, ζ_{obs} value for BSA^+ was very high across NCM, while for PCM it was low. Progressive alteration in the ζ_{obs} with pH was observed due to nature of charge on the BSA molecule. Furthermore, BSA transmission for both membranes was identical at pH: 7.0. Thus their were three parameters such as applied pressure, electric gradient and charged nature of membrane matrix as well transmitting species governed membrane throughput and selectivity. It is important to record that membrane fouling was noticeably absent in all cases with less than 1% reduction in the membrane permeability after repeated use, due to applied electric gradient.

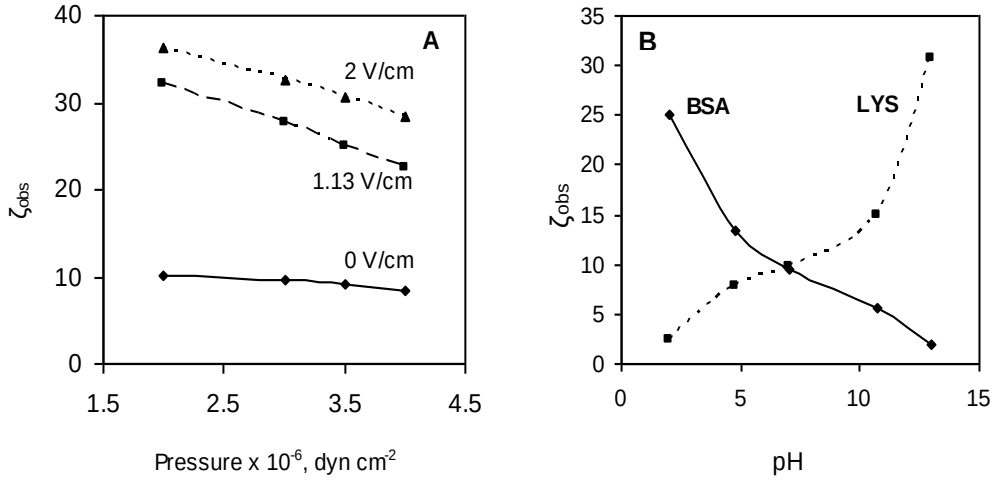

Figure 4.2.11. Variation of observed BSA transmission (ζ_{obs}) for NCM with: (A) applied pressure and under different electric gradient in equilibration with 5 mg/ml BSA solution at pH: 2; (B) pH of BSA solution (5 mg/ml) under 3.5 X 10^{-6} dyn cm^{-2} applied pressure and 1.13 V cm^{-1} electric gradient.

4.2.2.5. Protein selectivity in the mixture of BSA and LYS during their separation

Selective separation of BSA and lysozyme (LYS) from their mixed solution was carried out at different pH ranging between 2.0 to 13.0, where both transmitted across NCM and PCM in different ionic forms. Representative ζ_{obs} values for BSA and LYS separately, when protein mixture was used as feed, is presented against pH in Fig 4.2.12 (A&B) for NCM and PCM, respectively under 3.0 × 10^{-6} dyn/cm^2 applied pressure without or with 2.0 V cm^{-1} applied electric gradient. Transmission of both, BSA and LYS, was strongly dependent on the nature of the charge on the transmitting species (pH), nature of membrane and electric gradient. At pH: 2.0, BSA and LYS both existed as BSA^+ and LYS^+, and showed very high ζ_{obs} values across NCM (Fig. 4.2.12 (A)). While at pH: 4.8, BSA^0 showed extremely low ζ_{obs} value (less than 0.1), whereas, LYS^+ showed almost equal transmission across NCM. With further increase in the pH of both protein solutions, their transmission was decreased to minimum limit because of enhanced Donnan exclusions.

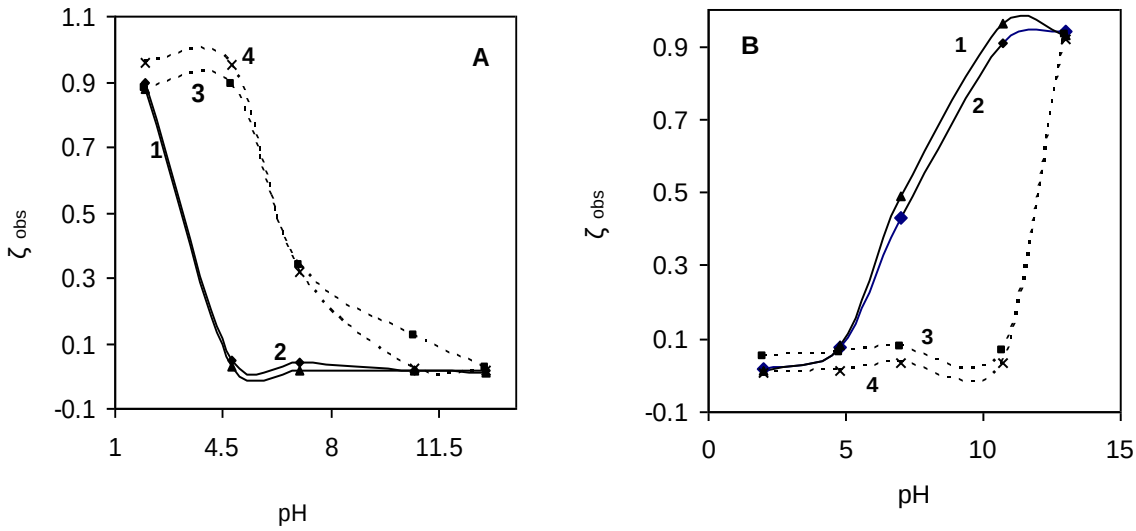

Figure 4.2.12. ζ_{obs} values for BSA (solid line) and LYS (dotted line) separately through: (A) NCM (B) PCM in equilibration with BSA, LYS mixed solution (5 mg/ml each) under 3.0 X 10^{-6} dyn cm^{-2} applied pressure and: 1 & 3- without any applied potential, 2 & 4 with 2.0 V cm^{-1} applied electric gradient.

Similarly, PCM showed highest transmission for BSA^- and LYS^- both (pH: 13.0), while transmission of LYS reduced to minimum at its p*I* value (pH: 10.7). PCM allowed extremely high transmission (close to 100%) for BSA^- at pH: 13.0 and 10.7 whereas its transmission across PCM was very low below p*I* (pH: 4.8). These variations in the ζ_{obs} were aroused due to variation in electrostatic attraction/repulsion or Donnan exclusion depending on the charged nature of transmitting protein species and charge on the membrane interfaces. Thus it is possible to separate LYS from the mixture of BSA-LYS at the p*I* of BSA (pH: 4.8) using NCM and BSA from its mixture with LYS at the p*I* of LYS (pH: 10.7) using PCM. This is a novel method where purity of separation was governed by nature of charge on the transporting species as well at the membrane interfaces, electrical polarity and pore size of the membrane. Also in al cases due to coupling of driving forces, filtrate flux and protein, transmission was enhanced under applied electrical gradient with constant pressure. Thus in this process, rate of protein separation can be controlled by varying two types of driving forces.

We can have further idea about separation and selectivity of a protein from the mixture by separation factor (SF) defined as the ration of transmission of individual proteins from their mixture. Estimated SF values for NCM and PCM under pressure alone (0 V cm^{-1}) or under coupled driving forces are presented in Fig. 4.2.13 (A&B), respectively as function of pH mixed protein feed solution. For NCM, SF value for the separation LYS from its mixture with BSA was close to 40 at pH: 4.8 (p*I* of BSA), while for PCM, SF value for the separation BSA from its mixture with LYS was close to 35 at pH: 10.7 (p*I* of LYS). At other pH, extremely low SF values revealed the possibility of protein separation by fixing one component at its p*I*. Furthermore, applied

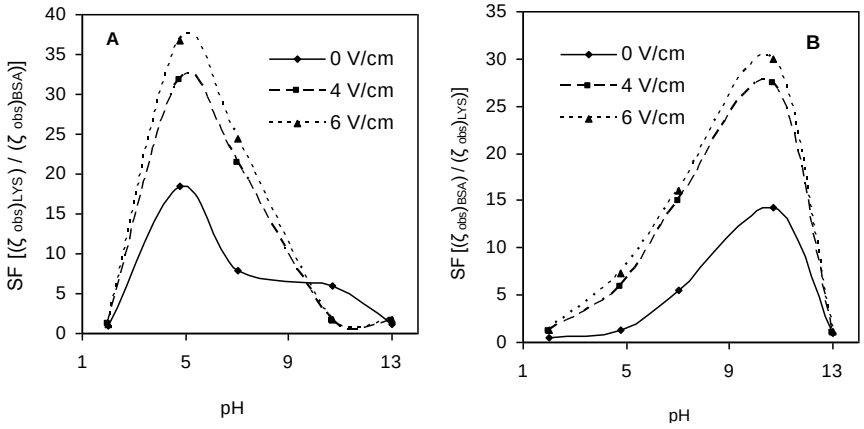

Figure 4.2.13. Separation factor as function of pH for the BSA and LYS mixed solution (5 mg/ml each) for: (A) NCM (B) PCM at 3.0 X 10^{-6} dyn cm^{-2} applied pressure and different electric gradient.

electric gradient progressively enhanced the SF values, suggesting their highly selective and fast separation under coupled driving forces. However, applied electric gradient was so low to avoid any possible denaturation of protein under given experimental conditions [47]. Using organic-inorganic type of charged membranes, it is possible to device a rapid and high selective method protein separation under coupled driving forces (pressure and electric gradient). In this case, two properties of BSA and LYS, such as their p*I* values and molecular size were taken into account, to separate/fractionate them with high degree of selectivity. Although under chosen system difference in p*I* values of two components was quite high, but this process

can be efficiently used for a system where p*I* values were very close by fine tailoring of pore texture and charge nature of the membrane matrix, fine control over the applied driving forces. In this process, no appreciable membrane fouling was observed due cleverly application of electric gradient and back flushing of foulants protein from the membrane interface and indirectly cleaning. In addition, charge on the membrane interface avoids any kinds of fouling and helps its cleaning. As whole, this separation method is a promising tool for down stream processes or separation/fractionation of protein with improved serration procedure.

4.2.3. Conclusions for organic-inorganic hybrid ultrafilter charged membranes

Organic-inorganic hybrid charged membranes were prepared in aqueous media by sol-gel and gelated in non-aqueous media for their tailoring the pore texture. Desired type negatively or positively charged groups were grafted on the membrane matrix, which was confirmed by recording their FTIR spectra, ion-exchange capacity. Conductivity and couter-ion transport numbers. Thermal properties of these membranes revealed their excellent thermal stability, whereas, electrochemical properties such as conductivity, surface charge density etc. revealed their mild charged nature due to grafting $–SO_3H$ or $–N^+(CH_3)$ groups respectively, for NCM or PCM. Interaction of these membranes and BSA was studied by adsorption, and it was concluded that BSA^+ was adsorbing to the NCM, while BSA^- to the PCM to very high extent due to the electrostatic attraction between adsorbing species and adsorbate. These hybrid charged with desired pore tailored membranes were used to develop a new method for rapid protein separation/fractionation from their mixture at the p*I* of one component under coupled driving forces. It was also studied that rapid and highly selective separation of LYS from the mixture of BSA-LYS at pH: 4.8 (p*I* of BSA) using NCM and separation of BSA from its mixture with LYS at pH: 10.7 (p*I* of LYS) using PCM was possible by newly developed protein separation method under coupled driving forces. Also due to coupling of driving forces, protein flux and

transmission was enhanced in all cases. In this process, membrane fouling was avoided due electric gradient and back flushing of foulants protein from the membrane interface and indirectly cleaning, charge on the membrane interface avoids any kinds of fouling and helps its cleaning.

In this process, charged nature of the protein, nature and extent of the charge on the membrane interfaces, polarity of electric gradient all are governing transmission of given protein and acted as additional three screening parameters. Thus is a new process using charged organic-inorganic hybrid membrane for improving product purity, and filtration velocity (throughput). Both, the electrophoretic migration of molecules and positive effect of electro-osmosis lead to increase in product purity. Reported process is a promising tool to make downstream processing faster and product purer to certain fields of application.

References

[1] Saksena S, Zydney AL. Biotechnol Bioeng 1994;43:960.

[2] Wan Y, Ghosh R, Cui Z. Biotechnol Prog 2004;20:1103.

[3] Muller CH, Agarwal GP, Melin Th, Wintgens Th. J Membr Sci 2003;227:51.

[4] Shukla R, Balakrishnan M, Agarwal GP. Bioseparation 2000;9:7.

[5] Iritani E, Mukai Y, Kiyotomo Y. J Membr Sci 2000;164:51.

[6] Nystrom M, Aimar P, Luque S, Kulovaara M, Metsamuuronen S. Colloids Surf. A: Physicochem Eng Aspects 1998;138:185.

[7] Ghosh R. Biotechnol Bioeng 2001;74:1.

[8] Ehsani N, Parkkinen S, Nystrom M. J Membr Sci 1997;123:105.

[9] Fane AG, Fell CJD, Suki A. J Membr Sci 1983;16:195.

[10] Pujar NS, Zydney AL. J Chromatogr Sect 1998;796:229.

[11] Saksena S, Zydney AL. J Membr Sci 1997;125:93.

[12] Burns DB, Zydney AL. AIChE J 2001;47:1101.

[13] Cheang B, Zydney AL. Biotechnol Bioeng 2003;83:201.

[14] Burns DB, Zydney AL. J Membr Sci 2000;172:39.

[15] Burns DB, Zydney AL. Biotechnol Bioeng 1999;64:27.

[16] Hulteen JC, Jirage KB, Martin CR. J Am Chem Soc 1998;120:6603.

[17] Jirage KB, Hulteen JC, Martin CR. J Membr Sci 1997;278:655.

[18] Ku JR, Stroeve P. Langmuir 2004;20:2030.

[19] Schoch RB, Bertsch A, Renaud P. Nano letters 2006;6:543.

[20] Chun KY, Stroeve P. Langmuir 2002;18:4653.

[21] Lee SB, Martin CR. J Am Chem Soc 2002;124:11850.

[22] Tsuneda S, Shinano H, Saito K, Furusaki S, Sugo T. Biotechnol Prog 1994;10: 76.

[23] Kubota N, Miura S, Saito K, Sugita K, Watanabe K, Sugo T. J Membr Sci 1996;117:135.

[24] Sunaga K, Kim M, Saito K, Sugita K, Sugo T. Chem Mater 1999;11:1986.

[25] Westermeier R, In Electrophoresis in Practice, 3rd ed.; Wiley-VCH: New York, 2001.

[26] Carlsson N, Sanandaji N, Voinova M, Akerman B. Langmuir 2006;22:4408.

[27] Locke BR. Ind Eng Chem Res 1998;37:615.

[28] Roche ME, Oda RP, Landers JP. Biotechnol Prog 1997;13:659.

[29] Wu XZ, Hosaka A, Hobo T. Anal Chem 1998;70:2081.

[30] Krylov SN, Dovichi NJ. Anal Chem 2000;72:111.

[31] Nolte R, Ledjeff K, Bauer M, Mulhaupt R. J Membr Sci 1993;83:211.

[32] Gohil GS, Nagarale RK, Binsu VV, Shahi VK. J Colloid Interface Sci 2006;298:845.

[33] Nagarale RK, Shahi VK, Schubert R, Rangarajan R, Mehnert R. J Colloid Interface Sci 2004;270:444.

[34] Koter S, Piotrowski P, Kerres J. J Membr Sci 1999;153:83.

[35] Capeci SW, Pintauro PN, Bennion DN. J Electrochem Soc 1989;136:10.

[36] Nagarale RK, Gohil GS, Shahi VK, Rangarajan R. J Colloid Interface Sci 2005;287:198.

[37] Wang DIC, Sinskey AJ, Sonoyama T. Biotechnol Bioeng 1969;11:987.

[38] Dukhin SS, Derjaguin BW, in E. Matijevic (Ed.), Surface and Colloid Science, Vol. 7, Wiley, New York, 1974, pp. 118 and 127.

[39] Larsson K. Desalination 1980;35:105.

[40] Breslau BR, Testa AJ, Milnes BA, Medjanis G, in A.R. Cooper (Ed.), Plenum Press, New York, 1980, pp. 109.

[41] Hiemenez PC, 2nd edn., Marcel Dekker, New York, 1986.

[42] Kim KJ, Fane AG, Nystrom M, Pihlajamaki A, Bowen WR, Mukhtar H. J Membr Sci 1996;116:149.

[43] Garcia-Aleman J, Dickson J, Mika A. J Membr Sci 2004;240:237.

[44] Saxena A, Shahi VK. J Membr Sci 2007;299:211.

[45] Bargman G, Houwing J, Recio I, Koops GH, Van der Horst C. Biontechnol Bioeng 2002;80:599.

[46] Li Y, Chung TS. J Membr Sci 2008;309:45.

[47] Kappler T, Posten C. J Biotechnol 2007;128:895.

[48] Binsu VV, Nagarale RK, Shahi VK. J Mater Chem 2005;15:4823.

[49] Ganesan V, Walcarius A. Langmuir 2004;20:3632.

[50] Ogoshi T, Chujo Y. J Mater Chem 2005;15:315.

[51] Saxena A, Tripathi BP, Shahi VK. J Phys Chem B 2007;111:12454.

[52] Jacob S, Cohet S, Poinsignon C, Popall M. Electrochim Acta 2003; 48:2181.

[53] Wu Y, Wu C, Yu F, Xu T, Fu Y. J Membr Sci 2008;307:28.

[54] Nakamura K, Matsumoto K. J Membr Sci 2006;285:126.

[55] Velasco CM, Ouammou JI, Calvo AH. J Colloid Interf Sci 2003;266:148.

[56] Nakamura K, Matsumoto K. J Membr Sci 2006;285;26.

[57] Martinez F, Martin A, Pradanos P, Calvo JI, Palacio L, Hernandez A. J Colloid Interf Sci 2000;221:254.

[58] Zhao ZP, Wang Z, Wang SC. J Membr Sci 2003;217:151.

[59] Martin A, Martinez F, Calvo JI, Pradanos P, Palacio L, Hernandez A. J Membr Sci 2002;207:199.

[60] Su TJ, Lu JR, Cui ZF, Thomas RK. J Membr Sci 2000;173:167.

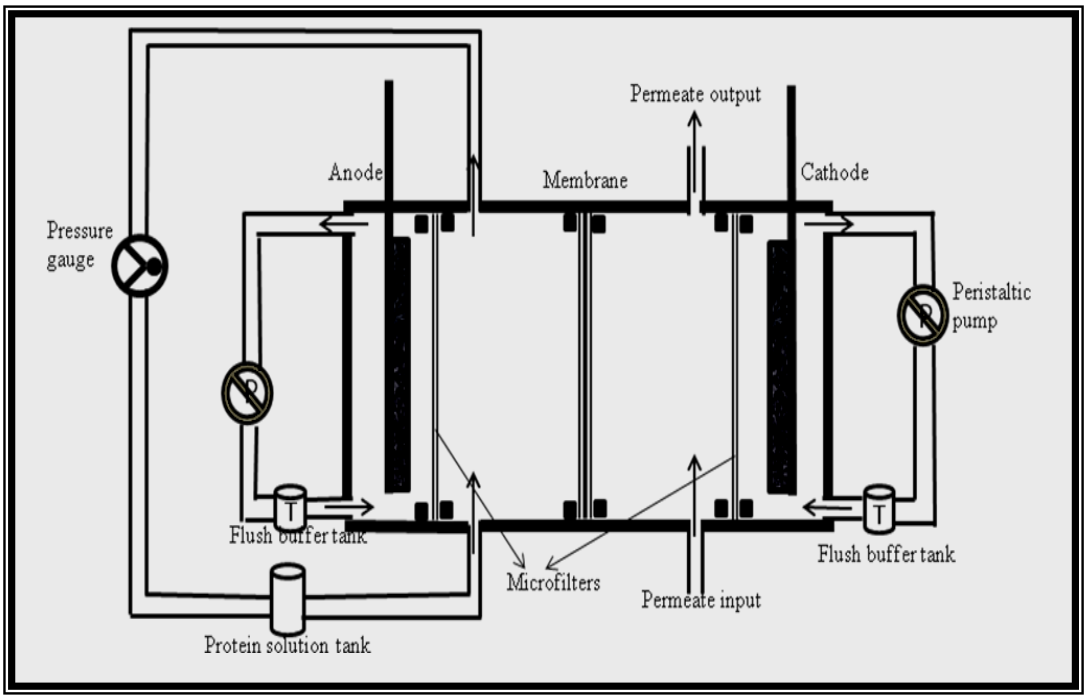

CHAPTER V

INTERPOLYMER CHARGED ULTRAFILTRATION MEMBRANES WITH POLY (VINYL CHLORIDE) AND STYRENE DIVINYL BENZENE

5.1. Interpolymer type of charged ultrafilter membranes with different functionality

It is often a requirement in the chemical and biochemical sciences to separate a component from mixture based on its molecular size or charge on individual component. The increasing complexity of chemical and in particular, biochemical, or biological systems has required more sophisticated, selective and efficient technique to resolve/separate individual components. Recently, membrane-based processes gained importance in biotechnology due to their ability for size and/or charge based protein separation with high purity and throughput [1-7]. Ultrafiltration (UF) of protein solution is gradually emerging as a powerful bio-separation process for diversified fields as biotechnology, biomedicine, dairy and food industry [8-12]. Although protein concentration using UF has become a routine and successful operation in biotechnology, fractionation of proteins using UF is still a technological challenge and its effectiveness and efficiency are strongly dependent on operating parameters such as pH, salt concentration, permeate flux, and system hydrodynamics [13-21]. Additionally, UF is a size based separation process, and it is difficult to achieve high selectivity with high throughput. To solve these problems, charged ultrafilter membranes were used for protein separation and electrostatic interactions between charged proteins and membranes were also studied [19,22-23]. Many processes with electric gradient as driving force such as electrophoresis, gel electrophoresis, capillary electrophoresis, etc. were also developed for commercial practice of protein separation [24-25].

In all these aforementioned processes only one property of given molecule either its molecular size or charge and iso-electric point was used to achieve its separation under only one driving force either pressure gradient or electrical gradient. All processes involve only one selectivity parameter (either molecular size or charge) and one driving force, which result less selectivity and membrane throughput. No report is available, in which, nature of charge on the protein, its molecular size, nature and extent of charge on the

membrane matrix was used to increase the selectivity of separation with high membrane throughput under coupled driving forces (pressure and potential gradient). In literature electro-ultrafiltration (UF under electric field) is also reported to achieve fractionation/separation of protein with enhanced throughput using uncharged UF membranes [26-27]. No report is available, in which, nature of charge on the protein, its molecular size, nature and extent of charge on the membrane matrix was used to increase the selectivity of separation with high membrane throughput under coupled driving forces (pressure and potential gradient).

In the present case, three types of acidic functionalized (sulphonated, carboxyleted and phosphorylated) ultrafilter membranes, based on the interpolymer of PVC and styrene–DVB copolymer has been prepared, for studying the transmission of proteins in different environments under simultaneous action of driving forces for achieving high selectivity and maximum membrane throughput because of three selectivity parameters (i.e., charge on the membrane matrix, nature of charge and molecular size of the protein) and dual driving forces. These charged ultrafilter membranes were characterized to investigate their physicochemical, electrochemical properties and protein binding capacity. Casein and lysozyme were used as model protein.

5.1.1. Preparation of charged ultrafilter membranes with different acid functionality

Acryl amide, phosphorous acid, maleic anhydride were received from Sigma-Aldrich Chemicals. Polyvinyl chloride (PVC), hexanone, formaldehyde, benzoyl peroxide (BP), styrene, divinyl benzene (DVB), sulphuric acid, sodium hydroxide, hydrochloric acid, sodium hydrogen phosphate, disodium hydrogen phosphate etc of AR grade were obtained from S.D. Fine Chemicals, India, and were used without any further purification. Casein (CAS; *Mw*: 20,000 Daltons) and Lysozyme (LYS; *Mw*: 14,600 Daltons) were received from HiMedia Laboratories Pvt. Ltd. India. Double distilled water was used in all experiments.

Three types of acidic functionalized (sulphonated, carboxyleted and phosphorylated) ultrafilter membranes, based on the interpolymer of PVC and styrene–DVB copolymer, were prepared. For the preparation of sulphonic acid functionalized ultrafilter membrane (M_{SO3H}), five grams of PVC was dissolved in 70.0 ml of hexanone. To the clear solution, styrene (5.0 g) and 50% DVB (1 g) were added. Temperature of the solution was raised up to 70 ^{0}C, and then initiator BP (0.02 g) was added. Afterwards the temperature was maintained for 6 h. A viscous solution was obtained, which was cast in the form of a thin film on a cleaned glass plate, which is covered with high-density poly (ethylene) sheet of desired thickness and partially dried for 2 h at ambient temperature (30 ^{o}C). Partially dried film was gelated by immersing it in the deionized water for 45 min at 5 ^{o}C. Thus obtained film was immersed in 85% sulphuric acid for sulfonation. Sulfonated membrane was washed with distilled water and then successively conditioned in 1M HCl and 1M NaOH and stored.

Carboxylic acid functionalized ultrafilter membrane (M_{COOH}) was prepared by dissolving PVC (5.0 g) in hexanone (70.0 ml). To a clear solution, maleic anhydride (5.0 g), styrene (4.0 g) and 50% DVB (1.0 g) were added at temperature 70 ^{o}C in the presence of BP (0.02 g). Temperature was maintained for 6 h. Resultant viscous solution was cast in the form of thin film of desired thickness on a cleaned glass plate and covered with high-density poly (ethylene) sheet for partially drying for 2 h at ambient temperature (30 ^{o} C). Partially dried film was gelated by immersing it in the deionized water for 45 min at 5 ^{o}C. Thus obtained membrane was kept in 1M NaOH to hydrolyze the anhydride group to carboxylic acid group. Carboxylated membrane was washed with distilled water and then successively conditioned in 1M HCl and 1M NaOH and stored.

For the preparation of phosphonic acid functionalized ultrafilter membrane ($M_{PO_3H_2}$), five grams of PVC was dissolved in 70.0 ml of hexanone. To the clear solution, acryl amide (5.0 g), styrene (4 g) and 50% DVB (0.5 ml) were added at temperature 70^{0}C in the presence of BP (0.02 g). Solution was

stirred for 6 h at temperature 70^{0}C and then further 6 hrs at room temperature. Resultant viscous solution was cast in the form of thin film on a cleaned glass plate covered with high-density poly (ethylene) sheet of desired thickness and partially dried for 2 h at ambient temperature (30 ^{o}C). Then dried film gelated by immersing it in the deionized water for 45 min at 5 ^{o}C. Thus obtained membrane was treated with the mixture of 37% formaldehyde (100 ml) and phosphorous acid (37 g) at 80 ^{o}C for 8 h, to introduce the phosphonic acid group. Phosphorylated membrane was washed with distilled water and then successively conditioned in 1M HCl and 1M NaOH and stored.

5.1.2. Result and discussion for acid functionalized ultrafilter membranes

5.1.2.1. Membrane preparation, their physicochemical and electrochemical properties

Inter-polymer of PVC and styrene–divinylbenzene was prepared and conventional methods were used to introduce sulphonic-, carboxylic- or phosphonic acid functionality in the polymer matrix. Schematic presentation for the preparations of M$_{SO_3H}$, M$_{COOH}$ and M$_{PO_3H_2}$ membranes and their structures are presented in Fig. 5.1.1 (A,B & C). Introduction of different functional groups was confirmed by the significant changes observed in IR peaks. The FT-IR spectra for three membranes (M$_{SO_3H}$, M$_{COOH}$ and M$_{PO_3H_2}$, are presented in Fig. 5.1.2. For M$_{PO_3H_2}$, peaks at 1300-1140 cm^{-1}assigned as P=O stretching while peaks around 3200, 2358 and 1040 cm^{-1}due to OH stretching. For M$_{COOH}$, peaks around 3200 and 2300 cm^{-1} give the information about the acidic proton while strong absorption around 1700 cm^{-1} confirms the C=O stretching present in the carboxylic acid. Strong characteristic peaks at 1030 and 1096 cm^{-1} were observed for M$_{SO_3H}$, due to symmetric and asymmetric stretching of sulfonate group. The presence of

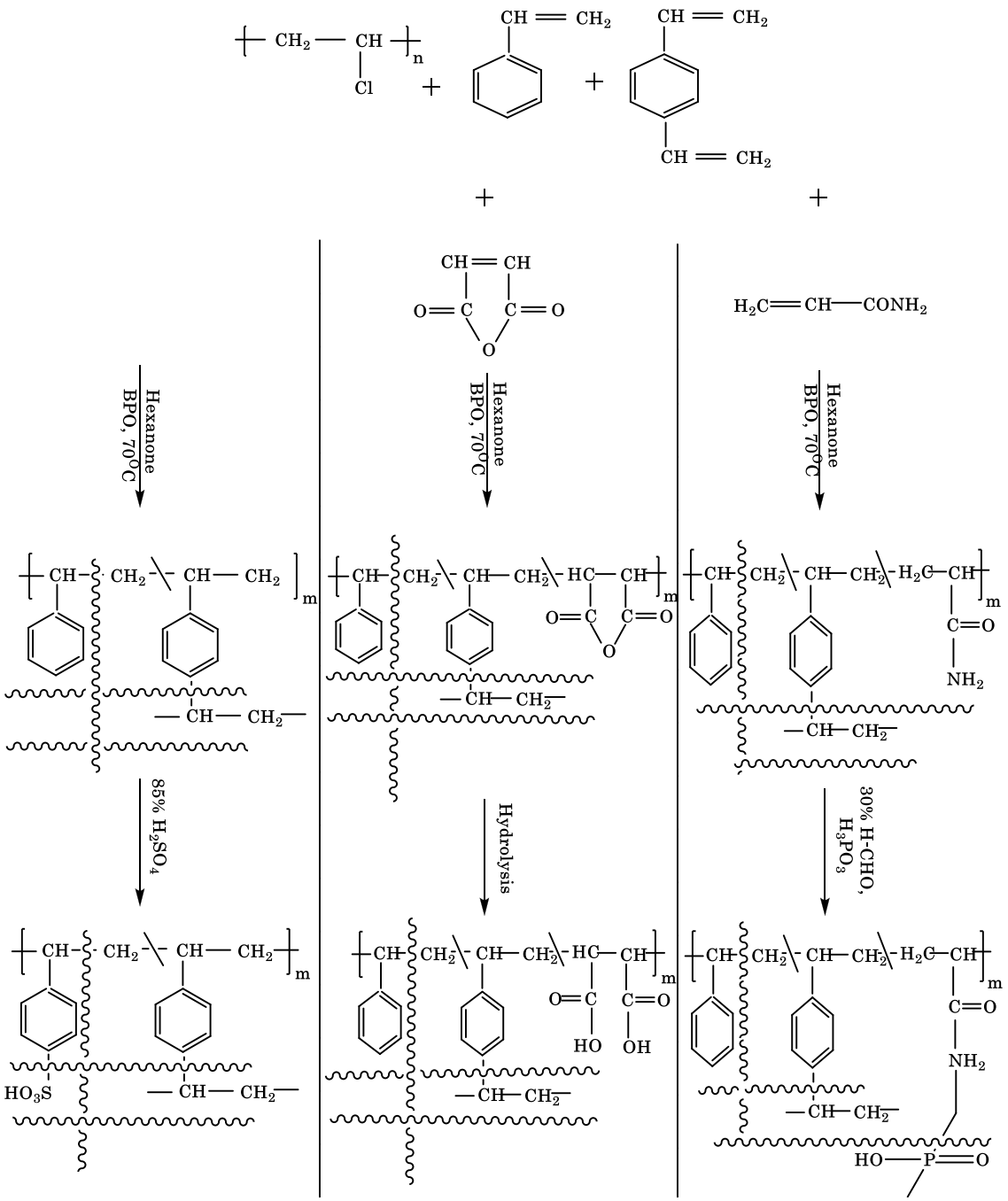

Figure 5.1.1. Schematic presentation of membrane preparations and chemical structures for: (A) MSO_3H; (B) MCOOH; and (C) MPO_3H_2 membranes.

different functional groups, were also supported by the elemental (CHNS) analysis data (Table 5.1.1).

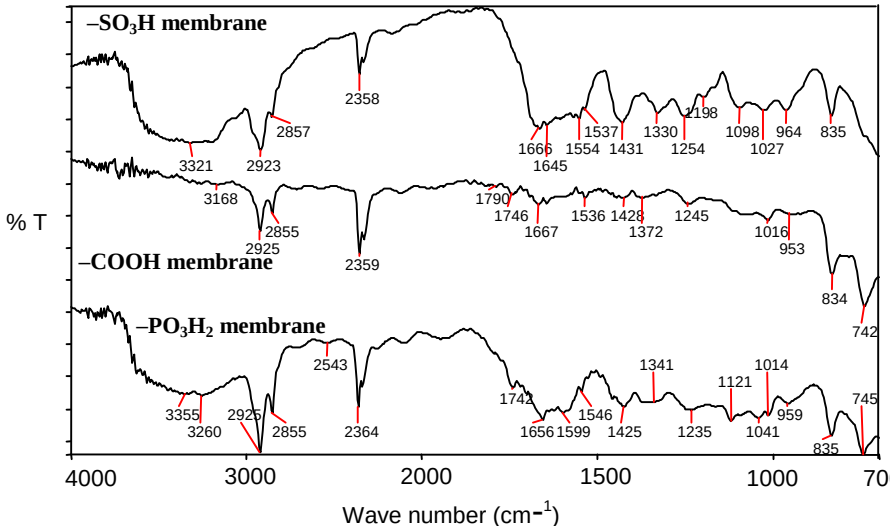

Figure 5.1.2. FT-IR spectra for MSO_3H; MCOOH; and MPO_3H_2 membranes.

Thermal strengths for different membranes were illustrated by TGA analysis, representative curves for MSO_3H; MCOOH; and MPO_3H_2 membranes under flowing nitrogen are presented in Fig. 5.1.3. Three membranes (MSO_3H; MCOOH; MPO_3H_2 membranes) showed two-stage thermal degradation (bound water loss and polymer loss) curve. The first weight loss occurred at below 100 °C, and was attributed to the loss of absorbed water molecules in the membrane matrix. The second weight loss started at about 350 °C for MPO_3H_2, while that for MSO_3H; and MCOOH; membranes started at about 250 °C, indicated thermal

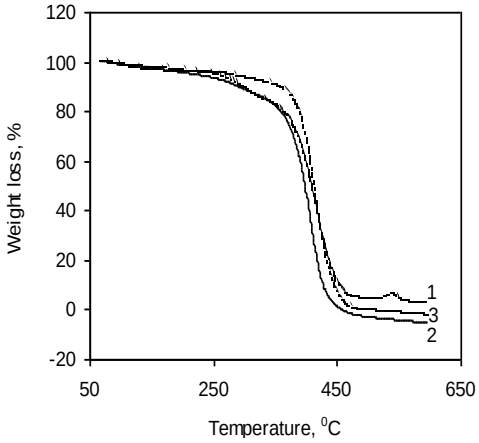

Figure 5.1.3. TGA curves for: (1) MSO_3H; (2) MCOOH; and (3) MPO_3H_2 membranes.

oxidation of membrane forming material. Complete weight losses for all membranes were attained in the final stage of the sample decomposition, starting at around 400 °C. The DSC analysis of these membranes were also carried out under nitrogen with a heating rate of 5°C/min, and the resulting curves for MSO_3H; MCOOH; and MPO_3H_2 membranes are presented in Fig. 5.1.4. These membranes exhibited *T*g values around 150, 120, and 117 °C, for MSO_3H; MCOOH; and MPO_3H_2, respectively. *T*g values for MCOOH; and MPO_3H_2 membranes are comparable, and relatively higher for MSO_3H membranes. These differences in *T*g values may be attributed due to nature of functional groups.

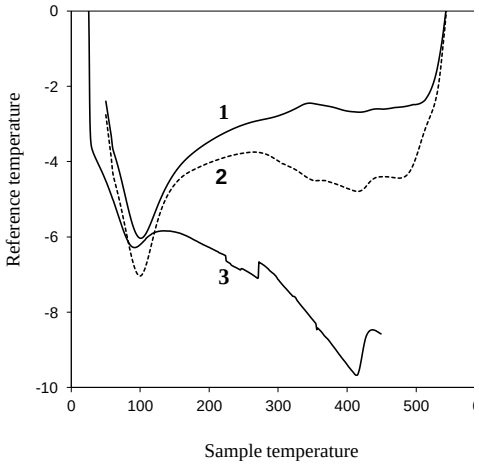

Figure 51.4. DSC curves for: (1) MSO_3H; (2) MCOOH; and (3) MPO_3H_2 membranes.

Fig. 5.1.5 shows the representative DMA analysis data for charged ultrafilter membranes with different functional groups, at applied forces of up to 50 N at room temperature and 1 Hz frequency. All membranes exhibited good mechanical stability and no breaking of the polymer film was observed under testing conditions.

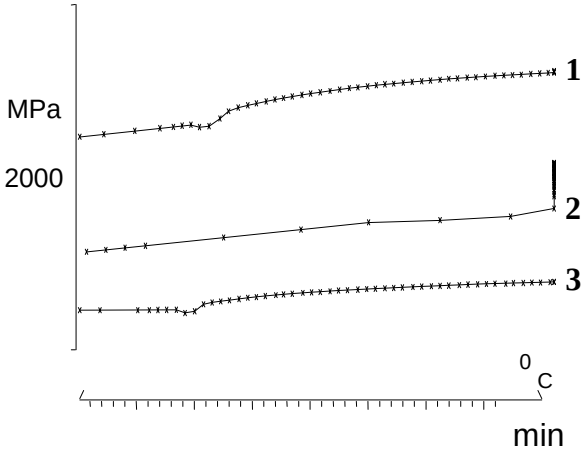

Figure 5.1.5. DMA curves for: (1) MSO_3H; (2) MCOOH; and (3) MPO_3H_2 membranes at room temperature and a constant frequency of 1 Hz.

Charged ultrafilter membranes with different functionality were also characterized by measuring their physicochemical properties such as water content, ion exchange capacity, contact angle MWCO values. The Water content values for different

types of membranes are summarized in Table 5.1.1, which follows the trend: M_{COOH} > M_{SO_3H} > $M_{PO_3H_2}$. High water content value for M_{COOH} membrane may be attributed to more hydrophilic nature of the carboxylic acid group in comparison with phosphonic and sulphonic acid group. In general membranes having the same chemical composition absorb same amount of water, when density of ionizable groups is the same throughout the membrane. Furthermore, we can have an idea about density of exchangeable functional groups from their IEC values presented in Table 5.1.1. IEC values for M_{SO_3H} was higher than those for M_{COOH}, because of high dissociation of sulphonic acid group at neutral pH in comparison to carboxylic acid group. IEC value of $M_{PO_3H_2}$ was very high due to the bi-functional nature of phosphonic acid groups, which indicates phosphonic acid groups completely introduced in the membrane matrix and no side reactions such as cross linking of the functional groups, had occurred. Water

Table 5.1.1. Physico-chemical properties for different membranes.

Membranes	Water content (%)[1]	IEC (mequiv./g of dry membrane)[2]	X^m (m mol dm^{-3})	CHNS analysis			
				C (%)	H (%)	N (%)	S (%)
M_{SO_3H}	48.3	0.59	0.32	38.25	3.95	0.01	2.95
M_{COOH}	59.4	0.29	0.34	42.46	4.13	0.01	0.01
$M_{PO_3H_2}$	41.3	0.86	0.28	20.31	4.89	0.01	0.01

content values in conjunction with IEC values can also be used for the determination of fixed ion concentration (X^m) of the membrane in units of (moles of sites)/ (unit volume of wet membrane) using Eq. 2.11. Void porosity (ε) was obtained by Eq. 2.8 and Eq. 2.9 [31,33]. X^m values for different membranes follow the trend: MCOOH > MSO_3H > MPO_3H_2 (Table 5.1.1). These values reveal moderate surface charge density on these membranes. The values of water contact angle presented in Table 5.1.2 reveals hydrophilic nature of these membranes. Among the prepared membranes, 80.70^0 contact angles obtained for M_{COOH}, which indicates its higher hydrophilic nature in

compare with others. SEM images of these membranes (Fig. 5.1.6) show smooth and homogeneous surfaces without any phase separation. The molecular weight cut off (MWCO) of these membranes by PEG rejection analysis was found to be in between 28-25 kDa (Table 5.1.2). These informations demonstrate mild charged, hydrophilic nature of these membranes with ultrafilter characteristics.

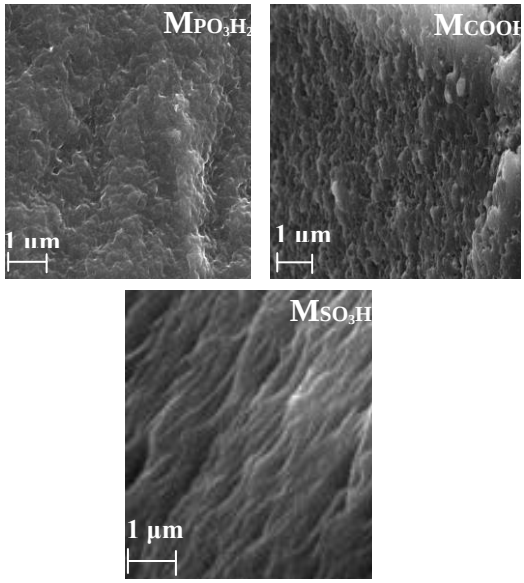

Figure 5.1.6. SEM images for membranes.

Mild charged nature of these ultrafilter membranes was also revealed by their electrochemical properties such as membrane conductivity (κ^m) and counter-ion transport number in the membrane phase $\left(t_i^m\right)$values presented in Table 5.2. Reasonably good conductivity (2.68-3.01 mS cm^{-1}) of these membranes indicates their suitability for electrochemical devices. Also, higher $\left(t_i^m\right)$values of these

Table 5.1.2. Contact angle, Membrane conductivity, Counter-ion transport number, Membrane porosity, Surface charge concentration for different membranes (0.15 mm thickness).

Membranes	MWCO (kDa)	Contact angle (°)	κ^m (mS cm^{-1}) [a]	t_i^m [b]
M_{SO_3H}	25	59.31⁰	2.89	0.75
M_{COOH}	28	80.70⁰	2.68	0.64
$M_{PO_3H_2}$	25	51.61⁰	3.01	0.69

membranes in compare with Na^+ transport number values in the solution phase (for NaCl solution of 0.055 mol/dm^3 concentration, Na^+ transport number is 0.392) reveal their cation selective nature due the negatively charged acidic functional groups on the membrane matrix. Based on these

characterizations we can conclude cation selective charged nature of developed ultrafilter membranes.

5.1.2.2. Protein adsorption on charged ultrafilter membranes

Charged ultrafilter membranes had higher dynamic, i.e., practical binding capacity for proteins and exhibited a higher through put for protein recovery. Introduction of a high density of functional groups in the membrane is required, while maintaining high selectivity for the protein adsorption/separation [34]. Several interactions, namely hydrophobic interactions, hydrogen bonding, and electrostatic interactions, simultaneously take part in controlling its behavior. In order to examine the interactions between negatively charged ultrafilter membrane, CAS and LYS binding capacities with different membranes were determined in batch mode at different pH of CAS or LYS solution with 5 mg/ml concentration for 6 h adsorption, and relevant data is presented in Figure 5.1.7 (A&B), respectively. For each type of membrane, protein binding capacity was highly dependent on pH of the solution as well nature of functional groups on the membrane matrix. At constant pH, CAS and LYS solutions show the trend: M_{SO_3H} >M_{COOH} > $M_{PO_3H_2}$. Further, binding capacity of CAS was almost constant in lower pH, and decreased with increase in the pH. At pH < 5 (p*I* of CAS), CAS carried positive charges (CAS^+) and its adsorption on negatively charged matrix was favored due to mutual electrostatic attraction. While for LYS carried positive charge at pH < 10.7 (p*I* of LYS), and adsorption of LYS^+ on the negatively charged ultrafilter was favored. At higher pH, both proteins carried negative charge and their binding capacity on negatively charged interface was very low due to electrostatic repulsive forces.

Furthermore, M_{SO_3H} & M_{COOH} membranes showed higher protein binding capacity in compare with $M_{PO_3H_2}$. Thus pH of the protein solution is an important parameter by varying which one can obtain its high adsorption and thus transport/separation across charged ultrafilter membrane.

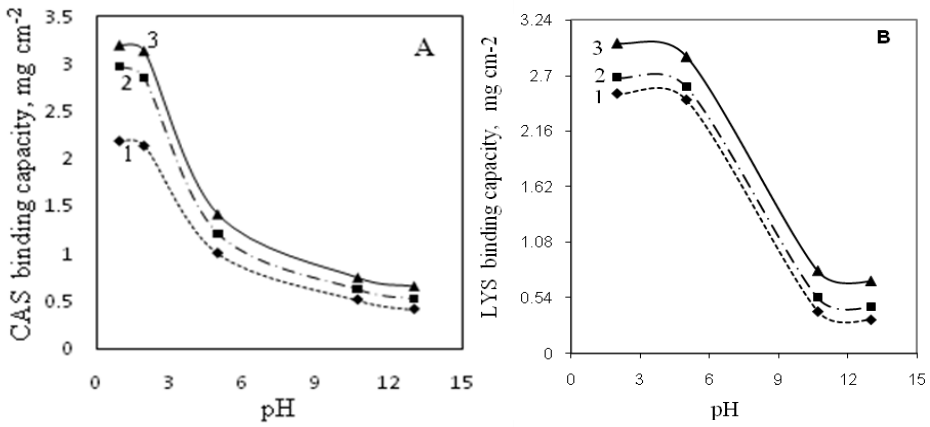

Figure 5.1.7. Binding capacity for: (A) CAS and (B) LYS solutions (5 mg/ml each separately) with 1- $M_{PO_3H_2}$; 2- M_{COOH}; and 3- M_{SO_3H} membranes at different solution pH for 6 h adsorption.

5.1.2.3. Membrane permeation studies

To investigate the impact of the membrane forming materials, nature of functional groups, optimum membrane casting and gelation conditions, permeation characteristics of charged ultrafilter membranes were evaluated by their volumetric flux (J_v) under applied pressure and electric gradient, relevant data are presented in Fig. 5.1.8 (A&B). In all cases, straight lines were obtained. Hydrodynamic and electro-osmotic permeability may be defined by phenomenological coefficients L_{12} and L_{11}, respectively by Eqs. 2.15 and 2.18. Phenomenological coefficients (L_{11} and L_{12}) were estimated from the slope of straight lines (Fig. 5.1.8) and are presented Table 5.1.3. Results revealed relatively high permeability values of these membranes. Among three types of functionalized membranes, M_{SO3H} showed highest permeabilities (hydrodynamic and electro-osmotic), may be due to highly charged nature and pore dimensions. Further, the L_{11} values were used with advantage for the estimation of apparent pore radius (r_p) using Hagen–Poiseuille equation (Eq. 2.19). Estimated r_p values are presented in Table 5.1.3, for different membranes. It can be seen that although pressure driven permeability value (L_{11}) for M_{SO_3H} membrane is high, its relatively low apparent pore radius may be explained due to its low water content (λ) values

in comparison to M_{COOH} membrane. Estimated apparent pore radius of these membranes also suggested ultrafilter nature of these membranes as observed

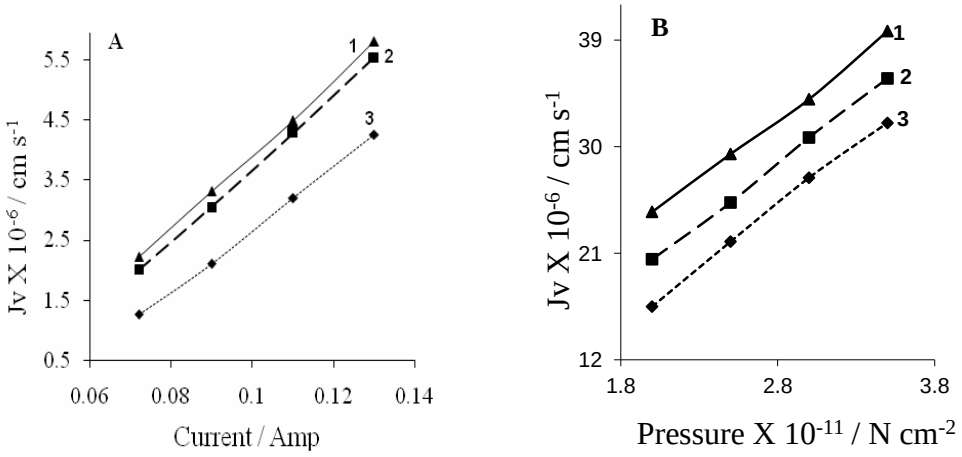

Figure 5.1.8. Variation of volumetric flux for: (1) M_{SO_3H}; (2) M_{COOH}; and (3) $M_{PO_3H_2}$ membranes (A) under applied current; (B) under applied pressure gradient.

by MWCO studies. Also, it can be clearly noticed that nature of functional groups (hydrophilic nature) has pronounced effect on membrane pore dimensions, in spite of same membrane forming material and casting conditions. Also, it was very interesting to find that nature and extent of charge in the membrane matrix influences their flux. Also surface charge on a membrane has significant influence on its separation properties.

Table 5.1.3. Hydrodynamic Permeability (L_{11}), Equivalent Pore radius (r_p), Electro-osmotic Permeability (Jv/I), and Membrane Zeta Potential (ξ) values for different membranes.

Membrane	L_{11} × 10^{-6} (cm^3 N^{-1} s^{-1})	$r_p{}^a$ (nm)	L_{12} × 10^{-3} (Amp^{-1} cm s^{-1})	ξ^b (mV)
M_{SO_3H}	1.62	11.31	0.33	5.22
M_{COOH}	1.13	15.27	0.30	4.25
$M_{PO_3H_2}$	1.23	10.21	0.28	4.63

Knowledge of the electrokinetic properties such as zeta potential of a particular membrane will be proved to be major contributing factor behind

the decision to implement that membrane for a specific separation process, as the surface charge on synthetic membrane has significant effect on its separation properties [35-36], and fouling tendency [37-38]. The zeta potential (ξ) can be obtained from electro-osmotic permeability (L_{12}) values presented in Table 5.1.3, using Smoluchowski equation (Eq. 2.16) [8,39]. Zeta potential values for membranes were also presented in Table 5.1.3. Usually, measurement of E_{eff} at the membrane interface is difficult, thus it is convenient to use current *(I)* for estimating electro-osmotic flux ($L_{12} = (Jv/I)$). In general, the zeta potential of the membranes is supposed to represent the charge characteristics of membrane-solution interfacial zone due to presence of charges at membrane surfaces. M_{SO_3H} showed relatively high ξ values (5.22 mV), because of presence of strong acidic functional groups. Mild charged nature for the ultrafilter membranes are responsible for the observed zeta potential, and it is evident from X^m values presented in Table 5.1.1, that these membranes are charged in nature. Furthermore, values of zeta potentials of these membranes suggest their capability for charge based selection/rejection.

5.1.2.4. Transmission on single protein under coupled driving forces

Protein transmissions across the charged ultrafilter membranes and its effect on the pH of the feed protein solution were studied under coupled driving forces (pressure and electric gradient) to investigate the effect of nature of charge on the protein molecule (CAS or LYS), membrane matrix and direction of electric polarity applied. Schematic diagrams for conventional UF and UF under coupled driving forces (pressure and electric gradient) using charged Ultrafilter membrane are presented in Fig. 5.1.9 (A&B), respectively. Polarity of the electric gradient (Fig. 5.1.9 (B)) was fixed in such a way, that positively charged protein (for example CAS^+, pH<p*I*) was facilitated to migrate through negatively charged membrane from anode side compartment towards cathode side compartment. Under this mode of operation, three

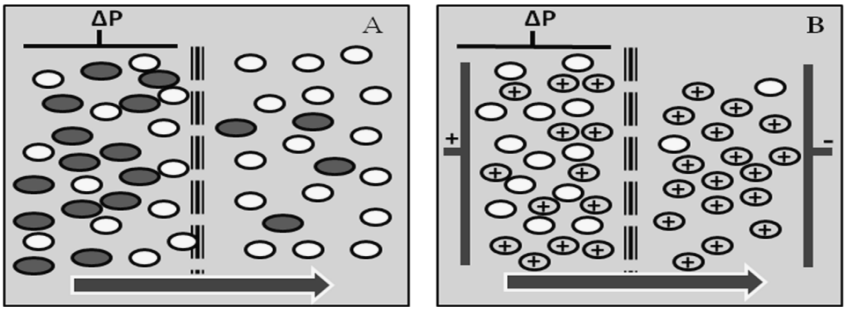

Figure 5.1.9. Schematic presentation of: (A) conventional UF, and (B) UF under coupled driving forces using charged membrane.

screening parameters such as pore size and nature of the charge on the membrane, and electric gradient not only enhance the protein transmission but membrane throughput will also increased due to the electrophoretic migration of the solvent along with protein. In the case, convective transport will be approaching towards zero and total volumetric flux obtained under the simultaneously active forces (pressure and electric gradient in this case) can be written as follows in the form of phenomenological equation (Eq. 3.8) based on non-equilibrium thermodynamic principle [8-32]. The experimental cell for this purpose has been shown in Fig. 5.1.10.

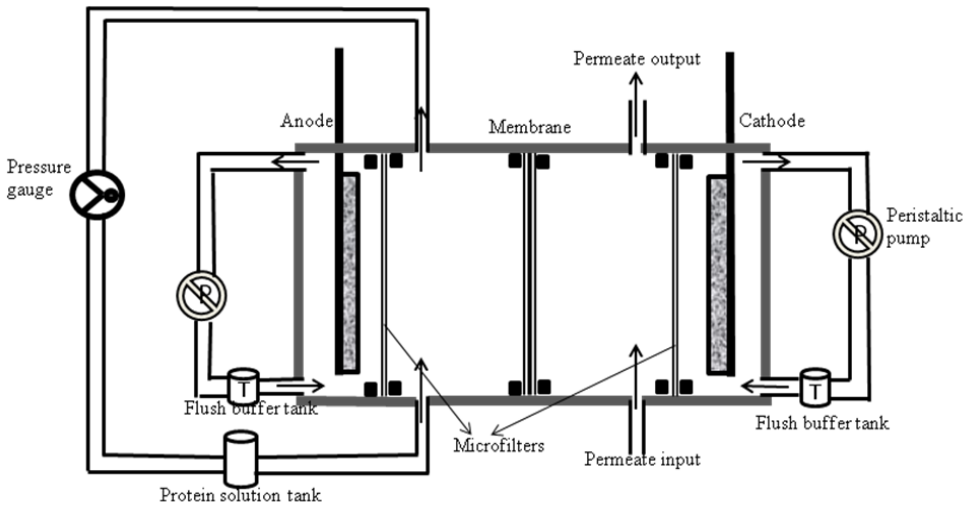

Figure 5.1.10. Experimental cell for protein separation under coupled driving forces.

In case of coupling of driving forces, $(J_v)_{\Delta E=0} < (J_v)_{coup} > (J_v)_{\Delta P=0}$. Fig. 5.1.11 presents volumetric flux of CAS solutions at different pH (between 2.0 to 10.7) across MSO_3H membrane, as a representative case, under constant applied pressure (3×10^{-11} N cm^{-2}) without or with applied electric gradient. It can be seen that without any electric gradient (at 0 V/cm) and under constant pressure, flux values were lowest, which were progressively increased with the increase in electric gradient, especially at pH: 2. Also at pH: 5 (p*I* of CAS) in J_v with increase in applied electric gradient, was very low. While at pH: 10.7 (CAS^-; pH>p*I*) no clear alteration in *Jv* was observed with the increase in applied electric gradient. The filtrate flux is an important parameter of amelioration when evaluating the separation/ fractionation process. After bio-production, the targeted product should be quickly separated because enzyme activity reduced with time [16]. Here it can be seen that filtration velocity was accelerated by coupling of driving forces, pressure and electric gradient, for both type of membranes.

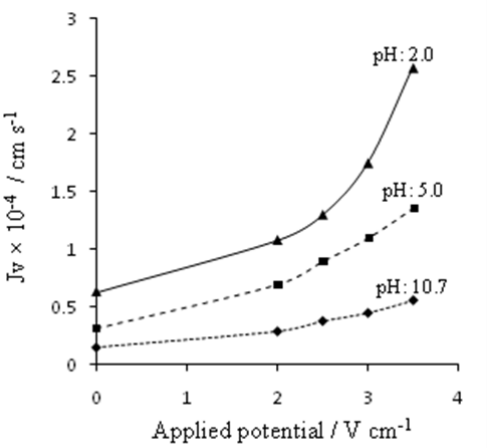

Figure 5.1.11. Variation of J_v at different pH of CAS solution (5 mg/ml) under 3×10^{-11} N cm^{-2} applied pressure and varied applied electric gradient for MSO_3H membrane.

pH of protein solution has marked effect on the permeation properties of protein during UF [7,40,41]. Volumetric flux data are also presented, as function of pH of the feed solution, in Fig. 5.1.12 for charged ultrafilter membranes under 3×10^{-11} N cm^{-2} applied pressure and 2.0 V/cm applied potential gradient. Filtrate flux was highly dependent on pH of the feed CAS or LYS solution. Interestingly, both protein showed highest flux below their p*I*, while at pH>p*I*, fluxes were almost constant. All three membranes showed similar type behavior, while MSO_3H membrane showed comparatively highest

filtrate flux, in spite of its low MWCO and apparent pore radius. These observations also verify the coupling of both the driving forces. This may be because of its comparatively high charge concentration (X^m) values. Also alteration in the filtrate flux under different experimental conditions may be attributed to the combined electrophoretic and electro-osmotic effects.

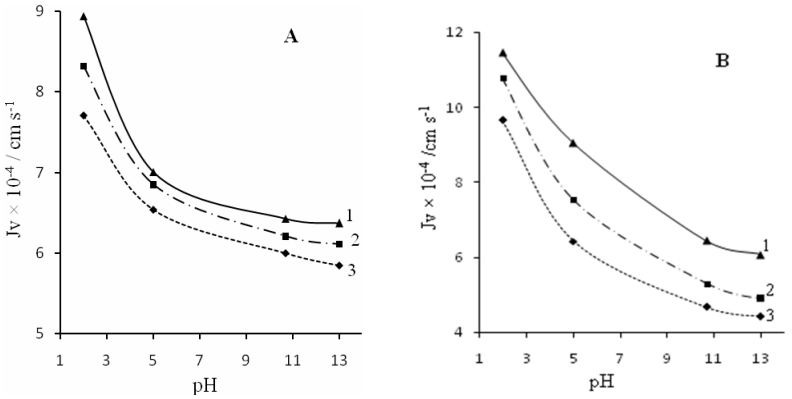

Figure 5.1.12. Variation of volumetric flux (J_v) for: (A) CAS solution and (B) LYS solution (5 mg/ml each) at different pH under 3 × 10^{-11} N cm^{-2} applied pressure and 2.0 V cm^{-1} applied electric gradient for: 1- MSO_3H; 2- MCOOH and 3- MPO_3H_2 membranes.

For the protein separation/ fractionation, transmission or selectivity of the targeted protein molecules is also an important parameter in addition to the throughput. Observed protein transmission (ζ_{obs}) was estimated from the ratio of protein concentration in the feed side to the concentrate side (Eq. 2.23). Representative curves for CAS or LYS transmission (ζ_{obs}) against pH of feed solution under 3 × 10^{-11} N cm^{-2} applied pressure and 2.0 V/cm applied potential gradient for three membranes are presented in Figure 5.1.13 (A&B). It was observed that under suitable experimental conditions, coupled driving forces not only influenced the filtrate flux but also enhanced the protein transmission for charged ultrafilter membrane with different functionalities. Similar to the filtrate flux values, ζ_{obs} value for CAS^+ or LYS^+ (pH below their respective p*I* values) was very high, which reduced significantly at their p*I* (CAS or LYS) or above due to alteration in charged nature of protein with respect pH. Among the three types of membranes, MSO_3H membrane showed comparatively high ζ_{obs} value, similar to data of filtrate flux. Also, these

observations revealed that, at p*I* of CAS (pH: 5.0), relatively high difference in ζ_{obs} value for both proteins can be used with advantage for their separation in mixture. This difference in their transmission aroused due to their different charged nature. At pH: 5, CAS was in zwitterionic form, whereas LYS was LYS^+ form. Thus their transmission of proteins was highly dependent on

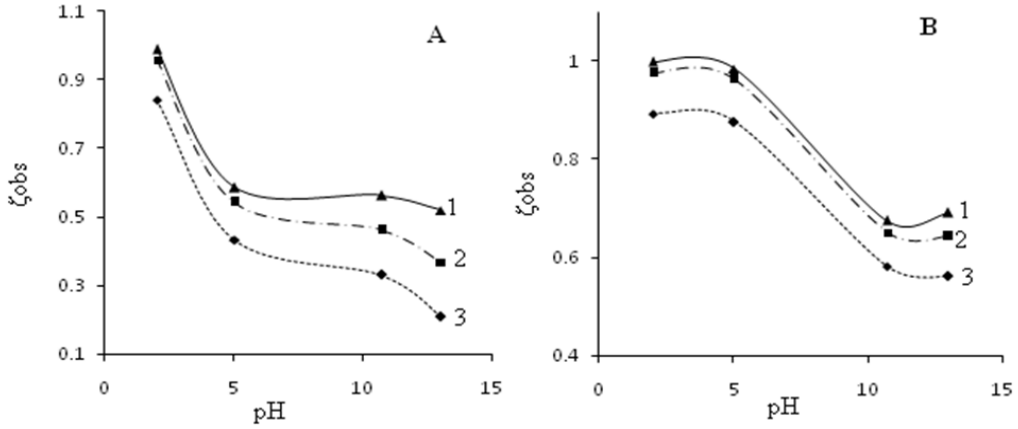

Figure 5.1.13. Variation of observed protein transmission (ζ_{obs}) for: (A) CAS solution and (B) LYS solution (5 mg/ml each) at different pH under 3×10^{-11} N cm^{-2} applied pressure and 2.0 V cm^{-1} applied electric gradient for: 1- MSO_3H; 2- M_{COOH} and 3- MPO_3H_2 membranes.

their charged nature along with applied electric gradient. Thus in this study, three parameters such as applied pressure, electric gradient and the nature of the charge on the membrane matrix govern the filtrate flux and protein transmission across the membranes with similar pore characteristics. Here it is important to record that, fouling was noticeably absent in all cases with less than 1% reduction in the membrane permeability after repeated use, due to applied electric gradient.

5.1.2.5. Protein transmission and selectivity in the mixture of CAS and LYS

The selective separation of CAS and LYS from their equi-gram mixed solution was carried out at different pH ranging between 2.0–13.0, where both existed in different ionic forms across the membranes. Representative ζ_{obs} values for CAS and LYS separately, when mixed protein solution was

used as feed, is presented against pH in Fig. 5.1.14, for three charged ultrafilter membranes, under 3×10^{-11} N cm^{-2} applied pressure and 2.0 V cm^{-1} applied electric gradient. For both protein, BSA and LYS, transmission was strongly dependent on the nature of the charge on the transmitting species (pH), charge nature of membranes and electric gradient. At pH: 2.0, CAS and LYS both existed in positively charged species (BSA^+ or LYS^+) and thus showed very high ζ_{obs} values due to negatively charged nature of membranes and applied electrical polarity. At pH: 5.0, transmission of CAS across charged ultrafilter membranes was relatively lower because of uncharged nature of permeating species (p*I:* 5.0). Transmission of the LYS^+ at pH: 5.0, across the membranes were even high due to electrostatic attraction between migrating species and membrane interface. Thus, at iso-electric point of CAS both proteins can be separated efficiently. Negatively charged membranes allowed high transmission of BSA^+ or LYS^+, while electrical gradient enhanced their flux in spite of similar pore dimensions. At pH: 10.7, while transmission of LYS^0 (p*I*: 10.7) and CAS^- were reduced significantly. Similar trends were also observed at higher pH. Thus selection of charged membranes with suitable pore dimensions and electrical polarity is very much necessary for electrostatic repulsion/attraction of permeating protein depending on the charged nature of transmitting protein species and the membrane interface. Also protein transmission depends on charge concentration and nature of functional groups on the membrane matrix. Thus it is possible to separate

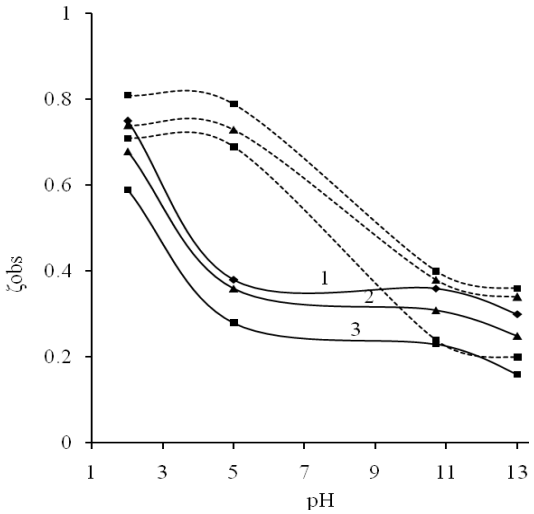

Figure 5.1.14. ζ_{obs} values for CAS (solid line); and LYS (dotted line) in equilibration with CAS-LYS mixed solution (1 mg/ml each) at different pH under 3×10^{-11} N cm^{-2} applied pressure and 2.0 V cm^{-1} applied electric gradient for: 1- MSO_3H; 2- M_{COOH} and 3- MPO_3H_2 membranes.

LYS from the mixture of CAS–LYS at pH: 5.0 (p*I* of CAS) using negatively charged ultrafilter membranes with high selectivity. Also in all cases due to coupling of driving forces, filtrate flux and protein transmission was enhanced.

Further idea about protein separation and selectivity, we can have from separation factor (SF) defined as the ratio of transmission of individual proteins from their mixture (Eq. 2.24). Estimated SF values for different charged ultrafilter membranes are presented in Fig. 5.1.15(A) as a function of pH of the mixed protein feed solution. For MPO_3H_2 membrane, SF values were comparable higher than M_{SO_3H} and M_{COOH} membrane, in spite of its low filtrate flux. Also from data it is clearly evident that separation of CAS and LYS can be efficiently achieved by using charged ultrafilter membrane. Also, SF values presented in Fig. 5.1.15(B) revealed that applied electric gradient further progressively enhanced the SF values, suggested highly selective separation of protein under coupled driving forces. However, applied electric

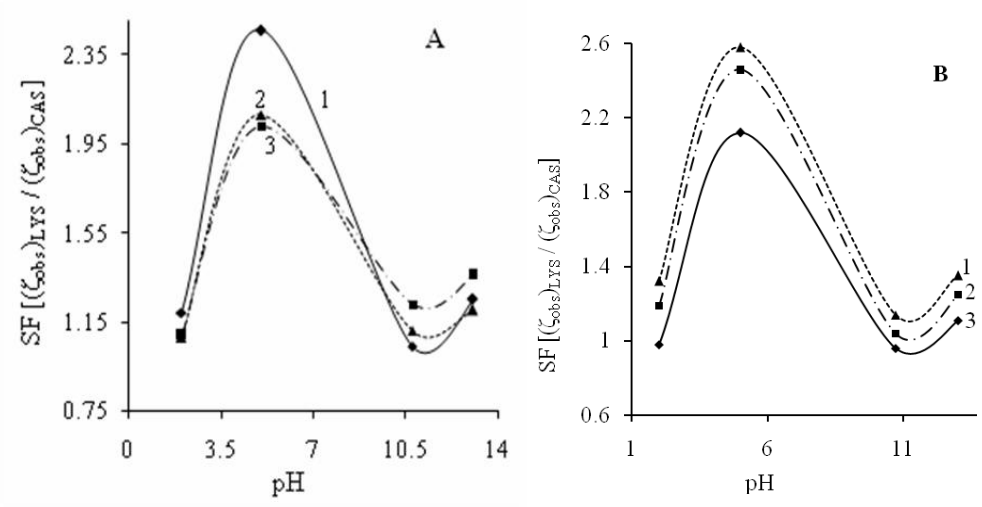

Figure 5.1.15. Separation factor (SF) as function of pH for LYS in its mixed solution with CAS (1 mg/ml each) under constant 3 × 10^{-11} N cm^{-2} applied pressure: (A) 2.0 V cm^{-1} applied potential for: 1- M_{PO3H2}; 2- M_{COOH} and 3- M_{SO3H} membranes; (B) for M_{PO3H2} membrane and varied applied potential: 1- 1.0 V cm^{-1}; 2- 2.0 V cm^{-1} and 3- 3.0 V cm^{-1}.

gradient was so small that no denaturation of protein is possible under given experimental conditions [9,32]. SF values for different membrane follows the

trend: $M_{PO_3H_2}$>M_{COOH}>M_{SO_3H}. Thus it is possible to develop a rapid and highly selective protein separation method using $M_{PO_3H_2}$ membrane under coupled driving forces (pressure and electric gradient). In this process no appreciable membrane fouling or protein denaturation was observed, while by focusing one component at its iso-electric point, other component in the charged state (depending on pH) may be effectively separated. In this case the difference in the p*I* values of LYS and CAS was quite high, but in general cases where p*I* values were nearby, this process also can be efficiently used by varying the pore size of the membrane according to the molecular weight of the protein to be separated and with fine variations in their pH. Two screening parameters such as p*I* values and molecular size were taken in account for achieving high degree of selectivity.

5.1.3. Conclusions for acid functionalized charged ultrafilter membranes

Inter-polymer of PVC and styrene–divinylbenzene was prepared and conventional methods and thin films of desired thickness were casted. Partially dried films were gelated by immersing it in the deionized water for under optimized conditions for tailoring the pore structure of the membrane matrix. Different functional groups such as sulphonic-, carboxylic- or phosphonic acid, were introduced in the membrane matrix for the preparation of charged ultrafilter membrane. Introduction of functional groups were also identified by FTIR and ion-exchange capacity studies. TGA, DSC and DMA testing of these membranes revealed their thermal and mechanical stabilities. Electrochemical characteristics such as membrane conductivity; surface charge density and counter-ion transport number of these membranes also revealed charged nature of the membrane matrix. It was observed that nature of functional groups (hydrophilic nature) has pronounced effect on membrane pore dimensions, in spite of same membrane forming material and casting conditions. These membranes were employed for the separation of proteins from their mixture under coupled driving forces. Coupling of forces were also confirmed by volumetric filtrate flux

under different charged state of permeating protein. Single protein transmission study revealed that, at p*I* of CAS (pH: 5.0), relatively high difference in ζ_{obs} value for both proteins can be used with advantage for their separation in mixture. It was concluded that separation of LYS from the mixture of CAS–LYS at pH 5.0 (p*I* of CAS) using negatively charged ultrafilter membranes, especially with MPO_3H_2 membrane, was possible with high selectivity. Also in all cases due to coupling of driving forces, filtrate flux and protein transmission was enhanced. Furthermore, applied electric gradient further progressively enhanced the SF values, suggested highly selective separation of protein under coupled driving forces.

In the present work product yield defined as transmission through the membrane could be highly raised due to coupling of driving forces and three screening parameters such as: charge on the protein; charge on the membrane matrix and superimposed electric gradient. Thus this is a novel process using charged ultrafilter membrane for improving product purity, and filtration velocity (throughput). Both, the electrophoretic migration of molecules and the positive effect of electro-osmosis, lead to increase in product purity. Also, an additional driving force (electric field) could raise filtration velocity even when the increase in applied pressure had reached to its limit. Reported process is a promising tool to make downstream processing faster and product purer in certain fields of application.

References

[1] Ulbricht M. Polymer 2006;47:2217.

[2] Baker RW, Membrane technology and applications. Wiley: Chichester, 2004.

[3] Blanch HW, Clark DS. Biochemical engineering. Marcel Dekker: New York, 1996.

[4] Van Reis R, Zydney AL. J Membr Sci 2007;297:16.

[5] Nagarale RK, Gohil GS, Shahi VK. Adv Colloid Interface Sci 2006;119:97.

[6] Saxena A, Gohil GS, Shahi VK. Ind Eng Chem Res 2007;46:1270.

[7] Saxena A, Tripathi BP, Kumar M, Shahi VK. Adv Colloid Interface Sci 2009;145:1.

[8] Saxena A, Shahi VK. J Membr Sci 2007;299:211.

[9] Kappler T, Posten C. J Biotechnol 2007;128:895.

[10] Ghosh R, Cui ZF. J Membr Sci 1998;139:17.

[11] Feins M, Sirkar KK. Biotechnol Bioeng 2004;86:603.

[12] Maruyama T, Katoh S, Nakajima M, Nabetani H. Biotechnol Bioeng 2001;75:233.

[13] Saksena S, Zydney AL. Biotechnol Bioeng 1994;43:960.

[14] Wan Y, Ghosh R, Cui Z. Biotechnol Prog 2004;20:1103.

[15] Muller CH, Agarwal GP, Melin Th, Wintgens Th. J Membr Sci 2003;227:51.

[16] Shukla R, Balakrishnan M, Agarwal GP. Bioseparation 2000;9:7.

[17] Iritani E, Mukai Y, Kiyotomo Y. J Membr Sci 2000;164:51.

[18] Nystrom M, Aimar P, Luque S, Kulovaara M, Colloids Surf. A: Physicochem Eng Aspects 1998;138:185.

[19] Ghosh R. Biotechnol Bioeng 2001;74:1.

[20] Ehsani N, Parkkinen S, Nystrom M. J Membr Sci 1997;123:105.

[21] Fane AG, Fell CJD, Suki A. J Membr Sci 1983;16:195.

[22] Burns DB, Zydney A. J Membr Sci 2000;172:39.

[23] Cheang B, Zydney AL. Biotechnol Bioeng 2003;83:201.

[24] Carlsson N, Sanandaji N, Voinova M, Akerman B. Langmuir 2006;22: 4408.

[25] Lilley KS, Razzaq A, Dupree P. Curr Opin Chem Biol 2001;6:46.

[26] Hulteen JC, Jirage KB, Martin CR. J Am Chem Soc 1998;120:6603.

[27] Chun KY. Langmuir 2002;18:4653.

[28] Kubota N, Miura S, Saito K, Sugita Watanabe K, Sugo T. J Membr Sci 1996;117:135.

[29] Wang DIC, Sinskey AJ, Sonoyama T. Biotechnol Bioeng 1969;11:987.

[30] Dukhin SS, Derjaguin BW, in: Matijevic E. (Ed.), Surface and Colloid Science, Wiley: New York, 1974.

[31] Larsson K. Desalination 1980;35:105.

[32] Breslau BR, Testa AJ, Milnes BA, Medjanis G. in: Cooper, A. R. (Ed.), Plenum Press: New York, 1980.

[33] Kim KJ, Fane AG, Nystrom M, Pihlajamaki A, Bowen WR, Mukhtar H. J Membr Sci 1996;116:149.

[34] Reis RV, Brake JM, Charkoudian J, Burns DB, Zydney AL. J Membr Sci 1999;159:133.

[35] Ricq L, Narcon S, Reggiani JC, Pagetti j. J Membr Sci 1999;156:81.

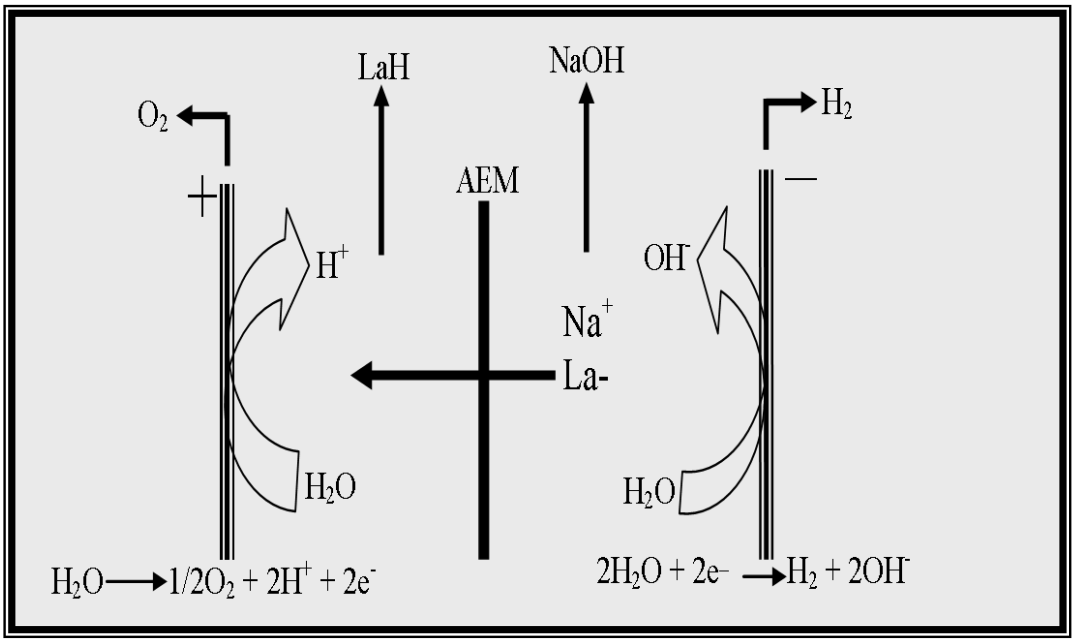

CHAPTER VI

ELECTROCHEMICAL MEMBRANE REACTOR

6.1. Separation and ion substitution for the recovery of lactic acid from lactates salt

Lactic acid has a wide range of applications in the food, pharmaceutical, and cosmetics industries [1-3]. In recent years, growing demand for biodegradable polymers, substitutes for conventional plastic materials, and new materials for specific uses such as controlled drug delivery or artificial prostheses have drawn attention to efforts to improve conventional processes for lactic acid production [4-6]. Lactic acid is currently manufactured either by fermentation or by chemical synthesis. Whereas the chemical synthesis route produces only a racemic mixture of lactic acid, a fermentation process can produce a single stereoisomer of lactic acid [7]. Approximately 50% of lactic acid is produced by microbial fermentation, whereas the remainder is manufactured by chemical synthesis [8]. Products of biological origin are preferred by the food industry and consumers; thus, microbial fermentation must be cost competitive with chemical synthesis. The efficiency and economics of lactic acid production by fermentation are still problematic from several points of view. The medium and composition of the fermentation broth play a vital role in the improvement of lactic acid production [3,9]. Therefore, current research efforts are focused on identifying effective, efficient, and economic downstream processes to recover lactic acid from the fermentation broth [1]. A number of processes for lactic acid recovery from fermentation broth without precipitation have been studied: solvent extraction [10] adsorption [11] direct distillation [12] and electrodialysis [7,13,14]. These processes can make lactic acid recovery simpler and can reduce waste generation. The solvent extraction process is disadvantageous because of unfavourable distribution coefficients. It also suffers from the environmental and economic problem of solvent loss. The adsorption process requires regeneration of the ion-exchange resin and adjustment of the feed pH to increase the sorption efficiency, necessitating large amounts of chemicals. Direct distillation can form high-boiling internal esters as dimers and polymers during the

distillation process [12]. Electrodialysis is an attractive process in terms of being a fast treatment, providing effective removal of non-ionic molecules, concentrating the product, and generating no by-products [15]. Several researchers have proposed the possibility of using electrodialysis for in situ lactate recovery to reduce product inhibition in batch fermentation [1,2,7,16,17]. Also, a two-stage electrodialysis method for the recovery of lactic acid from fermentation broth, involving desalting of lactate salt from fermentation broth and acidification of the purified lactate salt by water-splitting electrodialysis, has been reported in the literature [7,18]. In the first step of desalting, sodium lactate is recovered, purified, and concentrated. In the water-splitting or acidification step, lactic acid is regenerated from sodium lactate, and sodium hydroxide is recovered. Recently, bipolar membrane electrodialysis has been developed for the conversion of salts into the corresponding acid and base [19,20]. This is a two-step process and involves an electrodialysis unit with several cell pairs of cation- and anion-exchange membranes, which, in turn, increases the downstream processing cost of lactate fermentation. To develop a single-step and environment-friendly process for the separation of lactates from fermentation broth and their acidification to produce lactic acid, an electrochemical membrane reactor based on an anion-exchange membrane was developed. Its performance was studied using standard sodium and ammonium lactate solutions of known concentrations, separately under different experimental conditions. In this reactor lactate ions are crossing the anion-exchange membrane, which cannot be crossed by uncharged carbohydrates, polysaccharides, and other colouring agents even under an applied potential gradient. Thus, it is possible to separate the lactates from fermentation broth and acidify them using this technique. The influence of different operating conditions on the process was investigated to assess the economic suitability of the process.

6.1.1. Materials and preparation of interpolymer type of anion-exchange membrane

Analytical reagent grade lactic acid was purchased from Sigma-Aldrich Chemicals, and NaOH, NH_4OH, and other reagents were obtained from S. D. Fine Chemicals India and were used with out further purification. Sodium lactate (LaNa) solutions were prepared by titrating lactic acid (LaH) with NaOH at pH 7. Doubly distilled water was used for the preparation of all solutions. The anion-exchange membrane (AEM) used in this work was prepared in our laboratory by a procedure reported earlier [21,22]. Numerous versatile applications of electrodialysis with this membrane have been developed because of its high ionic conductivity and chemical and mechanical stabilities [23,24]. It is basically an interpolymer of polyethylene and styrene-divinylbenzene copolymer and was prepared by the polymerization of styrene and divinylbenzene in the presence of polyethylene (60-40% blend of HDPE and LDPE) as a binder and benzoyl peroxide as an initiator at 103 °C in xylene. The obtained polymer was precipitated and palletized. A thin film was obtained by blow film extrusion and was later converted into an AEM by subsequent cholromethylation and amination. The membrane was conditioned by treatment with 1M HCl and 1M NaOH successively and then washed thoroughly with distilled water before its use.

6.1.2. Results and discussion for electrochemical membrane reactor

The physicochemical and electrochemical properties of the anion-exchange membrane used in this investigation are presented in Table 6.1.1. The quite high permselectivity and low membrane resistance reveal that this membrane is suitable for electro-membrane applications. Furthermore, the chemical and mechanical stabilities of this membrane are also attractive features. For any electro-membrane application, it is necessary to have an idea of the membrane conductivity under actual operating conditions. The specific membrane conductivity (km) was estimated by the Eq. (2.20). The variation of km for the membrane in equilibrium with lactic acid and sodium lactate of different concentrations is depicted in Fig. 6.1.1. The conductivity values for the membrane in equilibrium with LaH decreased with

concentration, whereas in case of LaNa, they progressively increased. The membrane conductivity is highly dependent on the ionic concentration in the membrane/solution interfacial zone. This variation can be attributed to (i) ion association in the high-concentration LaH solution and/or (ii) formation of LaH molecular layers on the anion-exchange membrane surface. Factor (ii) is expected to reduce the membrane flux upon prolonged use, which was not observed experimentally in the present case. Factor (i), on the other hand,

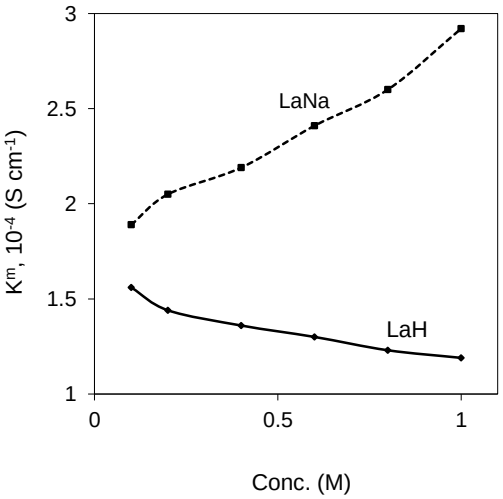

Figure 6.1.1. Membrane conductivity (κ^m) values in equilibration with lactic acid and sodium lactate solution of varied concentration.

Table 6.1.1. **Physicochemical and electrochemical properties of anion-exchange membrane.**

Properties	Anion-exchange membrane
thickness (mm)	0.15
water content (%)	16.0
ion-exchange capacity (mequiv/g of dry membrane)	1.69
permselectivity[a]	0.93
membrane resistance[b] (Ω cm^2)	5.32

[a] permselectivity value was estimated from membrane potential measurements in equilibration with NaCl solutions of 0.10 and 0.01 M concentrations.
[b] membrane resistance was measured in equilibration with 0.10 M NaCl solution.

would result in fewer free mobile ions at higher concentration and cause a decrease in the membrane conductivity. It seems that factor (i) is responsible for the observed variation of membrane conductivity with LaH concentration. The fraction of the organic acid species that exist in ionized form depends on the pH of the solution, which is, consequently, a strong influence on the performance of electro-membrane processes. The fraction can be obtained by consideration of appropriate dissociation reactions. For lactic acid (LaH) and sodium lactate (LaNa) in monovalent anionic form, we must consider Eq. 6.1 and 6.2, respectively.

$$LaH \Leftrightarrow La^- + H^+ \qquad \left[H^+\right]\left[La^-\right] \Leftrightarrow K_1\left[LaH\right] \qquad (6.1)$$

$$LaNa \Leftrightarrow La^- + Na^+ \qquad \left[Na^+\right]\left[La^-\right] \Leftrightarrow K_2\left[LaNa\right] \qquad (6.2)$$

The dissociation constant for LaH (K_1) is always lower than that for LaNa (K_2), which results in a relatively higher number of ionic species for a LaNa solution than for an LaH solution of the same molarity. Because of the higher concentration of ionic species in LaNa solution, the conductivity of a membrane in equilibrium with it is higher than that of a membrane in equilibrium with a LaH solution of the same concentration. Furthermore, the membrane conductivity values under both conditions were good, indicating the efficient performance of the AEM under the applied operating conditions.

6.1.2.1. Single step separation and ion substitution

Single-step separation and ion substitution of LaNa solution was carried out in the electrochemical membrane reactor as described in Fig. 2.12.1. This single-step process involves two stages: (i) In the transfer stage, lactate ion (La^-) is transferred from the catholyte to the anolyte across the AEM under an applied potential gradient. (ii) In the acid formation stage, La- forms the corresponding acid by combining with H^+ produced at the anode through the oxidative electrode reaction. A schematic representation of the

possible lactate-ion transfer and electrode reactions is depicted in Fig. 6.1.2. Lactic acid is inert to electrode reactions. Therefore, the cathode reaction is

$$2H_2O + 2e^- \longrightarrow 2OH^- + H_2\uparrow$$

And the anode reaction is

$$H_2O \longrightarrow 2H^+ + 1/2O_2\uparrow + 2e^-$$

Two electrons produced at the anode are consumed at the cathode, and thus, this is a two-electron process. The whole reaction can be regarded as a water splitting process. We can write the overall electrochemical reaction for the single-step separation and ion substitution of lactate as follows

$$\mathbf{LaNa + 3/2H_2O \rightarrow LaH + NaOH + O_2\uparrow + H_2\uparrow.} \qquad \mathbf{(6.3)}$$

Experiments on the single-step separation and ion substitution of LaNa were carried out at varied applied potential gradients using different concentrations of LaNa solution in the catholyte with water initially being fed through the anolyte at a fixed flow rate.

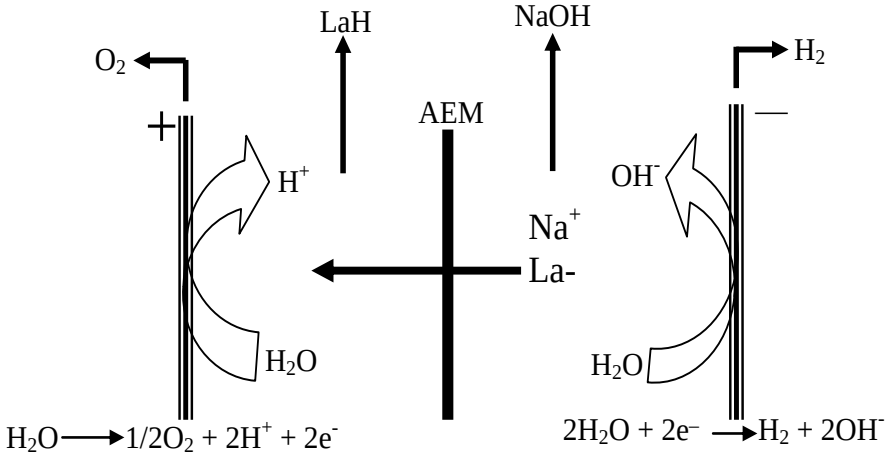

Figure 6.1.2. Schematic presentation of possible lactate ion transfer and electrode reactions.

The variations of the current density with time at different applied potential gradients for 0.50 M LaNa solution as the catholyte feed and for varied concentrations of LaNa at constant applied potential gradient (8.0 V cm^{-1}) are

presented in Fig. 6.1.3 (A and B), respectively. For both cases, the current increased with time and attained a limiting value. The mass transfer performance and water splitting of this process are highly dependent on the current. At the beginning of the experiments, anolyte through which water was initially recirculated offered high electrical resistance.

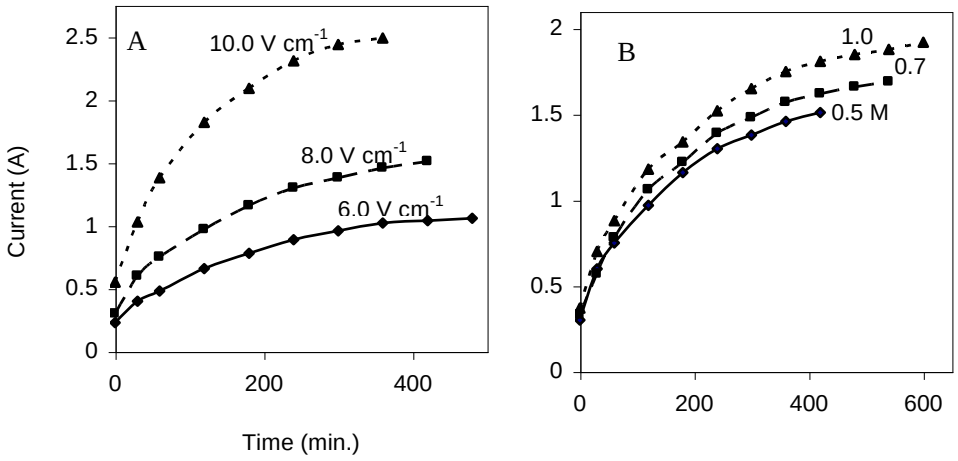

Figure 6.1.3. Variation of current with time during separation and ion substitution for the recovery of LaH (A) at different applied potential using 0.5 M LaNa in the catholyte; (B) at different concentration of LaNa in the catholyte and 8.0 V cm^{-1} applied potential,

With the onset of La^{-} migration from the catholyte to the anolyte and formation of LaH in the anolyte, the electrical resistance offered by the anolyte decreased progressively, resulting in an increase in the current at constant applied potential gradient.

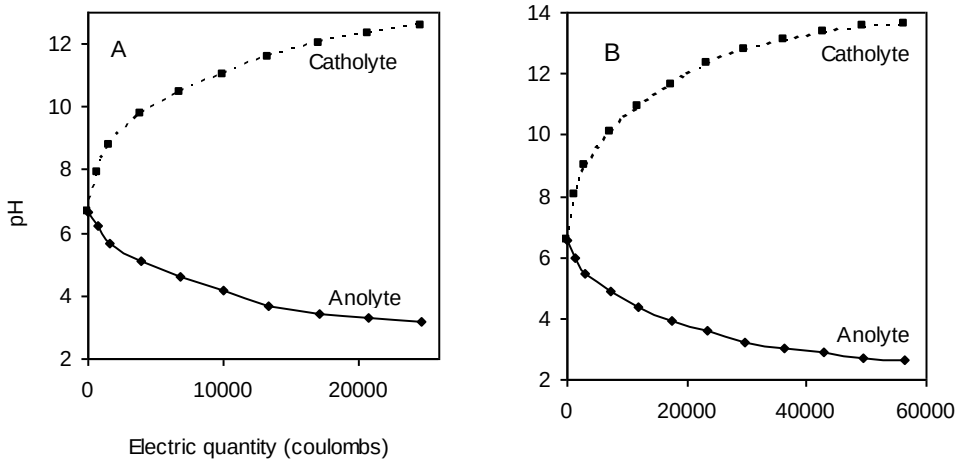

Figure 6.1.4. Variation of anolyte and catholyte pH values with electric quantity for: (A) 0.5 M LaNa in the catholyte at 6.0 V cm^{-1} applied potential; (B) 1.0 M LaNa in the catholyte at 8.0 V cm^{-1} applied potential.

After a certain time, both streams became conductive, and thus, the current passing through the electrochemical reactor attained the limiting value in all cases. Fig. 6.1.4 shows the variation of the pH values of the catholyte and anolyte during the progress of the separation and ion substitution as a function of the total number of coulombs passed for a representative case. As discussed above, there was progressive formation of alkali in the catholyte and lactic acid in the anolyte.

6.1.2.2. Influence of applied potential gradient and lactate concentration on lactic acid flux

The lactate flux from the catholyte to the anolyte or rate of formation of LaH in the anolyte (*J*) in case of negligible volume change can be defined as [25].

$$J = \frac{V_a}{A}\frac{C_t - C_0}{\Delta t} \qquad (6.4)$$

where C_0 and C_t are the initial and final (at time t) concentrations of LaH in the anolyte (mol m^{-3}), Δt is the time allowed for the electro-membrane process (s), V_a is the total volume of anolyte (m^3), and A is the effective membrane area (m^2). In this case, no appreciable volume changes were observed in either compartment during the

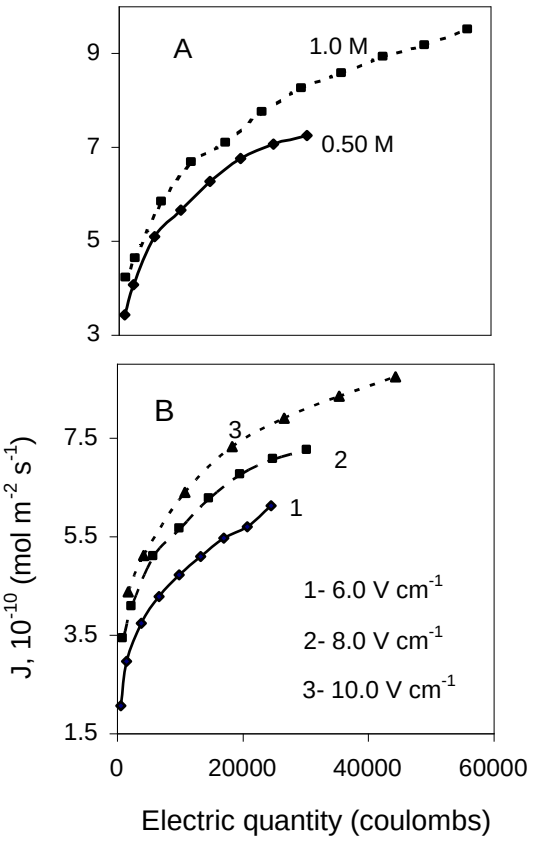

Figure 6.1.5. Dependence of lactate flux on the electric quantity (A) at different concentration of LaNa in the catholyte and 8.0 V cm^{-1} applied potential; (B) at different applied potential using 0.5 M LaNa in the catholyte.

experiments. The effects of the applied potential gradient and lactate concentration in the catholyte are presented in Fig. 6.1.5(A and B), respectively. For each case, the *J* values are proportional to the current passing through the membrane reactor cell under the given experimental conditions. At the beginning of the experiments, the electrical resistance of the membrane reactor was very high because one compartment (anolyte) was initially fed with distilled water and because the absence of electroactive species in the anolyte initially contributed to high membrane reactor resistivity. As the experiments progressed, La- was transferred from the catholyte to the anolyte, and simultaneously H+ was formed through water splitting and the oxidation of oxygen. These processes led to an increase in the concentration of electroactive species in the anolyte with time and, thus, to a simultaneous increase in the current of the system at constant

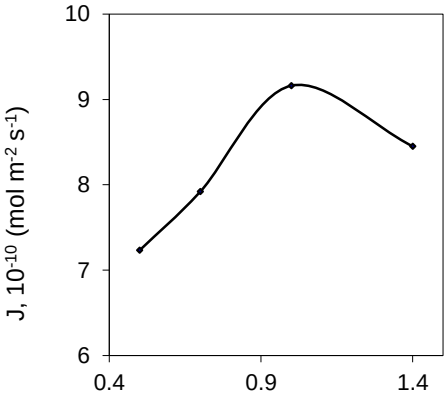

Figure 6.1.6. Variation of lactate flux with LaNa concentration in the catholyte at 8.0 V cm^{-1} applied potential for 6 h process time.

applied potential. The electrical resistance of the catholyte also decreased with time because of the formation of highly conductive OH- at the cathode. Furthermore, the rate of transfer of La-, and thus the rate of formation of LaH, depended on the applied potential gradient and concentration of LaNa. Thus, single-step separation and ion substitution for the recovery of LaH using a membrane reactor can be well optimized for a highly efficient process. Fig. 6.1.6 shows the variation of the La- flux with the initial LaNa concentration in the catholyte. The *J* value initially increased with the concentration of LaNa, and above a 1 M concentration of LaNa, it followed downward trend. Throughout the process of LaH production, OH- competes with La-. The transport number of these anions in the membrane phase depends on their concentration and mobility. Generally, the OH- concentration in the catholyte depends on the applied potential or current flowing through the membrane reactor. At constant applied potential, the current strength of the system also increases with the LaNa concentration or, equivalently, with the La- concentration in the catholyte, which, in turn, is associated with the formation of more OH- at the cathode, especially at higher LaNa concentrations. Thus, the resulting increase in the migration of OH- from the catholyte to the anolyte, in addition to La because of its extremely high concentration in catholyte, might be responsible for the observed downward trend in *J* at LaNa concentrations in the catholyte above 1M. The concentration of LaH recovered from the anolyte is also presented in Fig. 6.1.7 as a representative case at varied applied potential gradients and 0.50M LaNa initial concentration in the catholyte.

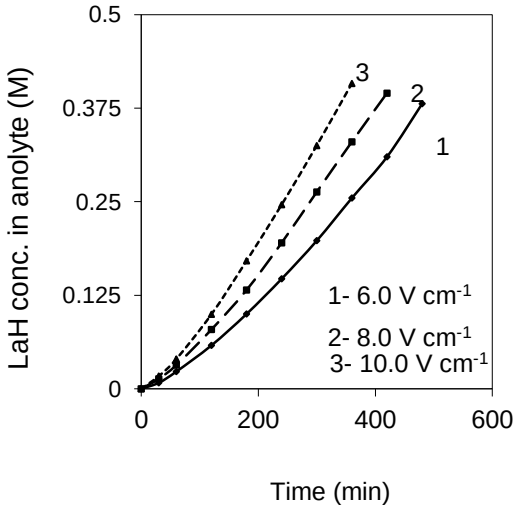

Figure 6.1.7. Lactic acid concentration in the anolyte *vs* time plots for 0.5 M LaNa was in the catholyte.

Moreover, for any process, study of the recovery of the product is highly important to predict its commercial viability. LaH recovery can defined as

$$LaH\ recovery = \frac{C_0\ V_0}{C_t\ V_t} 100 \qquad (6.5)$$

where C_0 and C_t are the initial concentration of LaNa in the catholyte and the concentration at time t of LaH in the anolyte, respectively, and V_0 and V_t are the volumes of the catholyte and anolyte, respectively, which are equal in this case. LaH recovery values are presented in Fig. 6.1.8 for different experimental conditions. The LaH recovery increased with the applied potential, and above 10.0 V cm^{-1}, it approached a limiting value of about 82% for the same feed of the catholyte (0.50 M LaNa). It seems that, under the experimental range and conditions, the electromigration of H+ occurs from the anode chamber to the cathode chamber, particularly at high applied potential gradient, which slows the transfer of La- from the cathode chamber to the anode chamber and, thus, slows the formation of LaH. Furthermore, the LaH recovery was highly dependent on the initial concentration of LaNa in the catholyte. Thus, it is necessary to optimize the applied potential and other process parameters, such as energy consumption and current efficiency, to achieve a high recovery of LaH.

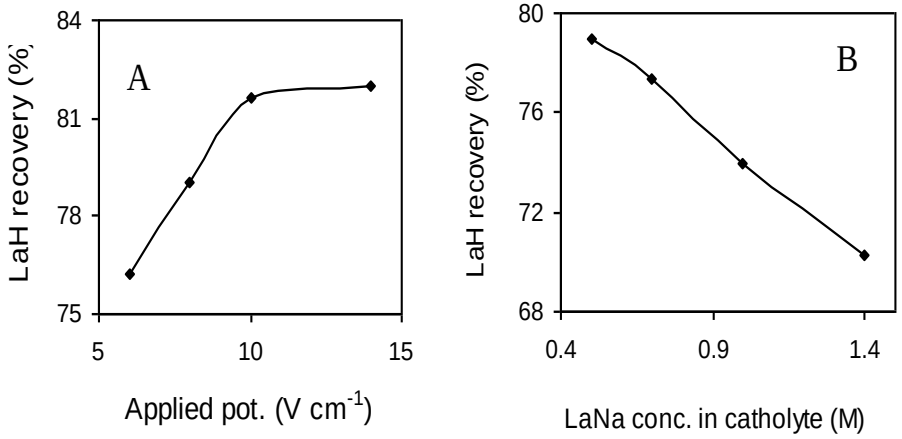

Figure 6.1.8. Dependence of lactic acid recovery, 6 h process time on: (A) applied potential for 0.5 M LaNa in the catholyte; (B) concentration of LaNa in the catholyte at 8.0 V cm^{-1} applied potential.

6.1.2.3. Energy Consumption and Current Efficiency

Energy consumption and current efficiency are important parameters for assessing the suitability of any electrochemical process for practical application. The energy consumption (*W*, kWh/kg of lactic acid produced) of single step separation and ion substitution process under recirculation mode of operation can be obtained from Eq. (6.6) [24]

$$W\left(kWh\,kg^{-1}\right)=\int_{0}^{t}\frac{V\,I\,dt}{w} \qquad (6.6)$$

Where *V* is the applied voltage, *I* the current, *t* the time allowed for electrochemical process and *w* is the weight of LaH formed in the anolyte. Also, current efficiency values were estimated by using Eq. (6.7) [24].

$$CE\,(\%)=\frac{w\,F}{M\,Q}100 \qquad (6.7)$$

where F is the Faraday constant (26.8 A h), M is the molecular weight of LaH (90.8 g/mol), and Q is the electric quantity (A h). An electrochemical process must not only be technically feasible, but should also be less expensive. To evaluate the economic feasibility of the modified process, the specific energy consumptions and current efficiencies values under different operation conditions were calculated, and the results are presented in Fig. 6.1.9 and Table 6.1.2 for different applied potentials and different initial LaNa concentrations in the catholyte. As seen in Fig. 6.1.9(B), the energy consumption increases with the applied potential, whereas the opposite trend can be observed for the CE

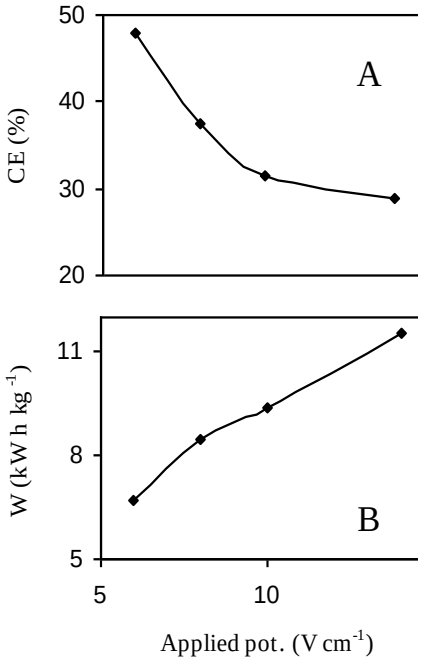

Figure 6.1.9. Current efficiency and energy consumption values for 6 h process time at different applied potential for separation and ion substitution of 0.5 M LaNa in the catholyte.

values under similar operating conditions Fig. 6.1.9(A). Interestingly, the *W* and CE values at constant applied potential for different initial concentrations of LaNa in the catholyte (Table 6.1.2) reveal that these process parameters are independent of the LaNa concentration. Thus, only the applied potential gradient has a high impact on the energy efficiency of the process. At high potential, the concentration of H+ in the anolyte will be quite large because of increased water splitting, and the electro-transport of H+ also consumes part of the energy, resulting in an increase in energy consumption and a decrease in the current efficiency of the process. Furthermore, the minimum value of energy consumption was 6.7 kWh/kg, and the maximum value was 11.6 kWh/kg, which indicates the economic feasibility of the single-step separation and ion substitution process using a membrane reactor.

Table 6.1.2. **Lactic acid concentration in the anolyte, energy consumption and current efficiency data at 8.0 V cm^{-1} applied potential for LaNa solutions with different concentration taken in the catholyte for different process time.**

LaNa conc. in catholyte (M)	Process time (h)	LaH conc. in anolyte (M)	energy consumption (kWh/kg of LaH)	current efficiency (%)
0.50	6.0	0.395	6.29	35.98
0.70	6.5	0.556	6.28	36.16
1.00	7.0	0.740	6.23	37.92
1.40	8.0	0.984	6.19	38.08

6.1.2.4. Single step separation and ion substitution synthetic $LaNH_4$ solution and fermentation broth

The single-step separation and ion substitution of an $LaNH_4$ solution with a 1.0M initial concentration in the catholyte at

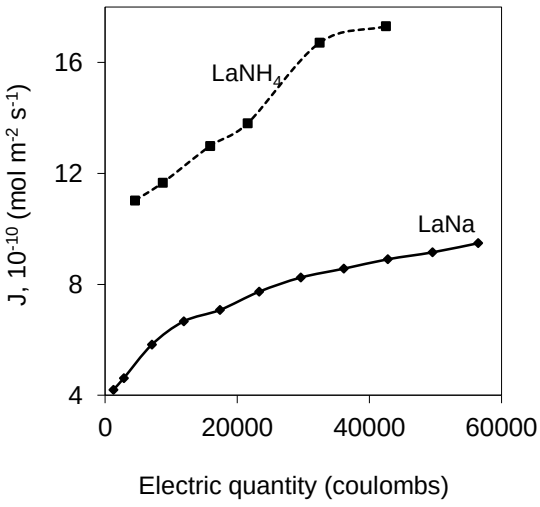

Figure 6.1.10. Dependence of lactate flux on electric quantity for 1.0 M LaNa or $LaNH_4$ catholyte input.

8.0 V cm^{-1} applied potential was also carried out in the electrochemical membrane reactor as a representative case, and flux data are presented in Fig. 6.1.10 in comparison to those for LaNa solution under similar conditions. The $LaNH_4$ solution exhibited a relatively higher flux than the LaNa solution. Here, the electro-migration of OH^- is competing with that of La^-, and it is easy for the former to be captured by NH_4^+, resulting in a higher flux of La^- across the anion-exchange membrane. For the fermentation broth containing Ca^{2+}, Mg^{2+}, and other cations, a similar case will exist. Detailed process parameters are presented in Table 6.1.3 in comparison to those for LaNa. It can be seen that, for about the same final degree of LaH recovery from 1.0M LaNa solution, many more coulombs were consumed than for an equi-molar $LaNH_4$ solution. Furthermore, in the former case, the energy consumption was quite high, and the current efficiency value was low in comparison to the latter case. Experimental data for the separation of La^- from the fermentation broth and its subsequent acidification are also presented in Table 6.1.3, along with the composition of the broth. Different parameter values reveal that the process was more efficient than that for the synthetic LaNa solution, possibly because of the high salt concentration in the broth, which might have contributed to a reduction in the membrane reactor resistance and thus resulted lower energy consumption and higher current efficiency.

Table 6.1.3. In situ separation and ion substitution data for synthetic LaNa and $LaNH_4$ (1.0 M) solutions and concentrated fermentation broth (37.5 g L^{-1} lactate concentration) taken in catholyte at 8.0 V cm^{-1} applied potential for 6 h process time.

Parameters	LaNa	$LaNH_4$	Fermentation broth
electric quantity (coulombs)	56484	42520	50124
recovery of LaH (%)	74.0	70.3	78.3
energy consumption (kWh/kg of LaH)	6.23	4.28	5.02
current efficiency (%)	37.92	55.15	47.64

*Compositions of fermentation broth - Conductivity: 35.8 mS cm^{-1}; pH: 4.04; Colour: dark brown; Cations: (K^+, Na^+, NH_4^+, Ca^{2+}, Mg^{2+}) 19.3 g L^{-1}; Anions: (Cl^-, NO_3^-, PO_43^-, $SO4^{2-}$) 15.5 g L^{-1}; Lactate: 37.5; Free amino acids: 26.13 g L^{-1}; Sugars: (glucose, fructose, sucrose, arabinose, xylose, galactose, mannitol) 38.34 g L^{-1}.

These data reveal that the separation of lactate from its ammonium salt and the conversion of LaH are relatively more efficient than the corresponding process for the sodium salt. Also, the results suggest that the electrochemical membrane reactor is an efficient and simple tool for the recovery lactates from uncharged molecules such as polysaccharides, carbohydrates, and other colouring agents because these molecules are not able to cross the anion-exchange membrane. Therefore, the single-step separation and ion substitution of lactates from fermentation broth also can be efficiently achieved for the production of LaH in downstream processing.

6.1.3. Conclusions for electro chemical membrane reactor

In downstream processing for the separation of lactates from fermentation broth and their conversion to lactic acid, a single step process using an electrochemical membrane reactor, based on an in-house-prepared anion-exchange membrane, was developed. It was observed that La^- ions were able to cross this membrane easily and efficiently under an applied potential gradient and in situ ion substitution was achieved by formation of H^+ in the anolyte as a result of oxidative water splitting, with OH^- formation occurring in the catholyte. The flux of lactate (J) was strongly dependent on the applied potential gradient and the initial concentration of La^- in the anolyte and about 70-82% recovery of lactic was achieved under different operating conditions. The minimum values of energy consumption for sodium lactate and ammonium lactate were found to be 6.23 and 4.28 kWh/kg, respectively. In addition, the energy consumption and current efficiency values for the recovery and ion substitution of LaNa from concentrated fermentation broth were observed to be about 5.02 kWh/kg and 47.64%, respectively, for a completely optimized experiment. The fact that these energy consumption values are higher than those reported for the separation of LaNa by conventional electrodialysis might be because of water oxidation

and reduction at the anode and cathode, which was essential for the in situ ion substitution. Nevertheless, it is necessary to develop a more efficient anion exchange membrane with low resistivity and high selectivity for lactate and hydroxyl ions, to reduce energy consumption and enhance current efficiency of the process. Moreover, the achievement of separation and ion substitution in a single step without any additive or regeneration is the novel feature of the reported process. In this process, La- crosses the AEM, which cannot be crossed by uncharged molecules such as polysaccharides, carbohydrates, and other colouring agents, so that the separation of lactates and conversion to lactic acid can be easily achieved using fermentation broth. Additionally, this new technique could provide a simple separation process for biomolecules such as citrate, format, gluconate, etc., and ion substitution to produce the corresponding acid in a simple manner with higher efficiency and recovery ratio and lower energy consumption.

References

[1] Lee KB. Bioresource Technol 2005;96:1505.

[2] Datta R, Tsai SP, Bonsignore P, Moon SH, Frank JR, FEMS. Microbiol Rev 1995;16:221.

[3] Hujanen M, Linko YY. Appl Microbiol Biotechnol 1996;45:307.

[4] Cheng P, Muller RE, Jaeger S, Bajpai R, Iannoti EL. J Ind Microbiol 1991;7:27.

[5] Goncalves LMD, Barreto MTO, Xavier AMB, Carrondo MJT, Klein J. Appl Microbiol Biotechnol 1992;38:305.

[6] Lipinsky ES, Sinclair RG. Chem Eng Prog 1986;82:26.

[7] Lee EG, Moon SH, Changa YK, Yoo IK, Changa HN. J Membr Sci 1998;145:53.

[8] VickRoy TB, Lactic acid. In Comprehensive Biotechnology vol 3; Blanch, H.W., Drew, S., Wang, D.I.C., Eds.; Pergamon Press, Oxford, 1985: pp 761–776.

[9] Arasaratnan V, Senthuran A, Balasubaramaniam K. Enzyme Microb Technol 1996;19:482.

[10] Yabannavar VM, Wang DIC. Biotech Bioeng 1991;37:1095.

[11] Kaufman EN, Cooper SP, Davison BH. Appl Biochem Biotech 1994;45:545.

[12] Cockrem MCM, Johnson PD, U.S. Patent 5, 210, 296, 1993.

[13] Heriban V, Skara J, Sturdik E, Ilavsky J. Biotech Tech 1993;7:63.

[14] Choi JH, Kim SH, Moon SH. Sep Puri Technol 2002;28:69.

[15] Cauwenberg V, Peels J, Resbeut S, Pourcelly G. Sep Puri Technol 2001;22:115.

[16] Hongo M, Nomura Y, Iwahara M. Appl Environ Microbiol 1986;52:31.

[17] Min-tian G, Koide M, Gotou R, Takanashi H, Hirata M, Hano T. Process Biochem 2005;40:1033.

[18] Glassner DA, Datta R, E. Patent 0 393 818 A1, 1990.

[19] Balster J, Stamatialis DF, Wessling M. Chem Eng Process 2004;43:1115.

[20] Xu TW, Yang WH. Chem Eng Process 2002;41:519.

[21] Narayanan PK, Adhikary SK, Harkare WP, Govindan KP. Indian Patent 1,60,880, 1987.

[22] Shahi VK, Makwana BS, Thampy SK, Rangarajan R. Desalination 2002;151:33.

[23] Gohil GS, Shahi VK, Rangarajan R. J Membr Sci 2004;240:211.

[24] Nagarale RK, Gohil GS, Shahi VK, Trivedi GS. J Colloid Inter Sci 2004;277:162.

[25] Yi SS, Lu YC, Luo GS. J Membr Sci 2005;255:57.

PUBLICATIONS/SYMPOSIA/ CONFRENCES

APPENDIX I:

1.1 List of research papers/review article/book chapter published during the investigation

[1] **Arunima Saxena**, Arvind Kumar, Vinod K. Shahi*, "Preparation and characterization of *N*-methylene phosphonic and quaternized chitosan composite membranes for electrolyte separations", ***Journal of Colloid & Interface Science*** 303 (2006) 484-493.

[2] **Arunima Saxena**, V. K. Shahi and Arvind Kumar*, "Thermodynamic study of functionally modified chitosan and their blends in aqueous media at 298.15 K", ***Journal of Molecular Liquid*** 135 (2007) 21-26.

[3] **Arunima Saxena**, G. S. Gohil, Vinod K. Shahi*, "Electrochemical Membrane Reactor: Single Step Separation and Ion Substitution for the Recovery of Lactic Acid from Lactates Salt", ***Industrial Engineering Chemistry Research*** 46 (2007) 1270-1276.

[4] **Arunima Saxena,** Bijay P. Tripathi, Vinod K. Shahi*, "Sulfonated poly (styrene-co-maleic anhydride)-poly (ethylene glycol)-silica nanocomposite polyelectrolyte membranes for fuel cell applications", ***Journal of Physical Chemistry B*** 111 (2007)12454-12461.

[5] **Arunima Saxena**, Vinod K. Shahi*, "pH Controlled selective transport of proteins through charged ultrafilter membranes under coupled driving forces: An efficient process for protein separation", ***Journal of Membrane Science*** 299 (2007) 211-221.

[6] Jeeshan Khan, Bijay P. Tripathi, **Arunima Saxena**, Vinod K. Shahi*, "Electrochemical membrane reactor: In situ separation and recovery of chromic acid and metal ions", ***Electrochimica Acta*** 52 (2007) 6719-6727.

[7] **Arunima Saxena**, Vinod K. Shahi*, "Recent developments on proton-exchange membranes for fuel cell applications", Chapter 1, ***Applied physics in the 21st Century*** (Ed. Xin Chen), Research Signpost, 2007.

[8] **Arunima Saxena**, Bijay P. Tripathi, Vinod K. Shahi*, "An improved process for separation of proteins using modified chitosan–silica cross-linked charged ultrafilter membranes under coupled driving forces: Isoelectric separation of proteins", ***Journal of Colloid & Interface Science*** 319 (2008) 252–262.

[9] **Arunima Saxena**, Vinod K. Shahi*, **"**Phosphonic acid grafted bis (4-γ-aminopropyldiethoxysilylphenyl) sulfone (APDSPS)-poly (vinyl alcohol) cross-linked polyelectrolyte membrane impervious to methanol, Bijay P. Tripathi", ***Journal of Membrane Science*** 318 (2008) 288–297.

[10] **Arunima Saxena**, Bijay P. Tripathi, Mahendra Kumar, Vinod K. Shahi*, "Membrane based techniques for the separation and purification of proteins: An Overview", ***Advances in Colloids and Interface Science*** 145 (2009) 1–22.

[11] Mahendra Kumar, Bijay P. Tripathi, **Arunima Saxena**, Vinod K. Shahi*, "Electrochemical membrane reactor: Synthesis of quaternary ammonium hydroxide from its halide by *in situ* ion substitution", ***Electrochimica Acta*** 54 (2009) 1630-1637.

[12] **Arunima Saxena**, Mahendra Kumar, Bijay P. Tripathi, Vinod K. Shahi*, Organic-inorganic hybrid charged membranes for proteins separation: Isoelectric separation of proteins under coupled driving forces, ***Separation and purification technology 2008 (Communicated).***

[13] Bijay P. Tripathi**,** Mahendra kumar, **Arunima Saxena** and Vinod K. Shahi*, Bifunctionalized organic-inorganic charged nanocomposite membranes for pervaporation separation of water-ethanol mixture, ***Industrial Engineering Chemistry Research* 2009 *(Under revision).***

[14] **Arunima Saxena**, Vinod K. Shahi*, Iso-Electric Separation of Proteins using Charged Ultrafilter Membranes with Different Functionality under Coupled Driving Forces, ***Industrial Engineering Chemistry Research* 2009 *(Under revision).***

APPENDIX II

2.1 Paper Presented/Accepted in Conference and Symposia

[1] **Arunima Saxena**, Arvind Kumar, Vinod K. Shahi, "Modified Biomaterial: N-Methylene Phosphonic and Quaternized Chitosan Composite Membranes for Electrolyte Separations" , paper presented in the Nation Symposium on Modern trends in Chemical Sciences, held at Kurukshetra University during October 6-7, 2006.

[2] **Arunima Saxena**, Vinod K. Shahi, " pH Controlled Transport of Proteins through Charged Membranes under Coupled Driving Forces" , poster presented in 9th CRSI National Symposium in Chemistry, Chemistry Department, Delhi University, Delhi, 1-4th February, 2007.

[3] **Arunima Saxena,** Bijay P. Tripathi, Mahendra Kumar, Vinod K. Shahi, Isoelectric-separation of proteins using modified chitosan-silica crosslinked charged ultrafilter membrane under coupled driving forces, oral presentation in DAE-BRNS Symposium on Emerging Trends in Separation Science and Technology SESTEC-2008, Chemistry Department, Delhi University, Delhi-10007, during March 12-14, 2008.